

2011

# Development of a Novel Methodology for the Identification of VOC Emission Sources in Indoor Environments based on the Material Emission Signatures and Air Samples measured by PTR-MS

Kwanghoon Han  
*Syracuse University*

Follow this and additional works at: [http://surface.syr.edu/mae\\_etd](http://surface.syr.edu/mae_etd)

 Part of the [Engineering Commons](#)

---

## Recommended Citation

Han, Kwanghoon, "Development of a Novel Methodology for the Identification of VOC Emission Sources in Indoor Environments based on the Material Emission Signatures and Air Samples measured by PTR-MS" (2011). *Mechanical and Aerospace Engineering - Dissertations*. Paper 57.

This Dissertation is brought to you for free and open access by the College of Engineering and Computer Science at SURFACE. It has been accepted for inclusion in Mechanical and Aerospace Engineering - Dissertations by an authorized administrator of SURFACE. For more information, please contact [surface@syr.edu](mailto:surface@syr.edu).

## ABSTRACT

One of the recent important challenges in the research field of indoor air quality is the identification of indoor Volatile Organic Compound (VOC) emission sources to clearly pinpoint the sources of concern in a field condition. This study represents the first attempt in developing a new technique to find the sources that may be invisible or hidden based on the inspection even of experts when a building with problems of indoor air quality is suspected. The objectives of this study were 1) to determine VOC emission signatures specific to nine typical building materials by using an on-line analytical monitoring device, Proton Transfer Reaction - Mass Spectrometry (PTR-MS), 2) to explore the correlation between the PTR-MS measurements and the measurements of acceptability by human subjects, 3) to develop and evaluate a methodology to identify individual sources of VOC emissions based on the measurements of mixed air samples and the PTR-MS material emission signatures, 4) to determine the long-term variation of VOC emission signatures over time, and 5) to develop a method to account for the long-term variation of emission signatures in the application of the emission source identification method. Samples of nine building materials were tested individually and in combination, including carpet, ceiling material, gypsum board, linoleum, two paints, polyolefine, PVC and wood. VOC emissions from each material were measured in a 50-liter small-scale chamber. Chamber air was sampled by PTR-MS to establish a database of emission signatures unique to each individual material. Sorbent tube sampling and TD-GC/MS analysis were also performed to identify the major VOCs emitted and to compare the resulting data with the PTR-MS emission signatures. The data on the acceptability of air quality assessed by human subjects were obtained from a previous

experimental study in which the emissions from the same batch of materials were determined under the same area-specific ventilation rates as in the case of the current measurements with PTR-MS. The same task was performed to measure combined emissions from material mixtures for the application and validation of a signal separation methodology and its source identification enhancement by the consideration of long-term emissions. The methodology was developed based on signal processing principles by employing the method of multiple regression least squares (MRLS) and a normalization technique. Source models were employed to track the change of individual material emission signatures by PTR-MS over a long period of time. It is concluded that: 1) PTR-MS can be an effective tool for establishing VOC emission signatures of material types, and there were sufficient correlations (i.e. Correlation coefficient  $r < -0.92$ ) between the PTR-MS measurements and the acceptability of air quality for the nine materials tested when the sum of selected major individual VOC odor indices was used to represent the emission level measured by PTR-MS; 2) the proposed method for source identification could identify the individual sources at high success rates under laboratory conditions with two, three, five and seven materials present; and 3) the long-term (over nine months) variation of emission factors of the tested materials could be well represented by an empirical power-law model or a mechanistic diffusion based model, and the model coefficients could be estimated based on relatively a short-term set of emission measurements (i.e.  $\leq 28$  days). The source models could also be used to predict the variation of material emission signatures, which could in turn be used for source identification. Further experiments and investigation are needed to apply the presented source identification method under real field conditions.

**Development of a Novel Methodology  
for the Identification of VOC Emission Sources in Indoor Environments  
based on the Material Emission Signatures and Air Samples  
measured by PTR-MS**

By

**Kwanghoon Han**

BS, at Seoul National University, 1999

MS, at Seoul National University, 2001

**DISSERTATION**

Submitted as the partial fulfillment of requirements for the  
Degree of Doctor of Philosophy in Mechanical and Aerospace Engineering  
of the Graduate School at Syracuse University

**May 2011**

**Advisor: Jensen S. Zhang, Ph.D**

Copyright © 2011 Kwanghoon Han

**All rights are reserved.  
Should be used by permission.**

**The Graduate School  
Syracuse University**

We, the members of the Oral Examination Committee,  
hereby register our concurrence that

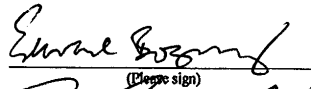
**Kwanghoon Han**

satisfactorily defended his dissertation on

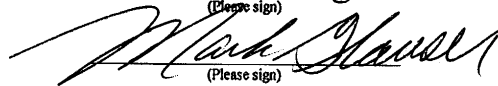
Monday, February 07, 2011

Examiners:

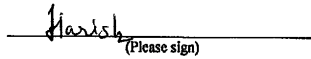
Edward Bogucz

  
(Please sign)

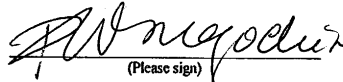
Mark Glauser

  
(Please sign)

Harish J Palanthandaram

  
(Please sign)

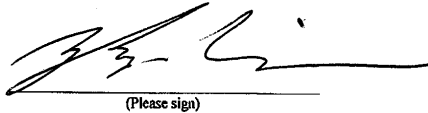
Pawel Wargocki

  
(Please sign)

(Please sign)

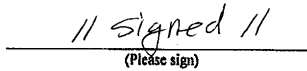
Advisor:

Jensen Zhang

  
(Please sign)

Oral Examination Chair:

Pramod K Varshney

  
(Please sign)

**Development of a novel methodology  
for the identification of VOC emission sources  
in indoor environments**

**TABLE OF CONTENTS**

ABSTRACT.....	VI
ACKNOWLEDGEMENTS.....	XVI
† CHAPTER 1. INTRODUCTION .....	1
1.1 Background of the Research .....	1
1.2 Objectives and Scope of the Research .....	2
1.3 Outcomes .....	5
† CHAPTER 2. LITERATURE REVIEW .....	7
2.1 PTR-MS Analysis Technology .....	7
2.1.1 Fundamentals .....	7
2.1.2 Other techniques that can be integrated with PTR-MS .....	11
2.1.3 On-going applications using PTR-MS.....	15
2.2 Studies on Human Perceived Air Quality .....	24
2.2.1 Methods of experimental sensory assessment studies .....	24
2.2.2 Quantification and composition studies of VOCs using other analyses .....	32
2.2.3 Integrated study cases using PTR-MS with sensory assessments .....	34
2.3 Material Emission Characteristics .....	35
2.3.1 Dry materials.....	37
2.3.2 Wet materials .....	38
2.4 Chemical Compositions and Dynamics of Indoor Air.....	40
2.4.1 Active and passive sources .....	40

2.4.2 Simulations of VOC emission dynamics in an indoor environment.....	41
2.5 Potential Techniques for Signature Separation and Identification .....	44
2.6 Summary and Conclusions .....	67
† CHAPTER 3. DETERMINATION OF MATERIAL ESs AND THEIR CORRELATIONS WITH SENSORY DATA .....	69
3.1 Introduction.....	69
3.2 Materials and Methods.....	73
3.2.1 Overview.....	73
3.2.2 Environmental conditions .....	76
3.2.3 Test specimens .....	77
3.2.4 PTR-MS analysis .....	79
3.2.5 GC/MS analysis .....	80
3.2.6 Test procedure.....	81
3.2.7 Data analysis procedure .....	82
3.3 Results and Discussion .....	85
3.3.1 Material emission signatures by PTR-MS .....	85
3.3.2 Relationship between acceptability and PTR-MS measurements ( <i>ncps</i> ) .....	90
3.3.3 VOCs responsible for the poor acceptability .....	92
3.3.4 Emission factor characteristics measured by PTR-MS.....	102
3.3.5 The existence of pair ion masses .....	107
3.4 Conclusions.....	108
† CHAPTER 4. NOVEL METHODOLOGY FOR INDOOR EMISSION SOURCE IDENTIFICATION.....	111
4.1 Introduction.....	111



4.2	Materials and Methods.....	116
4.2.1	Overview and basic assumptions .....	116
4.2.2	Algorithms for source identification module.....	118
4.2.3	Environmental chamber setup and conditions .....	123
4.2.4	Test specimens .....	124
4.2.5	PTR-MS setting .....	125
4.2.6	Test procedure.....	126
4.3	Results and Discussion .....	127
4.3.1	Relative signal intensity ( $\alpha$ ) and variance ( $\varepsilon$ ) of material emission signatures	127
4.3.2	Separation simulations of the algorithms for various material mixtures .....	129
4.3.3	Monte-Carlo simulations for the nine-material mixture .....	132
4.3.4	Experimental results of multi-material mixtures .....	134
4.3.5	Effects of adsorption.....	137
4.4	Conclusions.....	142
†	CHAPTER 5. VARIATION OF ESs OVER TIME AND ITS IMPACT ON SOURCE IDENTIFICATION.....	143
5.1	Introduction.....	143
5.2	Materials and Methods.....	146
5.2.1	Overview.....	146
5.2.2	Environmental chamber conditions .....	147
5.2.3	Test specimens .....	147
5.2.4	PTR-MS setting .....	148
5.2.5	Test procedure.....	149
5.3	Results and Discussion .....	151

5.3.1 Emission pattern at each long-term period .....	151
5.3.2 Long-term ES estimations by using source models .....	163
5.3.3 ES separation performance with the consideration of long-term ES change....	171
5.3.4 Recommendations on the practical establishment of a long-term ES library ...	175
5.4 Conclusions.....	196
† CHAPTER 6. SUMMARY AND CONCLUSIONS .....	199
6.1 Summary and Conclusions .....	199
6.2 Practical Implications.....	202
6.3 Limitations .....	203
† CHAPTER 7. RECOMMENDATIONS FOR FUTURE RESEARCH AND APPLICATIONS .....	205
7.1 Recommendations for Future Works .....	205
7.2 Possible Applications using the Emission Signature Technique .....	207
REFERENCES .....	209
APPENDIX A. A Library of ESs by PTR-MS for Nine Building Materials tested. ....	225 -
(a) Polyolefine:.....	225 -
(b) PVC: .....	226
(c) Ceiling: .....	227
(d) Gypsum: .....	228
(e) Paint 1:.....	229
(f) Paint 2: .....	230
(g) Carpet: .....	231
(h) Linoleum: .....	232
(i) Wood:.....	233
Biographical Sketch .....	234

## LIST OF TABLES

[Table 3.1] Flow rates and specimen areas for PTR-MS chemical measurements. ....	81
[Table 3.2] List of possible VOCs responsible for poor acceptability. ....	96
[Table 4.1] Flow rates and specimen areas determining the concentrations of emissions for the PTR-MS experiments. ....	124
[Table 4.2] Comparison of signature separation performance results of the two algorithms for various cases. ....	131
[Table 5.1] Flow rates and specimen areas for the PTR-MS experiments. ....	148
[Table 5.2] Summary of emission signature estimation results by source models. ....	170
[Table 5.3] Comparison of signature separation performance results of the two algorithms for various cases. ....	173
[Table 5.4] Summary of the prediction errors by two source models (w/ short-term data). .....	186
[Table 5.5] Summary of ES predictions by the power-law model (w/ 28-day short-term data). ....	187
[Table 5.6] Comparison of source identification performance by the ES prediction of the power-law at the 9-month period via the two algorithms for various emission mixtures (w/ 28-day short-term data). ....	190

## LIST OF FIGURES

[Figure 1.1] Study scope and contents.....	4
[Figure 2.1] (a) Schematic diagram of a PTR-MS device. (b) PTR-MS system illustration (in BEESL/SU). .....	8
[Figure 2.2] An example of acceptability and context question. ....	27
[Figure 2.3] An example of a test chamber with a diffuser. . ....	28
[Figure 2.4] (a) Dry material emission characteristics and modeling. (b) For wet materials. ....	37
[Figure 2.5] (a) Concentration dynamics per VOC. (b) Concentration dynamics per material. ....	41
[Figure 2.6] Test example of signal separation. (a) Top, no noise. (b) Bottom, with 20% noise. .....	66
[Figure 3.1] Experimental setup.....	74
[Figure 3.2] Data analysis procedure exemplified for Linoleum. ....	83
[Figure 3.3] Emission signature of Linoleum. ....	85
[Figure 3.4] Consistency of PTR-MS emission signature exemplified for Linoleum over different sampling time. (a) Top, from the raw signals. (b) Bottom, from the filtered signals. ..	87
[Figure 3.5] Pattern of PTR-MS emission signature for Polyolefine over different sampling time. (a) Top, from the raw signals. (b) Bottom, from the filtered signals. ....	88
[Figure 3.6] Consistency of PTR-MS emission signature exemplified for Linoleum among different $Q_v/A$ . ....	89
[Figure 3.7] Emission signatures of the tested nine building materials by PTR-MS.....	89
[Figure 3.8] Correlation of the PTR-MS measurements with the acceptability for Linoleum. ....	90
[Figure 3.9] VOC concentrations in the chamber air from the GC/MS analysis results (Test #1). .....	92

[Figure 3.10] Odor index status of all measured VOCs in each material (The name of VOC for each spot displayed in each column can be found in order in Table 3.2 only for the major ones).....	97
[Figure 3.11] Correlation between acceptability and VOI.....	98
[Figure 3.12] Correlation between acceptability and VOC odor index (VOI) with Tokyo set used. ....	99
[Figure 3.13] The relationship between VOI and acceptability.....	101
[Figure 3.14] Signal trend of each ion mass for Linoleum over $\log(Q_v/A)$ .....	103
[Figure 3.15] Signal trend of each ion mass for Paint 2 over $\log(Q_v/A)$ . ....	104
[Figure 3.16] Trend of equilibrium emission factors of VOCs in each material over different area-specific ventilation rates. ....	106
[Figure 4.1] Experimental setup for source ID validation. ....	117
[Figure 4.2] Relative signal intensity factors ( $\alpha$ ) and variances ( $\varepsilon$ ) of the emission signatures for the nine building materials.....	128
[Figure 4.3] Monte-Carlo simulation results for 9-material mixture under various conditions...	132
[Figure 4.4] Optimal separation results of the measured emission signature for the Carpet/Linoleum mixture in the sense of MRLS. ....	135
[Figure 4.5] Optimal separation results of the measured emission signature for the five-material mixture ([3 6 7 8 9]) in the sense of MRLS. ....	136
[Figure 4.6] Comparison of the superposed and measured signatures for the two-material mixture ([7 8]). ....	137
[Figure 4.7] The measured signature intensity/profile change of the Linoleum-plus mixtures mainly due to adsorption effect as other materials were added to the mixture. ....	141
[Figure 5.1] Measurement schedule for constructing 9-month long-term emission signatures...	150
[Figure 5.2] PTR-MS raw emission signal vs. filtered signal patterns of the major ion masses for Linoleum. ....	153

[Figure 5.3] Emission patterns of major compounds from Linoleum during the initial 2 days...	154
[Figure 5.4] PTR-MS raw vs. filtered signal patterns of the major ion masses for Paint 2. ....	156
[Figure 5.5] Emission patterns of major compounds from Paint 2 during the initial 2 days. ....	156
[Figure 5.6] Stable emission signatures for Paint 2 after 7-month long-term emissions. ....	158
[Figure 5.7] Stable emission signatures for Carpet after 7-month long-term emissions.....	159
[Figure 5.8] Stable emission signatures for Linoleum after 7-month long-term emissions.....	160
[Figure 5.9] Stable emission signatures for Wood after 7-month long-term emissions. ....	161
[Figure 5.10] Unstable emission signatures for Gypsum at 7 & 8 months due to low SNR. ....	162
[Figure 5.11] Long-term emission fitting by the double-exponential model for major compounds of Linoleum.....	164
[Figure 5.12] Long-term emission fitting by the double-exponential model for several major compounds of Paint 2.....	165
[Figure 5.13] Long-term emission fitting by the power-law model for major compounds of Linoleum.....	168
[Figure 5.14] Long-term emission fitting by the power-law model for several major compounds of Paint 2.....	168
[Figure 5.15] Estimation of emission signatures exemplified by the Linoleum case using the double-exponential model at the time of 7 months (Long-term 2). ....	170
[Figure 5.16] Reconstructed emission signatures based on the estimation results at the time of 9 months.....	172
[Figure 5.17] Comparison of the emission profiles of the two different groups of measurements for selected ion masses of Linoleum.....	176
[Figure 5.18] Comparison of the emission profiles of the two different groups of measurements for selected ion masses of Paint 2. ....	178
[Figure 5.19] Prediction of the future concentrations at 7, 8 & 9 months by source models with short-term meas. exemplified with ethanol ( $m/z=47$ ) from Linoleum. ....	181

[Figure 5.20] Conc. predictions by the double-exp for selected compounds of Linoleum.....	181
[Figure 5.21] Conc. predictions by the power-law model for selected compounds of Linoleum. .....	182
[Figure 5.22] Prediction of the future concentration trends at 7, 8 & 9 months by source models with short-term measurements ( $\leq$ Day 28) exemplified with propanoic acid (with a small portion of ethanol, $m/z=75$ ) from Paint 2. ....	184
[Figure 5.23] Conc. predictions by the double-exp for selected compounds of Paint 2. ....	185
[Figure 5.24] Conc. predictions by the power-law model for selected compounds of Paint 2. ...	185
[Figure 5.25] Reconstructed emission signatures based on the prediction results at 9 months (w/ short-term data).....	188
[Figure 5.26] Prediction of the long-term emissions at 7, 8 & 9 months by a mechanistic diffusion model with short-term measurements ( $\leq$ Day 28).....	193
[Figure 7.1] Schematic diagram of a source detection/localization system for VOC emissions.	207

## Prologue

When I look back upon the past three years of my study and consider great findings hidden for a long time in nature He created, especially in the science of material emissions, I can not help confessing a song in praise of His greatness and majesty:

O Lord my God! When I in awesome wonder,  
 Consider all the works Thy hands have made.  
 I see the stars, I hear the rolling thunder,  
 Thy power throughout the universe displayed.

Then sings my soul, my Saviour God, to Thee;  
 How great Thou art, how great Thou art!

When Christ shall come with shouts of acclamation,  
 And take me home, what joy shall fill my heart!  
 Then I shall bow in humble adoration,  
 And there proclaim, my God, how great Thou art!

Refrain:

Then sings my soul, my Saviour God, to Thee;  
 How great Thou art, how great Thou art!  
 Then sings my soul, my Saviour God, to Thee;  
 How great Thou art, how great Thou art!

**“<sup>19</sup>since what may be known about God is plain to them, because God has made it plain to them. <sup>20</sup>For since the creation of the world God’s invisible qualities – his eternal power and divine nature – have been clearly seen, being understood from what has been made, so that people are without excuse.”**

(Romans 1:19, 20)



## ACKNOWLEDGEMENTS

### ***So very special thanks to:***

*My one and only Lord God: Father God, my Lord Jesus Christ and the Holy Spirit - The wonderful creator and wisest One with full of love for His children, who Himself started the present study by granting His insight on His little child, guided each step and finally completed the work powerfully in His time, granting a splendid victory to this little child of Him in this highly-competitive academic arena. Thank God, Amen.*

### ***Special thanks to:***

*Dr. Jensen Zhang, my dear advisor and professor - He was the best advisor and most considerate supporter I have ever met in my life, a great blessing of the Lord.*

### ***Thanks to:***

*I want to thank the Syracuse Center of Excellence for funding the present study;*

*My dear prayer partners – Mijung, lovely wife; Kwangjae, one and only brother; Eld. Sungduk and Keumduk, Eld. Jongwon and Hyunsoo, parents; Chooncha Nam, my aunt and sincere prayer supporter; Rev. Jee and Samonim. Soo Jee, best mentors in my life; Chanwoong and Sangrim, best friends; Yunhee, ultra super excellent general secretary; Dr. Kern Chang, servant of the HOP fellowship; Eunah, Soojin, Caroline, Vanessa, Tran Phuong, Hui, Jessie, Andrew, dear pals of HOP; Junghoon and Haeree, a cheerful and beautiful couple met in the Lord; Esq. Gloria Chung, my baksoo friend and nunim; Every member of the church's intercessory prayer team;*

*My dear labmates – Beverly; Zhiqiang and Jingjing Pei; Kevin; Jingjing Wang; Shewan; Korbaga; Dr. Zhi; Yixing; Zhigao; Meng;*

*Dear co-workers – Dr. Pawel Wargocki; Dr. Henrik Knudsen; Dr. Pramod Varshney; Dr. Hao Chen; Dr. Harish; Dr. Edward Bogucz; Dr. Mark Glauser.*

# † CHAPTER 1. INTRODUCTION

---

## 1.1 Problem Definition and Hypothesis

A large number of emission sources of Volatile Organic Compounds (VOCs) exist in indoor and outdoor environments that can adversely affect the indoor air quality (IAQ) which is vital to human health, comfort and productivity. When IAQ problems are reported, it is often difficult to determine where and what the source of pollution is because many factors affect the measured or perceived IAQ such as: the number of pollutants in the air, the inter-zonal airflow patterns, the existence of many emission materials and human activities in a building, the interaction between the indoor and outdoor environment, and the variation of the climate and pollution conditions.

Building materials and furnishings are major contributors to indoor VOC concentrations that impact IAQ. Over the past two decades, many research works have been conducted to determine the emission characteristics of these materials under laboratory conditions. Each material typically emits a series of compounds, and their emission rates decrease over a long period of time. As a result, the VOCs emitted from building materials are often detected, but the specific material sources cannot be identified and pinpointed. Source identification has been a challenging research topic in the area of indoor and

outdoor air quality, and solutions to this problem may lead to new approaches for source control and removal to improve IAQ. A first step toward a source identification would be to determine if a unique emission signature exists for each material or each type of material, and if the emission decay of individual VOCs and hence the variation in emission signature can be predicted. The fundamental hypotheses of the present study are: 1) each type of material has a unique emission signature defined by its emission compounds and emission rates; 2) the variation of the signature over time due to the emission rate decay of individual compounds can be modeled by emission source models. If these hypotheses are proven to be valid, with the additional information about the inter-zonal airflow pattern (e.g. determined by a tracer gas technique, which is out of the scope of this study), it is then possible to identify the emission sources of VOCs of concern in a complex indoor environment. This study is the first of its kind to develop a source identification method by using a near-real time measurement technique, Proton Transfer Reaction - Mass Spectrometry (PTR-MS).

## 1.2 Objectives and Scope of the Research

The ultimate goal of this study is to develop a novel methodology for identifying and locating emission sources of VOC in buildings based on multiple air samples and the emission signatures of individual types of materials used in buildings. This goal is achieved through the following three staged specific objectives:

- 1) **Stage 1:** Develop a method for determining the emission signatures of individual building materials by using PTR-MS, and to explore the correlations between the PTR-

MS measurements and the assessments of acceptability by human subjects. This has been accomplished by testing nine typical building materials that were previously studied using human subjects at two leading-edge institutions, DTU (Technical University of Denmark) and SBI (Danish Building Research Institute) in the area of the human exposure-response research to building material emissions as part of the collaboration between SU and DTU/SBI on indoor air quality research. Results obtained have confirmed that unique emission signatures exist for the same types of materials. A paper has been published in **Indoor Air Journal** (Han et al., 2010) for this work.

2) **Stage 2**: Develop and validate a methodology based on signal processing principles that can identify/recognize the emission signatures of individual materials from mixed signals due to simultaneous emissions from multiple materials present. This work deals with mathematical modeling and laboratory experiments with multiple (up to seven) as well as individual materials. The outcome of this task is a methodology and procedure to identify individual sources based on the measurements of a mixed air sample. A paper has been submitted to **Atmospheric Environment Journal** (Han et al., 2011) for this work.

3) **Stage 3**: Extend the application of the developed identification methodology by considering the long-term change of emission signatures of the studied building materials for enhancing the performance of source identification, and to provide a practical protocol for establishing a library of material emission signatures for future works. A paper has been submitted to **Indoor Air 2011 Conference** for this work (Han et al., 2011b).

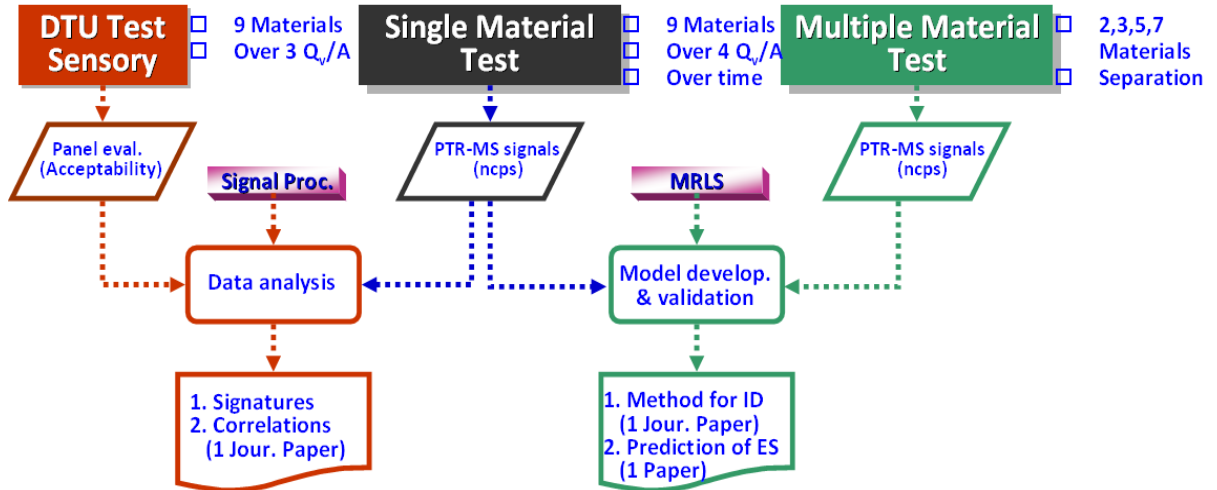


**Figure 1.1 Study scope and contents.**

In the present study (Figure 1.1), emissions from nine (9) common building materials, the same types previously studied by DTU and SBi to investigate the human exposure-response relationship in terms of acceptability, were first measured individually in a 50-liter small-scale chamber with specified airflow rates resulting in the similar pollution levels. Exhaust air was sampled by PTR-MS to determine emission signatures followed by sorbent tube sampling for identifying major VOCs emitted from each material and for comparing with the PTR-MS emission signatures. Because the subjective relationships have been established for these key building materials, the quantification and composition of VOCs in each material causing acceptability difference are discussed by use of PTR-MS and GC/MS analyses. In addition, the feasibility of emission signature separation by a novel and effective methodology of signal processing for identifying each emission signature under material mixture conditions and for determining VOC emission sources in indoor environments are challenged with the consideration of emission signature change over a long-term period. Finally, a practical testing schedule for establishing a

library of material emission signatures are presented as well as possible applications with the use of a complete database of PTR-MS emission signatures (Figure 1.1).

### 1.3 Outcomes

The results of the present study can be further used to develop methods for: 1) on-line material identification and detection, 2) VOC source detection in a field condition, and 3) deeper understanding of VOC behaviors in material mixtures and its impact on human health and perception. Results of this study have shown that unique emission patterns may indeed exist for different types of building materials. These patterns, or signatures, can be established by using PTR-MS. A correlation between the measurements from PTR-MS and the acceptability of air quality assessed by human subjects have also been established, so the PTR-MS measurements can provide a reliable and convenient way of assessing perceived indoor air quality.

In the following sections, previous research works related to the PTR-MS technology, VOC emission studies by use of analytical measuring devices and human subjects, and the development of VOC source identification are reviewed (Chapter 2) to find out knowledge gaps, research niches and possible applications in the areas of indoor air quality. The detailed procedures and results on the three stages of the present study are dealt with afterwards: 1) the determination of VOC emission signatures for building materials and their correlations with the acceptability assessments by human subjects (Chapter 3), 2) the development of a novel methodology for indoor VOC source identification (Chapter 4), and 3) the consideration of the emission signature change over

long-term emissions for the enhancement of the source identification (Chapter 5). Finally, the major concluding findings are summarized (Chapter 6) with some recommendations for future works and possible promising applications of this study (Chapter 7).

## † CHAPTER 2. LITERATURE REVIEW

---

Literature reviews are performed in the five major areas for the present study as follows:

- A novel analytical monitoring technology, PTR-MS and its related techniques/applications
- Past and on-going studies on human perceived indoor air quality
- Characteristics of building material emissions
- Chemical compositions and dynamics in indoor environments
- Potential techniques for source identification

The purpose of this chapter is to provide an overview of relevant methodologies and techniques, and to identify research needs.

### 2.1 PTR-MS Analysis Technology

#### 2.1.1 Fundamentals

W. Lindinger et al. (1998) and Taipale et al. (2008) described the principles of PTR-MS and its operating conditions in detail. Hence, only a brief description is provided in this section.



PTR-MS is based on the principle of measuring the ion products of proton transfer reaction between the compound to be measured and a reagent (Figure 2.1). As a reagent source, the hydronium ions ( $\text{H}_3\text{O}^+$ ) are generated from pure water vapor in a hollow cathode discharge. A controlled water vapor flow of 6.0 STP  $\text{cc}/\text{min}$  (STP stands for Standard conditions for Temperature of 293.15 K and Pressure of 1 atm by NIST's version) is continuously pumped into the reaction region via the source. The air to be analyzed is continuously pumped into a drift tube reactor, and a fraction of VOCs is ionized in proton-transfer reactions with hydronium ions ( $\text{H}_3\text{O}^+$ ) as a chemical reagent. At the end of the drift tube, the reagent and product ions are measured by a quadrupole mass spectrometer, and the signal of the product ion, the detected mass of which equals the VOC mass plus one, is proportional to the VOC concentration sampled (Figure 2.1).

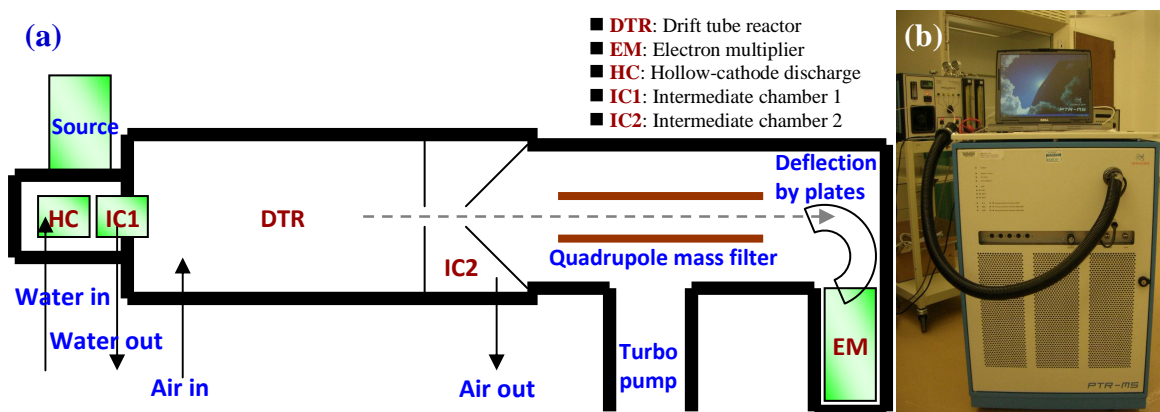


Figure 2.1 (a) Schematic diagram of a PTR-MS device. (b) PTR-MS system illustration (in BEESL/SU).

The hydronium ions are not reactive with some compounds having lower proton affinity (PA) than that of water (165.2  $\text{kcal}/\text{mol}$ ) such as CO, CO<sub>2</sub>, O<sub>3</sub>, NO, CH<sub>4</sub>, C<sub>2</sub>H<sub>2</sub> and etc., but does react with most of organic compounds of interest in a non-destructive proton transfer reaction shown as the following:



where  $R$  represents a target organic compound in the drift tube,  $H_3O^+$  is a primary hydronium ion,  $RH^+$  is a product ion, and  $k$  is the proton transfer reaction rate constant.

In the quadrupole mass spectrometer, the ions are mass-selected and counted with an electron multiplier. The chemical reaction rate occurring in a closed system under constant volume conditions can be expressed as follows:

$$r = -\frac{d[H_3O^+]}{dt} = \frac{d[RH^+]}{dt} = k \cdot [H_3O^+] \cdot [R] \quad (2.2)$$

where [ ] indicates the number density of trace species or the concentration.

Assuming the first-order reaction conditions (in other words, the pseudo first-order approximation is valid due to  $[R] \gg [H_3O^+]$  keeping a constant value of  $[R]$  within the short reaction time for most of the general applications), the concentration of  $[H_3O^+]$  can be calculated by setting  $k[R]$  as a constant:

$$[H_3O^+] = [H_3O^+]_0 \cdot \exp(-k \cdot [R] \cdot t) \quad (2.3)$$

Then, the number density of a trace compound in the drift tube,  $[R]$ , can be obtained by the following:

$$[RH^+] = [H_3O^+]_0 \cdot (1 - e^{-k[R]t}) \cong [H_3O^+]_0 \cdot k \cdot [R] \cdot t \quad (2.4)$$

$$[R] = \frac{1}{kt} \cdot \frac{[RH^+]}{[H_3O^+]_0} \quad (2.5)$$

where  $t$  is the drift time of the primary hydronium ions in the reaction region.

As the ion count rates measured at the device (counts per second, *cps*) are proportional to the respective densities of the ions, the densities can be substituted with the measured count rates, and the volume mixing ratios of the target compounds in *ppbv* can be calculated by the following equation:

$$[R]_{ppbv} = \frac{[R]}{[air]} \times 10^9 = \frac{1}{const \cdot kt} \cdot \frac{(RH^+)_{count}}{(H_3O^+)_{count}} \cdot \frac{Tr_{H_3O^+}}{Tr_{RH^+}} \quad (2.6)$$

where *const* is a constant value determined by the temperature and pressure conditions of the reference air,  $( )_{count}$  indicates the measured count rates of the ions, and *Tr* represents the instrument specific relative transmission efficiency of the ions, whose value ranges from zero to one, and is mainly mass-dependent but vary also over time (de Gouw et al., 2003; Steinbacher et al, 2004).

The transmission efficiencies can be found from transmission curves. In this way, from the well-defined conditions in the reaction region, the volume mixing ratios of trace-level VOCs can be calculated by use of gas standards without any further calibration. For more accurate measurements, sensitivity calibration for a target compound can be performed. In this dissertation, the count rates of the product ions (*cps*) were normalized by per million hydronium ion ( $H_3O^+$ ) count rates to compensate the variations in the hydronium ions as other researchers in this area usually do (e.g. de Gouw and Warneke, 2007; Jobson

et al., 2005; Whyte et al., 2007). This normalized ion count rates (*ncps*) becomes directly proportional to the concentration level of a target VOC.

In order to get VOC volume mixing ratios, another method can be utilized based on calibrating the sensitivity factors of the device (*ppbv/ncps*) with gas standards. However, because the device tries to measure a large number of different compounds for which gas standards may not be available at all times, the use of Eq. (2.6) for determining the VOC concentrations is still required.

## **2.1.2 Other techniques that can be integrated with PTR-MS**

### **2.1.2.1 GC/MS**

Gas Chromatography / Mass Spectrometry (GC/MS) is an analysis method by means of integrating the features of gas/liquid chromatography and mass spectrometry together for identifying different species taken in a test sample. The use of a mass spectrometer as a detector in gas chromatography was traced back to the late 1950s developed by R. Gohlke (1959). At that time, this sensitive instrument was huge, fragile and initially limited to laboratory settings only. The development of personalized and small-sized computers has motivated the simplification of the use of this tool, with great improvements in the processing time of a sample. In 1996, a state-of-art high-speed GC/MS unit succeeded in accomplishing the analysis of fire accelerants in less than 90 seconds, whereas the first generation of GC/MS would have required at least 16 minutes. These improvements in GC/MS technology have stimulated its widespread adoption in a number of areas.

Applications of GC/MS include drug detection, fire investigation, environmental analysis, identification of unknown samples and investigation of explosives. GC/MS can also be utilized in airport security to detect any dangerous compounds in luggage or on human bodies. In addition, it can identify trace species in materials that were previously thought to be beyond identification. Especially, GC/MS has been widely used as a gold standard for forensic investigation because this instrument can be used to perform a specific test. A specific test positively identifies the actual presence of a particular element in a given sample, whereas a non-specific test can indicate only that a particular sample falls into a category of some elements.

GC/MS consists of two major components: gas chromatograph and mass spectrometer. The gas chromatograph utilizes a capillary column mostly depending on the column's dimensions (length, diameter and film thickness) as well as phase properties. The difference in the chemical properties among different compounds in a mixture will separate each compound as the sample travels the length of the column. Each compound takes a different amount of time, called retention time ( $RT$ ), to elute from the gas chromatograph, allowing the downstream mass spectrometer to capture, ionize, accelerate, deflect and detect the ionized molecules separately. The mass spectrometer performs this task by breaking each compound into ionized fragments and detecting these fragments in terms of their mass to charge ratio ( $m/z$ ).

These two components, when utilized together, allow a much finer degree of compound identification than when either unit is used separately. Actually, it is impossible to make an accurate identification of a particular compound by either of gas chromatography or

mass spectrometry alone because there is ambiguousness in retention time and pattern of ionized fragments in a mass spectrum for some compounds. Combining the two processes together makes the possibility extremely unlikely that two different compounds behave in the same way from both a gas chromatographic point of view and a mass spectrometric point of view (de Gouw et al., 2003; de Gouw and Warneke, 2007; Warneke et al., 2003).

This GC/MS technique can be integrated with PTR-MS to solve the specificity issue of PTR-MS indentifying and relating each ion mass detected from PTR-MS to possible specific compounds (e.g. VOCs).

#### **2.1.2.2 GC-PTR-MS**

As mentioned in short from the introduction, though PTR-MS allows numerous VOCs of interest in air to be monitored and measured with a high sensitivity and rapid response time, only the masses of ionized VOCs and their fragments (if any) can be detected, which means it is not a unique indicator of the VOC identity. To resolve this ambiguous issue on the VOC identity, the specificity of PTR-MS has been studied by coupling a gas chromatographic column to the device (GC-PTR-MS). The column separates VOCs in a sample prior to the injection into PTR-MS, allowing the different VOCs detected at the same mass to be separated at the cost of the rapid response time of PTR-MS. Overall, this combined technique is a highly valuable tool for studying the specificity of PTR-MS for individual samples. Karl et al. (2001) introduced this method, and it was further improved in laboratory conditions to determine the specificity of PTR-MS measurements from urban air by de Gouw and Warneke (2007) and Warneke et al. (2003). It was

demonstrated that the ions associated with methanol, acetonitrile, acetaldehyde, acetone, benzene, toluene and higher aromatic VOCs were free from significant interference (Warneke et al., 2003). A quantitative inter-comparison between PTR-MS and GC-PTR-MS measurements of target VOCs was performed and showed that they were accurately measured by PTR-MS.

The GC-PTR-MS analysis is highly valuable in determining which species contribute to the signal at a certain mass. Until now, GC-PTR-MS has been used to analyze certain types of biogenic emissions (Karl et al. 2001) and urban air (de Gouw and Warneke, 2007; Warneke et al., 2003). It will be meaningful that further work can be done to investigate the specificity of PTR-MS in other areas.

### 2.1.3 On-going applications using PTR-MS

The analytical tools traditionally used in environmental research and industry areas for analyzing related VOCs and its effects are Gas Chromatography (GC), High Pressure Liquid Chromatography (HPLC), Isotopic Ratio Mass Spectrometry (IRMS), sensory assessments and several non-destructive/direct techniques such as electronic tongues and noses, Nuclear Magnetic Resonance (NMR) spectroscopy and Atmospheric Pressure Chemical Ionization (APCI) (Boscaini et al., 2004). These techniques can be used in a highly selective and reliable way, but the major disadvantages in the use of them include expensive instrumentation, experienced operators required, not-readiness of fully automated test operation, off-line operation, time-consuming sample preparation and etc. Meanwhile, one of the non-destructive and direct analysis tools, PTR-MS, has revealed its far-beyond merits compared with other techniques aforementioned in the recent few years, including compact/robust experimental setup, easy operation, low fragmentation in the ionization process compared with electron impact ionization, no sample preparation necessary, outstanding low detection limit (10-100 *pptv*), real-time measurement and monitoring (Usually, the response time is less than 100 *ms*), real-time quantification of absolute concentrations possible without any previously direct calibration measurements, but losing some information of chemical details. By utilizing the strong advantages mentioned above, the following seven (7) areas are establishing the major on-going trend of the applications of this new technique, PTR-MS.



### 2.1.3.1 Atmospheric research

By utilizing the merit of PTR-MS enabling real-time measurements of VOCs in different regions of the atmosphere, de Gouw and Warneke (2007) expanded the use of PTR-MS in atmospheric research, aiming to establish a firm foundation for this area in using this device with the coupling of a gas chromatographic interface in order to solve the specificity issue of PTR-MS and to enhance the accuracy of the device for many VOCs of atmospheric interest. Some highlights of airborne measurements by PTR-MS in a global scale were presented including the results obtained in fresh and aged forest-fire and urban plumes. After an extensive scale of examination about this device, they concluded that PTR-MS had become a useful tool for atmospheric research because 1) it could give a chemical fingerprint of the origin and history of an air mass, 2) air masses impacted by forest-fire, urban, marine and vegetation emissions could be readily distinguished from another, and 3) the degree of photochemical processing could be inferred from the data. In addition, they added one more important mention that this kind of information had proven to be useful in many studies other than those aimed specifically at VOCs.

### 2.1.3.2 Automotive engineering

Jobson et al. (2005) used PTR-MS to measure VOC concentrations on-line in diesel engine exhaust as a function of engine load. The purpose of the study was to evaluate the device as an analytical tool for the abatement study of diesel engine emissions. Measured sensitivities determined from gas standards were found to agree well with calculated sensitivities for non-polar species. The diesel exhaust mass spectra were complex, but displayed a pattern of strong ion signals at  $14n+1$  ( $n = 3, 4, 5, 6, 7, 8$ ) masses with a

relative ion abundance similar to those obtained from electron impact ionization of alkanes. As a conclusion, they wrote down their impression on this device, saying on-line analysis of diesel exhaust using this technology may be a valuable tool for diesel engine emission research.

### 2.1.3.3 Food and flavor research/industry

PTR-MS has been used in this area to classify different kinds of food products by utilizing the analysis of PTR-MS volatile profiles: 1) different types of Gana Cheeses concerning the original place, 2) different types of Mozzarella with regard to raw material and production process, 3) different types of juices based on pasteurization treatment, 4) different types of wine depending on its variety and 5) different types of strawberries based on cultivars.

Granitto et al. (2007) coupled PTR-MS's direct injection and fast analysis merits with data mining techniques in order to extract a reliable and fast way for the automatic characterization of agro-industrial products. They tested the validity of this approach to identify several samples of strawberry cultivars by measuring the signals from single intact fruits collected over 3 years and harvested in different locations. Three data mining techniques were applied to the full PTR-MS spectra without any preliminary projection or feature selection. After all, they succeeded in demonstrating that strawberry cultivars could be identified by the PTR-MS rapid non-destructive measurements of single fruits.

Another significant example of the identification/detection application of PTR-MS in this area was done by C. Lindinger et al. (2008). They developed a robust and reproducible

model to predict sensory profiles of different types of espresso coffee from instrumental headspace data. The model was derived from 11 different espresso coffees and validated using 8 additional espressos. The input of the model consisted of 1) sensory profiles from a trained panel and 2) on-line PTR-MS data. The experimental PTR-MS conditions were designed to simulate those for the sensory evaluations. Sixteen (16) characteristic ion traces in the headspace were quantified by PTR-MS, requiring only 2 min of headspace measurements per espresso. The correlation was based on the knowledge-based standardization and normalization of both datasets, selectively extracting the differences in the quality of the samples, while reducing the impact of variations on the overall intensity of coffees. Their work represents a significant progress in the sense of the correlation extraction between sensory evaluations and PTR-MS instrumental measurements.

Besides the above examples, Van Ruth et al. (2007) evaluated this tool for the classification of milk fats (butters and butter oils) in terms of quality and authentication issues. Three different analysis methods were employed and compared together: PTR-MS analysis, sensory analysis and classical chemical analysis. After this examination, they concluded that their suggested combination method with PTR-MS seemed to be a promising approach with potential applications in quality control and regulation control.

#### 2.1.3.4 Forensic investigation

Instead of using the current techniques for the forensic analysis of fire debris to detect the presence of arson accelerants normally accomplished by use of off-line sampling with the collection of accelerant vapors on activated charcoal strips and further pre-chemistry prior to the analysis, Whyte et al. (2007), by using PTR-MS, tried an alternative method for the direct detection of arson accelerants requiring no sample pre-treatment. VOC fingerprints of given fire accelerants from PTR-MS were collected by the simple headspace analysis of accelerant burned materials. Using a set of four most common arson accelerants and four common household building materials, they successfully demonstrated that characteristic VOC fingerprints could provide satisfactory identification of the accelerants used to burn each material.

#### 2.1.3.5 Environmental science and technology

As an example of the power of on-line monitoring capability of PTR-MS, Filella and Penuelas (2006) studies the daily, weekly and seasonal patterns and possible origins of air concentrations of VOCs by using PTR-MS measurements taken on a minute-by-minute basis in the vicinity of a highway in a semi-urban site near Barcelona. Their results showed that diurnal, weekly, and seasonal fluctuations in measured VOC concentrations depended on variations in the strength of sources, as well as on photochemical activity and meteorological conditions. All of their data provides useful information on the dynamics of VOCs in an area where ozone levels in summer exceed quite often the standard protection thresholds.

### 2.1.3.6 Medical research

Wehinger et al. (2007) investigated the diagnostic usefulness of PTR-MS for detecting primary lung cancer through the analysis of VOCS in exhaled human breath. They chose this device as their analysis tool because, unlike gas chromatographic analyses, PTR-MS could be used without time-consuming preparation and pre-concentration of gas samples. Exhaled breath samples from patients with primary lung cancer (n=17) were analyzed and compared with both an overall control collective (controls total, n=170) and three sub-collectives: hospital personnel (controls hospital, n=35), age-matched persons (controls age, n=25) and smokers (controls s, n=60), respectively. The leading product ions at  $m/z = 31$  (protonated formaldehyde) and  $m/z = 43$  (a fragment of protonated isopropanol) were found with significantly higher concentrations in the breath gases of the primary lung cancer patients as compared to the healthy controls, suggesting that the two VOCs identified could be the best determinants between the exhaled breath of primary lung cancer cases and the healthy controls. As a conclusion, they foretold that PTR-MS might become a new valuable tool for diagnosing primary lung cancer because simple and time-saving breath gas analysis by PTR-MS could be possible even for a larger scale of clinical evaluations.

### 2.1.3.7 Indoor air quality related

Bunge et al. (2008) attempted an analysis method for VOCs from microbial cultures by using PTR-MS. A newly developed sampling system was coupled with a PTR-MS instrument to allow on-line monitoring of VOCs in the dynamic headspaces of microbial cultures. Headspace VOCs in sampling bottles containing actively growing cultures and un-inoculated culture medium controls were sequentially analyzed by PTR-MS, which led to the detection of characteristic marker ions for certain microbial cultures, demonstrating the potential of this method to differentiate between even closely related microorganisms. Although temporal profiles of some VOCs were similar to growth dynamics of microbial cultures, most VOCs showed different temporal profiles, characterized by constant or decreasing VOC levels or by single or multiple peaks over 24-hour of incubation. Their findings strongly indicated that the temporal evolution of VOC emissions during growth should be considered if characterization or differentiation based on microbial VOC emissions is attempted. They established an analysis method of VOCs by on-line PTR-MS as a routine method in microbiology and as a tool for monitoring environmental and biotechnological processes.

The above illustrations of PTR-MS applications have been utilizing the merits of this device mostly in terms of its on-line monitoring, practical/handy identification and detection of VOCs. Especially as for source/quality identification, several researchers have tried to use PTR-MS, as aforementioned, in extracting a VOC composition profile specific to a given material so called as material signature. However, most of them have been focused on the identification of each single source one by one, transforming key ion masses measured from PTR-MS onto an indirect/implicit domain by using several feature

extraction methods such as data mining techniques, PCA (Principal Component Analysis) and PLS-DA (Partial Least Square-Discriminant Analysis).

For instance, Whyte et al. (2007) applied this PTR-MS technique to detect the presence of arson accelerants in arson sample candidates as an on-line simple sampling and rapid detection method, instead of other classical methods using off-line sampling. In the process of this identification, they used a method of PCA for their analyses. As a closing mention, they suggested that it was possible that all of the recorded fingerprints (i.e. VOC mass profiles) could be collated into a database, so that this database could be used for comparison against other external and blind samples, and that additional work using multiple sources of accelerant and material would be required to enhance its application. More specific investigation on the potential of PTR-MS applications in source/quality identification was performed by Van Ruth et al. (2007). They observed the potential of PTR-MS as a tool for classification of milk fats by dealing with the quality (Good or Poor) and authentication issues (Matrix: Butter or Butter Oil) of treated milk fat samples. In order to investigate the effect of the treatments: heat and off-flavoring, they employed PTR-MS analysis, sensory analysis and classical chemical analysis, and compared each result to the PTR-MS identification method implemented by using PCA and PLS-DA. 84% of the 37 samples in total were successfully classified into butter and butter oil matrix groups, and 89% of the samples were correctly classified in terms of sensory quality (good/poor sensory quality).

As indentified from the above literature review, the material identification from multiple sources by using PTR-MS measurements itself without any implicit data transformation

or pre-conception can be a good research topic enhancing its scope of applications, because a novel signal separation technique can be entrained to raw measurement signals. This is one of the research niches identified.

In addition, during the last several decades, many attempts have been made to explain human complains on perceived indoor air quality and its relevance to symptoms related to buildings, human performance and its associated usage of energy on the basis of physiological effects of chemical polluting compounds such as VOCs. However, those researches have not been satisfactory or successful. Due to the lack of proper techniques and methods in determining the quantification and composition of VOCs affecting human sensory response, indoor air quality researches on the human exposure-response relationships to VOC emissions have been done mostly by human sensory assessments. As suggested by Wolkoff and Nielsen (2001), it would be a better approach in evaluating VOC impacts on perceived air quality to consider the compound-by-compound effects rather than from a total VOC point of view. In this regard, this new technique, PTR-MS, can be integrated in human sensory research on perceived indoor air quality, trying to reveal the correlations of sensory response results to its quantification and composition of VOCs in materials used in the sensory tests. As indicated by other researchers foretelling the powerful potential of this device, the extraction of the correlations between sensory analysis and VOC quantity/composition analysis would be very significant task, which was identified as a niche in this area of indoor air quality research and is tried in this study as a brilliant subject required to be researched.



## 2.2 Studies on Human Perceived Air Quality

### 2.2.1 Methods of experimental sensory assessment studies

#### 2.2.1.1 Study trend

Evidence from many building investigations and systematic studies suggested that among several sources of indoor pollution, VOC emissions from building materials either as structural materials or as furnishings could be considered the major contributor of the pollution typically encountered indoors, due to its complex chemical composition, large surface area and permanent exposure to indoor air (Haghighat and Donnini, 1993). Moreover, these VOC emissions are supposed to be perceived by workers or residents in a building usually as odors (Fang et al., 2008). A lot of experimental studies using both sensory and chemical measurements have been tried to demonstrate that emissions from building materials depend on air velocity (Haghighat and Zhang, 1999; Iwashita and Kimura, 1994; Zhang and Haghighat, 1997), humidity (Berglund and Cains, 1989; Bluysen et al., 1996; Fang et al., 1996; Haghighat and DeBellis, 1998; Reinikainen, 1993), surface treatments, temperature, time after manufacture, transformations on surfaces, ventilation rate (Gunnarsen et al., 1993) and pollution adsorbed on building materials from other activities (Wolkoff et al., 1991).

Among these studies, Knudsen et al. (1998) developed a novel experimental procedure for sensory assessments (which is described in the following section) for determining the human exposure-response relationships for building materials. Using this procedure, they established several exposure-response curves for eight materials, observing that for some

materials, the exposure-response relationship was rather flat, and that the effect of increased ventilation for those materials would be limited. Their final conclusion was that source control by using low polluting materials could be often the most practical way to improve indoor air quality. And then, Knudsen et al. (1999) investigated the impact of mixing the emissions from building materials on perceived indoor air quality. They placed three materials in three chambers and then mixed the exhausts from these chambers into a fourth chamber. This experiment was performed to exclusively investigate human perception on pollutant mixture from different building materials, meaning that the interaction among materials was ignored. So, this approach could overestimate the level of human sensory response because in a field condition, the assessment of perceived air quality would be affected by the interaction among building materials.

In practice, a number of different materials are used to build and furnish a building, and there is interaction between materials and their emissions. In this regard, Haghghat et al. (2001) investigated from a series of experiments the impact of HVAC system operation and the combination of building materials on perceived indoor air quality, by employing a similar concept and method for human sensory tests in terms of acceptability and odor intensity. Experiments were performed in test chambers to establish human exposure-response relationships for three building materials, and in office buildings as well. They assumed that the systematic quantification and assessment on the impact of the emissions from building materials on perceived air quality is possible at different varying concentration levels, resulting in a human exposure-response relationship.

The scope and quality of the human sensory study started to be extended by conflating chemical evaluations using GC/MS from Knudsen et al. (1999) and using GC-O/MS in other following studies. From then on, researchers tried to explain the causes and the differences of their sensory assessments by using VOC chemical data.

As the use of low-polluting materials as a means of indoor pollution source control on perceived air quality was known to be more effective than other methods such as ventilation control or air-cleaning techniques, a well controlled study considering psychological/physical/physiological factors with several different building materials was performed in small-scale chambers and also under realistic full-scale conditions by Wargocki and Knudsen (2007). The main objective of their study was to investigate the potential of reducing the energy used for building ventilation by using low-polluting building materials without compromising indoor air quality. To quantify this potential, the exposure-response relationships were established for rooms furnished with different categories of polluting building materials, and the energy used for the ventilation was calculated by simulation. The exposure-response relationships were based on a summary of data reported by Knudsen et al. (2006) for materials tested with laboratory settings in small-scale glass chambers and in full-scale climate chambers, test rooms or normal offices. New experiments were also performed to examine the effect of using low-polluting materials on perceived air quality in terms of acceptability. The experiments were conducted in test rooms ventilated with different rates of outdoor supply air. The low-polluting materials were selected by utilizing small-scale glass chamber tests. The results suggested that the exposure-response relationships could vary among different building materials and that the perceived air quality could be improved considerably

when polluting building materials were replaced with low-polluting substitutes. The preliminary energy simulations also indicated that the selection of low-polluting materials would result in considerable energy savings as a result of reducing the ventilation requirements to achieve acceptable indoor air quality.

Although the human exposure-response relationships between acceptability of air quality and ventilation rate have been fully established for these key building materials in a subjective sense, the quantification and composition of VOCs in each material causing the human acceptability difference were not quite revealed. Challenging this issue using a new technology such as the combined analyses of PTR-MS and GC/MS will be a good research topic, leading to a significant progress in indoor air quality research.

#### 2.2.1.2 Acceptability of indoor air quality

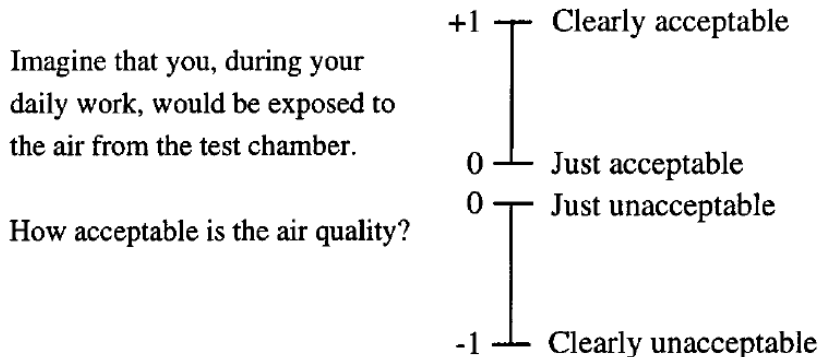


**Figure 2.2** An example of acceptability and context question (Wargocki et al., 2007).

As a means of sensory assessments, an index with a continuous scale from -1 to +1 named as acceptability was developed by Gunnarsen and Fanger (1992) and modified by Knudsen et al. (1998), coded as follows: Clearly not acceptable = -1, Just not acceptable/Just acceptable = 0, Clearly acceptable = 1 as shown in [Figure 2.2](#). The

acceptability of air quality is assessed by an untrained human panel with the following question: “Imagine that you, during your daily work, would be exposed to the air in this diffuser. How acceptable is the air quality?” The assessments are usually performed following a random order among established test chambers. In order to minimize the effect of human sensory adaptation, at least several minutes break should be taken between each assessment. Knudsen et al. (1998) provides a full description of the acceptability.

### 2.2.1.3 Experimental design

Knudsen et al. (1998) suggested a novel experimental procedure for a human sensory assessment concerning the effects of building materials. The followings are based on their test procedure.

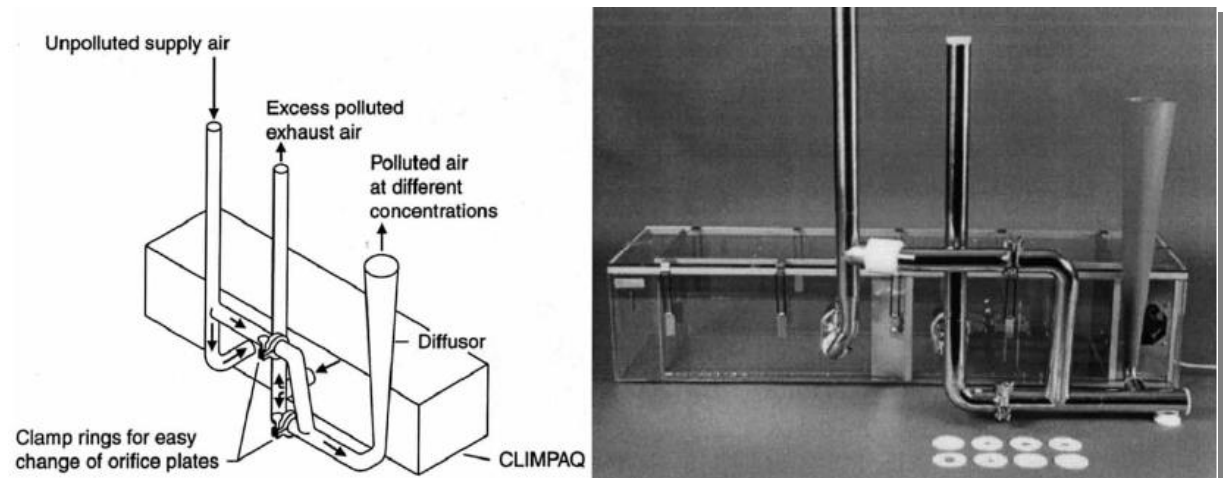


**Figure 2.3** An example of a test chamber with a diffuser (with permission from Knudsen, 1998).

Usually, an air-dilution system is designed to provide different concentrations of polluted air for sensory assessments. The system is connected to the exhaust of a small-scale test chamber (**Figure 2.3**). Material samples are placed in test chambers each connected to a

dilution system. The sizes of material samples are selected so that the area-specific ventilation rates in the test chamber correspond to the area-specific ventilation rate in a typical room. A sensory panel assesses the immediate acceptability and odor intensity of polluted air at different concentration levels for each building material. Sample collection, test specimen preparation, specimen conditioning and handling for the sensory tests are in accordance with the “Protocol for testing of building materials” (Clausen et al., 1995) developed in the research program “European Data Base on Indoor Air Pollution Sources in Buildings” (Clausen et al., 1996).

### *Sensory Panel*

A sensory panel consisting of around 40 to 50 untrained subjects performs the sensory assessments. The subjects are recruited in the neighborhood taking a set of consecutive tests to document their normal sense of smell. The tests consist of two parts to estimate their smell abilities: 1) to discriminate among odorous substances (matching test), and 2) to rank different odor intensities of the same odorous substance (ranking test). The leader of the experiment assesses and documents each subject’s attitude and motivation concerning the experiment and the subject’s personal hygiene. Those passing the tests satisfactorily become a part of the sensory panel. The following distributions should be considered: male/female, age (young/old) and smokers/non-smokers. These person-related data are collected via a questionnaire to be filled in by the subjects upon recruitment. The subjects receive written and oral instructions concerning sensory assessments.

### *Procedure*

On each day of the experiment, the panel is divided into four to five groups of approximately 10 persons. Each group finishes the assessments within a 2-hour period. The subjects stay in a hall outside the test room, which is used as a waiting room between assessments called antechamber. Before doing the assessments in the main chamber, the subjects wait for at least three (3) minutes in the antechamber between assessments to minimize the effect of human sensory adaptation. This procedure is conducted to adapt the panel members to the general background air delivered to the small-scale chambers and the full-scale chambers. Then, the subjects enter the main test room and assessed the immediate acceptability of air exhausted from one diffuser and marked their assessments on acceptability scale and odor intensity exemplified in **Figure 2.2**. Before doing the assessments, the panel is to be instructed on how to use the scale. During this instruction, it should be emphasized that they are not allowed to mark between just acceptable and just unacceptable. Rather, they are requested to decide on whether the air is acceptable or unacceptable, and then to rate the degree of acceptability and odor intensity. They are also to be instructed on how to use the exposure equipment.

The first day of experiments is a practice session day, but this is not communicated with the subjects. The assessments collected during this day are to be discarded. Sensory measurements may be made for several consecutive weeks to obtain a reasonable mean value of the sensory assessment for each test. Exposures are randomly assigned to the subjects in a random order. The subjects enter the test room one by one at a time. Pollution sources are hidden to the subjects by a special cabinet, so that the exposure conditions are not revealed to them. The assessments in the test room are made

immediately upon reaching a marked spot on the floor in the middle of the room, by marking on the continuous acceptability scale and odor intensity printed on the paper. This procedure is used to standardize the test position and the approximate time spent prior to the assessments of indoor air quality. The assessments are made upon taking one inhalation of polluted air exhausted from one diffuser. The doors to the test room are to be closed during assessments. A break of at least three minutes is taken between assessments in a well-ventilated antechamber for the next assessment.



## 2.2.2 Quantification and composition studies of VOCs using other analyses

### 2.2.2.1 with GC/MS

Knudsen et al. (1999) studied over a period of 50 days the emissions from five commonly used building materials in small-scale test chambers having a diffuser for sensory assessments, similar to that shown in **Figure 2.3**. Odor intensities and concentration levels of selected VOCs of interest for indoor air quality were assessed and measured, respectively. By using GC/MS, they performed a screening of VOCs emitted from each building material prior to sensory assessments. The measurements were done 2 days after the placement of the building materials. About 30 different VOCs were identified from each building material. For each building material, several VOCs of interest were selected on the basis of low odor threshold, abundance and persistence, assuming that VOCs with low odor thresholds might have an impact on perceived air quality. The impacts of VOC concentrations in air and of air velocity over building materials on the odor intensities and emission rates of the VOCs of concern were studied.

By using GC/MS the selection of the effectual VOCs and these VOCs' quantity analysis could be integrated with the results of sensory assessments through this study, providing a more firm foundation for validating a proposed hypothesis on the impacts of VOC emissions. Still, the extensive preparation time and cost required to track each VOC's concentrations are the burden of this method to be improved.

### 2.2.2.2 with GC-O/MS

Knudsen et al. (2007) investigated how perceived indoor air quality could be influenced by emissions from building materials with linseed oil compared with similar conventional synthetic substitutes without linseed oil. The emissions from two types of materials had been monitored over one year in small ventilated test chambers. The odorous emissions were evaluated by sensory panel assessments of odor intensity and acceptability, and by chemical analysis of odor-active VOCs and carbonyl compounds using GC/MS combined with olfactometry (GC-O/MS). The results of the GC-O/MS investigations and VOC measurements indicated that almost constant emissions of odor-active VOCs with low odor thresholds resulted in the persistency of odors. They demonstrated that the acceptability for the emission from floor oil was influenced by linseed oil used as a raw element, suggesting that systematic use of less odorous linseed oils might improve the acceptability for emissions from building materials with linseed oils. As a closing mention, they concluded that the combination of sensory assessments of perceived air quality and GC-O/MS seemed to be a useful approach in the effort to eliminate unwanted odors from building materials.

GC-O/MS opened a new way for the research of VOC emissions, but still has the same drawbacks as those of GC/MS. However, this method caught the importance of odors in perceived air quality researches.

### 2.2.3 Integrated study cases using PTR-MS with sensory assessments

Fang et al. (2008) conducted two experiments to investigate the use of the co-sorption effect of a desiccant wheel for improving indoor air quality. One experiment was conducted in a climate chamber to investigate the co-sorption effect of a desiccant wheel on the chemical removal of indoor air pollutants; another experiment was conducted in an office room to investigate the resulting effect on perceived air quality. A dehumidifier with a silica-gel desiccant wheel was installed in the ventilation system of the test chamber and office room to treat the recirculation airflow. Human subjects, flooring materials and four pure chemicals (formaldehyde, ethanol, toluene and 1,2-dichloroethane) were used as air pollution sources. PTR-MS and sensory assessments were used to characterize the effectiveness of chemical and sensory pollution removal of the desiccant wheel. The experiments revealed that all the measured VOCs were removed effectively by the desiccant wheel with an average efficiency of 94% or higher; more than 80% of the sensory pollution load was removed and the percentage dissatisfied with the air quality decreased from 70% to 20%, concluding that the incorporation of a regenerative desiccant wheel in a ventilation system is an efficient way of removing indoor VOCs.

Instead of revealing the quantification and interaction of VOCs in a polluted space, this study monitored the reduction effect of a new air-cleaning technique by using the ability of PTR-MS for on-line monitoring of emitted VOCs. In addition, only several target VOCs were traced, leaving a large space of other VOCs' important contributions on perceived air quality.

In this regard, this dissertation study tries to apply this new technique, PTR-MS, opening a new gate to the areas of indoor air quality assessment and VOC identification/detection, particularly using it as a tool for determining VOC emission signatures of building materials and furnishings.

### **2.3 Material Emission Characteristics**

Although the emission signatures by PTR-MS might have been established at a certain representative time, due to the time decay of VOC emission rates and changing indoor emission dynamics, the shape of each emission signature could change over a long period of time and over different ventilation scenarios. To extend the applicability of the emission signature technique to be developed from this study, these aspects affecting VOC emission signatures should be considered, so that the probable emission signatures at a later different time can be predicted based on the information contained in the established database of material emission signatures by PTR-MS. The following two sections (2.3.1 & 2.3.2) will deal with these aspects by reviewing the related literature.

Chemicals present in indoor air can affect indoor air quality in buildings. Building materials may be significant sources of chemicals found in indoor environments. Due to this aspect, the material emission characteristics are considered important and found to have different trends significantly according to dry materials and wet materials. To address indoor air quality claims resulting from the emissions of various building materials, a Consortium-supported project on Material Emission and Indoor Air Quality Modeling (CMEIAQ) was initiated in April, 1996 at the Institute for Research in

Construction, National Research Council of Canada (NRC/IRC). One report among its several tasks deals with how to measure VOC emissions from typical building materials using chamber test methods developed by CMEIAQ. Two small chamber test methods have been developed by the CMEIAQ project. CMEIAQ Final Report 1.2 describes a test method using small-scale chambers for VOC emissions from dry building materials, and CMEIAQ Final Report 1.3 deals with a test method using small-scale chambers for measuring VOC emissions from wet building materials. In addition, chemical analysis procedures for chamber methods are reported in CMEIAQ Final Report 1.1. Using the test methods described in the CMEIAQ Final Reports 1.2 and 1.3, forty-eight (48) typical building materials after extensive considerations on the selection of typical and commonly used building materials for testing were tested for VOC emissions using small-scale dynamic chambers. 30 of these were dry materials (e.g. acoustic tile, carpet, gypsum wallboard, oriented strandboard, particleboard, plywood, solid wood, vinyl flooring and underpad), and 18 were wet materials (e.g. adhesive, caulking/sealant, floor wax, paint, polyurethane and wood stain).

For dry materials, only the power-law part of the segmented model was used to describe the emission characteristics over time between 24 and 100 hours of the dynamic chamber tests.

For wet materials, coefficients were calculated to fit a general empirical “Segmented VB + Power-law” model to the experimental TVOC and selected VOC data.

### 2.3.1 Dry materials

VOC emissions from dry building materials between 24 and 100 hours of a dynamic chamber test may be characterized by a single power-law equation (Eq. 2.7) using the following steps:

$$E(t) = a \times t^{-b} \quad (2.7)$$

where  $E$  = emission factor,  $mg/(m^2h)$ , and  $a$ ,  $b$  = empirical constants in the power-law.

1. Calculate the emission factor,  $E(t)$  at time  $t$  directly from the chamber concentration.
2. Fit the power-law equation (Eq. 2.7) to the  $E(t)$  data to determine coefficients  $a$  and  $b$ .

**Figure 2.4a** shows the typical example of the emission characteristics of a dry material, gypsum wallboard over time and the performance of the prediction modeling.

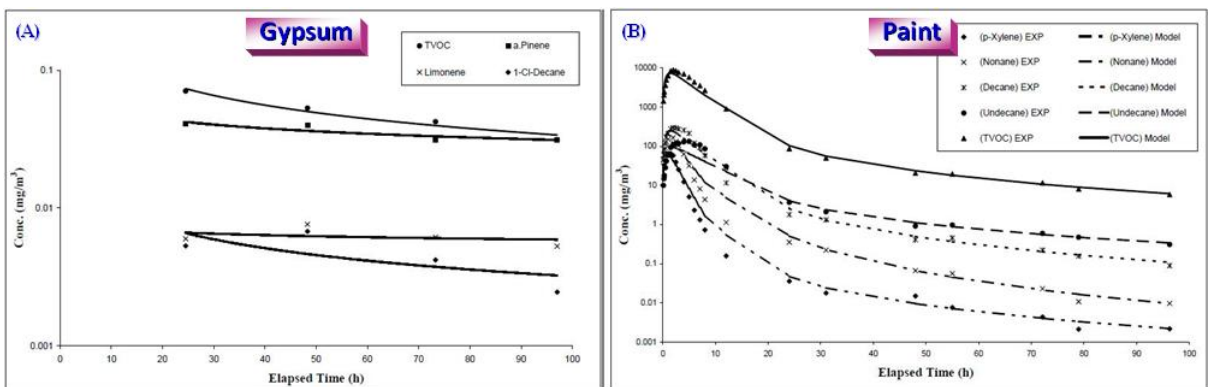


**Figure 2.4** (a) Dry material emission characteristics and modeling. (b) For wet materials (Zhu et al., 1999).

### 2.3.2 Wet materials

VOC emission characteristics from wet coating materials can be divided into three emission periods. During the first period, the emission is mainly controlled by evaporation and thus the emission factor is high and decreasing rapidly. During the third period, the emission is mainly controlled by internal diffusion after the material is dried, and the emission factor is low and slowly decreasing. In between, the second period, transition period shows the emission behavior controlled by both evaporation and internal diffusion. The following “Segmented VB + Power-law” model has been used to describe the emission factor in the three periods:

For  $t \leq t_1$  (evaporation-controlled emission period):

$$E(t) = E_e = K_m \times [(C_v \times M(t) / M_{01}) - C(t)] \quad (2.8)$$

For  $t_1 \leq t \leq t_2$  (transition emission period):

$$E(t) = E_{ed} = E_e(t_1) \times \exp(-k_{ed} \cdot (t - t_1)) \quad (2.9)$$

For  $t \geq t_2$  (internal diffusion-controlled emission period, or IDC period):

$$E(t) = E_d = a \times t^{-b} \quad (2.10)$$

where

$E$  = emission factor,  $mg/(m^2h)$

$E_e$  = emission factor during the evaporation-controlled period,  $mg/(m^2h)$

$E_d$  = emission factor during the diffusion-controlled period,  $mg/(m^2h)$

$E_{ed}$  = emission factor during the transition period,  $mg/(m^2h)$

$K_m$  = gas phase mass transfer coefficient,  $m/h$

$C_v$  = initial surface concentration,  $mg/m^3$

$M_{0l}$  = initial pollutant mass for evaporation,  $mg/m^2$

$a, b$  = empirical constants in the power-law equation

$t_1, t_2$  = hour time points dividing the emission process into the three,  $h$ .

$k_{ed} = \ln[E_d(t_1)/E_e(t_2)]/(t_2-t_1)$ , exponential decay constant for the transition period,  $h^{-1}$

**Figure 2.4b** illustrates the typical example of the emission characteristics of a wet material, paint over time and the modeling performance.



## 2.4 Chemical Compositions and Dynamics of Indoor Air

### 2.4.1 Active and passive sources

In an indoor environment, there are many sources of indoor air pollution including bioeffluents from human beings, building materials (e.g. carpets, ceilings, engineered woods, insulations and wall materials), combustion sources (e.g. gas, oil and tobacco products), electronic equipments (e.g. computers, copiers, radios, printers, televisions and etc.), HVAC systems, humidification/cleaning devices and outdoor air pollution (Ilka, 2005). The relative importance of these sources can be determined by their amount of emitting pollutants, hazardous levels of their components in them and the ages of the sources. These sources of indoor emissions can be divided into two categories: active and passive sources. Active sources generate heat as well as pollutants, depending on the operating modes and processes of devices which activate emissions. The examples of these sources are personal computers, printers and copiers. On the contrary, passive sources in an office environment include building materials, furniture and other emission sources not involving heat generation or machine operations.

By considering these representative sources, Ilka (2005) determined the experimental emission properties of several active and passive sources typical in an office indoor environment by using small-, mid- and full-scale chambers. After that, he used these emission data to simulate the holistic impacts of the sources on VOC concentrations in a typical office environment by utilizing a simulation program called MEDB-IAQ (Zhang et al. 1999).

## 2.4.2 Simulations of VOC emission dynamics in an indoor environment

This simulation (Ilka, 2005) was performed for a period of three days (72 hours). Printers were operating from 9:00 to 10:00, and copiers from 13:00 to 14:00, everyday.

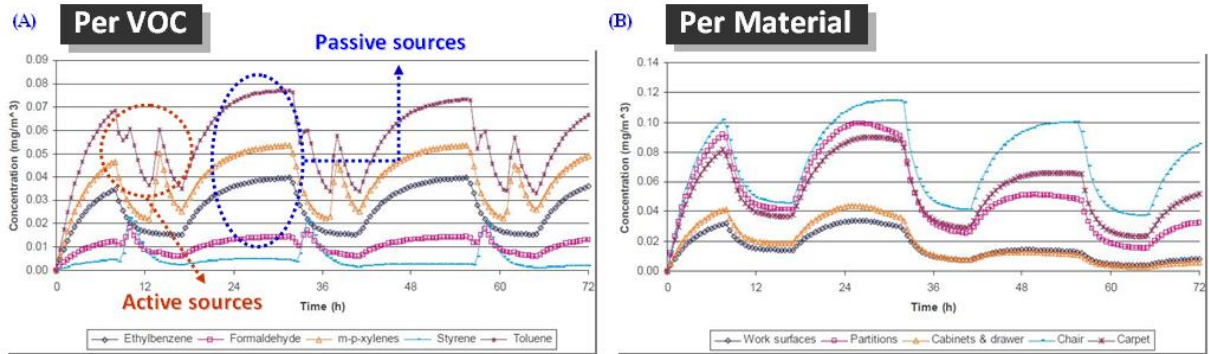


**Figure 2.5 (a) Concentration dynamics per VOC. (b) Concentration dynamics per material (Ilka, 2005).**

**Figure 2.5a** shows the concentration levels of selected eminent VOCs such as ethylbenzene, formaldehyde, m,p-xylene, styrene and toluene. Toluene, which emitted from carpet, computer, copier, drawer, panel and printer, was largely influenced by the active source emissions and its decay behavior over time was caused by the emissions from the passive sources. Formaldehyde and m,p-xylene came only from computer and copier emissions, so their peaks at different days had the same tendency due to the same amount of emissions during the same hours of the day. Styrene was generated mostly from printer emissions. Ethylbenzene was emitted from computer only as a constant source.

**Figure 2.5b** illustrates the concentration behaviors for the period of three days. From this, the concentration decays of the passive source materials over time can be seen evidently, but not all of them at the same rate. The concentration due to cabinet was the one that was fast decayed showing the decrease of 70% during the period of 24-48 hours. In addition, chair was the most eminent passive source material having higher emission while work surfaces were the lowest contributor on the indoor pollutant concentration until the first 2 days.

Li and Niu (2007) developed a novel single-zone mass-transfer-based IAQ model verified by the comparison with the results from another model that has been experimentally validated. Their model consists of a multi-phase emission and sorption model for multi-layer floor, ceiling and wall materials with varying ventilation schemes entrained, considering reasonably realistic aspects typical in indoor environments, as a decision-making tool not alone for predicting indoor VOC concentrations, but also to quantitatively evaluate various IAQ strategies assessing their potential health impacts. In their paper, the variation of indoor VOC concentrations over time was the result of diffusion/sorption within individual layers of materials and interaction of the indoor air with interior building materials under a certain ventilation scheme. Sometimes, an air cleaner could be used indoor to further reduce VOC concentrations. The proposed model is useful in analyzing the level of contaminant buildup that would occur during no ventilation period for intermittent ventilation schemes and in determining the amount of outdoor air and the lead-time hours required to flush out the accumulated contaminants to maintain the acceptable IAQ level prior to occupancy.

In this way, by using this kind of well-established models, the impact of changing indoor emission dynamics on the shape of emission signatures over time can be traced and predicted compensating the shape change of emission signatures over time and different ventilation scheme of a given indoor environment.

## 2.5 Potential Techniques for Signature Separation and Identification

Several techniques are reviewed in detail below to identify their pros and cons for possible applications in the current study.

### 2.5.1 Principal Component Analysis method (PCA)

#### 2.5.1.1 Overview

Principal Component Analysis (PCA) was invented in 1901 by Karl Pearson (Pearson, 1901). PCA involves a mathematical procedure that transforms a number of possibly correlated variables into a smaller number of uncorrelated variables called principal components. The first principal component accounts for as much of the variability in the data as possible, and each succeeding component accounts for as much of the remaining variability as possible. Depending on the field of application, it is also named as discrete Karhunen-Loève Decomposition (KLD), Hotelling Transform or Proper Orthogonal Decomposition (POD).

Now it is mostly used as a tool in exploratory data analysis and for making predictive models. PCA involves the calculation of the eigenvalue decomposition of a data covariance matrix or singular value decomposition of a data matrix, usually after making a given dataset mean-centered for each attribute. The results of PCA are usually discussed in terms of component scores and loadings. PCA is the simplest of the true eigenvector-based multivariate analyses. Often, its operation can be thought of as revealing the internal structure of the data in a way which best explains the variance in the

data. If a multivariate dataset is visualized as a set of coordinates in a high-dimensional data space (1 axis per variable), PCA provides with a lower-dimensional picture, a shadow of this object when viewed from its most informative viewpoint. PCA is closely related to factor analysis. Indeed, some statistical packages deliberately combine the two techniques.

In most of the identification/detection researches aforementioned using PTR-MS in the literature review, this PCA method was employed for the purpose of authentication/quality /source/type/VOC identifications and its classifications.

#### 2.5.1.2 Underlying model

Let's define an N state variable vector adjusted  $v(x, t)$  as follows, given an observation data vector  $U$ :

$v(x,t) = U - \langle U \rangle$ , then  $\langle v \rangle = 0$ ; where the brace  $\langle . \rangle$  means ensemble average.

\* Because the basis (mode) is derived from the ensemble of observation sets  $\{U\}$ , the eigenfunctions  $\{\varphi_n\}$  that we have to find are usually called empirical eigenfunctions.

The PCA is a generalized Fourier expansion of a random space expressing  $v(x,t)$  that has the meaning of variation from the mean value, as the sum of orthonormal basis functions  $\{\varphi_n\}$  as follows:

$$v(x,t) = \sum_{n=1}^{\infty} a_n(t) \varphi_n(x) \rightarrow v^N(x,t) = \sum_{n=1}^N a_n(t) \varphi_n(x)$$

where

$$a_n(t) = \int \varphi_n^H(x) v(x,t) dx \quad \leftarrow \text{Random Fourier coefficients, H denotes its conjugate transpose}$$

$$(\varphi_i, \varphi_j) = \int \varphi_i^H(x) \varphi_j(x) dx = \delta_{ij} \quad \leftarrow \text{Orthonormality}$$

Minimizing the mean square error from a partial sum of N terms leads to a homogeneous Fredholm integral equation of the second kind like the below,

$$\int R(x, x') \varphi_i(x') dx' = \lambda_i \varphi_i(x) \quad \text{--- (*)}$$

where

$$R(x, x') = \langle v(x,t) v^H(x',t) \rangle$$

By Mercer's theorem, R can be expressed by the following form with the random Fourier coefficients being orthogonal variables having its mean square values equal to the eigenvalues  $\lambda_n$ .

$$R(x, x') = \langle v(x,t) v^H(x',t) \rangle = \sum_{i=1}^{\infty} \lambda_i \varphi_i(x) \varphi_i^H(x')$$

where

$$\langle a_i(t) a_j^*(t) \rangle = \lambda_i \delta_{ij}$$

And also, the equation (\*) can be reduced to matrix eigenvalues problems using the trapezoidal quadrature. Then, we can solve the eigenvalues problem getting eigenfunctions, its eigenvalues and  $a_n$ .

And then,

$$v^N(x, t) = \sum_{n=1}^N a_n(t) \varphi_n(x) = a_1 \varphi_1 + a_2 \varphi_2 + \Lambda + a_N \varphi_N = \begin{bmatrix} \varphi_1 & \Lambda & \varphi_N \end{bmatrix} \begin{bmatrix} a_1 \\ M \\ a_N \end{bmatrix} = \Phi z(t)$$

where

$$z(t) = [a_1(t) \quad a_2(t) \quad \Lambda \quad a_N(t)]^T$$

When the approximation of  $v^N$  is expressed by only M eigenfunctions,

$$v^N(x, t) = \sum_{n=1}^M a_n(t) \varphi_n(x) + r \cong \sum_{n=1}^M a_n(t) \varphi_n(x) = \Phi_M z_M(t)$$

where

$$\Phi_M = [\varphi_1 \quad \varphi_2 \quad \Lambda \quad \varphi_M], \quad z_M(t) = [a_1(t) \quad a_2(t) \quad \Lambda \quad a_M(t)]^T, \quad M \ll N$$

these eigenfunctions  $\{\varphi_i\}_{i=1}^N$  are optimal in the sense of minimizing the approximation error (residual r).

As a conclusion, this PCA eigenfunctions obtained using the above process can be used effectively in getting huge data compression due to the use of  $\{z_M(1), z_M(2), \Lambda, z_M(N), \varphi_1, \varphi_2, \Lambda, \varphi_M, \langle U \rangle\}$  : (2M by N)+N components, not of



$\{U^{(1)}, U^{(2)}, \Lambda, U^{(N)}\}$  : (N by N) components when expressing a given sample set like snapshots, conserving the energy level of over 99.99%.

Usually,  $2M \ll N$  because  $M < \frac{1}{100} N$ .

To reduce the order of system states, the M vector  $Z_M$  is utilized instead of the N vector U.

To reconstruct the original state vector U, we can use this relation:

$$U(x, t) \cong \Phi_M z_M(t) + \langle U \rangle$$

### 2.5.1.3 Assumptions and limitations of PCA

PCA is theoretically an optimal linear scheme in terms of least mean square error, for compressing a set of high dimensional vectors into a set of lower dimensional vectors and then reconstructing the original set. It is a non-parametric analysis, and the answer is unique and independent of any hypothesis about data probability distribution. However, the latter two properties are regarded as weakness as well as strength, in that being non-parametric, no prior knowledge can be incorporated and that PCA compressions often incur loss of information. The applicability of PCA is limited by the assumptions made in its derivation. These assumptions are:

1) Assumption on linearity:

The observed data set is assumed to be linear combinations of certain basis. Non-linear methods such as kernel PCA have been developed without assuming linearity.

2) Assumption on the statistical importance of mean and covariance:

PCA uses the eigenvectors of the covariance matrix, and it only finds the independent axes of the data under the Gaussian assumption. For non-Gaussian or multi-modal Gaussian data, PCA simply de-correlates the axes. When PCA is used for clustering, its main limitation is that it does not account for class separability since it makes no use of the class label of the feature vector. There is no guarantee that the directions of maximum variance will contain good features for discrimination.

3) Assumption that large variances have important dynamics:

PCA simply performs a coordinate rotation that aligns the transformed axes with the directions of maximum variance. It is based on the common idea, when the observed data has a high signal-to-noise ratio, that the principal components with larger variance correspond to interesting dynamics and lower ones correspond to noise. Essentially, PCA involves only rotation and scaling. The above assumptions are made in order to simplify the algebraic computation on the data set. Some other methods have been developed without one or more of these assumptions.

## 2.5.2 Partial Least Squares - regression method (PLS)

### 2.5.2.1 Overview

Partial Least Squares regression (PLS) was developed by a Swedish statistician, Herman Wold. In statistics, the method of PLS bears some relation to principal component analysis; instead of finding the hyperplanes of minimum variance, it finds a linear model describing some predicted variables in terms of other observable variables. It is used to find the fundamental relations between two matrices ( $\mathbf{X}$  and  $\mathbf{Y}$ ), i.e. a latent variable approach to modeling the covariance structures in these two spaces. A PLS model will try to find the multidimensional direction in the  $\mathbf{X}$  space that explains the maximum multidimensional variance direction in the  $\mathbf{Y}$  space. PLS-regression is particularly suited when the matrix of predictors has more variables than observations, and when there is multi-collinearity among  $\mathbf{X}$  values. On the contrary, standard regression will fail in these cases.

PLS-regression is an important step in PLS path modeling, a multivariate data analysis technique that employs latent variables. This technique is often referred to as a form of variance-based or component-based structural equation modeling. It is widely applied in the field of chemometrics, in sensory evaluation, and more recently, in chemical engineering process data (see John F. MacGregor) and the analysis of functional brain imaging data (see Randy McIntosh).

Van Ruth et al. (2007) and Granitto et al. (2007) used this method with PCA in their researches for resolving their identification issues when utilizing PTR-MS.

### 2.5.2.2 Underlying model

The general underlying model of multivariate PLS is

$$\begin{aligned}\mathbf{X} &= \mathbf{TP}^T + \mathbf{E} \\ \mathbf{Y} &= \mathbf{TQ}^T + \mathbf{F}\end{aligned}\tag{2.11}$$

where  $\mathbf{X}$  is an  $n \times m$  matrix of predictors,  $\mathbf{Y}$  is an  $n \times p$  matrix of responses,  $\mathbf{T}$  is an  $n \times l$  matrix (*score, component or factor matrix*),  $\mathbf{P}$  and  $\mathbf{Q}$  are, respectively,  $m \times l$  and  $p \times l$  *loading matrices*, and matrices  $\mathbf{E}$  and  $\mathbf{F}$  are the error terms, assumed to be independent and identically distributed Gaussian.

### 2.5.2.3 Algorithm

A number of variants of PLS exist for estimating the factor and loading matrices  $\mathbf{T}$ ,  $\mathbf{P}$  and  $\mathbf{Q}$ .

Most of them construct estimates of the linear regression between  $\mathbf{X}$  and  $\mathbf{Y}$  as follows:

$$\mathbf{X} = \mathbf{Y}\tilde{\mathbf{B}} + \tilde{\mathbf{B}}_0\tag{2.12}$$

Some PLS algorithms are only appropriate for the case where  $\mathbf{Y}$  is a column vector, while others deal with the general case of a matrix  $\mathbf{Y}$ . Algorithms also differ on whether they estimate the factor matrix  $\mathbf{T}$  as an orthonormal matrix or not.

### 2.5.3 Chemical Mass Balance method (CMB)

#### 2.5.3.1 Overview

The Chemical Mass Balance (CMB) is one of several receptor models that have been applied to air resources management. The atmosphere is a very complex system, and it is necessary to greatly simplify the descriptions of reality to produce a mathematical model capable of being calculated on even the largest and fastest computers. Thus, although significant improvements have been made over the past 20 years in the mathematical modeling of dispersion of pollutants in the atmosphere, there are still many cases where the models are insufficient to permit the full development of effective and efficient air quality management strategies. Thus, it is necessary to have other methods available to assist in the identification of sources and the apportionment of the observed pollutant concentrations to those sources. Such methods are called receptor-oriented or receptor models since they are focused on the behavior of the ambient environment at the point of impact, as opposed to the source-oriented dispersion models that focus on the transport, dilution and transformations that occur at the source and follow the pollutants to the sampling or receptor site.

Receptor models use the chemical and physical characteristics of gases and particles measured at sources and receptors to both identify the presence of sources and to quantify source contributions to receptor concentrations. Receptor models are generally contrasted with dispersion models that use the estimates of pollutant emission rates, the meteorological transport and the chemical transformation mechanism to assess the

contribution of each source to receptor concentrations. The two types of models are complementary, with each type having its own advantages that compensate for the drawbacks of the other.

The CMB receptor model was first applied by Winchester and Nifong (1971). The original applications used unique chemical species associated with each source type, the so-called “tracer” solution. Friedlander (1973) introduced an ordinary weighted least-squared solution to the CMB equations, and this had the advantages of relaxing the constraint of a unique species in each source type and of providing estimates of uncertainties associated with the source contributions.

#### 2.5.3.2 Underlying model

##### Assumptions:

- Compositions of source emissions are constant over the period of ambient and source sampling.
- Chemical species do not react with each other (i.e. can be linearly added). For many assessments, secondary formation of particles is important. While CMB is not formulated to explicitly treat secondary transformation, a surrogate procedure is available to give some information on at least the extent of secondary materials in the ambient data.
- All sources with a potential for significantly contributing to the receptor have been identified and have had their emissions characterized.
- The source compositions are linearly independent of each other with random, uncorrelated and normally distributed measurement uncertainties.

- The number of sources or source categories is less than the number of chemical species.

The fundamental principle of receptor models is that mass conservation can be assumed and a mass balance analysis can be used to identify and apportion sources of airborne particulate matter in the atmosphere. This methodology has generally been referred within the air pollution research community as receptor modeling. The approach to obtaining a dataset for receptor modeling is to determine a large number of chemical constituents such as elemental concentrations in a number of samples. Alternatively, automated electron microscopy can be used to characterize the composition and shape of particles in a series of particle samples. In either case, a mass balance equation for the pollutant concentrations at a sampling location can be written as the summation of the contributions to account for all  $m$  chemical species in the  $n$  samples as contributions from  $p$  independent various sources as follows:

$$x_{ij} = \sum_{k=1}^p s_k \cdot a_{kj}, \quad j = 1, 2, \dots, m \quad \text{for } \forall i = 1, 2, \dots, n \quad (2.13)$$

where  $x_{ij}$  is the predicted concentration of compound  $j$  measured in sample  $i$  at the sampling location,  $s_k$  is the contribution of source  $k$  (which is the unknown and to be solved), and  $a_{kj}$  is the source profile for compound  $j$  from source  $k$ .

The value of  $s_k$  can be found by minimizing the difference between the measured ( $C_j$ ) and the predicted ( $x_j$ ) concentrations for all target compounds:

$$\xi^2 = \sum_{j=1}^m \left[ \frac{1}{\sigma_j^2} \cdot \left( C_j - \sum_{k=1}^p s_k \cdot a_{kj} \right)^2 \right] \quad (2.14)$$

This is the common multiple regression analysis problem. When the uncertainties ( $\sigma_j$ ) in the measurements are assumed to be constant among compounds, the solution can be found by using least squares.

The collection of  $p$  source profile vectors forms a source profile matrix. Initially, ordinary least squares were employed for the estimation (Friedlander, 1973). Since different elements have quite different scales for their values (major elements at  $\mu\text{g}/\text{m}^3$  concentrations, minor elements at concentrations of hundreds of  $\eta\text{g}/\text{m}^3$  and trace elements at  $\eta\text{g}/\text{m}^3$  values), a weighted least squares regression analysis has been used to fit sources with several elements for measured ambient samples. In these analyses, the ambient elemental concentrations are weighted by the inverse of the square of the analytical uncertainty in that measurement.

It was recognized that there is uncertainty in source profile values. The inclusion of this error is the statistical ‘error in x’ problem that has been examined by a large number of investigators. A mathematical formulation called effective variance weighting was independently suggested, which included the uncertainties in the measurements of the source composition profiles as well as the uncertainties in the ambient concentrations. As part of this analysis, a method was also developed to calculate the uncertainties in the mass contributions. This effective variance least squares (EVLS) method has been



incorporated into the standard personal computer software developed by the US Environmental Protection Agency, or EPA (Watson et al., 1990). Because of the distribution of this model approved by EPA, it has become virtually mandatory to use EVLS in receptor modeling for regulatory purposes. It has thus been widely applied and those results are summarized in an EPA report (EPA, 1996).

### 2.5.3.3 Limitations and on-going improvements

In fact, the assumptions mentioned in the previous section pose a limitation of the model because source compositions are not constant (varying with changes in process inputs, loads and cycles); components do react with each other and systems are not linear; it is not rarely known exactly how many sources are contributing to a receptor; there are many more sources than components which can be practically measured; many sources have very similar compositions; measurement errors are not necessarily random, uncorrelated or normally distributed; and very few sources have their own unique tracer components. In addition, the ordinary weighted least squared solution was limited in that only the uncertainties of the receptor concentrations were considered; the uncertainties of the source profiles, which were typically much higher than the uncertainties of the receptor concentrations, were neglected.

While the implicit assumptions are fairly restrictive and will never be totally obeyed in actual practice, CMB can tolerate deviations from these assumptions with some penalty in uncertainty. Several studies have been published that document CMB's tolerance to such deviations. The limitations of receptor models may be offset by their advantages. They are relatively simple compared to source-oriented models of comparable accuracy and

precision. In addition, because an analytical method of determining the effects of systematic errors on the mass balance equations has been developed, the precisions required for measurements can be estimated to provide a target precision for the model output.

Because of limitations of performing the least squared analysis, it is useful to have additional techniques that can help to determine the applicability of source profiles to a particulate apportionment problem to be solved. These methods have been developed as solutions to the problem of calibrating multivariate chemical analysis instruments, but these methods can be applied to the receptor modeling problem. The methods applied until now include partial least squares, simulated annealing, genetic algorithms and back propagation artificial neural networks. Especially, the artificial neural networks showed a better performance with respect to collinearity of sources. However, these methods have not been extensively tested in solving actual chemical mass balance problems.

## 2.5.4 Positive Matrix Factorization method (PMF)

### 2.5.4.1 Overview

The Positive Matrix Factorization (PMF) is a recent type of receptor model, developed by Dr. Pentti Paatero (Department of Physics, University of Helsinki, Finland) in the middle of the 1990s (Paatero and Tapper, 1994). PMF incorporates error estimates of the measured data to solve matrix factorization of a linear model as a constrained, weighted least squares problem. These error estimates account for sampling errors, detection limits, missing data observations and outliers. The input data must be finite, positive numbers. One portion of the model solution is a matrix of factors. These factors, which are roughly interpreted as source profiles, represent the relative amounts of each compound in each source. Each factor is constrained to be nonnegative. This requirement decreases the rotational freedom used to produce meaningful factors, and often, the result is fully unique with no rotational freedom.

If the number and the profiles of sources are known, the chemical mass balance method (CMB) can be used to estimate the contribution of each source to the pollution where regression methods are used to provide quantitative results. However, in many cases, source information is unknown a priori, so factor analysis (multivariate analysis) needs to be used to extract the sources information. Hopke and co-workers applied principal component analysis (PCA) to source identification, but Paatero and Tapper (1994) showed that PCA cannot provide a true minimal variance solution since they are based on an incorrect weighting. In view of the limitations of PCA, a new technique, positive

matrix factorization (PMF), was developed for sources identification and apportionment. The distinct advantages of PMF over PCA are that non-negative constraints are built in PMF models and PMF does not rely on the information from the correlation matrix, but utilizes a point-by-point least-squares minimization scheme. It has been reported that the source profiles produced by PMF are better and more reasonable in describing the source structure than those by PCA (Huang et al., 1999). Over the past few years, PMF has been applied to a number of particle composition data sets. Recently, the PMF analysis can be expanded by using a more general model, and a new analysis tool called the multilinear engine (ME) was developed to solve such problems (Paatero, 1999). ME is very flexible and provides a general framework for fitting any of the multilinear model, so it becomes possible to obtain not only the sources profiles, but also other interesting parametric factors that may be important for source identification and pollution control/planning. For example, wind directional information can help locate the potential sources.

This becomes increasingly important with the introduction of the Guide for Expression of Measurements (GUM) and the derived Guide for Quantification of Analytical Measurements (QUAM), which are nowadays commonly accepted references underlying numerous national and international standards (Ellison et al., 2000; ISO/IEC, 2008).

#### 2.5.4.2 Underlying model

Positive Matrix Factorization is as a weighted factorization problem with non-negativity constraints. A measured dataset can be considered as an input data matrix  $\mathbf{X}$  of  $i \times j$  dimensions (i.e. VOCs' concentrations in this study), in which  $i$  number of samples and  $j$  chemical species were measured. The matrices  $\mathbf{X}$  and  $\boldsymbol{\sigma}$  (uncertainty data matrix) and a

selected number of factors  $p$  are known or given. The goal of the multivariate receptor modeling is to identify the species profile  $f$  of each source and the amount of mass  $g$  contributed by each factor to each individual sample (see Equation 2.18):

$$\mathbf{X} = \mathbf{G}\mathbf{F}^T + \mathbf{E}, \quad \mathbf{G} : n \times p, \quad \mathbf{F} : m \times p \quad (2.15)$$

$$g_{ik} \geq 0, \quad f_{jk} \geq 0 \quad (2.16)$$

$$J \equiv \sum_{i=1}^n \sum_{j=1}^m \left( \frac{e_{ij}^2}{\sigma_{ij}^2} \right) \quad (2.17)$$

$$\{\mathbf{G}, \mathbf{F}\} = \arg \min_{\{\mathbf{G}, \mathbf{F}\}} J \quad (2.18)$$

where  $\mathbf{X}$  is the matrix of VOCs' concentrations,  $\mathbf{G}$  is the matrix of source contributions,  $\mathbf{F}$  is the matrix of source profiles, and  $\mathbf{E}$  is the residual matrix. Their elements  $x_{ij}$ ,  $g_{ik}$  and  $f_{jk}$  can be respectively understood as the concentration of compound  $j$  measured in sample  $i$ , the strength of source  $k$  on sample  $i$ , and the concentration of compound  $j$  in the emission of source  $k$ .  $\sigma_{ij}$  is the standard deviation representing the uncertainty in the observation  $x_{ij}$ .

Results are constrained, so that no sample can have a negative source contribution. PMF allows each data point to be individually weighed. This feature allows the analyst to adjust the influence of each data point, depending on the confidence in the measurement. For example, data below detection can be retained for use in the model, with the associated uncertainty adjusted, so these data points have less influence on the solution

than measurements above the detection limit. The PMF solution minimizes the object function  $J$  (Equation 2.17), based upon these uncertainties ( $\sigma$ ).

The problem is symmetric with respect to the rows and columns of the matrix  $\mathbf{X}$  and the factors  $\mathbf{G}$  and  $\mathbf{F}$ : this is a ‘bilinear model’. Its resolution is a difficult task, because it has two different non-linearities: inequalities and products of unknowns. Two are the main algorithms used to solve this problem: PMF2 (Paatero, 2000) and ME (Multilinear Engine; Paatero, 1999). The PMF2 program that implements PMF includes non-negativity constraints, but it is not written in such a manner that additional constraints can be applied to the problem. Additional constraints can be imposed using the ME program and it can also provide the other options available for PMF. However, it is currently more complicated to use as one has to script the constraint model for the problem. It would be possible to produce a preprocessing program that would prepare the input files for the ME program that could incorporate all of the constraints that are appropriate for any given problem.

Variability in the PMF solution can be estimated using a bootstrapping technique, which is a re-sampling method in which new data sets consistent with the original data are generated. Each data set is decomposed into profile and contribution matrices, and the resulting profile and contribution matrices are compared with the base run. Instead of inspecting point estimates, this method allows the analyst to review the distribution for each species to evaluate the stability of the solution.

### 2.5.4.3 Limitations and comparisons with PCA and CMB

One limitation of PMF is its inability to extract factors that fit widely varying exposure concentrations, which is apparent when comparing modeled concentrations from the regression analysis with measured concentrations. When the measured concentrations analyzed include both very high and very low values, the modeled concentrations are generally much higher or lower than the true values. When the measured concentrations are restricted to a smaller range, the modeled concentrations reflect measured concentrations much more closely. In addition, PMF (also in other multivariate receptor models) cannot resolve sources/components when: (a) profiles are too similar, and (b) sources/components show similar temporal variation. Another limitation of PMF is that the characteristics of the sources to be identified should be inferred from or interpreted by the characteristics of the profiles for several key factors identified. PMF is also known to have high bias for some cases having high variability and complexity of the measurements, which makes the results from PMF as rough estimates on the profiles of sources, not knowing the true profiles.

Both CMB and PMF provide quantitative estimates of source contributions. In the CMB analysis, source profiles are provided whereas in PMF, the source profiles are estimated. If some of the source profiles are known, they can be used in PMF to constrain the extracted source profiles and thereby reduce the rotational indeterminacy. Both CMB and PMF are employing least squares fitting, but there are some important differences in how the underlying error structures are modeled and how many unknowns are being estimated. With PMF, it is not possible to precisely assign errors to the source profiles and contributions. With CMB, it is possible to assign error estimates to each source

contribution value. However, there are no diagnostics provided in the CMB model that would alert the analyst to misspecification of the source profiles. In addition, since the CMB analysis is done on a sample-by-sample basis, there can be errors in the estimated source contributions because of the variations that can occur in the source profiles. PMF uses all of the data and thus, estimates the average source profile over the time interval, during which samples were collected. Thus, there are some similarities in the process and the outcome, but there are also some important differences in what is being estimated, the input data that are required, and the estimates of the uncertainties in the calculated values.

PCA and PMF have the main difference in that the solution of PCA forms a hierarchy and a higher number of factors contain all the factors of the lower dimension, whereas the factors of PMF are not orthogonal and, as a result, there is no hierarchy. However, when rotation is applied to PCA, the factors are not anymore orthogonal. Usually, in physical sciences, the factors do not have the property of orthogonality, so the missing of this property in PMF may not be problematic. In addition, PMF produces non-negative distributions (factors) by definition and this aspect precludes the orthogonality. However, resolving PMF algorithms is slower than PCA's because PCA is simpler to use because of less parameters to control. Other different aspects between these two methods concern the rank of the standard deviation matrix ( $\sigma$ ) and the p-rotatable property of SVD (Singular Value Decomposition). The comparison of different cases can be found elsewhere (Paatero and Tapper, 1994), and the results are summarized as follows:

- The matrix  $\sigma$  is of rank one and SVD of  $\mathbf{X}$  is p-rotatable: With PCA the matrix can be scaled correctly and factorization by SVD is optimal. The factorization by



PMF is always optimal, because it always uses the correct standard deviations. When the solution given by SVD is p-rotated, then it becomes a solution of the PMF task, because both have the same residuals and  $J(\text{PMF}) = J(\text{PCA})$  (Refer to Equation 2.17 for the definition of  $J$ ). However, PMF produces a desired non-negative solution directly, whereas the solution by PCA must be rotated in order to obtain a nonnegative solution.

- The matrix  $\sigma$  is of rank one, but SVD of  $\mathbf{X}$  is not p-rotatable: It's impossible to rotate the SVD-derived factorization, while PMF will produce the desired solution. PMF solves the problem, but PCA does not.
- $\text{Rank}(\sigma) > 1$ : Correct scaling is not possible with SVD; it's only possible to approximate the  $\sigma$  with a matrix of rank one, leading to loss of information. It may also happen that the solution by SVD is not p-rotatable, preventing the solution by PCA. However, PMF solves the original problem correctly.

From these considerations, it becomes apparent that in conclusion, PMF is generally more powerful than the best possible PCA, or at least equivalent to PCA. On the other hand, PCA is much faster than PMF in calculating the solution via SVD.

### 2.5.5 Method proposed in this study

Using the feature of material emission signatures to be established in a later chapter, we proposed a methodology toward a source identification based on signal processing principles. The following is an introductory section aiming for this direction, and the detailed descriptions and validation of the methodology will be presented in Chapter 4.

#### 2.5.5.1 No noise case in the x-axis (e.g. RT, $m/z$ , etc.)

The combined signal intensity from a measured sample signal can be defined as:

$$S_{sp}(x) = \alpha \cdot S_1(x) + \beta \cdot S_2(x) + \Lambda + w, \quad \alpha, \beta, \Lambda > 0$$

Then,

- (1) If  $Ind(S_{sp}) \supset Ind(S_{db})$ , then find  $\{db\}$ .
- (2) Find  $\alpha, \beta, \dots$  by regression. In this case, LSE (Least Squares Estimation) such that

$$J = \min \sum_{x \sim \text{measured}} (S_{sp}(x) - \alpha \cdot S_1 - \beta \cdot S_2 - \Lambda)^2$$

#### 2.5.5.2 Noisy case

The combined signal intensity from a measured sample signal with noise can be defined:

$$S_{sp}(x) = \sum_i [\alpha_i \cdot S_i(x) + w_i(x)], \quad \alpha_i > 0, \quad \forall i$$

Then,

$$(1) \text{ If } \text{Ind}(S_{sp}) \stackrel{\varepsilon}{\supset} \text{Ind}(S_{db}), \text{ where } \varepsilon = \sum_{i \sim \text{missed}} (x_{sp}^i - x_{db}^i)^2, \quad \varepsilon \leq \text{Thresh},$$

then, find  $\{db\}$ .

(2) Find  $\alpha_1, \alpha_2, \dots, \alpha_n$ , which minimize the following (MMSE, Minimum Mean Square Estimation in this case). Check the magnitude of  $Err$ .

$$J = \min \quad Err \equiv \min \quad E \left\{ \left( S_{sp}(x) - \sum_i \alpha_i \cdot S_i(x) \right)^2 \right\}$$

### 2.5.5.3 Example of preliminary tests

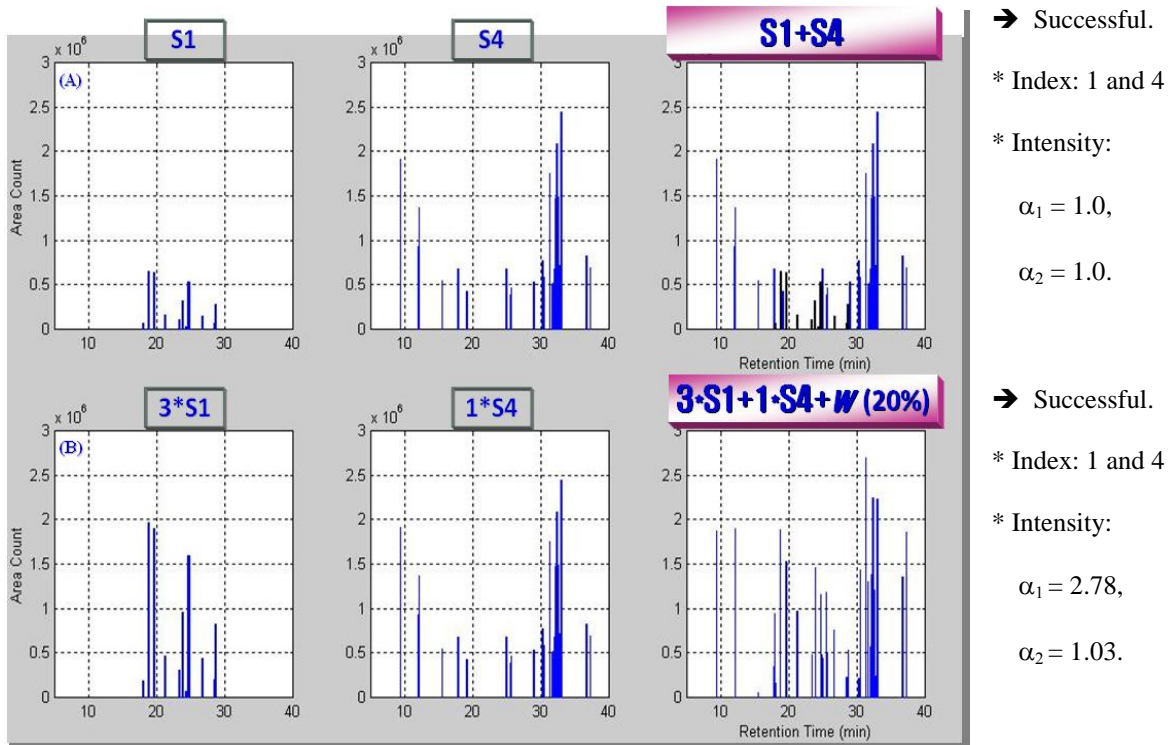


Figure 2.6 Test example of signal separation. (a) Top, no noise. (b) Bottom, with 20% noise.

## 2.6 Summary and Conclusions

◆ Several studies performed in the areas of food engineering, medical research, forensic investigations, etc. implied that a pollutant mass spectrum measured by an on-line analytical device, PTR-MS, had the potential to be used for origin/quality characterizations and source identifications.

◆ Extensive works of sensory assessments by human subjects have been done to evaluate the impact of VOC emissions from building materials on indoor air quality, and attempts have been made to correlate human sensory assessments and chemical evaluations to assess the human response on perceived air quality (PAQ) more practically and efficiently. To expedite the establishment of human exposure-response relationships caused by indoor VOC emissions from building materials and to elucidate the understanding of the relationships, a more convenient and faster analytical methodology for the evaluation of PAQ needs to be developed with a much wider detection window for indoor VOCs.

◆ Many studies claimed that building materials might be significant sources of chemical pollutants found in indoor environments. For this reason, the emission characteristics of building materials were considered important and reported to have significantly different emission profiles over time as per dry or wet materials.

◆ VOC long-term emission profiles can be accounted for by considering elapsed time and dynamic conditions via proper source models, which can also be applied to emission signatures.

◆ For the purpose of food origin/quality characterization and pollutant source apportionment, several factor analyses and receptor-based methods are being used in several research disciplines to get rough estimates. Considering that polluting compounds indoors mostly have multiple types of sources, the conventional techniques using factor analysis and the correlation with several elemental data are limited and difficult to be used in clearly pinpointing the source or material from which the target compounds are emitted. A new approach needs to be developed to account for this source identification issue specific to indoor environments.

## † CHAPTER 3. DETERMINATION OF MATERIAL ESs AND THEIR CORRELATIONS WITH SENSORY DATA

---

### 3.1 Introduction

Odors from building materials may be an important factor in their own right and for human health effects in working or residential environments. During the last two decades, there have been many attempts to understand human complaints because of poor indoor air quality and their impact on occupant health, comfort and performance. Wolkoff and Nielsen (2001) reported that after formaldehyde was focused on as a major indoor pollutant, there had been a considerable amount of interest in VOCs as potential causes of sensory health effects such as odor annoyance, eye/airway irritation, headache and other health effects. They argued that perceived indoor air quality largely should be evaluated from the sensory effects of specific indoor compounds, suggesting that VOC evaluations in terms of its impact on perceived air quality should be switched over from the use of total VOCs to a compound-by-compound approach. Evidence from many building investigations and systematic studies suggested that among several sources of indoor pollution, VOC emissions from building materials (structural or furnishing) could be considered as a major contributor to indoor air pollution, because of their complex chemical composition, large surface area and permanent exposure to indoor air

(Haghighat and Donnini, 1993). These VOC emissions cause sensory effects on building occupants because of odors and/or irritants (Fang et al., 2008).

Experimental studies using sensory measurements by human subjects have been performed to examine the impact of VOC emissions from building materials on perceived indoor air quality, and to establish human exposure-response relationships for building materials. Knudsen et al. (1998) suggested a novel experimental procedure to determine this exposure-response relationship. Their final conclusion was that source control by using low-polluting materials could often be the most effective way to improve indoor air quality. It is generally acknowledged that the exposure-response relationships can be a useful tool to systematically quantify and assess the impact of emissions from building materials on perceived air quality at different concentrations (Haghighat et al., 2001; Knudsen et al. 1998).

Attempts have been made to correlate sensory assessments and chemical evaluations using Gas Chromatographic (GC) methods (Knudsen et al., 1999) and using GC-O/MS with olfactometry (Clausen et al. 2008; Knudsen et al. 2007). Although detailed and accurate, the traditional methods for the trace analysis of VOC chemical data require extensive preparation time, and long measurement and analysis time (> 3 hours) even for one sample. In order to expedite and elucidate the understanding of human exposure-response relationships caused by the impact of VOC emissions from building materials, the advent of a more convenient and faster chemical measurement method with a much wider detection window for indoor VOCs than any traditional chemical analysis methods is urgently called for.

An analytical method, PTR-MS, was developed to overcome the disadvantages of GC methods, providing on-line measurements of individual compounds at trace levels (i.e. down to *ppb* or even *ppt* level for some VOCs, depending on the concentration level of background air). In PTR-MS, the air to be analyzed is continuously pumped into a drift tube reactor, and a fraction of VOCs is ionized in proton-transfer reactions with hydronium ions ( $\text{H}_3\text{O}^+$ ) as a chemical reagent. The advantage of utilizing proton transfer is that it is a soft ionization method, meaning that it generally does not lead to the fragmentation of product ions, and the mass of each product ion equals the VOC mass plus one. At the end of the drift tube, the reagent and product ions are measured by a quadrupole mass spectrometer, and the product ion signal is proportional to the VOC concentration sampled. PTR-MS allows numerous VOCs of interest to be monitored with a high sensitivity (Usually, the detection limits are within 10-100 *pptv*) and a rapid response time for sampling ( $< 100$  *ms*). In addition, this technique does not require any sample pre-treatment such as drying or pre-concentration, and is thus well suited for oxygenated VOCs, which cannot be quantified from canister samples used in a traditional chemical analysis method. PTR-MS has been widely used in atmospheric, food, environmental science, forensic investigation and medical research (Blake et al., 2009; Boscaini et al., 2004; de Gouw and Warneke, 2007; Filella and Penuelas, 2006; Granitto et al., 2007; Hewitt et al., 2003; Jobson et al., 2005; Kato et al., 2004; C. Lindinger et al., 2008; W. Lindinger et al., 1998, 2001; Lirk et al., 2004; Mayr et al., 2003; Steeghs et al., 2004; Van Ruth et al., 2007; Wang and Stout, 2007; Warneke et al., 2003; Wehinger et al., 2007; Whyte et al., 2007). On the other hand, there have been rare studies in the field of indoor air quality utilizing this technique with a few exceptions (Bunge et al., 2008; Fang et al., 2008; Weschler et al., 2007; Wisthaler et al., 2007).



One of the important research challenges in the field of indoor air quality is the identification of emission sources of indoor VOCs (Hodgson et al., 2000). Even though several possible compounds with great potency have been chemically measured and reported through indoor field studies, the sources of the detected compounds can not often be pinpointed. To establish an effective countermeasure against unwanted VOC emissions, emission sources need to be identified. A first step toward a source identification would be to determine a material emission signature if it is unique for each material or each type of material. This is similar to human's fingerprint for personal identification. In addition, if a correlation exists between measured emissions and odor assessments by human subjects, the emission signatures may be used for identification of the responsible odor source that causes perceived air quality problems in a building. The objectives of the present study in Chapter 3 were to determine the VOC emission signatures of nine building materials using PTR-MS as a primary method for VOC analysis, and to study the correlations between the PTR-MS measurements and the acceptability of air quality perceived by human subjects.

## 3.2 Materials and Methods

### 3.2.1 Overview

Nine typical individual building materials previously used in an odor assessment study of air quality by human subjects (Wargocki et al., 2007) were placed one by one in a 50-liter small-scale chamber. The materials included carpet, ceiling material, gypsum board, linoleum, paint 1 (water-based), paint 2 (with linseed oil), polyolefine, PVC and wood. To achieve similar concentrations as in the previous human assessment tests, area-specific ventilation rates defined as the ratio of ventilation rate to emitting surface area were set to be similar in the two series of experiments. Chamber exhaust air polluted by the emissions from the materials was sampled by PTR-MS to determine material emission signatures. The signature is the PTR-MS ion mass ( $m/z$ , which is a physical quantity denoting the mass-to-charge ratio widely used in the electrodynamics of charged species) spectrum of the air sampled for each material test. Tests were done for low, medium and high airflow rates. Tenax sorbent tube samples were also taken from the same exhaust air to identify the major VOCs emitted from the materials using GC/MS analysis and for comparison with the emission signatures from the PTR-MS measurements. The experimental setup is shown in [Figure 3.1](#), and the detailed illustrations of the test equipment and facilities can be found in [Appendix B](#). The PTR-MS measurements were then analyzed to obtain the correlation with the odor assessments by human subjects – the ratings of acceptability of air quality. Their changes with area-specific ventilation rates were also examined.

An effective signal processing method to extract a VOC emission signature for each material from the relatively noisy signals of the PTR-MS device was developed as well as a dataset (See [Appendix A](#)) of the PTR-MS emission signatures for the materials tested. This method is outlined in the coming section of Data analysis procedure.

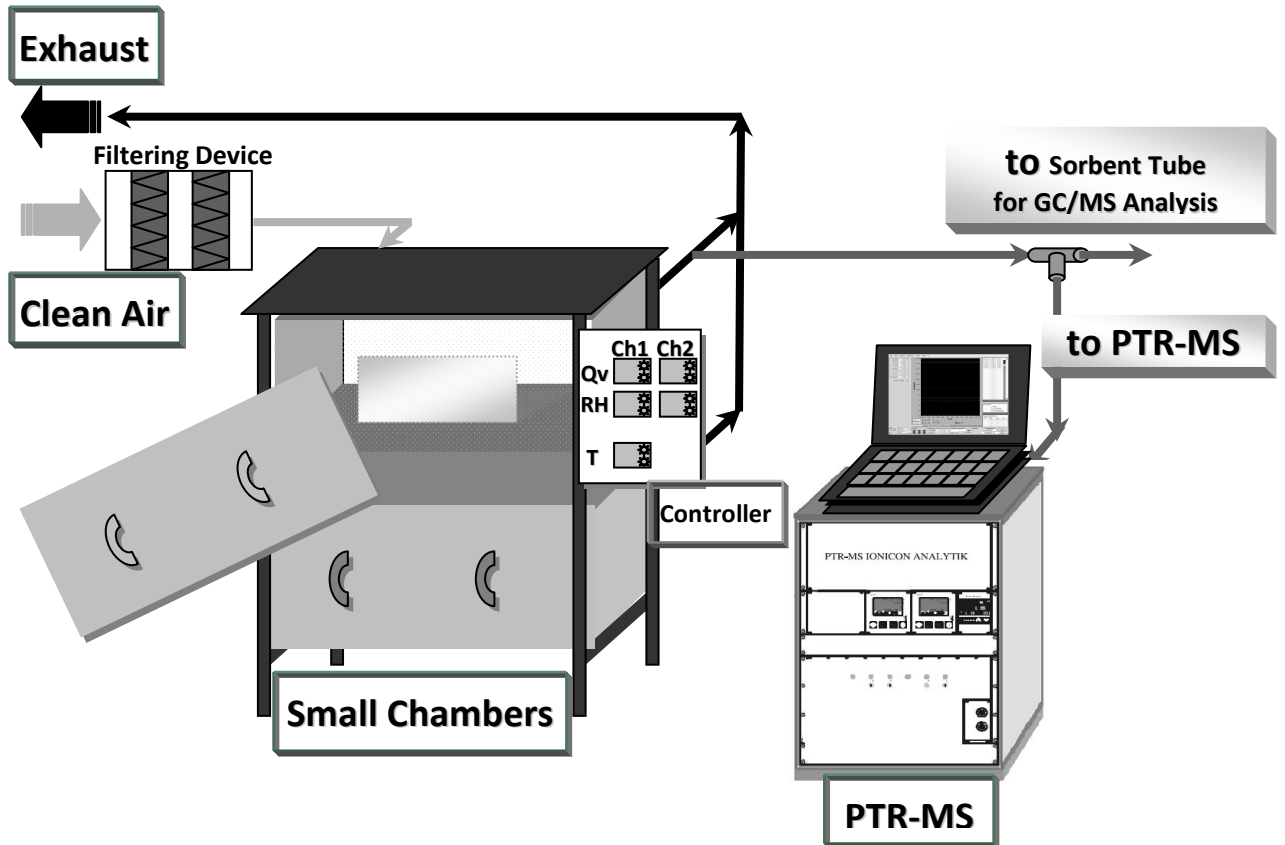


**Figure 3.1** Experimental setup.

The data on the acceptability of air quality were obtained from the previous experimental study (Wargocki et al., 2007). The temperature and relative humidity in the test chambers were  $22 \pm 0.1^\circ\text{C}$  and  $31 \pm 6\%$  RH, respectively. The study was performed by DTU (Technical University of Denmark) and SBi (Danish Building Research Institute, AAU) in small-scale glass chambers employing 38 untrained human subjects. The acceptability

was evaluated as a continuous scale from -1 to +1, defined as follows: Clearly not acceptable = -1, Just not acceptable/Just acceptable = 0 and Clearly acceptable = 1. The values of acceptability for the building materials were assessed with the following context question: “Imagine that you, during your daily work, would be exposed to the air in this diffuser. How acceptable is the air quality?” The assessments were performed following a random order among the established exposures in the small-scale glass chambers. During the assessments, the subjects could not see the materials. In order to minimize the effect of human sensory adaptation, at least 3 minute-break was taken between each assessment. The average ratings of the assessments were used in the analysis.

### 3.2.2 Environmental conditions

A 50-l small-scale environmental chamber ( $0.5\text{ m} \times 0.4\text{ m} \times 0.25\text{ m}$  high) made of electro-polished stainless steel was used in the present study. It was placed in a well-ventilated laboratory maintained at a positive pressure to ensure high air quality. The chamber assembly was comprised of four small-scale chambers stacked in a two-story frame having a flow controller (*Alicat Scientific*, accuracy  $\pm 0.1\%$  of measured values) and a humidity controller (*Vaisala INTERCAP HMP50*, accuracy  $\pm 1\%$  of measured values) for each chamber, to set and maintain the desired airflow rate and relative humidity. The temperature in the chamber was maintained by controlling the temperature in the laboratory (accuracy  $\pm 0.5^\circ\text{C}$ ). The chamber was ventilated with external air which passed through a dedicated filtering device (*Wilkerson* 3-stage carbon filters with micro filtration), ensuring conditioned and clean air supply.

In order to emulate the test conditions used in the previous human subject experiments, the air temperature and relative humidity in the chamber were maintained constant at  $23.7\sim 24.7^\circ\text{C}$  (During each sampling period, the variation was less than  $\pm 0.02^\circ\text{C}$  from the mean) and  $31 \pm 0.1\%$  RH during the tests. Before the tests, the inner surface of the chamber was scrubbed with a paper towel that was saturated with isopropanol and DI water (*SATPAX 1000*, pre-saturated non-woven polyester/cellulose wipers). After that, they were ventilated for at least 24 hours with clean air at 2 ACH (Air Change per Hour). To confirm the effectiveness of this cleaning process, the background concentrations of

individual VOCs inside the empty chamber were measured and were found to be below 1  $\mu\text{g}/\text{m}^3$ .

### 3.2.3 Test specimens

Nine typical building materials were investigated:

- ① Ceiling: 10-*mm* plain gypsum board covered with plastic coated material
- Wood: 14-*mm* untreated beech wood parquets
- Carpet: 6.4-*mm* tufted loop polyamide carpet with supporting layer of polypropylene web and polypropylene backing
- Linoleum: 2.5-*mm* linseed-oil-based flooring, 52% wood meal
- PVC: 2.0-*mm* homogenous single layered vinyl flooring, reinforced with polyurethane
- Polyolefine: 2.0-*mm* homogenous polyolefine-based resilient flooring, reinforced with polyurethane
- Gypsum: 13-*mm* plain gypsum board lined with cardboard
- Paint 1: 13-*mm* plain gypsum board painted with one coat ( $0.14 \text{ l}/\text{m}^2$ ) of water-based acrylic wall paint
- Paint 2: 13-*mm* plain gypsum board painted with one coat ( $0.14 \text{ l}/\text{m}^2$ ) of water-based wall paint with linseed oil

Detailed descriptions of these materials were reported elsewhere (Wargocki et al., 2007).

It was the same batch of materials used in the previous acceptability study by human subjects. In other words, the originally sealed materials from the same batch were used

instead of the same materials tested previously. The materials were shipped after the purchase from Denmark to Syracuse University by air mail, wrapped with aluminum foil, tightly double-taped piece by piece to minimize any permeation, and packed together in a thick package box leaving almost no space inside. Specimens were cut and prepared according to the sizes specified in **Table 3.1**. Most of them except for gypsum, paint 1 and 2 were stapled back to back together in order that both sides of each specimen were exposed to the air in the test chamber, and a VOC-free aluminum tape (*3M 2113*) was applied to seal all edges. The prepared specimens were placed vertically, parallel with the airflow in the chamber (the same direction of the long side of the chamber). The same range of area-specific ventilation rates as in the previous experiments with human subjects was set by adjusting the airflow to the chamber while keeping the size of specimen unchanged. In the previous acceptability study, airflow rate was constant at 0.9 *l/s* and specimen areas were varied to achieve the desired area-specific ventilation rates. Keeping the area-specific ventilation rates the same ensured that the resulting concentration levels at the quasi-steady state were similar between the PTR-MS measurements and the previous human subject assessments.

### 3.2.4 PTR-MS analysis

A PTR-MS device (*Ionicon Analytik high-sensitivity model with a detection limit as low as 1 pptv, Austria*) was operated at the standard conditions (Drift tube pressure: 2.3~2.4 mbar, PC: 455 mbar, FC: 6.5 STP cc/min, U SO: 75 V, U S: 100 V, Drift tube voltage: 600 V and Source: 6.0 mA). Detailed descriptions of the device and its principle can be found in W. Lindinger et al. (1998).

The instrument measures ion count rates (counts per second, *cps*) which are proportional to the respective densities of the ions. These densities can be substituted with the measured count rates, and the volume mixing ratios of the target compounds in *ppbv* can be calculated. The count rates of the product ions (*cps*) in the present work were normalized by per million hydronium ion ( $\text{H}_3\text{O}^+$ ) count rates to compensate the variations in the hydronium ions as done by other researchers in this area (e.g. de Gouw and Warneke, 2007; Jobson et al., 2005; Whyte et al., 2007). This normalized product ion count rate measured in normalized counts per second (*ncps*) is then directly proportional to the concentration level of a target VOC.



### 3.2.5 GC/MS analysis

For the identification and semi-quantification of VOCs, air samples collected by Tenax sorbent tubes were analyzed using a conventional GC/MS instrument (*Perkin Elmer Auto System XL GC, TurboMassGold MS EI detector, Thermal desorber TurboMaxtrix ATD-GC/MS system and Elite-624 GC Column* were used). Sample volumes were from 6-l to 10-l. All sorbent tubes were double pre-conditioned at 330°C for 40 minutes. To ensure clean tubes, the cleaned sample tube was pre-analyzed before sample collection. The total VOC mass for a clean tube was less than 8.0 ng (equivalent to 0.80  $\mu\text{g}/\text{m}^3$  if a 10-l sample was assumed). All abundant peaks in the gas chromatogram were selected and identified by using the NIST MS library, but only those confirmed by spiking using individual standards were reported. For the quantification of compounds, only the response factor of toluene from the GC/MS calibration was used as a semi-quantitative measurement since the main purpose of the GC/MS analysis was to identify the VOCs emitted and to determine the relative abundance of various VOCs identified. The amount of VOCs calculated by GC/MS was divided by its sampling volume for each tube sample to determine the VOC concentrations in the chamber air.

### 3.2.6 Test procedure

**Table 3.1 Flow rates and specimen areas for PTR-MS chemical measurements.**

Material	Flow Rate – $Q_v$ (l/min) / Specimen Area – $A$ ( $cm^2$ ) $Q_v/A$ (l/s/m <sup>2</sup> )				Range of $Q_v/A$ in the previous study (l/s/m <sup>2</sup> )
	Test #0	Test #1	Test #2	Test #3	
<b>Ceiling</b>	0.50 / 290.7	1.55 / 290.7	4.64 / 290.7	1.72 / 36.0	0.89 ~ 7.96
	0.29	0.89	2.66	7.96	
<b>Wood</b>	0.50 / 265.5	1.30 / 265.5	3.85 / 265.5	1.54 / 36.0	0.81 ~ 7.14
	0.31	0.81	2.42	7.14	
<b>Carpet</b>	0.50 / 240 0.35	1.28 / 240 0.89	3.83 / 240 2.66	1.72 / 36.0 7.96	0.89 ~ 7.96
<b>Linoleum</b>					
<b>PVC</b>					
<b>Polyolefine</b>					
<b>Gypsum</b>	0.50 / 416	1.03 / 416	3.08 / 416	1.80 / 81.0 3.70	0.41 ~ 3.70
	0.20	0.41	1.23		
<b>Paint 1</b>	0.50 / 402	0.99 / 402	2.97 / 402	1.80 / 81.0 3.70	
	0.21	0.41	1.23		
<b>Paint 2</b>	0.50 / 490.2	1.21 / 490.2	3.63 / 490.2	1.80 / 81.0 3.70	
	0.17	0.41	1.23		

The nine building materials were tested at four different area-specific ventilation rates (Table 3.1). A total of 36 tests were conducted. For each test, the mass spectra for the background emission signal from the empty chamber and for the sample emission signal with each prepared specimen inside the chamber were measured all after three volumetric air changes from the start of ventilation to allow concentrations in the chamber to reach

over 95% of the quasi-steady state level (*i.e.*  $\Delta t_{\text{lapse}} = \frac{3}{N_v} = \frac{3}{(Q_v \times 60/50L)} = \frac{2.5}{Q_v}$  hours, where  $N_v$  is air change rate, and  $Q_v$  is airflow rate in  $l/min$ ). PTR-MS was set to scan from  $m/z = 21$  to  $m/z = 250$  once every 12 seconds with an ion mass resolution interval of 50  $ms$ . The total sampling period was 10 minutes (600 seconds) with 50 ion mass spectra collected for each dataset. During each test, another set of duplicate mass spectra was scanned to verify the collected data. For the identification of VOCs from each material, a Tenax sorbent tube sample for GC/MS analysis was taken at the end of Test #1 for each material (**Table 3.1**) under the same chamber airflow condition.

### 3.2.7 Data analysis procedure

A dataset measured by PTR-MS has a raw signal set (in  $cps$ ) and a calculated concentration set (in  $ppbv$ ), each of which has a three dimensional data structure consisting of the time of air sampling ( $sec$ ), ion counts ( $cps$ ) and ion mass ( $m/z$ ) axes. The sample signal from PTR-MS is a random variable assumed to have at least three components: true concentration signal of each ion mass, system noise and periodic random bias – the last one seems to come from the small fluctuation of airflow rate as a result of the airflow control effort by the flow rate controller, having an amplitude of  $\pm 1.0\%$  of measured values. The system noise part can be modeled as Gaussian random noise. After considering this random noise structure, the following procedure was used for analyzing the data and is illustrated in **Figure 3.2** with the corresponding step numbers:

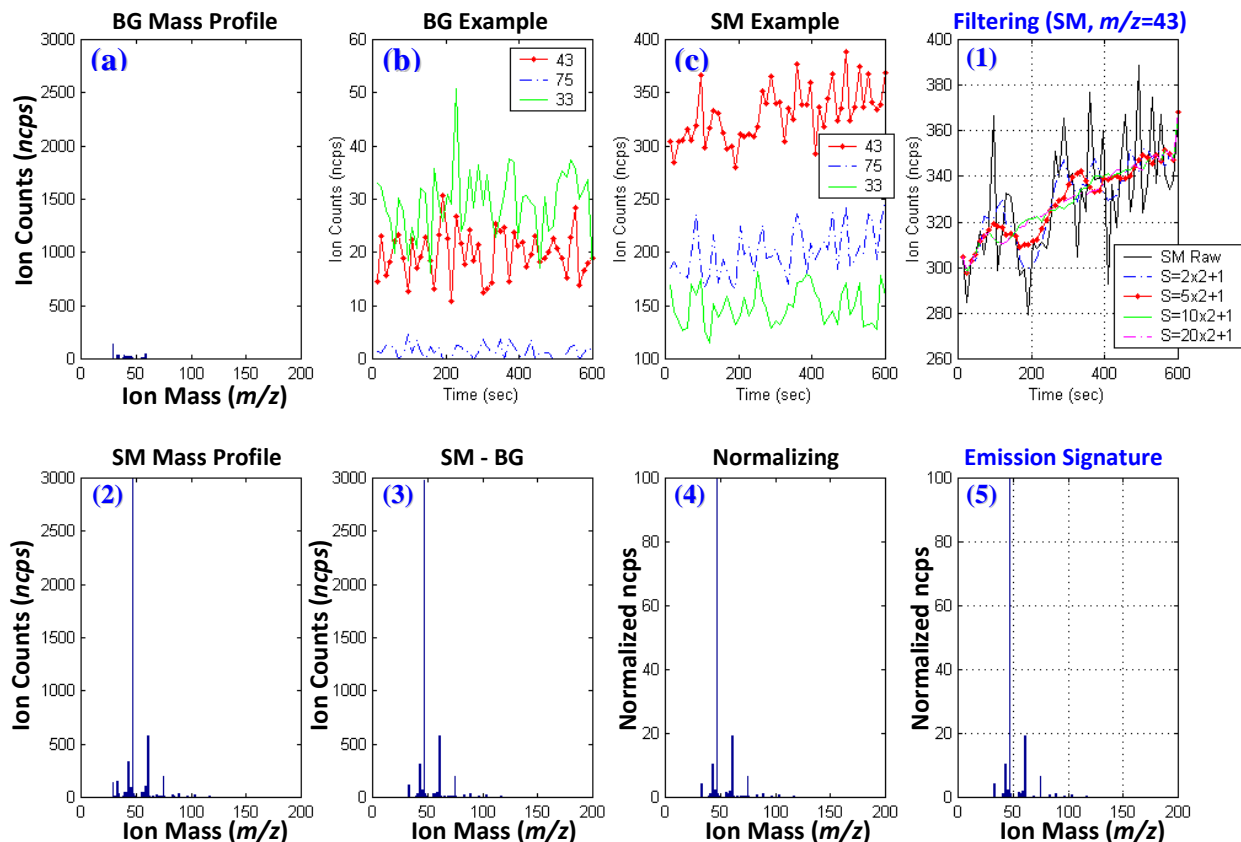


**Figure 3.2 Data analysis procedure exemplified for Linoleum.**

(a) The background mass profile. (b) The background signals. (c) The sample signals at the ion masses:  $m/z = 43, 75$  and  $33$ . Numbers (1) through (5) correspond to the steps described in the data analysis procedure.

\* BG: Background air, SM: Sample air.

\* The letter 'S' in Graph (1): Selected window size in data points for the moving-average.

(1) Filtering PTR-MS signal (**Figure 3.2(1)**): To remove noise in the PTR-MS raw data, both for the background air in the empty chamber (**Figure 3.2b**) and for the sample air with a test specimen inside the chamber during a test (**Figure 3.2c**), a moving-average estimator (Kenney and Keeping, 1962) instead of the maximum likelihood estimator (i.e. general averaging method) was applied to each dataset with two filtering objectives: 1) lowering the standard deviation of the filtered signal less than half the original signal's noise level, and 2) keeping the signal dynamics over time not deviating from the original

mean value (in other words, not to be overfitted). Eleven samples were determined to be sufficient for removing the system noise from the raw signal (i.e. the window size of the moving average for this case:  $S = 11$ ).

(2) Filtered mass profile: After the moving average filter was applied for each ion mass, consistent and stable mass profiles were obtained for both the background air (**Figure 3.2a**) and the sample air (**Figure 3.2(2)**).

(3) Material-specific mass profile: To obtain a material-specific mass profile, the mass profile for the background air was subtracted from the profile for the corresponding sample air (**Figure 3.2(3)**).

(4) Normalization: By normalizing the resulting material-specific mass profile expressed in percentage ratio using the maximum peak of the count rate of the ion mass (*ncps*), a consistent mass profile could be established (**Figure 3.2(4)**).

(5) Creating emission signature (**Figure 3.2(5)**): To establish an emission signature, any ion mass component was excluded, whose peak value was less than three times the standard deviation of the value at the same ion mass in the corresponding background mass profile. This additional step was done to remove any ion mass peaks that could occur because of the background noise signals (i.e. within the uncertainty).

In addition, by using the GC/MS analysis results together with the ion mass identification data from the literature, each detected ion mass was related to individual VOCs as a probable or tentative identification. Together these identified VOCs constitute a material emission signature.

### 3.3 Results and Discussion

#### 3.3.1 Material emission signatures by PTR-MS

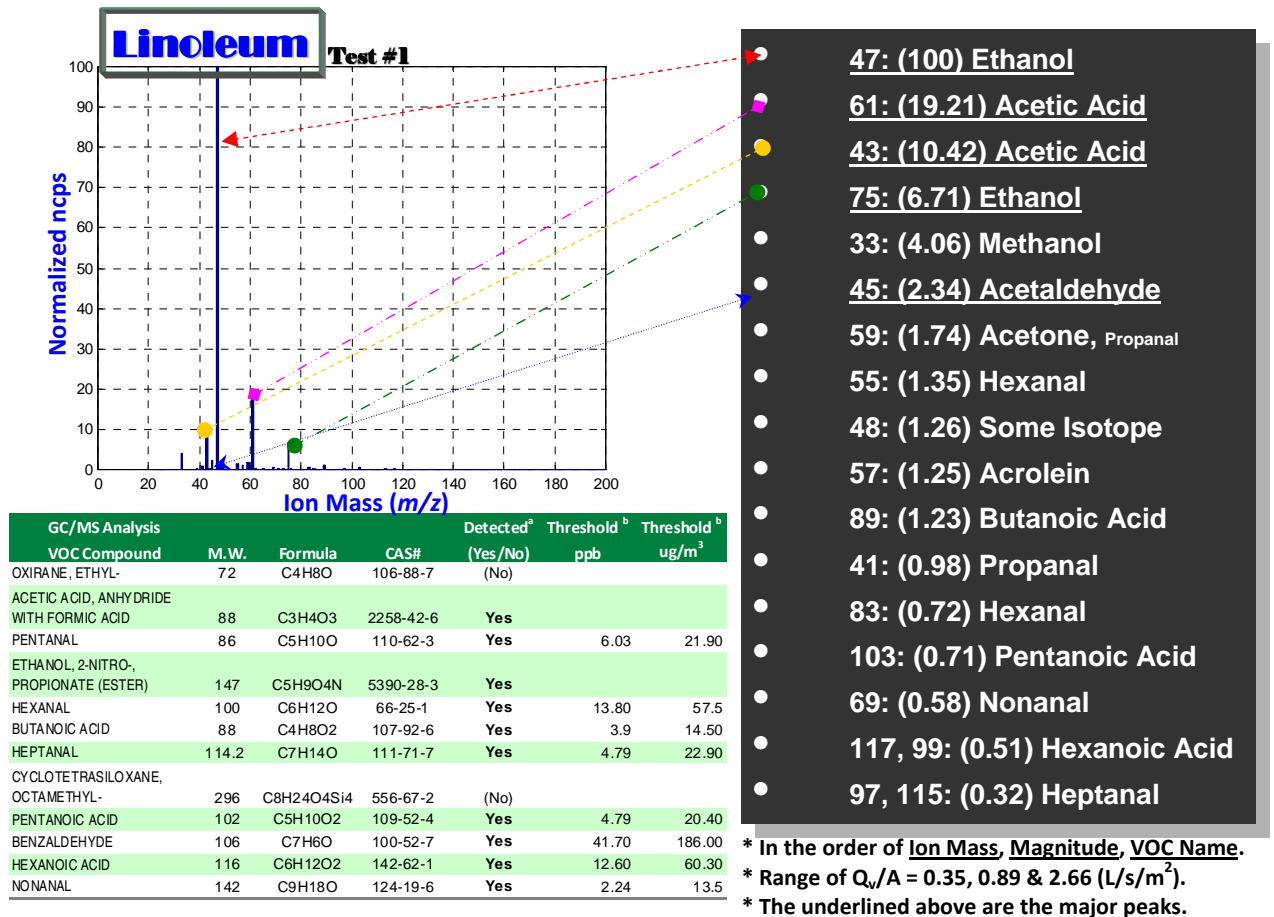


**Figure 3.3** Emission signature of Linoleum.

\* The detected compounds in the table of GC/MS analysis result indicate that the corresponding VOCs were confirmed by individual compound spiking.

A complete dataset of the PTR-MS emission signatures for the nine building materials tested was obtained (See [Appendix A](#)). As an illustration, [Figure 3.3](#) shows the emission signature for Linoleum. The signatures were established by using the test results from Test #1 as a reference because, in that experiment, the GC/MS samples were taken by

using Tenax sorbent tubes for VOC identification. In other tests with different airflow rates (Test #0, #2 and #3), signatures with the same pattern were obtained. As for the table of the GC/MS analysis, listed were only common VOCs detected by the GC/MS analysis among all the materials and considered to have an important role in the odor assessments because of their low odor thresholds. The mass assignment to each VOC was done by utilizing the GC/MS results and the identification information from the literature. Unless confirmed by the GC/MS spiking analysis, the VOCs identified in the PTR-MS results should be considered as probable or tentative.

**Figure 3.4** indicates the shape consistency of the emission signature over time for Linoleum, a high polluting material (maximum peak of  $m/z = 47$  at Test #1: Mean  $\pm$  SD =  $2974 \pm 157$  *ncps*). The result for Polyolefine, a low polluting material (maximum peak of  $m/z = 33$  at Test #1: Mean  $\pm$  SD =  $6.6 \pm 1.5$  *ncps*), which was one of the most difficult cases to measure a signal because of its low signal intensity, is presented in **Figure 3.5**. This shape consistency over time was also seen in other materials investigated in this study, indicating the effectiveness of the filtering technique used. The filtering method led to the signature that was stable during the 10-minute sampling period by eliminating the effect of noise observed in the raw signals (**Figure 3.4a**).

The pattern of the emission signatures also did not change under the different area-specific ventilation rates tested (**Figure 3.6**). There were also identifiable differences in the VOC emission signatures measured by PTR-MS among the different types of building materials as shown in **Figure 3.7**. The differences include the type of ion mass present, its relative amount or both. An effective index for quantifying the differences is under

development as part of a pattern recognition method. PTR-MS emission signatures were specific to each material tested. Therefore, it is possible to identify the material based on the emission pattern of the same material measured by PTR-MS. The differences in emission patterns may potentially be used to identify emission sources (e.g. in buildings) based on air samples measured by PTR-MS, but a specific signal processing and separation method for pattern recognition is yet to be developed.

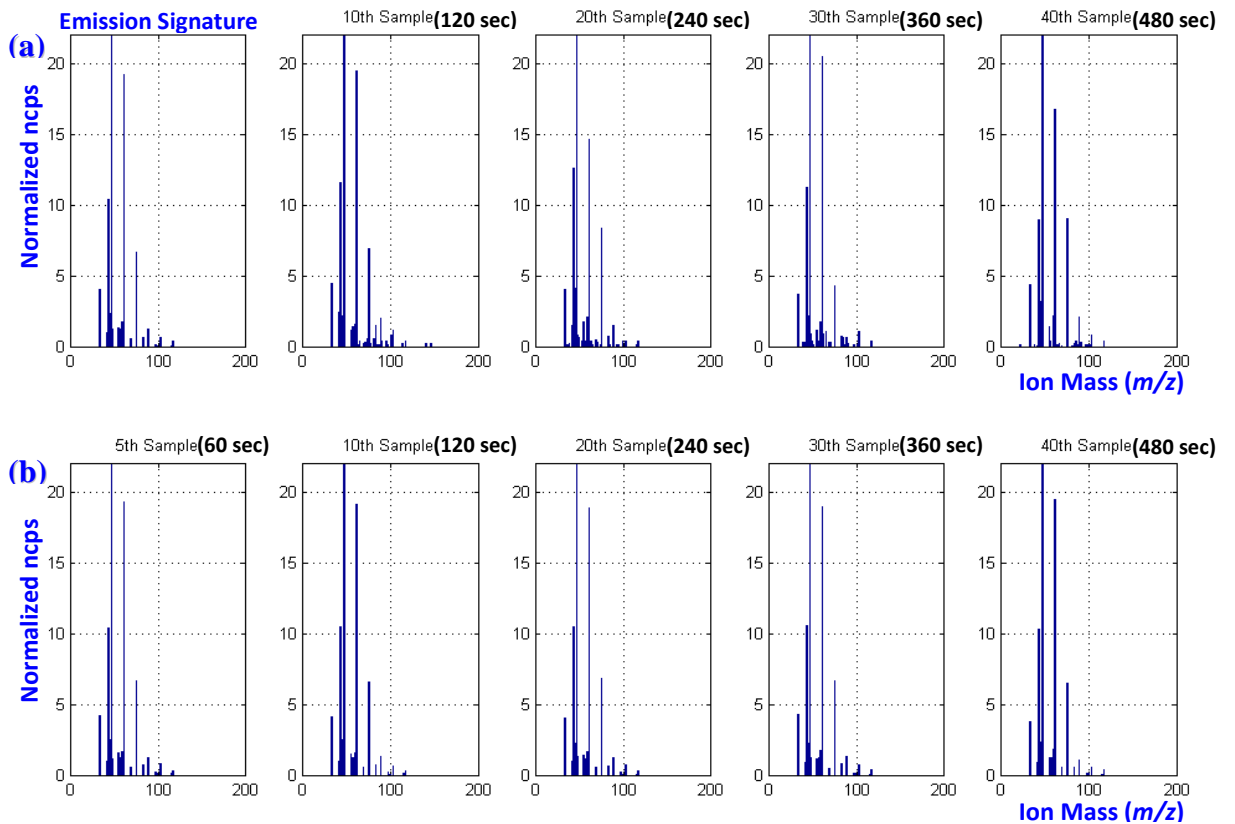


Figure 3.4 Consistency of PTR-MS emission signature exemplified for Linoleum over different sampling time. (a) Top, from the raw signals. (b) Bottom, from the filtered signals.



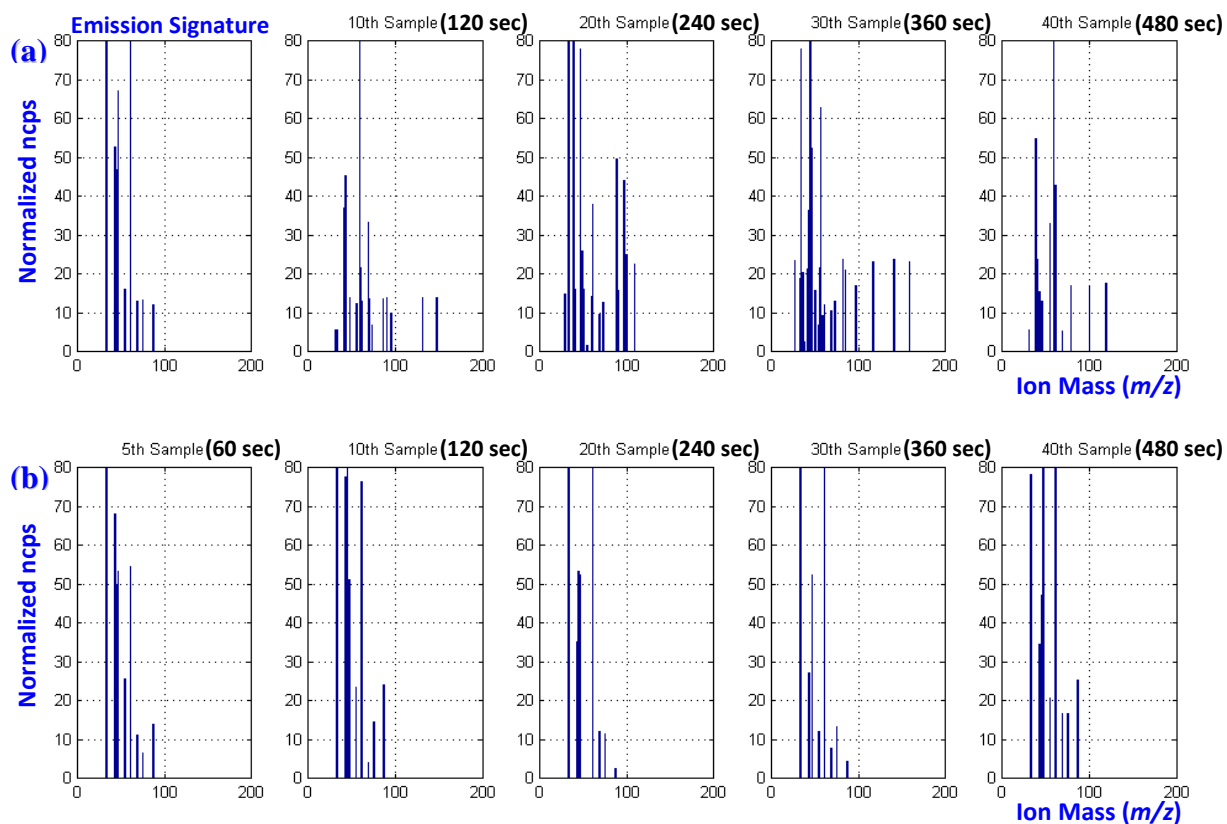
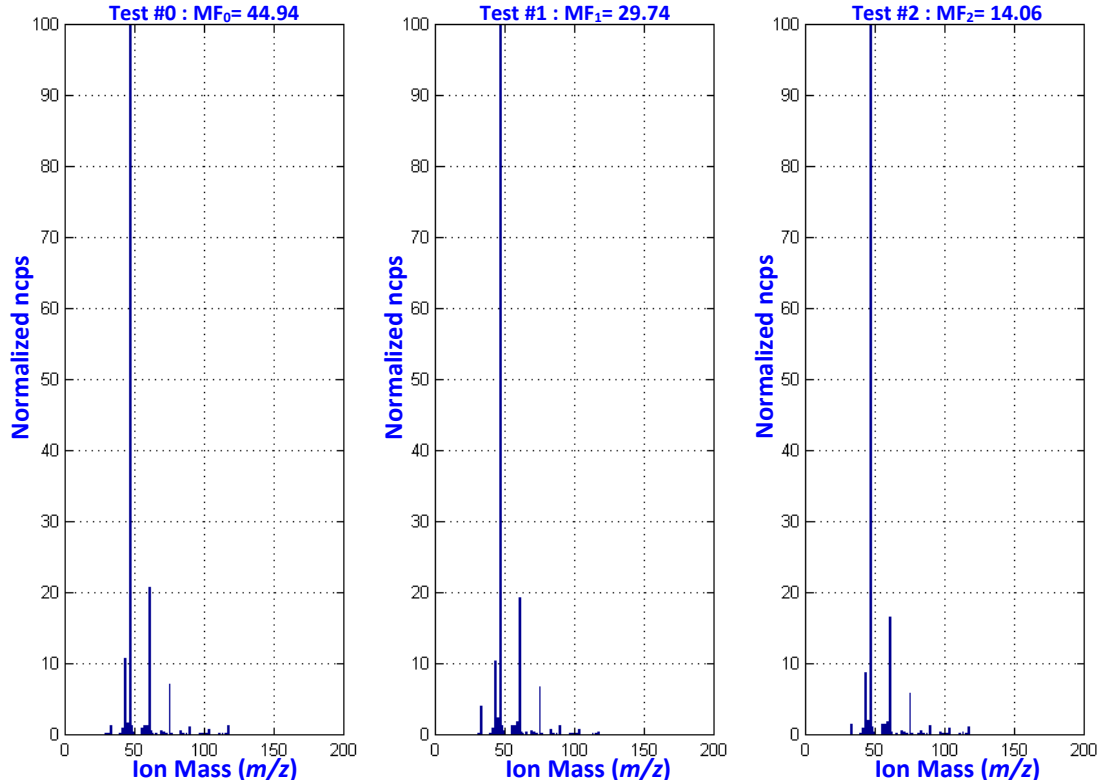
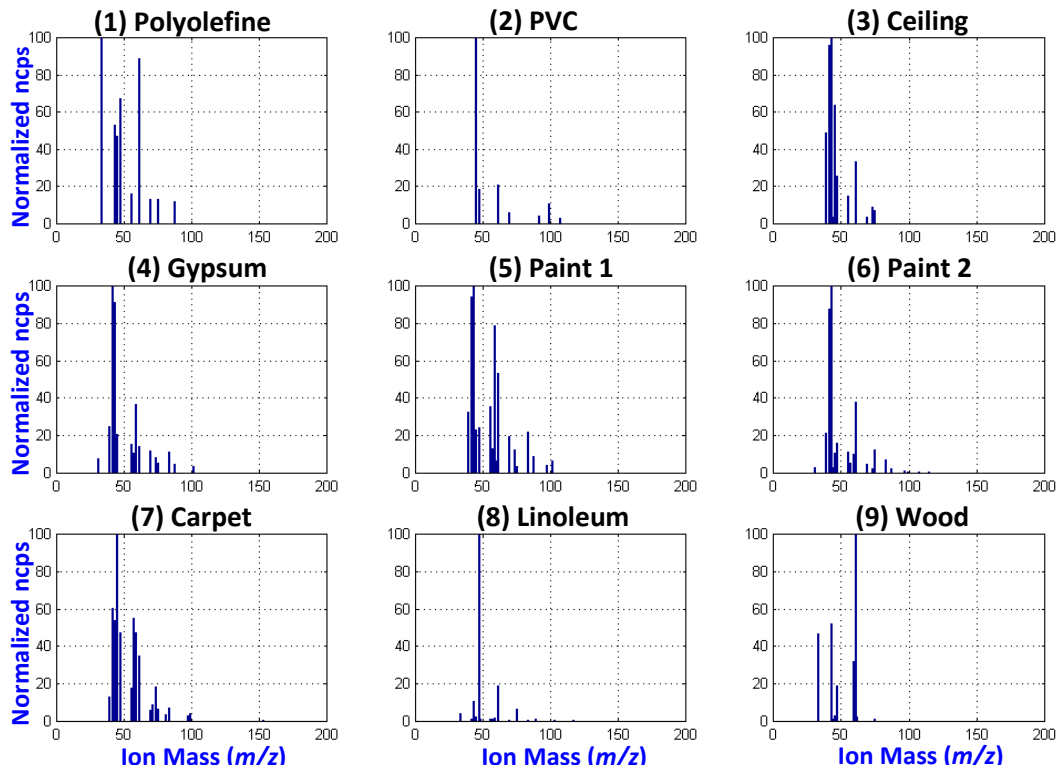


Figure 3.5 Pattern of PTR-MS emission signature for Polyolefine over different sampling time. (a) Top, from the raw signals. (b) Bottom, from the filtered signals.



**Figure 3.6** Consistency of PTR-MS emission signature exemplified for Linoleum among different  $Q_v/A$ .

\* MF: Multiplying factor to get the concentration level of each peak in *ncps* from each profile above (i.e. Conc. = Normalized ncps × MF).



**Figure 3.7** Emission signatures of the tested nine building materials by PTR-MS.

### 3.3.2 Relationship between acceptability and PTR-MS measurements (*ncps*)

In order to examine the relationship between the PTR-MS measurements and the acceptability assessed by human subjects in the previous study (Wargoeki et al., 2007), the *ncps* trend of each ion mass was correlated with  $\log(Q_v/A)$ . As shown in **Figure 3.8a**, for Linoleum as an example, there is a linear decrease of the *ncps* values as  $Q_v/A$  increases logarithmically (i.e. Correlation coefficient:  $-1 < r < -0.93$ ) except for  $m/z = 33$ , methanol. This linear trend was also observed for other eight materials.

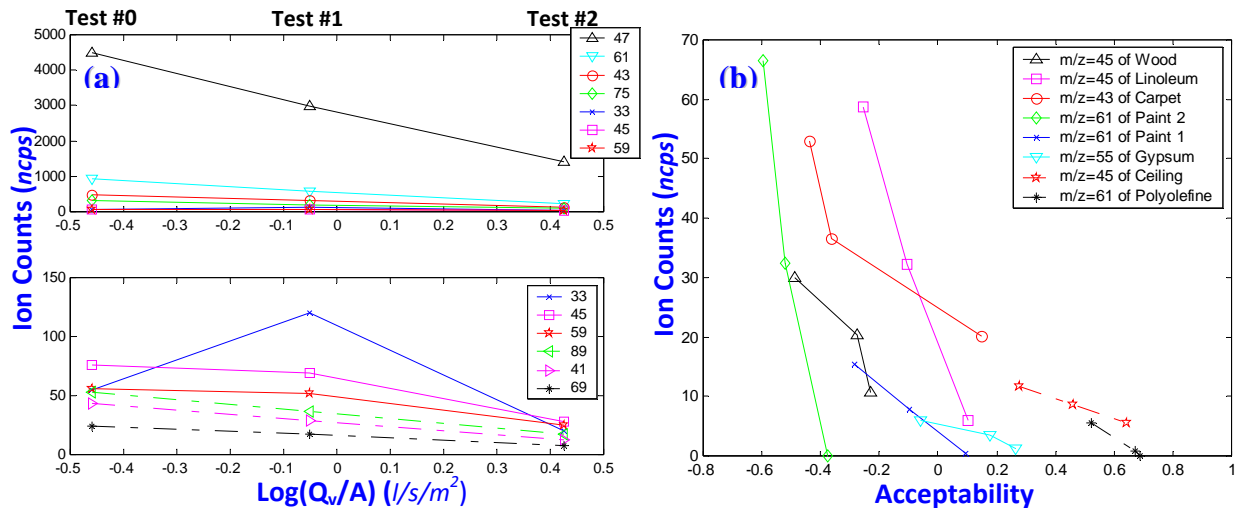


**Figure 3.8 Correlation of the PTR-MS measurements with the acceptability for Linoleum.**

(a) Left, PTR-MS measurements over  $Q_v/A$ . (b) Right, acceptability vs. *ncps* for several materials at the corresponding  $Q_v/A$ .

\* Note: Figure (a) does not contain every trend, but only for selected ion masses with a high level of concentrations or probable to have small odor threshold values.

\* For Figure (b), a good representative ion mass from each material was selected to have a similar range of *ncps* values among different materials for comparison.

The previous human subject study showed that the acceptability had a linear relationship with the change of area-specific ventilation rates in a logarithmic manner (with a positive slope). When combining this result with the findings above from this study, one may

conclude that, within each material investigated in this study, the acceptability is linearly correlated (with a negative slope) with the PTR-MS measurements (*ncps*) which represent the concentration levels of VOCs emitted from each material (i.e. Correlation coefficient  $r < -0.92$  for all trends presented). The higher the values (*ncps*), the lower the acceptability is as expected (**Figure 3.8b**).

### 3.3.3 VOCs responsible for the poor acceptability

What are the major VOCs affecting the human olfactory response to material emissions, which resulted in the acceptability difference as reported in the previous study?

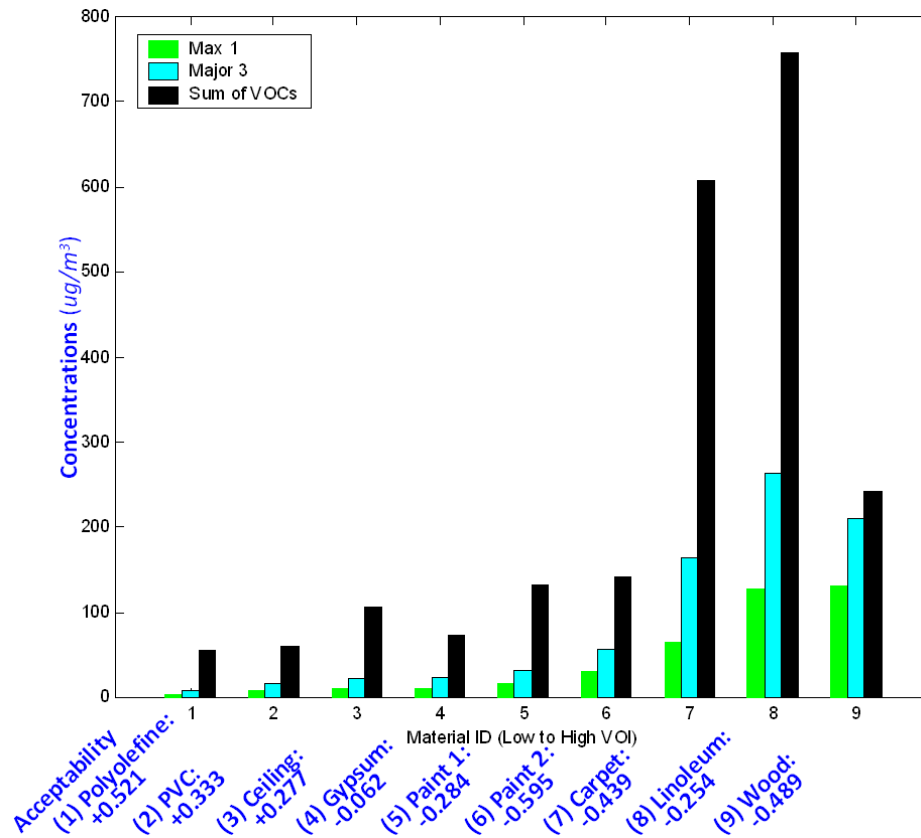


**Figure 3.9** VOC concentrations in the chamber air from the GC/MS analysis results (Test #1).

\* “Max 1”: The maximum individual VOC concentration.

\* “Major 3”: The sum of the top three highest individual VOC concentrations.

\* “Sum of VOCs”: The sum of the concentrations of all VOCs measured.

**Figure 3.9** illustrates how all three quantities of VOC concentrations defined in the figure may be related to the acceptability determined by human subjects (Wargocki et al., 2007): maximum individual VOC concentration (Max 1), sum of the top three highest individual VOC concentrations (Major 3) and sum of the concentrations of all VOCs measured in

reference to toluene (Sum of VOCs). It shows that the three quantities all had lower concentration values for the materials with higher acceptability values, indicating that the outcome of subject assessments might be correlated with the level of most abundant individual VOCs. However, in general, the perceived odor intensity of an individual VOC is better correlated with the ratio of its concentration to the corresponding odor threshold - i.e. the odor index (Knudsen et al., 1999).

We proposed to define a VOC odor index (VOI) as follows:

$$VOI \equiv \sum_{i=1}^N C_i / C_{Th\_i} \quad (3.1)$$

where  $C_i$  represents the PTR-MS concentration level in *ppbv* for each selected VOC,  $C_{Th\_i}$  is its odor threshold in *ppbv* based on the VOCBASE database of the Danish National Institute of Occupational Health (Jensen and Wolkoff, 1996), and  $N$  is the total number of VOCs used in VOI calculation in a given material, selected as follows:

$$N = \begin{cases} 1, & \text{if } OI_2/OI_1 < 20 \% \\ 2, & \text{if } OI_3/(OI_1 + OI_2) < 20 \% \\ 3, & \text{otherwise} \end{cases} \quad (3.2)$$

where  $OI_i$  is the  $i^{th}$  highest OI value.

In Equation (3.2), we applied “80-20% rule” (i.e. do not include an additional compound if its OI (odor index) value is less than 20% of the OI sum for the major VOCs already selected), and only included up to 3 VOCs with the highest OI values to calculate VOI.

The rationale behind this selection is: 1) odor is most likely influenced by the VOCs having high OI values assuming that similar types of odors are present, and 2) threshold values may not be available for all compounds detected and limiting up to 3 major compounds appeared to be practical while sufficient for correlating with the acceptability to be shown from the data in this study. It should be noted that PTR-MS has a much broader detection window of VOCs than other traditional methods (W. Lindinger et al., 1998).

Note also that one may have a cautious mind about applying any database values of odor thresholds for VOCs due to the uncertainty associated with the establishment of these odor thresholds because of methodological differences and wide possible variations in individual human responses (Amoore and Hautala, 1983; Cain and Schmidt, 2009). Because of this caveat that may limit the usefulness of any odor threshold data, Cain and Schmidt (2009) suggested using a homogeneous database of VOC odor thresholds collected by use of a uniform methodology to reduce the limitation of its applicability, presenting an example of this kind of database quoted as Tokyo set (Refer to Nagata, 2003). The present study used the threshold values in the VOCBASE database (which was derived from 3 multiple sources on odor threshold values for the VOCs measured in this study) because of its wide collection of VOC odor thresholds (Jensen and Wolkoff, 1996). Most of the data on odor threshold values for all measured VOCs by PTR-MS in this study could be found in the VOCBASE database except for ethyloxirane,  $m/z = 91$  of PVC,  $m/z = 44$  of Ceiling,  $m/z = 60$  of Paint 1,  $m/z = 44$  of Paint 2,  $m/z = 48$  of Linoleum and  $m/z = 44,60,62$  of Wood. Although this database is a heterogeneous one, most of the values in the database are an order of magnitude larger than those in the Tokyo set,

keeping a similar trend in the relative magnitude (at least for the measured VOCs used in this study). This means that the resulting OI values will be increased when the Tokyo set is applied instead of the VOCBASE used in this study, but still maintaining a similar correlation trend (This trend will be dealt with in the following paragraphs) between the odor assessments and the ratios of VOC concentrations to odor threshold values (because all resulting ratios would be increased altogether with the relative ratio differences among the materials unchanged; see **Figure 3.12** for the result when the Tokyo set is applied)

Both the contribution ratios in **Table 3.2** and the NOI values in **Figure 3.10** illustrate that the odor acceptability is likely determined by a few dominant VOCs that have highest OI values. **Table 3.2** illustrates the possible dominant VOCs among all measured VOCs in each material tested, having relatively high OI values. The corresponding fractional contribution of the selected VOCs to the overall odor index (CR) is also calculated. As shown in **Table 3.2**, the selected VOCs have major contributions (CR = 57~98%) to odor from the materials. In order to compare in a visual sense the portion of the odor impact of the dominant VOCs on human nasal perception compound by compound and material by material, the OI value of each VOC was normalized with the sum of all OIs for the VOCs within the corresponding material, called a normalized OI (NOI) as shown in **Figure 3.10**. The OI value for each compound listed in **Figure 3.10** can be retrieved by multiplying to its NOI value in the figure the sum of odor indices (SOI) for all measured VOCs by PTR-MS in the corresponding material (Note: SOI is given in **Figure 3.10**). The range of SOI for each material was about 0.1~6.7. When the odor threshold values in the Tokyo set are applied, this range of SOI is increased to an order of magnitude larger than that in this study.



Table 3.2 List of possible VOCs responsible for poor acceptability.

Material (ID)	Possible Dominant Odor VOCs	Contribution Ratio (%) <sup>b</sup>
Polyolefine (1)	<u>Nonanal</u> <sup>a</sup> , <u>acetic acid</u> , <u>pentanal</u> ,	81.43
PVC (2)	<u>Nonanal</u> , <u>acetaldehyde</u> , acetic acid	92.21
Ceiling (3)	<u>Nonanal</u> , <u>acetaldehyde</u> , <u>hexanal</u> , acetic acid	89.03
Gypsum (4)	<u>Nonanal</u> , <u>hexanal</u> , pentanal, acetaldehyde, acetic acid	82.76
Paint 1 (5)	<u>Nonanal</u> , <u>hexanal</u> , pentanal, acetic acid, acetaldehyde	79.04
Paint 2 (6)	<u>Nonanal</u> , <u>hexanal</u> , acetic acid, propanoic acid, pentanal	63.66
Carpet (7)	<u>Propanal</u> , nonanal, acetaldehyde, hexanal, acetic acid	65.01
Linoleum (8)	<u>Acetic acid</u> , <u>butanoic acid</u> , <u>propanal</u> , nonanal, pentanoic acid, hexanoic acid	56.50
Wood (9)	<u>Acetic acid</u> , acetaldehyde	97.55

<sup>a</sup> The underlined are included in the VOI calculations defined in Equation (3.1).

<sup>b</sup> The contribution ratio is defined as the ratio of VOI to the total sum of odor indices for all measured/identified species in a material

(i.e.  $CR \equiv 100 \times VOI / \left( \sum_{i \sim \text{every}} C_i / C_{Th\_i} \right)$ , where  $C_i$ :  $i^{\text{th}}$  VOC's PTR-MS concentration, and  $C_{Th\_i}$ : its odor threshold).

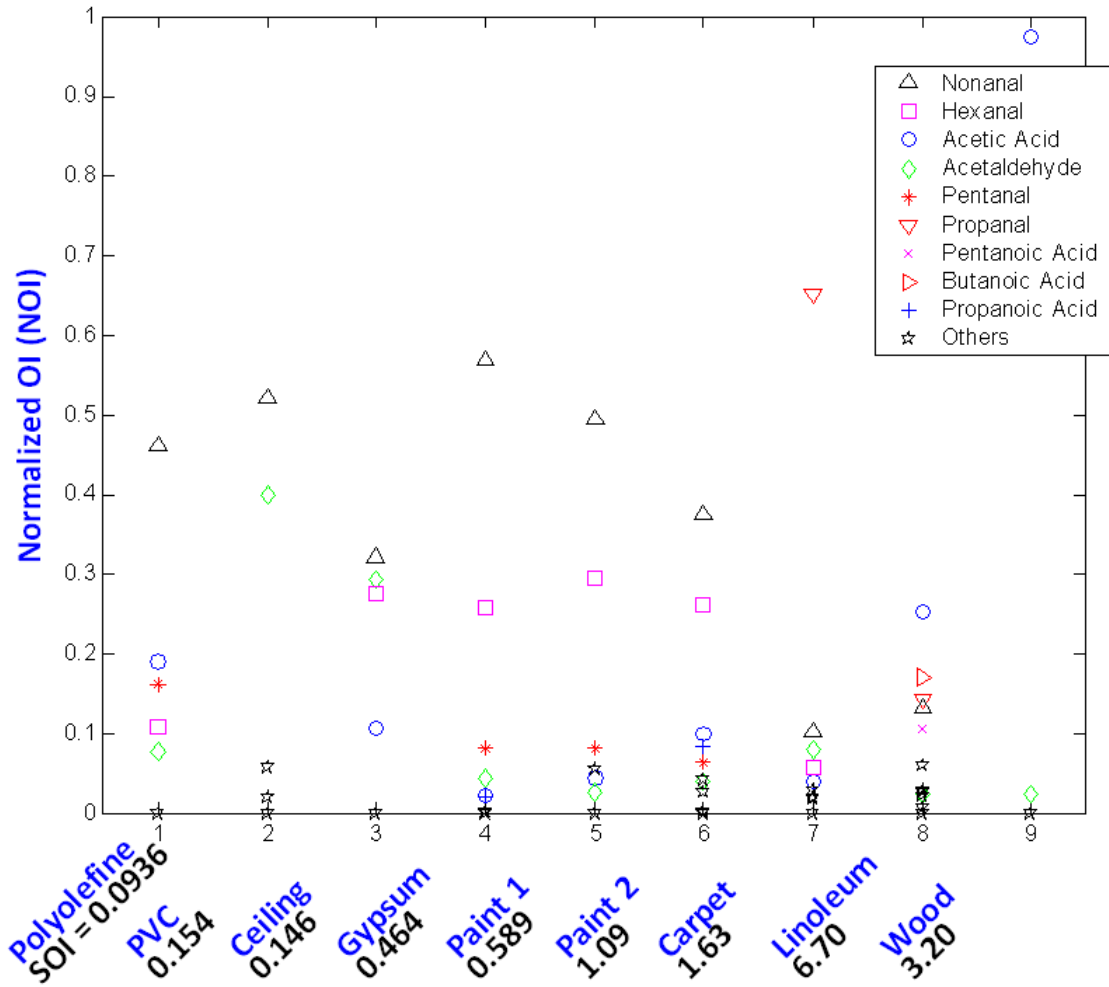
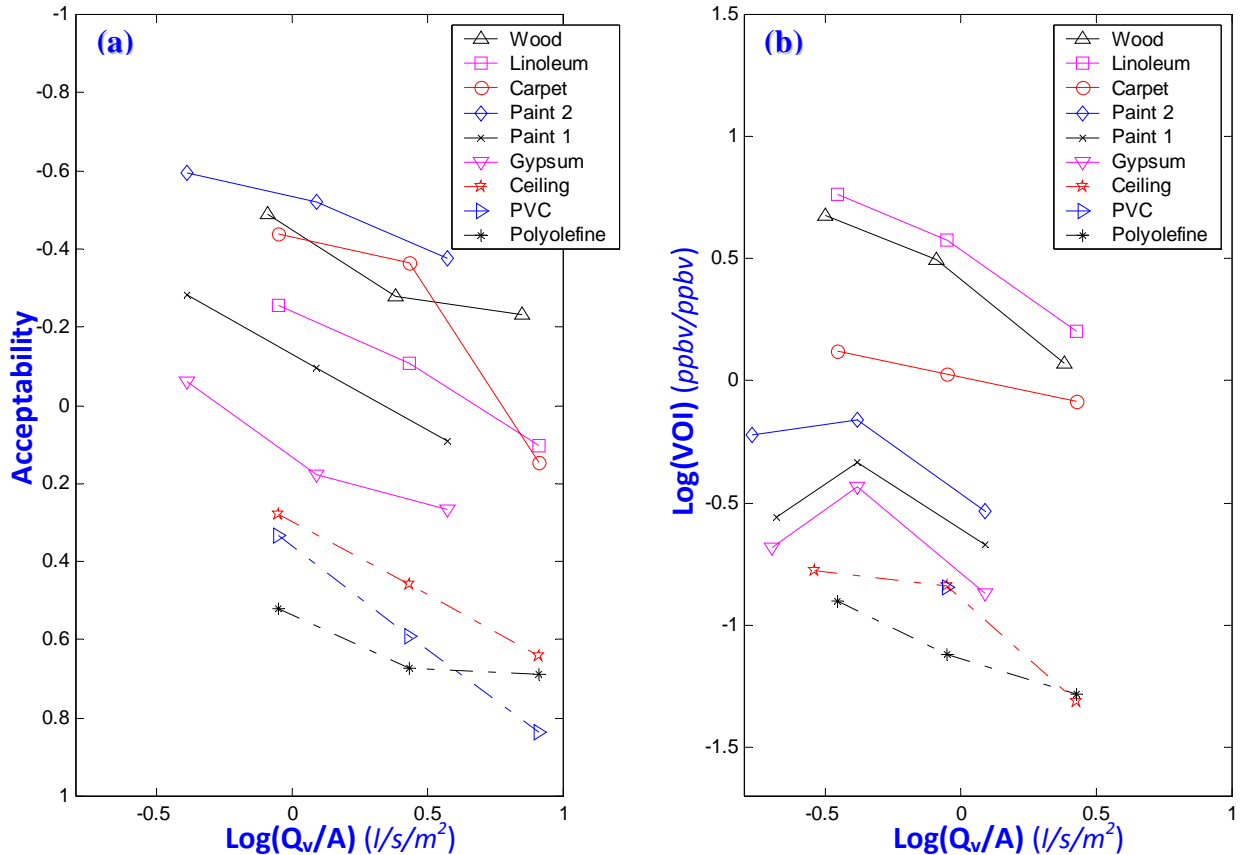


Figure 3.10 Odor index status of all measured VOCs in each material (The name of VOC for each spot displayed in each column can be found in order in Table 3.2 only for the major ones).

\*  $SOI \equiv \sum_{i \sim \text{every}} \frac{C_i}{C_{Th\_i}}$ , where  $C_i$ :  $i^{th}$  VOC's PTR-MS concentration, and  $C_{Th\_i}$ : its odor threshold.

SOI: The sum of odor indices for all measured VOCs by PTR-MS in the corresponding material. This value can be used to restore the OI values of VOCs at Test #1 for each material (i.e.  $OI = NOI \times SOI$ ).



**Figure 3.11 Correlation between acceptability and VOI.**

(a) Material rank according to odor assessments (Note: The axis values of the acceptability are reversed for the purpose of comparison). (b) Material rank according to VOI.

Together with the rank list according to the acceptability from the previous study (Figure 3.11a), Figure 3.11b illustrates the list of material emission ranks in terms of VOI. Except for Paint 2 and Carpet, the relative ranking based on VOI reasonably coincides with that based on the acceptability, keeping similar slopes and relative gaps between each material. Paint 2 had the lowest acceptability in the previous human subject study, while its VOI was not the highest in this study most likely because of the relatively fast decay rate in its emissions over time. Although the materials have been sealed at all times before the tests in the present study, the PTR-MS tests were conducted about three months after receiving the materials, while the human subject study in Denmark had been

performed for the same batch of materials within two months after the purchase. Carpet became a less odorous material than Linoleum based on the VOI value, while it was determined to be more odorous in terms of acceptability, again possibly because of emission decay over time.

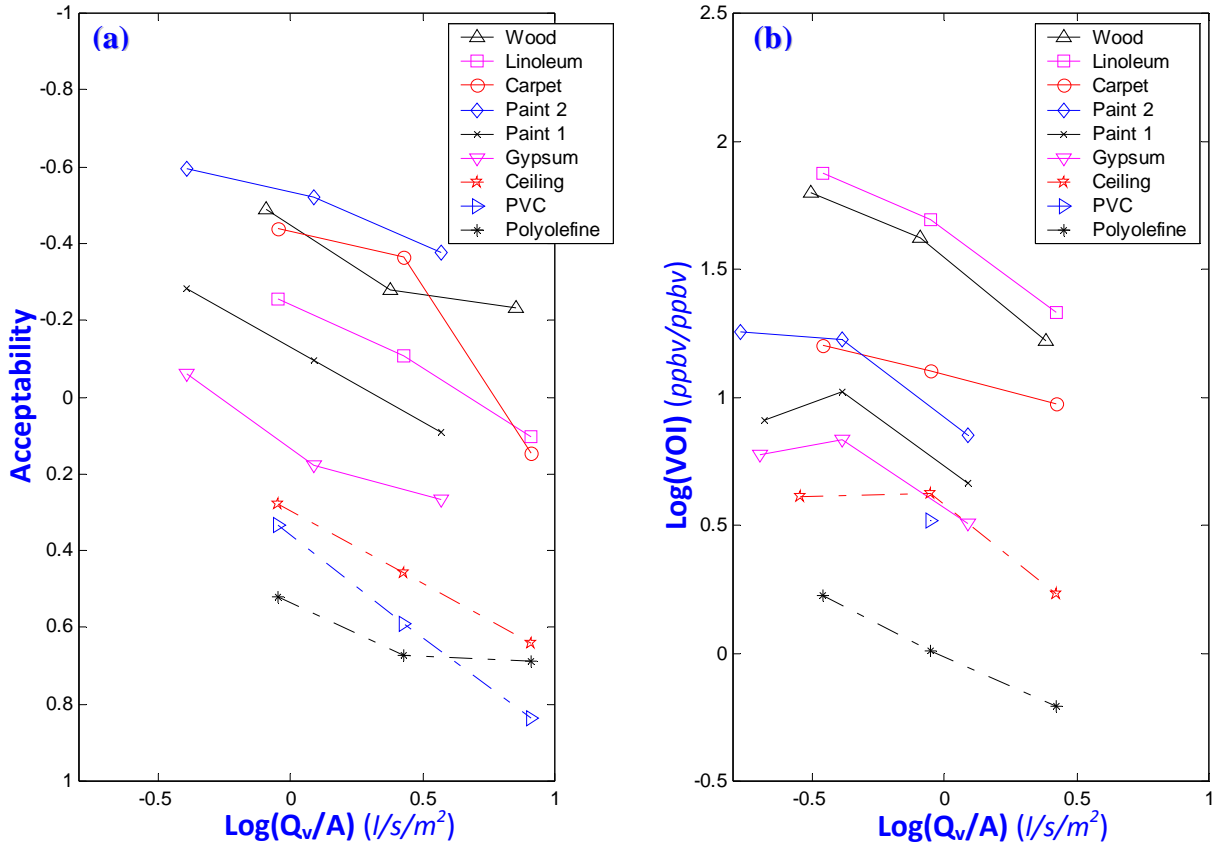


Figure 3.12 Correlation between acceptability and VOC odor index (VOI) with Tokyo set used.

(a) Material rank according to odor assessments. (b) Material rank according to VOI with Tokyo thresholds

Combining the test results from the subject evaluations and the VOC quantity measurements using PTR-MS and GC/MS, the relationship between measured concentration level (represented by VOI in logarithm) and human sensory response (represented by acceptability) can be extracted as shown in **Figure 3.13**. The combined results form an S-shaped curve relationship inversely correlated between concentration quantity and sensory response (Note: Usually, human perceptions to physical stimuli related to stimulus concentration levels have the sigmoid relationship exemplified in Fechner's Law. In other words, at both the edges of stimulus strength, the slope of the human response is decreased, while the response slope is steeper at the middle range of the stimulus strength than those at the edges. In this sense, the term of S-shape was used, although the detailed S-shape was not revealed clearly because there were only three data points for each material). This kind of exposure-response relationship can be found and reported in the literature when researchers tried to reveal the linkage between measured concentration quantity and human sensory response (Knudsen et al., 1998; Sheynin, 2004). From the viewpoint of this relationship, it seems to be possible to estimate the expected impact of each building material on human's perceived air quality and also to label each material's ranking list concerning its potential pollution level based on this kind of odor impact evaluation for the given material using PTR-MS on-line measurements instead of relying completely on human subjects.

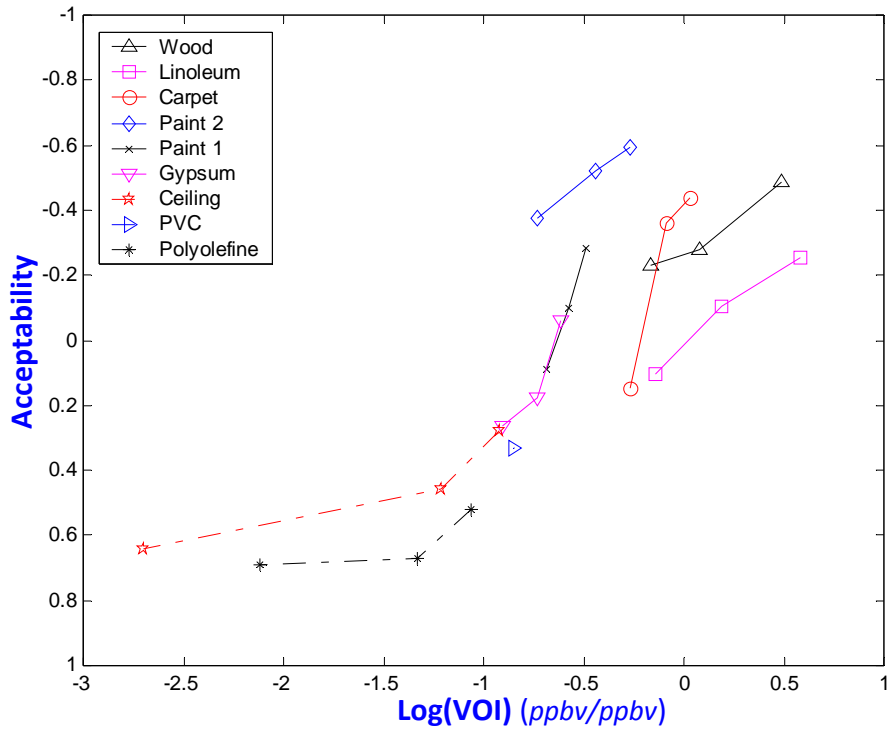
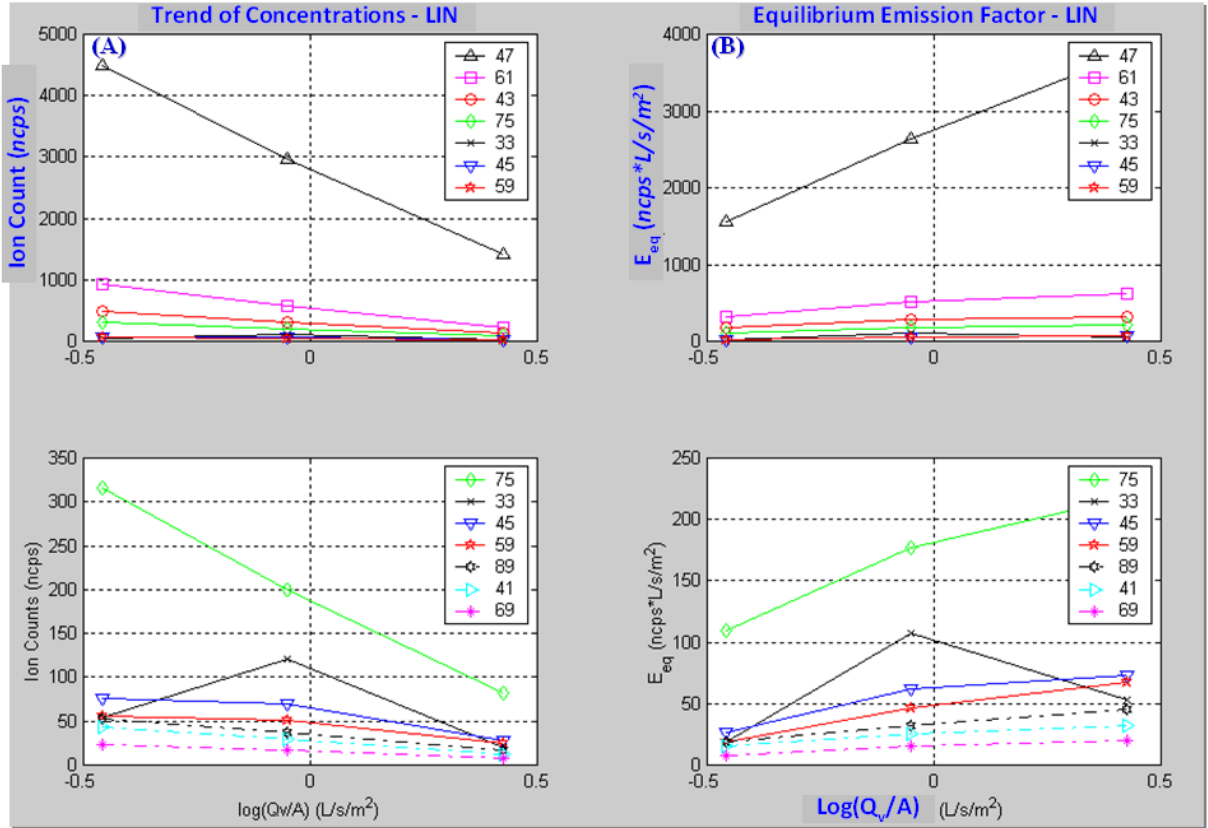


Figure 3.13 The relationship between VOI and acceptability.

### 3.3.4 Emission factor characteristics measured by PTR-MS

The shape steadiness of the emission signatures is related to the different emission factor characteristics of different VOCs in materials, and can be explained from the decomposed plot of the ncps signal trend by each ion mass as shown in **Figure 3.14**. Each ion mass corresponds to a VOC. Sometimes, two or three ion masses represent one VOC due to the fragmentation of the product ions in PTR-MS (e.g. For ethanol,  $m/z = 47, 75$ ; For isopropanol,  $m/z = 41, 43, 39$ ). The investigation on this kind of plots for all the materials tested suggests that building materials may contain VOCs that are either slowly or fast decreasing (decaying) in emission rates. For slow decaying compounds, a clear linear relationship can be established between concentrations and area-specific flow rates ( $Q_v/A$ ) on a log scale (**Figure 3.14**). To clearly see this trend mentioned here, the order of the tests was intentionally conducted as follows, so that there was a time difference among the three consecutive tests: medium level of  $Q_v/A$  (Test #1, in the middle of the figure)  $\rightarrow$  high level of  $Q_v/A$  (Test #2, on the far right)  $\rightarrow$  low level of  $Q_v/A$  (Test #0, on the far left). When this order of the tests was followed, methanol ( $m/z = 33$ ), which is considered to be one of the fast decaying compounds over time in the material, did not show a highest concentration at the lowest  $Q_v/A$  as it would have done so for a slowly decaying (nearly constant over time) emission compound (**Figure 3.14**).



**Figure 3.14** Signal trend of each ion mass for Linoleum over  $\log(Q_w/A)$ .  
 (a) Left,  $ncps$  vs.  $\log(Q_w/A)$ . (b) Right, equilibrium emission factor ( $E_{eq}$ ) vs.  $\log(Q_w/A)$ .



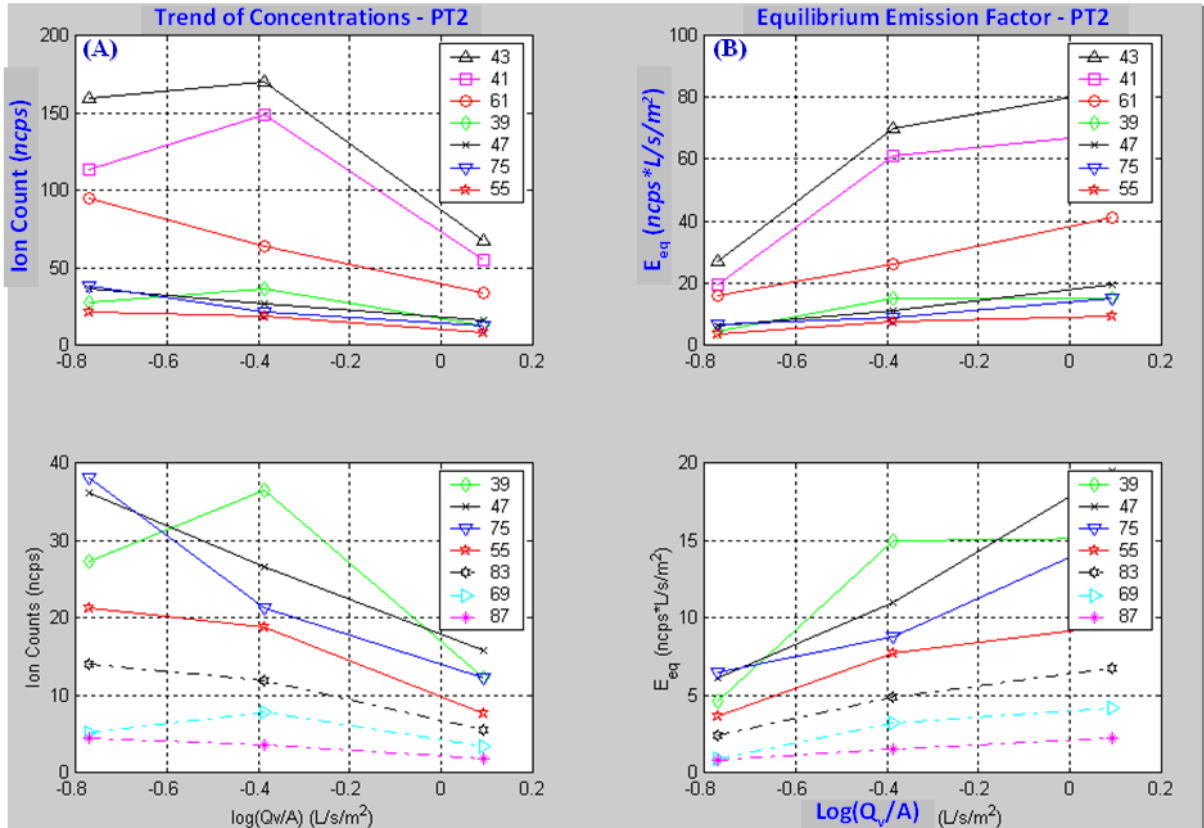


**Figure 3.15** Signal trend of each ion mass for Paint 2 over  $\log(Q_v/A)$ .

(a) Left,  $ncps$  vs.  $\log(Q_v/A)$ . (b) Right, equilibrium emission factor ( $E_{eq}$ ) vs.  $\log(Q_v/A)$ .

**Figure 3.15** shows the  $ncps$  trend of VOCs contained in Paint 2, one of the representative materials having many of the fast decaying compounds over time. Many more of the major compounds in this material exhibited the behavior of VOCs with fast decaying emission rates over time. Those compounds are, for instance, isopropanol ( $m/z = 41, 43, 39$ ), hexanal ( $m/z = 55, 83$ ) and methanol ( $m/z = 33$ ). However, there are still several compounds even in this material having the aforementioned strong linear relationship of concentration with the logarithm of  $Q_v/A$  due to the different emission characteristics like those of the major compounds in Linoleum 2. Acetic acid ( $m/z = 61$ ) and ethanol ( $m/z = 47$ ) are the cases.

**Figures 3.14 and 3.15** show that for many VOCs in a material there is a linear relationship between the logarithm of  $Q_v/A$  and PTR-MS measurements ( $ncps$ , which is proportional to a concentration level) with a negative slope. These findings are in agreement with the experimental results of Lin et al. (2009) and the mass-transfer based diffusion model simulation results of Wang et al. (2006) on VOC emissions. It is also noted that with the exception of methanol (a fast decaying source over time), **Figures 3.14 and 3.15** show a higher emission rate for a higher area-specific flow rate. Anderson et al. (1996) also observed and reported this phenomenon between pollutant concentrations in the air emitted from building materials and VOC emission rates in their paper. This means that the mass transfer across the boundary layer played a significant role in limiting the material emissions from these materials, even though they are considered as dry materials and conventional reasoning was that emissions from such materials had been considered to be primarily internal-diffusion controlled. A higher area-specific flow rate would result in a lower concentration in the chamber air, leading to a higher concentration difference between the material surface and the chamber air, and hence resulting in the increase of a convective mass transfer rate across the boundary layer over the emitting surface. This convective mass transfer rate effect caused by the flow rate change on the emission factor can be seen generally at least in all the building materials tested in this study except for Polyolefine and PVC from which most of the major compounds have almost constant emission factors independent of the flow rate change (**Figure 3.16**). Still, in these two materials, there are some lightweight compounds showing the dependence of their emission rates on the flow rate change, which are acetaldehyde ( $m/z = 45$ ) from Polyolefine and ethanol ( $m/z = 47$ ) from PVC.

The same compound may have a slight different emission characteristic in a different material. But, several compounds still show similar emission characteristics even over different material surfaces. Isopropanol ( $m/z = 39$ ) from Gypsum and Paint 2, and methanol ( $m/z = 33$ ) from Linoleum 2 and Wood (having a fast emission-decaying characteristic over time) are the cases over similar ranges of area-specific ventilation rates. Another observation taken from **Figure 3.16** is that a heavier compound seems to be less affected by the change of a flow rate keeping rather a constant emission factor over the emission surface. On the contrary, a lighter compound can get a huge effect from the flow rate change on its emission factor due to the change of the corresponding concentration difference of the air between the material surface and the chamber air.

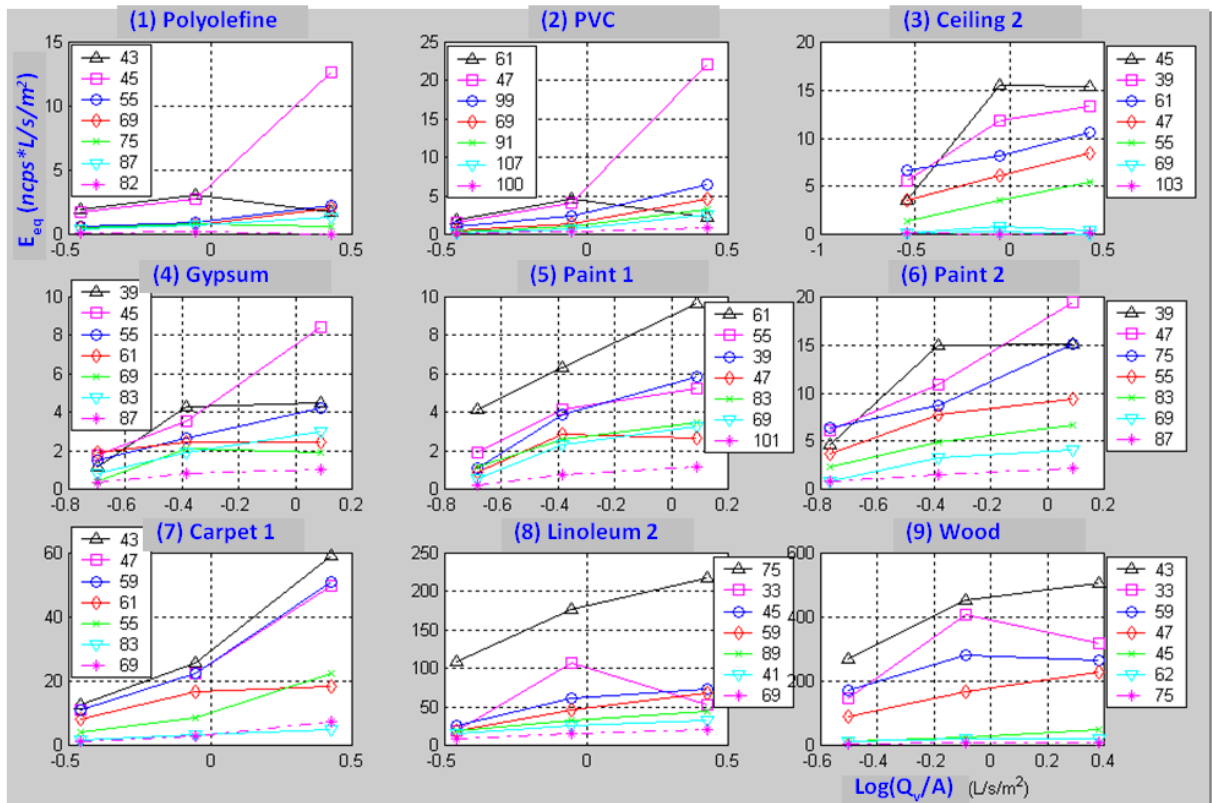


**Figure 3.16** Trend of equilibrium emission factors of VOCs in each material over different area-specific ventilation rates.

\* Note: For the purpose of good visual comparison, any VOC having very high emission factor was not plotted in the above figure.

### 3.3.5 The existence of pair ion masses

During the present experiments, in several cases,  $m/z = RH^+ + 1$  ion masses had also been detected with  $m/z = RH^+$ . For example, as for Wood, one of the major VOCs detected by PTR-MS was  $m/z = 61, 43$  tentatively identified as acetic acid. Together with these ion masses,  $m/z = 62, 44$  were also detected at a relatively small portion, but were not specified as any VOC in the emission signature herein (See [Appendix A\(i\)](#)). One possible way to explain the existence of these pair ion masses is to consider the theoretical isotopic abundances of a given species able to be detected by the device. If the well-established isotopic abundances of  $^2H$  and  $^{13}C$  are taken into consideration, the relative signal intensity of PTR-MS for a given pair ion mass containing the  $^2H$  or  $^{13}C$  atom can be calculated and compared with the intensity of the main ion mass (For the wood case, the main ion masses are  $m/z = 61, 43$ , and the pair ones,  $m/z = 62, 44$ ). The measured isotope ratios defined as  $(RH^+ + 1)/RH^+$  in percentage were observed within the range of 1~8% in the test results, which coincides with the abundance levels of the expected isotope ratios for examined species (e.g.  $m/z = 47, 75; 57; 59; 61, 43$ ). Jobson et al. (2005) also observed this phenomenon, and reported it in their research paper on diesel engine exhaust using PTR-MS. They used this isotopic consideration in testing and detecting the mass interferences of several species laid in one ion mass.

### 3.4 Conclusions

A new method and procedure using PTR-MS was developed to determine the emission signature specific to each building material. The emission signatures of nine common building materials were determined. The measured PTR-MS concentrations were compared to the acceptability of air quality assessed in the previous study for the same batch of materials to investigate the relationships between the quantity and composition of VOCs emitted from the materials and the acceptability determined by human subjects. In addition, a VOC odor index (VOI) was proposed to assess the impact of individual material emissions on perceived air quality that correlates well with the acceptability assessed by human subjects for the materials tested.

The following major conclusions could be drawn from the findings of the study (*Stage 1*) described in Chapter 3:

- ◆ A stable VOC emission signature specific to each type of building material can be established by using PTR-MS with the signal processing method and procedure developed in the present study. A dataset for the nine common building materials tested was obtained using the procedure. The signatures were found not to vary with area-specific ventilation rates for the duration and conditions of testing.
- ◆ The signal intensity (*ncps*, which corresponds to a concentration level) of the PTR-MS measurements had a tendency to linearly decrease with the change of area-specific ventilation rates,  $\log(Q_v/A)$  in a logarithmic manner for most compounds emitted from the building materials studied.

- ◆ The acceptability of chamber air decreased linearly with the PTR-MS measurements (*ncps*) for the materials studied.
- ◆ The logarithm of VOI, defined as the sum of ratios of concentrations to odor threshold values of up to three compounds with highest concentration-to-odor threshold ratio, was found to be inversely correlated with the acceptability. This is in agreement with the previous findings on the relationship between concentration measurements and odor responses, suggesting the validity of the proposed VOI.
- ◆ The material ranking based on the VOI using the PTR-MS measurements provided a similar ranking of the tested materials to that in terms of acceptability, and may be used for evaluating the impact of each material on perceived air quality.

The correlation between VOI and perceived air quality derived in this study may be valid only for the nine building materials investigated here because the materials tested appeared to have similar types of odors. A broader range of materials and types of odors should be investigated before the approach can be widely applied. The selection of up to three VOCs in defining VOI is somewhat arbitrary, and its implementation may be difficult if the VOCs are not known or the corresponding odor thresholds are not determined. In addition, emission signatures may change over the course of long-term emissions. Further study is needed to account for such variation over time (e.g. by using appropriate emission source models).

This page is intentionally left blank.

## † CHAPTER 4. NOVEL METHODOLOGY FOR INDOOR EMISSION SOURCE IDENTIFICATION

---

### 4.1 Introduction

Source identification has been a challenging research topic in the area of indoor and outdoor air quality because this issue may have the key to open a new gate to develop optimal control protocols for protecting and improving human's life and welfare for the coming ages. Over the last several decades, emissions of VOCs and Particulate Matter (PM) have been of global concern because of their significant impact on human's health, comfort and performance. Exposure to these air pollutants has been reported to have various critical impacts on human performance and cardiovascular/respiratory related diseases in a negative way (Pope and Dockery, 2007; Wargocki and Wyon, 2006). For example, Corbett et al. (2007) examined the link between PM emissions from ships and human's health, assessed their potential impact leading up to 60,000 premature deaths on a global scale annually and expected a further mortality increase by 40% by 2012 under current regulations and activity conditions. In addition, VOCs have been shown to act as precursors of many secondary air pollutants such as organic aerosols and ozone (Buzcu and Fraser, 2006). High level of ozone beyond the specified limit in the standard is also posing another severe concern of global air quality, which is in an increasing trend



especially in many cities of USA. Moreover, this widespread concern about the critical potency of VOC and PM emissions on human's life and health is expected to increase far more than the present situations in the coming years because of the fast growing rate of global-scale commercial trade and worldwide distributed manufacturing, the associated increase of vehicle/ship/air traffics and the corresponding massive use of diesel/gasoline fuels (Corbett et al., 2007; EPA, 2009).

Although the predicted threats of these emissions have succeeded in attracting worldwide attention for reducing these emissions, it has been generally agreed that the present countermeasures for dealing with these emissions were not sufficient to protect human's health (EPA, 2009). Because different sources of air pollution may affect the exacerbation of human's health effects in different ways, it has been suggested as a desirable countermeasure to identify and quantify the partial contribution each type of major air pollution source makes to the overall air quality condition (Lin et al., 2010). In addition, the accurate and complete apportionment of these pollution sources is regarded as an essential step to the development of optimal control protocols for global and built environments (Lin et al., 2010).

Source identification and apportionment has been an active research subject for outdoor air quality, but existing methods have shortcomings. Many receptor modeling studies have been performed on ambient air quality data collected for this apportionment purpose (Cass, 1998; Cincinelli et al., 2003; Didyk et al., 2000; Edwards et al., 2001; Hagler et al., 2006; Graham et al., 2004; Lewis et al., 2004; Simoneit, 2002; Wu et al., 2007). Traditional receptor modeling methods require site-specific source profiles to accurately

estimate the contribution of different sources. Previous source apportionment studies have used Chemical Mass Balance (CMB) model (Fujita et al., 2003; Schauer et al., 1996). The CMB model assumes that the concentrations of target species in the ambient air are linear sums of each contributing source and that all potential sources for significant contribution to the receptor have been identified and characterized. This approach has a limitation in identifying any new or unknown sources. On the other hand, Positive Matrix Factorization (PMF) is an advanced multivariate receptor modeling technique (Paatero and Tapper, 1994), identifying source profiles for the major sources present by cluster analysis and calculating site-specific source profiles together with time variations of these sources based on correlations embedded in the ambient air data (Begum et al., 2004; Buzcu and Fraser, 2006; Kim et al., 2003, 2004, 2008; Ramadan et al., 2000; Viana et al., 2009). The limitation of this method is that the characteristics of the sources to be identified should be inferred from or interpreted by the characteristics of the profiles for several key factors identified. With the mentioned drawbacks of the two apportionment methods above, there is another critical limitation of these traditional tools. These two receptor-based apportionment methods, CMB and PMF, are most common techniques used nowadays for the source apportionment purpose, but are known to have high bias for some cases because of high variability and complexity of VOC/PM emissions, which makes the results from these methods as rough estimates on the profile of sources not knowing the true profile of emission sources (Zhao et al., 2007). Most compounds can be emitted from multiple types of sources, and thus identifying and quantifying sources on the basis of their correlation with several elemental data is limited and difficult because of similar emission characteristics of different sources.

Different from the area of outdoor air quality, indoor source identification has rarely been studied with a few exceptions (Arhami et al., 2010; Jia et al., 2010; Liu and Zhai, 2007, 2008; Zhang and Chen, 2007), and the problem has its challenge because of both indoor and outdoor sources. The global issues VOC/PM emissions are posing and the corresponding human health concerns are also important in the area of indoor air quality, because indoor air has been reported to be strongly affected by outdoor air via traffic emissions and long-range transport pollutants (Edwards et al., 2001; Zhao et al., 2007) as well as indoor sources. In many cases, it has been known that the strength of indoor emissions has a more significant influence on indoor VOC concentrations than the effect of infiltration from outdoor air (Kim et al., 2001). One of the recent important research challenges in the field of indoor air quality is the identification of emission sources of indoor VOCs. In several field studies performed for residential buildings to measure VOC emissions, it was possible to identify several active compounds with great potency to human health and perception, and their chemical measurements were reported. However, it was hard to trace the emission sources of the detected compounds clearly. As an example, Hodgson et al. (2000) reported that source reduction treatment via substitution of materials or modification of building practices could be generally the preferred method for reducing occupants' exposures to VOCs. They identified acetic acid as one of the important compounds, but were not certain about the sources of acetic acid in the studied houses. To establish an effective countermeasure against unwanted VOC emissions, emission sources need to be identified. A first step toward a source identification would be to determine a material emission signature if it is unique for each material or each type of material. This is similar to human's fingerprint for personal identification. A study previously conducted to deal with this issue (Han et al., 2010)

showed that unique emission patterns appeared to exist for different types of building materials. These patterns, or signatures, could be established by using PTR-MS. Several studies performed in other research areas such as food engineering, medical research, forensic investigations, etc. implied that pollutant mass spectra measured by this on-line analytical device, PTR-MS, could be useful tools for detection and identification purposes (Granitto et al., 2007, 2008; Lirk et al., 2004; Mayr et al., 2003; Moularat et al., 2008; Van Ruth et al., 2007; Wehinger et al., 2007; Whyte et al., 2007). With the definition of emission signatures of different building materials, it may be possible to develop a signal processing technique that can help pinpoint the materials responsible for certain VOCs of concern in indoor air. The objectives of the study in Chapter 4 were to explore the feasibility of a signal processing methodology for emission pattern recognition, validated by Monte-Carlo simulations by setting related simulation variables based on PTR-MS experimental measurements, and to apply the method to several actual data of material mixture emissions for identifying the individual sources of emissions based on the measurements of mixed air samples and the PTR-MS emission signatures of individual building materials.

## 4.2 Materials and Methods

### 4.2.1 Overview and basic assumptions

In a previous study (Han et al., 2010), chamber exhaust air polluted by the emissions from nine individual building materials in a 50-l small-scale chamber was sampled by PTR-MS at low, medium and high airflow rates to establish a set of material emission signatures stable over different sampling time and over different area-specific ventilation rates, and to determine their variances because of noise. The signature is the PTR-MS ion mass ( $m/z$ , which is a physical quantity denoting the mass-to-charge ratio widely used in the electrostatics of charged species) spectrum of the air sampled from each material. Five actual emission cases of material mixtures were studied to validate source identification methods developed. The experimental setup is shown in **Figure 4.1**, and the detailed illustrations of the test equipment and facilities can be found in **Appendix B**. Two signal separation methods were proposed, tested using measurement-based Monte-Carlo simulations, and validated on the five multi-material mixtures. Before going into details, it would be useful to formally state the basic assumptions the separation methods were based on: 1) Emission signature exists and is unique for each material type, 2) Interaction effects between material emissions are small and can be modeled as noise or compensated, and 3) Emission signatures for material mixtures can be established by the superposition of individual emission signatures of the co-located materials.

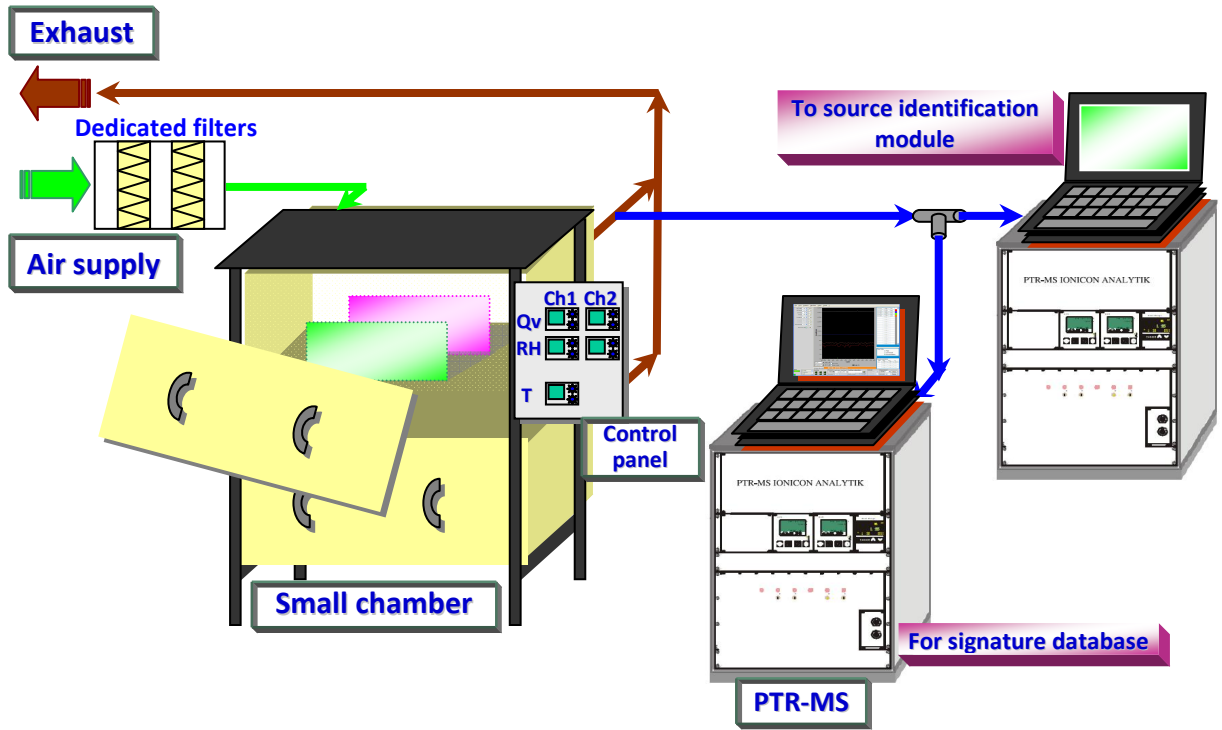


Figure 4.1 Experimental setup for the validation of source identification method.

## 4.2.2 Algorithms for source identification module

### 4.2.2.1 Algorithm 1

Under the basic assumptions stated in the overview, the source identification problem to be examined in this study can be configured as the estimation of the set of materials present in the chamber {ID} expressed in terms of a set of integer material identification numbers, or IDs (i.e.  $i = 1, 2, \dots, 9$  defined in **Table 4.1** for each material) and the corresponding emission concentration level of each identified material expressed as a positive real number  $\alpha_i$  which is the signal intensity multiplication factor of material  $i$ . The measured output from PTR-MS is a mass spectrum of the emissions from a material mixture, consisting of ion mass  $\mathbf{x}$  (related to VOC) and its signal intensity  $S_{sp}(\mathbf{x})$  (related to concentration level) for all scanned ion masses  $\mathbf{x}=[x_1, x_2, \dots, x_N]$ . Measurements from single material emission tests have shown that measured signal noise  $w(x_n)$  of PTR-MS for each ion mass  $x_n$  (where  $n=1, 2, \dots, N$ ) can be roughly modeled as independent Gaussian noises having the same variance throughout the target ion masses (Note: Several ion masses for the background air such as  $m/z = 29, 30, 32$  and  $37$  had larger variances than others, so those were excluded from the target ion masses). Now, the measured emission signature of a material mixture by PTR-MS can be modeled as follows:

$$S_{sp}(x_n) = \sum_i [\alpha_i \cdot S_i(x_n) + w_i(x_n)] \text{ for } \forall x_n, \text{ with } \alpha_i > 0 \text{ for } \forall i, n = 1, 2, \dots, N \quad (4.1)$$

where  $sp$  represents ‘the measured sample’,  $i$  indicates the material ID of the correct material set for the mixture, defined in the database of material emission signatures,  $S_{sp}(x_n)$  is the PTR-MS signal intensity (not normalized) of the measured sample for a

given ion mass  $x_n$ ,  $S_i(x_n)$  is the normalized magnitude of emission signature for a given ion mass  $x_n$  of material  $i$  (Note: An emission signature for each studied material is recorded in the database in a normalized form having a peak magnitude of 100 as its maximum. For details, see Chapter 3),  $w_i(x_n)$  is the independent measurement noise for the ion mass  $x_n$  contained in the signal for material  $i$ , and  $\alpha_i$  is the signal intensity multiplication factor of the emission signature for material  $i$ .

The measured sample signature can also be expressed in a vector form as follows:

$$\mathcal{S}_{sp}^{\mathcal{P}}(\mathbf{x}) = \sum_i [\alpha_i \cdot \mathcal{S}_i^{\mathcal{P}}(\mathbf{x}) + \mathcal{W}_i^{\mathcal{P}}(\mathbf{x})] \quad (4.2)$$

where  $\mathcal{S}_{sp}^{\mathcal{P}}(\mathbf{x})$  represents the sample signal intensity vector measured for all scanned ion masses  $\mathbf{x}$  defined as  $\mathcal{S}_{sp}^{\mathcal{P}}(\mathbf{x}) \equiv [S_{sp}(x_1), \Lambda, S_{sp}(x_n), \Lambda, S_{sp}(x_N)]^T$ ,  $\mathcal{S}_i^{\mathcal{P}}(\mathbf{x})$  is the normalized magnitude vector of the emission signature for material  $i$  defined as  $\mathcal{S}_i^{\mathcal{P}}(\mathbf{x}) \equiv [S_i(x_1), \Lambda, S_i(x_n), \Lambda, S_i(x_N)]^T$ ,  $\alpha_i$  is given in Equation (4.1),  $\mathcal{W}_i^{\mathcal{P}}(\mathbf{x})$  is the corresponding signal noise vector for material  $i$  defined as  $\mathcal{W}_i^{\mathcal{P}}(\mathbf{x}) \equiv [w_i(x_1), \Lambda, w_i(x_n), \Lambda, w_i(x_N)]^T$ , and  $x_n$  is the  $n^{\text{th}}$  ion mass in the scanned range (Note: If there is no corresponding peak for the  $n^{\text{th}}$  ion mass recorded in the emission signature of material  $i$ , then  $S_i(x_n) = 0$  in this representation).

To perform a signature separation and identification when  $\mathcal{S}_{sp}^{\mathcal{P}}(\mathbf{x})$  is the measurement from PTR-MS, let us define  $Ind(\mathcal{S}^{\mathcal{P}}(\mathbf{x}))$ , where  $Ind(.)$  is the set of ion mass indices



corresponding to a given emission signature intensity vector  $\overset{p}{S}(\mathbf{x})$ , with positive (or non-zero) signal intensities. Then, in the first step, the set of possible material candidates  $\{db\}$  in the database can be searched by comparing the ion mass components (related to VOC components in a physical sense) of each material emission signature  $Ind(\overset{p}{S}_i(\mathbf{x}))$  with the measured ones  $Ind(\overset{p}{S}_{sp}(\mathbf{x}))$  under the epsilon condition ( $\varepsilon$ ) to be defined below. While performing the comparison between the measurement and the database signatures, if all ion mass components of a signature are found in the measurement, then that material  $i$  related to the signature will be selected as a possible material candidate (i.e.  $i \in \{db\}$ ), having all VOC components to be found. However, due to noise, some ion masses that should be found in the measurement might be missed or measured falsely as any near ion masses. For example, the emission signature for Wood (Material ID=9) has ten ion mass indices including  $m/z = 33, 43, 44, 45, 47, 59, 60, 61, 62$  and  $75$ , so  $Ind(\overset{p}{S}_9(\mathbf{x})) = \{33, 43, 44, 45, 47, 59, 60, 61, 62, 75\}$ . If the component indices of the measurement from PTR-MS are given as  $Ind(\overset{p}{S}_{sp}(\mathbf{x})) = \{33, 43, 44, \mathbf{46}, 47, 59, 60, 61, 62, 69, \mathbf{76}, 83\}$ , in order for Wood or  $i=9$  to be selected as a possible material candidate, the mismatched two ion masses ( $m/z = 45$  and  $75$ ) should be checked whether they are present in the actual emissions, but measured wrongly (as  $m/z = 46$  and  $76$ ) due to noise. For this case, the epsilon condition, which considers the tolerable square error level along the ion mass axis, was considered. We assume that the noise occurring along ion masses can be modeled as an independent Gaussian noise having much lower variance than that of signal intensity for each ion mass. The missing of any correct materials due to this noise along ion masses can now be considered in the Chi-square distribution by setting a threshold value

enabling the detection of the material at a 95% confidence level. This threshold value is a one-sided detection limit and can be determined based on actual PTR-MS measurements.

These considerations can be summarized as Step 1 such that:

**Step 1.** If  $Ind(S_{sp}^p(\mathbf{x})) \supset^{\varepsilon} Ind(S_{db}^p(\mathbf{x}))$  where  $\varepsilon = \sum_{n\text{-no matched}} (x_{n\_sp}^{(near)} - x_{n\_db})^2$  and  $\varepsilon \leq Thresh$

(95% confidence level), then find  $\{db\}$ .

Here,  $x_{n\_sp}^{(near)}$ , which is an element of  $\{x_n\}$  of the measured sample, denotes the nearest ion mass component in the sample emission signature with a positive signal intensity to an ion mass ( $x_{n\_db}$ ) for which there was no match in the attempted emission signature in the database because of noise. For example,  $\varepsilon = (46-45)^2 + (76-75)^2 = 2$ . If the calculated threshold value for detection (in this case, for two degrees of freedom) is larger than 4, Wood or  $i=9$  can be selected as a possible material candidate. But, if the detection threshold is less than 2, Wood or  $i=9$  will not be included in the candidate set.

Assuming  $w_i(x_n)$  is an i.i.d. Gaussian noise (Note: i.i.d. stands for ‘independent and identically distributed’), the signal intensity factor of each material candidate  $\alpha_i$ , where  $i \in \{db\}$ , can be determined via the following linear regression approach such that:

**Step 2.** Find an optimal value of each  $\alpha_i$  for  $i \in \{db\}$ , which minimizes the following performance index  $J$  (i.e. in the sense of MRLS, multiple regression least squares. For detailed descriptions, see Cohen et al., 2003).

$$J \equiv \min_{\{\alpha_i\}} \sum_{n \sim \text{all scanned}} \left( S_{sp}(x_n) - \sum_{i \in \{db\}} \alpha_i \cdot S_i(x_n) \right)^2 \quad (4.3)$$

Here, it should be noted that  $\alpha_i$ s are unknown control variables to be estimated in the sense of MRLS while  $S_{sp}(x_n)$  is measured by PTR-MS and  $S_i(x_n)$  is given in the database for all scanned ion masses, where  $n=1, 2, \dots, N$ .

The first step of the algorithm is the scanning of the ion mass components in the measured sample emission signature by the comparison with those in the database. Because of noise, several components can have small deviations from the exact values of ion masses. So, the algorithm tries to find any matching emission signatures in the database (a set of materials denoted as  $\{db\}$ ), having the same ion mass components under the  $\varepsilon$  condition described above. Next, by using only the selected set of material emission signatures  $\{db\}$ , the algorithm attempts to find the optimal set of signal intensity factors  $\alpha = [\alpha_{ID_1}, \dots, \alpha_{ID_j}, \dots, \alpha_{db}]$ , where  $ID_j$  is the  $j^{\text{th}}$  material ID in the set of  $\{db\}$  selected as possible material candidates. If the final value of  $\alpha_i$  is less than a specified small threshold value (e.g. 10% of the smallest signal intensity factor in the database, 0.007), then material  $i$  will be excluded from the final set of the material candidates  $\{ID\}$ .

#### 4.2.2.2 Algorithm 2

Let us set up the problem as  $w_i(x_n)$  being a function of the spectrum of  $x_n$ , where  $n=1, 2, \dots, N$ . In Algorithm 1, the error value for a relatively small signal peak contributes less (although it might be an important peak for detection and identification) to the overall performance index than larger peaks. So, a normalization technique for adjusting the

weight for each term might be useful to reflect in the overall error terms the contributions of the errors for any small peaks in the proportion comparable with those of larger peaks. The other definitions and procedure are the same as those of Algorithm 1 except for the definition of the performance index  $J$  as follows:

$$J \equiv \min_{\{\alpha_i\}} \sum_{n \sim \text{all scanned}} \left[ \left( S_{sp}(x_n) - \sum_{i \sim \{db\}} \alpha_i \cdot S_i(x_n) \right)^2 / S_{sp}(x_n) \right] \quad (4.4)$$

#### 4.2.3 Environmental chamber setup and conditions

A 50-l small-scale environmental chamber (0.5 m × 0.4 m × 0.25 m high) made of electro-polished stainless steel (**Figure 4.1**) was operated with a precise airflow controller (*Alicat Scientific*, accuracy ±0.1% of measured values) and a humidity controller (*Vaisala INTERCAP HMP50*, accuracy ±1% of measured values), using external supply air passing through a dedicated filtering assembly (*Wilkinson* 3-stage carbon filters with micro filtration). The chamber was maintained at a constant stable temperature in the range of 23.5-25.4°C (with a small variation of < ±0.02°C during each sampling period) and at a stable relative humidity of 31 ± 0.1% RH during the tests. The background concentrations of individual VOCs in the empty chamber were maintained clean to be less than 1 µg/m<sup>3</sup>.

#### 4.2.4 Test specimens

**Table 4.1 Flow rates and specimen areas determining the concentrations of emissions for the PTR-MS experiments.**

Material (ID#)	Flow rate – $Q_v$ (l/min) / Specimen area – $A$ (cm <sup>2</sup> ) $Q_v/A$ (l/s/m <sup>2</sup> )							
	Meas. #1	Meas. #2	Meas. #3	Meas. #4	Meas. #5	Meas. #6	Meas. #7	Meas. #8
<b>Ceiling (3)</b>	0.50 / 290.7 0.29	1.55 / 290.7 0.89	4.64 / 290.7 2.66				1.55 / 290.7 0.89	1.28 / 290.7 0.73
<b>Wood (9)</b>	0.50 / 265.5 0.31	1.30 / 265.5 0.81	3.85 / 265.5 2.42		1.28 / 265.5 0.80	1.21 / 265.5 0.76	1.55 / 265.5 0.97	1.28 / 265.5 0.80
<b>Carpet (7)</b>	0.50 / 240 0.35	1.28 / 240 0.89	3.83 / 240 2.66	1.28 / 240 0.89			1.55 / 240 1.08	1.28 / 240 0.89
<b>Linoleum (8)</b>	0.50 / 240 0.35	1.28 / 240 0.89	3.83 / 240 2.66	1.28 / 240 0.89	1.28 / 240 0.89	1.21 / 240 0.84	1.55 / 240 1.08	1.28 / 240 0.89
<b>PVC (2)</b>	0.50 / 240 0.35	1.28 / 240 0.89	3.83 / 240 2.66					1.28 / 240 0.89
<b>Polyolefine (1)</b>	0.50 / 240 0.35	1.28 / 240 0.89	3.83 / 240 2.66					
<b>Gypsum (4)</b>	0.50 / 416 0.20	1.03 / 416 0.41	3.08 / 416 1.23					
<b>Paint 1 (5)</b>	0.50 / 402 0.21	0.99 / 402 0.41	2.97 / 402 1.23					1.28 / 402 0.53
<b>Paint 2 (6)</b>	0.50 / 490.2 0.17	1.21 / 490.2 0.41	3.63 / 490.2 1.23			1.21 / 490.2 0.41	1.55 / 490.2 0.53	1.28 / 490.2 0.44

\* Meas. stands for 'Measurement'.

\* Measurements #1-3: from single material tests.

\* Measurements #4-8: from material mixture tests with the selected materials put in the chamber together.

Nine typical building materials were used including ceiling, wood, carpet, linoleum, PVC, polyolefine, gypsum, paint 1 (water-based acrylic) and paint 2 (with linseed oil) applied on gypsum board. The detailed descriptions of the materials tested can be found elsewhere (Han et al., 2010). Specimens were cut and prepared according to the sizes

specified in **Table 4.1**. The specimens except for Gypsum, Paint 1 and 2 were stapled together back to back in order that only the material upper surface was exposed to the air in the test chamber. A VOC-free aluminum tape (*3M 2113*) was applied to seal all edges. The prepared specimens were placed vertically, parallel with the airflow in the chamber (the same direction of the long side of the chamber). The range of area-specific ventilation rates defined as the ratio of ventilation rate to emitting surface area was set by adjusting the airflow to the chamber while keeping the size of specimen unchanged.

#### 4.2.5 PTR-MS setting

A PTR-MS device (*Ionicon Analytik high-sensitivity model with a detection limit as low as 1 pptv, Austria*) was operated at the standard conditions (Drift tube pressure: 2.3~2.4 mbar, PC: 455 mbar, FC: 6.5 STP cc/min, U SO: 75 V, U S: 100 V, Drift tube voltage: 600 V and Source: 6.0 mA). Detailed descriptions of the device, its principle and applicability can be found elsewhere (Blake et al., 2009; de Gouw et al., 2003; Han et al., 2010; Hewitt et al., 2003; Lindinger et al., 1998, 2001; Lirk et al., 2004; Steeghs et al., 2004). The signal intensity of VOC emissions used in the present study was measured by the instrument in the unit of ion count rates (counts per second, cps), which were then normalized by per million hydronium ion ( $\text{H}_3\text{O}^+$ ) count rates to compensate the variations in the hydronium ions as other related works in this area (e.g. de Gouw and Warneke, 2007; Jobson et al., 2005; Whyte et al., 2007). This normalized product ion count rate (*ncps*) becomes directly proportional to the concentration level of a target VOC.

#### 4.2.6 Test procedure

The nine building materials were previously studied at three different area-specific ventilation rates (Measurements #1, #2 and #3) as shown in **Table 4.1** to establish a database of emission signatures by PTR-MS specific to each individual material. Five multi-material mixture tests were conducted (Measurements #4-#8) in the present study to obtain combined emission signatures for the studied mixtures and to validate the feasibility of the proposed source identification methods. The mixture tests were performed within two weeks after the single material measurements were finished. For each measurement, the mass spectra for the background emission signal from the empty chamber and for the sample emission signal with each prepared specimen inside the chamber were measured all after three volumetric air changes from the start of ventilation to allow concentrations in the chamber to reach over 95% of the quasi-steady state level. PTR-MS was set to scan from  $m/z = 21$  to  $m/z = 250$  once every 12 s with an ion mass resolution interval of 50 ms. The total sampling period was 10 min (600 s) with 50 ion mass spectra collected for each dataset. During each measurement, another set of duplicate mass spectra was scanned to verify the collected data.

## 4.3 Results and Discussion

### 4.3.1 Relative signal intensity ( $\alpha$ ) and variance ( $\sigma$ ) of material emission signatures

The previous section (Chapter. 3) determined the identification of each ion mass with a related VOC by using GC/MS and PTR-MS together. Now, each ion mass ( $m/z$ ) of PTR-MS represents a VOC, and its signal intensity ( $ncps$ ) corresponds to the concentration level of VOC.

To perform a signal separation simulation using the Monte-Carlo method, some reasonable ranges of signal intensities (mean) and noise levels (variance) for material emission signatures are needed. To conduct a measurement-based simulation, the experimental data collected using PTR-MS through Measurements #1, #2 and #3 were used to get the range information. The pattern of material emission signatures determined by PTR-MS with a special filtering method employed were found to be consistent and stable in a normalized mass spectrum domain even under different area-specific ventilation rates tested and also over different sampling time (Han et al., 2010). There were also identifiable differences in the VOC emission signatures measured by PTR-MS among different types of building materials. The differences include the type of ion mass present, its relative amount (signal intensity) or both. This study used the emission signatures collected at Measurement #2 (medium airflow rate) as a reference, and the variance of signal intensity for each material was determined based on the variations of



all collected data from the corresponding reference signature. **Figure 4.2** summarizes the results.

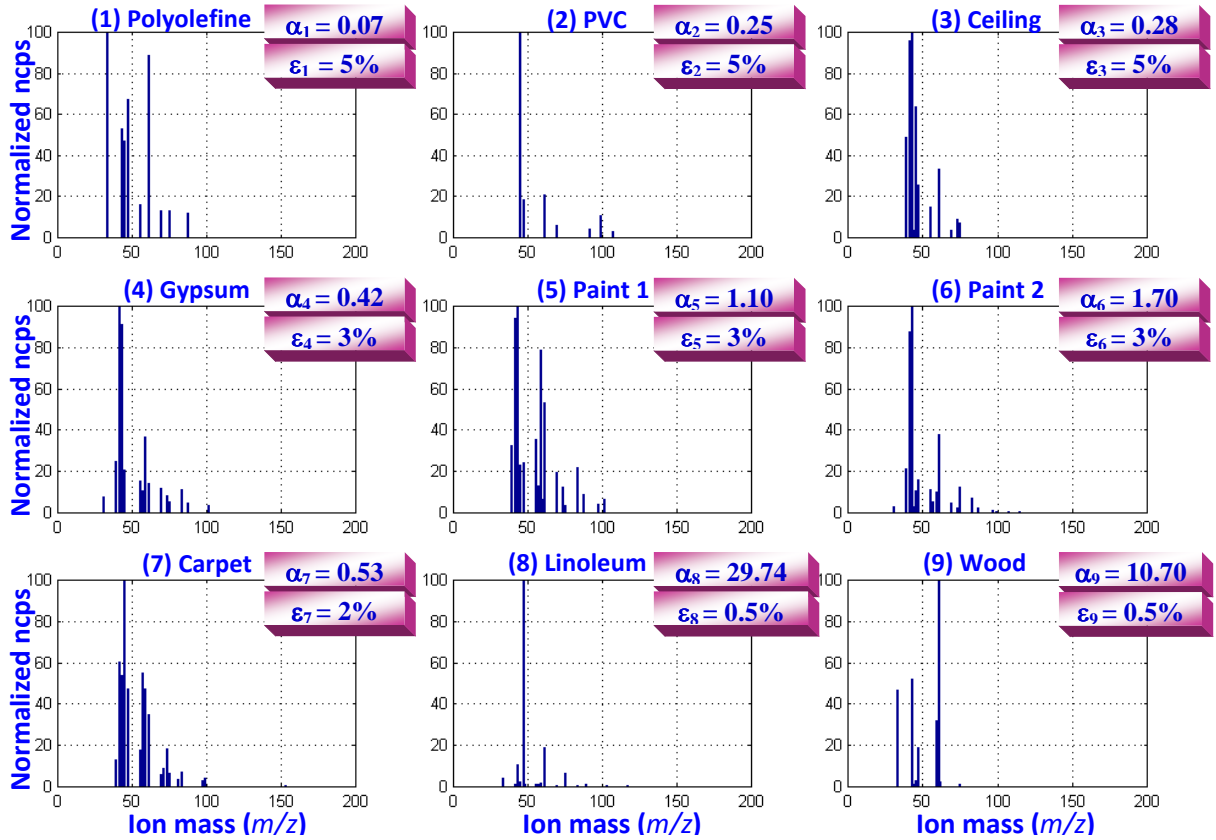


**Figure 4.2** Relative signal intensity factors ( $\alpha$ ) and variances ( $\epsilon$ ) of the emission signatures for the nine building materials.

\* The number in the parenthesis indicates the corresponding material ID (1-9) of each studied material.

\*  $\alpha$  is the signal intensity multiplication factor to be applied to each material emission signature to get the corresponding concentration level of each peak related to VOC concentration at Measurement #2 (i.e. Concentration level in *ncps* = Normalized *ncps* of each peak  $\times \alpha$ ).

\*  $\epsilon$  is the variance of emission signature caused by noise. This value is defined as the standard deviation of the maximum peak variation of a signature sample (worst case among all scanned ion masses) from the corresponding reference signature for the material. This value is obtained using all measured samples for each material, and expressed in the percentage of the maximum peak value in the corresponding reference emission signature for the material.

### 4.3.2 Separation simulations of the algorithms for various material mixtures

To compare the performances of the suggested algorithms, Monte-Carlo simulations were conducted by setting the design parameters based on PTR-MS measurements (for relative signal intensities and noise levels). The Monte-Carlo method is a class of computational algorithms that rely on repeated random sampling to compute the performance results for a given method when simulating physical and mathematical systems, which tend to be unfeasible to compute an exact result with a deterministic algorithm. The noise component,  $w$ , was modeled as white Gaussian random noise, and its variance was determined by the corresponding percentage of noise level ( $\varepsilon$ ) which represents the standard deviation of the noise with respect to the maximum peak value of the corresponding reference material emission signature. The number of random samples,  $N$ , was determined to make the variance of the final simulation results less than 1% (e.g.  $\sigma$  of Success Rate < 1% out of 100%) with a computational time as small as possible. With these considerations,  $N=1000$  was selected in this study. For the performance comparison of the algorithms, three indices were introduced as follows:

$$Err \equiv E \left\{ \left\| \bar{\alpha}_{est} - \bar{\alpha}_{true} \right\|_2 \right\}, \quad Score \equiv E \{ scr(N) \}, \quad SR \equiv (N - N_{fail}) \times 100 / N \quad (4.5)$$

where  $Err$  is the expected value of the 2-norm of the difference between the estimated value of signal intensity factor vector and the true one,  $N_{fail}$  indicates the number of material identification failures that occurred during the simulation (If every material in the sample is correctly identified with several wrong candidates, this case is classified as success. However, if there is any missing material identified in the final set of the

material candidates, then it is declared as failure. For example, for [5 6 8], if the ID result is [1 3 5 6 8], this is considered as success. But, if the result is [3 5 6 7], this is failure), *Score* is the expected value of success score (*scr*) which is defined as follows: for each simulation, if the ID result is success with exact identification, then  $scr = 100$ ; if success with  $n$  wrong candidates, then  $scr = 100 - 10 \times n$ ; and if failure,  $scr = 0$ , and SR represents the success rate in material identification defined in percentage.

Note: To differentiate the ID performance result with less wrong candidates from that with more wrong candidates (e.g. For [5 6 8], [1 5 6 8] ( $scr = 90$ ) vs. [1 3 4 5 6 8] ( $scr = 70$ )), *Score* index was introduced.

The results in **Table 4.2** indicate five noticeable aspects concerning the performance of the two algorithms. The algorithm performance for signature separation and identification may rely mainly on key factors such as the number of materials in a mixture, the signal intensity ratio and the variance of each composing signature. Algorithm 1 always showed by far the better performance than Algorithm 2 in the present simulations in terms of error expectation (*Err*), which implies that Algorithm 2 may get affected more susceptibly to the variation of emission signature because of noise than Algorithm 1. For some conditions, Algorithm 2 could show a better performance than Algorithm 1 in the sense of success rate and score, which suggests that the performance of the two algorithm can vary depending on given environmental and material conditions affecting the performance difference. A mixture case having no possible false ID can show a better performance in terms of success rate and score than that with several possible false IDs potentially under similar conditions (e.g. [2 8 9] vs. [3 6 8] or [1 7 9]). The material number in a mixture seemed to strongly affect the performance difference because of complexity increase (e.g. the low success rate of the 9-material mixture case), but when

focusing only on several major materials having higher signal intensities, the two algorithms suggested in this study still showed reasonably high success rates (> 95%).

**Table 4.2 Comparison of signature separation performance results of the two algorithms for various cases.**

Materials	Possible false ID	Max ratio ( $\gamma$ ) <sup>c</sup>	Err1 <sup>a</sup>	Err2 <sup>a</sup>	Score1	Score2	SR1 (%)	SR2 (%)
[8 9]	-	2.8	0.18	1.78	100.00	100.00	100.00	100.00
[7 8]	-	56.1	0.16	0.78	100.00	99.90	100.00	99.90
[1 8]	-	425	0.16	1.40	74.00	73.30	74.00	73.30
[2 3 4]	-	1.7	0.04	0.20	100.00	99.30	100.00	99.30
[5 6 7]	3, 4	3.1	0.25	0.67	90.69	88.68	100.00	99.60
[6 7 9]	1, 3	6.3	0.21	0.77	90.66	87.81	100.00	100.00
[6 8 9]	1, 3	17.5	0.50	1.53	90.30	89.73	100.00	99.80
[5 6 8]	1, 3, 4	27	0.67	1.45	86.03	82.37	100.00	96.40
[7 8 9]	3	55	0.26	1.14	95.26	94.35	100.00	99.80
[3 6 8]	1	106	0.35	1.27	83.04	<b>90.26</b>	87.20	<b>93.90</b>
[2 8 9]	-	119	0.23	1.65	94.60	<b>96.10</b>	94.60	<b>96.10</b>
[1 7 9]	3	153	0.09	0.16	80.58	<b>89.40</b>	84.10	<b>94.50</b>
[1 6 8]	3	425	0.34	1.20	68.53	61.97	71.80	65.30
[3 6 7 8 9]	1	106	0.54	1.55	73.39	<b>89.74</b>	76.60	<b>93.60</b>
[2 3 5 6 7 8 9]	1, 4	119	1.16	1.53	88.22	<b>92.04</b>	94.20	<b>98.70</b>
[1 2 3 4 5 6 7 8 9]	-	425	1.15	1.75	17.60	<b>27.10</b>	17.60 ( <b>95.60</b> ) <sup>b</sup>	<b>27.10</b> ( <b>98.50</b> ) <sup>b</sup>

<sup>a</sup> 1: of Algorithm 1, 2: of Algorithm 2.

<sup>b</sup> indicates the success rate of separation/identification performance of the algorithms when considering only the major five materials (Material 5, 6, 7, 8 and 9) having higher signal intensities.

<sup>c</sup> This ratio is defined as the maximum peak value (*ncps*) in the emission signature of the material with the highest signal intensity over the maximum peak value (*ncps*) of the material with the lowest signal intensity (e.g. For [3 6 7 8 9],  $\gamma = \alpha_8 / \alpha_3 = 106$ ).

\* For dual-material mixture cases, except for the case of [1 8], most of the cases showed > 95% of success rate when the two algorithms were applied.

### 4.3.3 Monte-Carlo simulations for the nine-material mixture

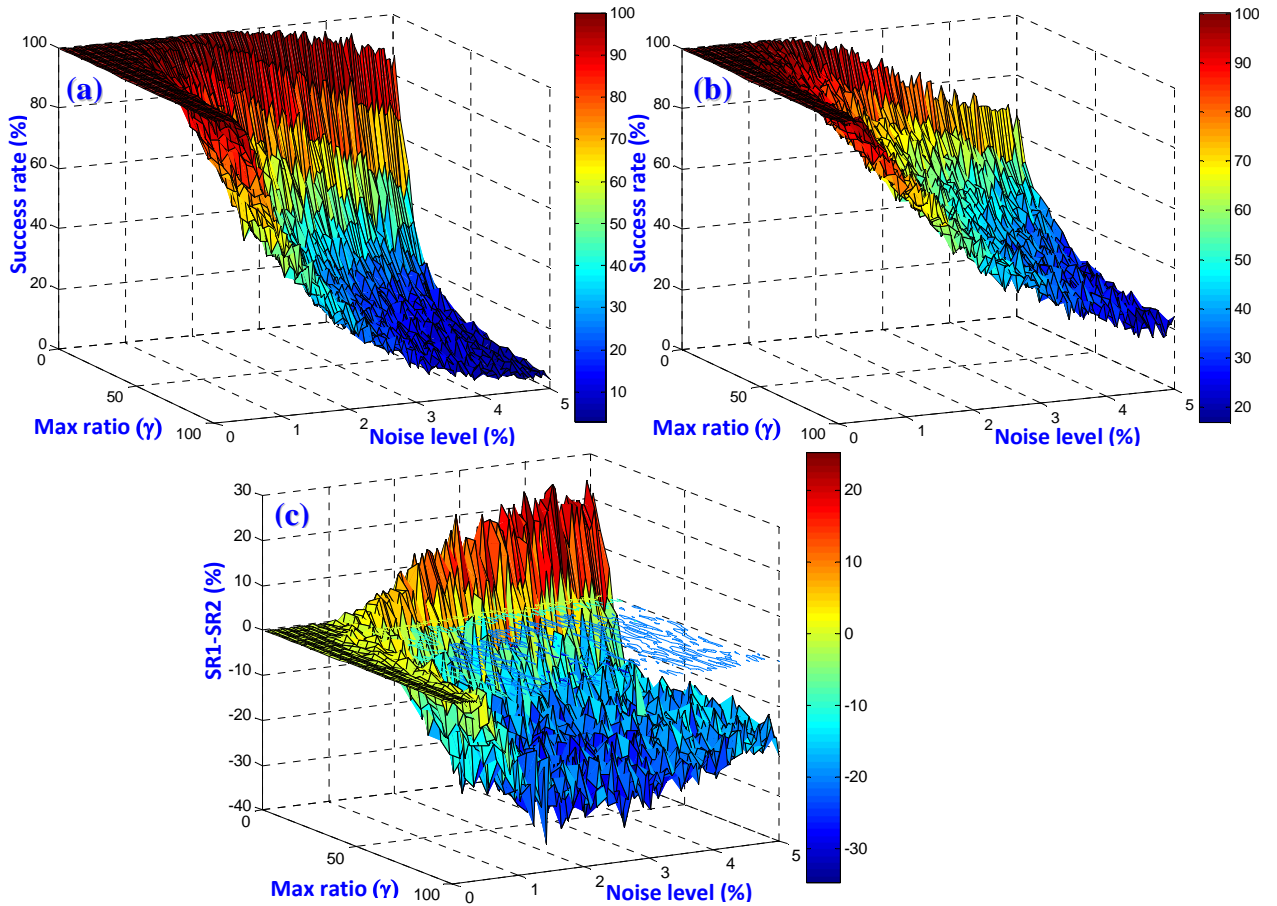


**Figure 4.3** Monte-Carlo simulation results for 9-material mixture under various conditions.

(a) Trend of success rate of Algorithm 1 (*SR1*). (b) Trend of success rate of Algorithm 2 (*SR2*). (c) Performance difference between the two algorithms (*SR1* - *SR2*) within the realistic ranges of  $\gamma$  and  $\varepsilon$ .

The results in [Table 4.2](#) suggest that the two proposed algorithms in this study exhibited a different quality of performance depending on given conditions of the two key factors – the maximum ratio of signal intensity factors ( $\gamma$ ) and the variance ( $\varepsilon$ ). To examine this aspect of the two algorithms as the two key parameters change, the most complicated case in this study, 9-material mixture, was selected, and the success rates of the two for this

case were explored at various combinations of  $\gamma$  and  $\varepsilon$ , varying within their corresponding realistic ranges (i.e.  $1.0 \leq \gamma \leq 100$ ,  $0 \leq \varepsilon \leq 5.0\%$ ). **Figure 4.3** shows the results.

As expected, the trends in **Figure 4.3a** and **4.3b** represent the decaying performance of both algorithms as the maximum ratio and the variance increase, although the slope of the decreasing performance of each algorithm is slightly different. Both algorithms exhibited high success rates within narrow decent ranges of the maximum ratio ( $1.0 \leq \gamma \leq 20$ ) and the variance ( $0 \leq \varepsilon \leq 1.0\%$ ) even for this complicated mixture. Within these decent ranges, Algorithm 1 showed a better performance than Algorithm 2 in terms of success rate. However, out of these ranges (more general ranges), the latter seemed better than the former in the sense of success rate (**Figure 4.3c**).

#### 4.3.4 Experimental results of multi-material mixtures

- Case 1: [7 8] = Carpet + Linoleum (Measurement #4)

The algorithms validated by measurement-based Monte-Carlo simulations were applied to actual emission measurements obtained from five multi-material mixtures. For comparison, the ground truths for the correct material IDs and the corresponding emission levels (represented by signal intensities) were known and obtained by the optimal separation of each measured signature in terms of MRLS (The exemplary separation profile of the signature for Case 1 is shown in [Figure 4.4](#)). Case 1 was comprised of Carpet (Material ID=7) and Linoleum (ID=8). Both algorithms identified the correct sources of material emissions with some false materials: for Algorithm 1, Gypsum (ID=4), so success score ( $scr$ )=90; for Algorithm 2, Gypsum (ID=4) and Wood (ID=9), so success score ( $scr$ )=80. In addition, the corresponding emission levels from the two materials could be estimated by both algorithms with reasonably small errors (Error expectations, or  $Err$ , were  $< 1.0$  for both cases). The performance results of the two algorithms for the actual emission measurement from Carpet and Linoleum could be summarized as below in terms of the performance indices defined in the previous section:

Algorithm 1:  $\mathbf{ID}_{est1} = [4 \mathbf{7} \mathbf{8}]$ ,  $\mathcal{A}_{est1}^p = [0.68 \mathbf{0.50} \mathbf{13.44}]$ ,  $Err1 = 0.81$ ,  $scr1 = 90$

Algorithm 2:  $\mathbf{ID}_{est2} = [4 \mathbf{7} \mathbf{8} 9]$ ,  $\mathcal{A}_{est2}^p = [0.28 \mathbf{0.53} \mathbf{13.63} 0.02]$ ,  $Err2 = 0.39$ ,  $scr2 = 80$ .

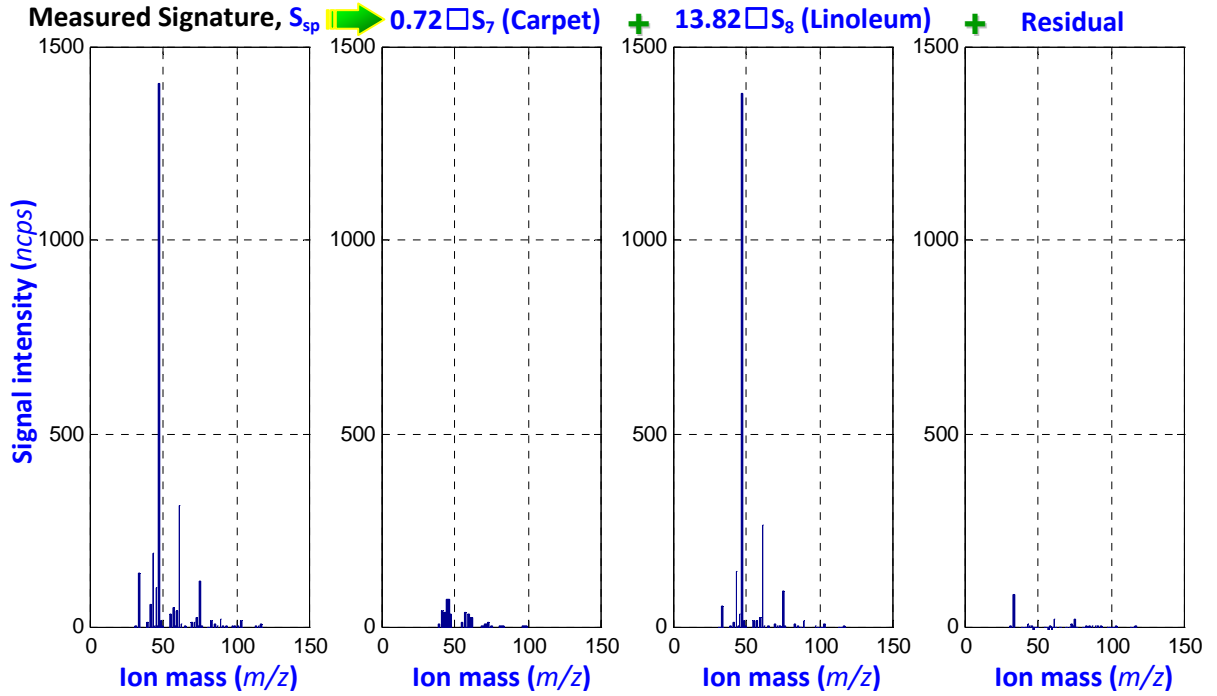


Figure 4.4 Optimal separation results of the measured emission signature for the Carpet/Linoleum mixture in the sense of MRLS.

- Case 2: [8 9] = Linoleum + Wood (Measurement #5)

The optimal signal intensity factors for this case were  $\hat{\alpha}_{true}^p$  for [8 9] = [18.42 8.23] in the MRLS sense. The following are the performance results:

Algorithm 1:  $\mathbf{ID}_{est1} = [8 \ 9]$ ,  $\hat{\alpha}_{est1}^p = [19.20 \ 9.63]$ ,  $Err1 = 1.60$ ,  $scr1 = 100$

Algorithm 2:  $\mathbf{ID}_{est2} = [8 \ 9]$ ,  $\hat{\alpha}_{est2}^p = [20.47 \ 4.82]$ ,  $Err2 = 3.98$ ,  $scr2 = 100$ .

- Case 3: [6 8 9] = Paint 2 + Linoleum + Wood (Measurement #6)

The optimal signal intensity factors for this case were  $\hat{\alpha}_{true}^p$  for [6 8 9] = [6.09 5.96 4.41] by MRLS. The following are the performance results:

Algorithm 1:  $\mathbf{ID}_{est1} = [6 \ 8 \ 9]$ ,  $\hat{\alpha}_{est1}^p = [1.71 \ 6.51 \ 5.78]$ ,  $Err1 = 4.62$ ,  $scr1 = 100$

Algorithm 2:  $\mathbf{ID}_{est2} = [6 \ 8 \ 9]$ ,  $\hat{\alpha}_{est2}^p = [3.63 \ 6.76 \ 3.75]$ ,  $Err2 = 2.67$ ,  $scr2 = 100$ .



- Case 4: [3 6 7 8 9] = Ceiling + Paint 2 + Carpet + Linoleum + Wood (Measurement #7)

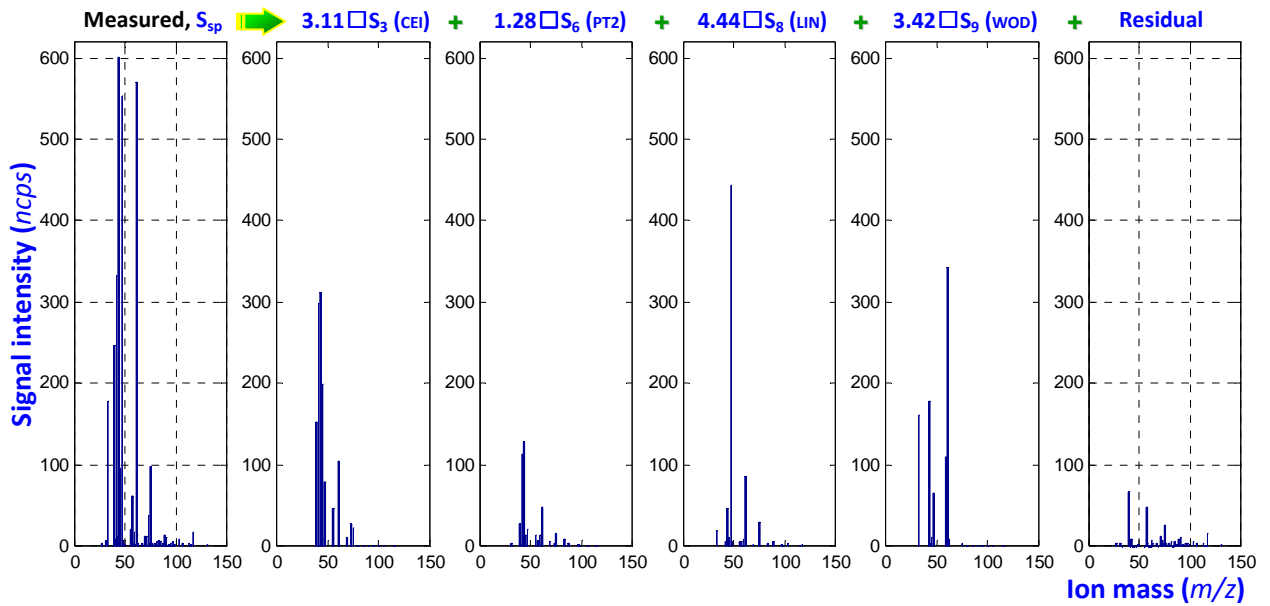


**Figure 4.5 Optimal separation results of the measured emission signature for the five-material mixture ([3 6 7 8 9]) in the sense of MRLS.**

The optimal signal intensity factors were  $\hat{\alpha}_{true}^p$  for [3 6 7 8 9] = [3.11 1.28 0.00 4.44 3.42] by MRLS (The detailed signature profile is given in **Figure 4.5**). The following are the performance results:

Algorithm 1:  $\mathbf{ID}_{est1} = [1 \ 8 \ 9]$ ,  $\hat{\alpha}_{est1}^p = [0.16 \ 4.28 \ 3.58]$ ,  $Err1 = 0.28$

Algorithm 2:  $\mathbf{ID}_{est2} = [1 \ 3 \ 6 \ 8 \ 9]$ ,  $\hat{\alpha}_{est2}^p = [0.38 \ 2.33 \ 1.84 \ 4.87 \ 1.51]$ ,  $Err2 = 2.21$ .

- Case 5: [2 3 5 6 7 8 9] = PVC + CEI + PT1 + PT2 + CAR + LIN + WOD (Measurement #8)

The optimal signal intensity factors for this case were  $\hat{\alpha}_{true}^p$  for [2 3 5 6 7 8 9] = [0.00 1.05 0.00 0.00 0.19 1.38 2.30] in terms of MRLS. The following are the performance results:

Algorithm 1:  $\mathbf{ID}_{est1} = [6 \ 7 \ 8 \ 9]$ ,  $\hat{\alpha}_{est1}^p = [0.40 \ 0.32 \ 1.26 \ 2.32]$ ,  $Err1 = 0.44$

Algorithm 2:  $\mathbf{ID}_{est2} = [1 \ 3 \ 6 \ 7 \ 8 \ 9]$ ,  $\hat{\alpha}_{est2}^p = [0.02 \ 1.04 \ 2.27 \ 0.04 \ 1.50 \ 1.63]$ ,  $Err2 = 2.37$ .

### 4.3.5 Effects of adsorption

The experimental results indicate three important aspects concerning the proposed technique, which may provide a new insight on adsorption effects occurring under material mixture conditions and open a new gate to quantitatively analyze and assess this adsorptive phenomenon inherent in material emissions:

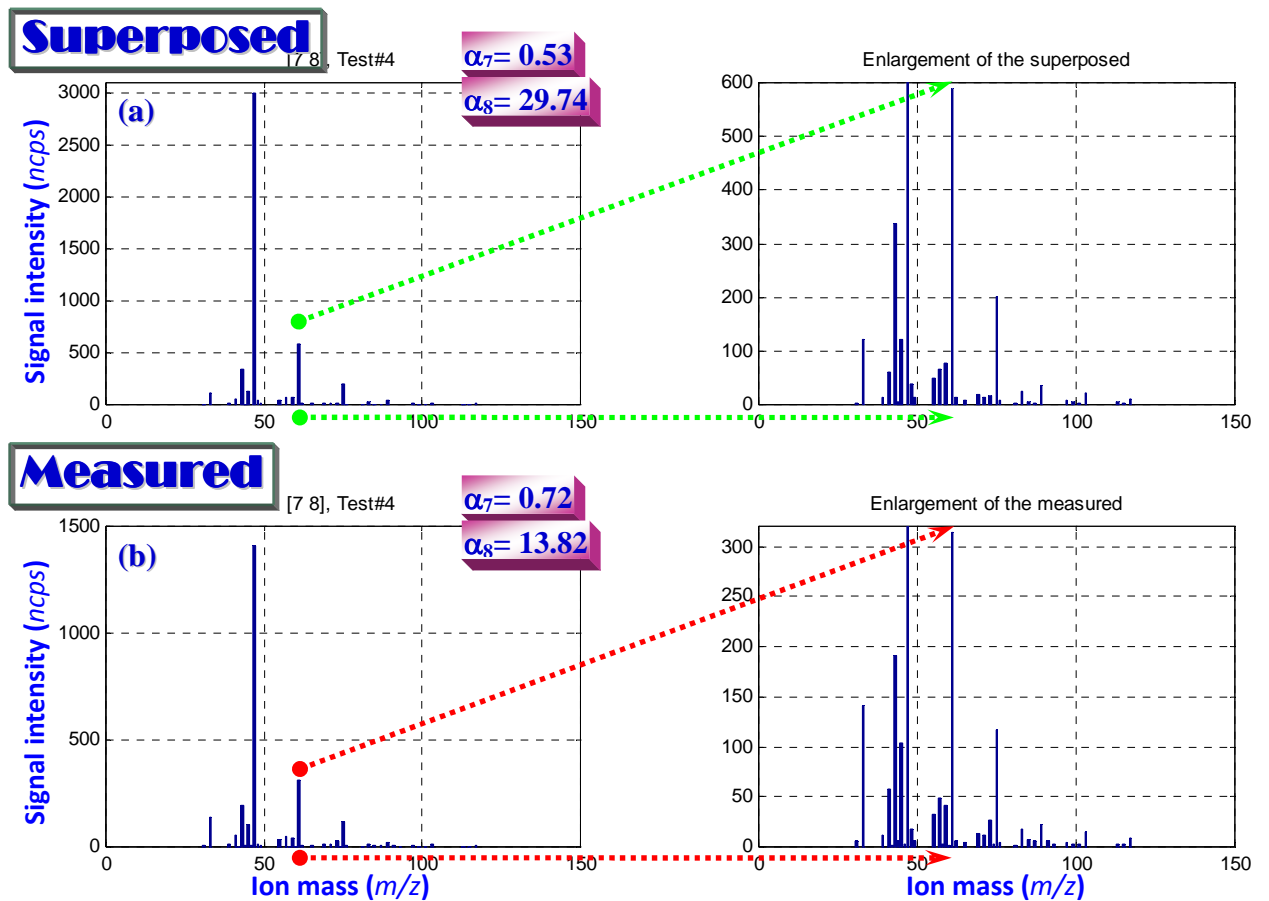


**Figure 4.6 Comparison of the superposed and measured signatures for the two-material mixture ([7 8]).**

(a) The superposed signature and its enlarged figure composed of the two individual signatures of Carpet and Linoleum. (b) The measured signature of the two-material mixture and its enlarged figure.

First, although there were some interactions among VOC emissions from a material mixture (which was observed in the measured signatures of the tested material mixtures having several different ion masses other than the ones found in the emissions from the original individual materials, with very small signal intensities), the chemical-interaction effect appeared to be small enough to allow the algorithms developed for separation and identification on the basis of the superposition assumption of the co-located materials' emission signatures.

In addition, the emission signatures of the mixtures maintained the individual emission signature pattern of each material almost unchanged even in a mixture. For example, note the similar pattern of the measured signature (Refer to the enlarged figure shown in [Figure 4.6b](#)) of a material mixture (Case 1 - Carpet and Linoleum) to the superposed signature of the two individual materials ([Figure 4.6a](#)), considering the given area-specific ventilation rates in [Table 4.1](#). Generally, it was observed that the similar patterns of the measured signatures to the superposed ones were maintained for all mixture cases tested, but the measured signal intensities were reduced significantly (meaning a lowered level of VOC concentrations emitted from material mixtures) compared with the superposed ones, mainly because of sorption effect among materials. Another possible reason for this reduction of signal intensity may be the effect of VOC emission decay over time, but this might be small or negligible considering that the mixture tests were performed right after the measurements of the single materials. Because of these special phenomena, the algorithms could be applied to the actual emissions of the studied material mixtures and yield satisfactory performances.

The second aspect examined in this study is that the sorption effect among materials can be quantitatively assessed in an accurate manner for each mixture by using this technique (Refer to another previous study on the assessment of sorption impact among material mixtures on perceived indoor air quality by human assessments, which is done by Sakr et al., 2006). The approach derived from the present study is based on the reduced percentage of the estimated signal intensity of emission signature from a material mixture when compared with that of the stand-alone emission signature for each individual material obtained under the same emission conditions (RH, temperature and area-specific ventilation rate). For example, the mixture of Carpet and Linoleum (Case 1) should have the relative signal intensity factors as  $\alpha_7 = 0.53$  for Carpet and  $\alpha_8 = 29.74$  for Linoleum under the given mixture emission conditions in **Table 4.1** (Measurement #4) if there are no interaction and no sorption effect between the two. However, the experimental results showed that the intensity factors were different as  $\alpha_7 = 0.72$  for Carpet and  $\alpha_8 = 13.82$  for Linoleum (**Figure 4.4**). Because of large porous areas in the surface of Carpet, the major portion of the VOC emissions from Linoleum might be trapped (i.e. adsorbed) in those porous areas of Carpet because of adsorption, and the reduction effect of VOC emissions from Linoleum could be estimated at the percentage of 53.5% (from 29.74 to 13.82). This sorption effect became more apparent when sorptive materials such as Carpet (material ID = [7]) and Gypsum ([4]) or gypsum-based materials such as Ceiling ([3]), Paint 1 ([5]) and Paint 2 ([6]) were present in the studied material mixture. This enhanced effect could be seen in the consecutive study of material mixtures as shown in **Figure 4.7**. The initial signature for Linoleum (the main emitting material in this case)

could be measured again with a similar level of signal intensities after other added materials were taken out of the chamber as shown in [Figure 4.7h](#).

Lastly, by using this technique, emission sources and their corresponding signal intensities (i.e. concentration levels of VOC emissions) can be identified and estimated in a laboratory condition. PTR-MS emission signatures were specific to each material tested, and the interactions among different material emissions may not significantly affect the pattern change of the individual emission signatures at least for the studied material mixtures. Therefore, it is possible to identify the related material based on the emission pattern of the same material measured by PTR-MS at least in a conditioned laboratory environment. The differences in emission patterns may potentially be used to identify emission sources (e.g. in buildings) based on air samples measured by PTR-MS. However, emission signatures may change over the course of long-term emissions, which will be further investigated in Chapter 5.

If there is a VOC related problem in an indoor air environment, different relevant sources can be identified and screened individually by PTR-MS. Finding the source(s) would help eliminating the problem efficiently and effectively. An advantage of this technique is that it may find the sources invisible or hidden when a building with problems of indoor air quality is suspected. Further studies are needed for extending this technique into a practical tool for emission source identification in real indoor environments because of the higher number of possible emission sources, the more complicated adsorption and desorption effects and the change of emission pattern over time for a given source. The pattern change of material emission signatures over a long-term period may be accounted for by using appropriate emission source models as to be discussed in the next chapter.

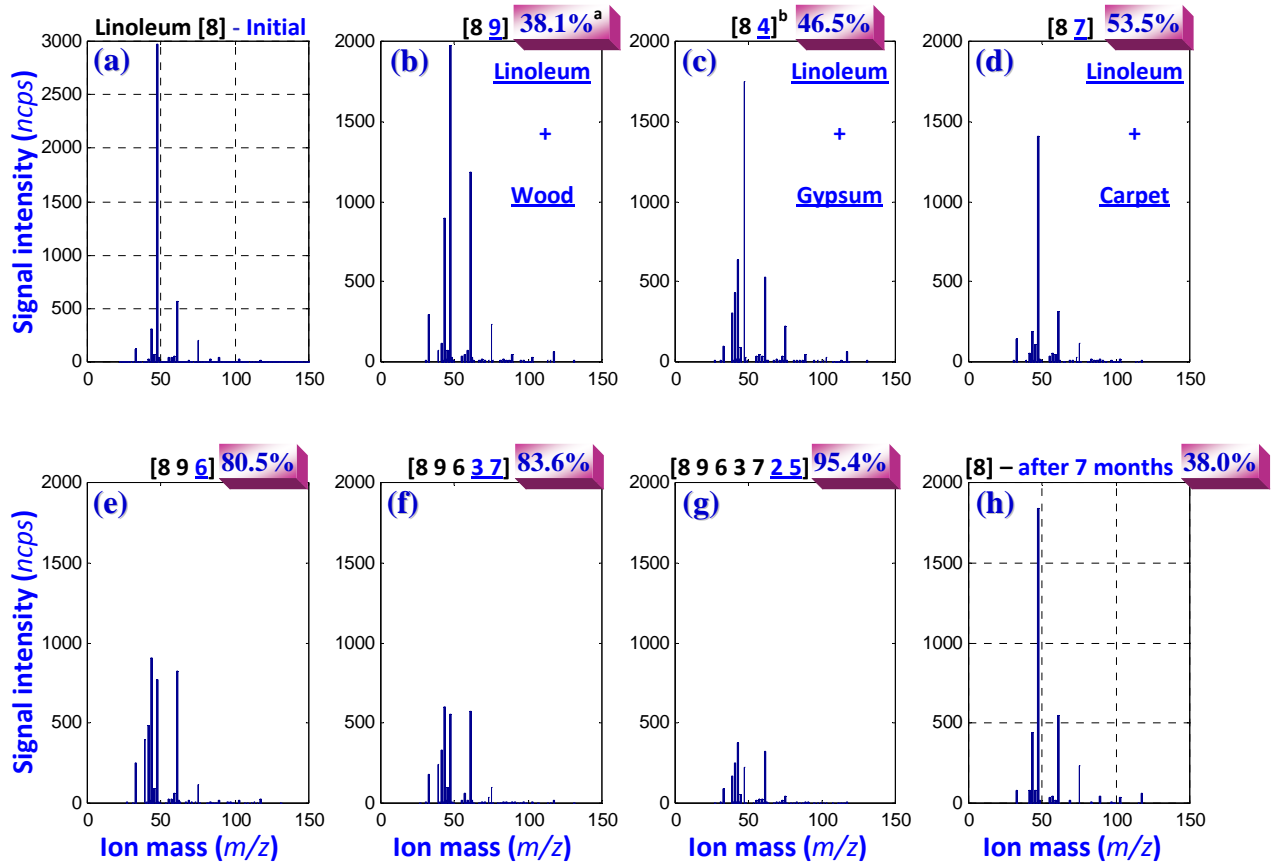


**Figure 4.7** The measured signature intensity/profile change of the Linoleum-plus mixtures mainly due to adsorption effect as other materials were added to the mixture.

(a) The initial emission signature of Linoleum (Measurement #2 described in Table 1). (b) The signature with Wood (Measurement #5). (c) With Gypsum. (d) With Carpet (Measurement #4). (e) The signature when Paint 2 added to the mixture of Linoleum/Wood (Measurement #6). (f) When Ceiling and Carpet added (Measurement #7). (g) When PVC and Paint 2 added (Measurement #8). (h) The signature of Linoleum obtained from another single material emission test after the 7-month conditioned storage of the material, with other materials taken out of the chamber (with the same test conditions as Measurement #2 for Linoleum).

<sup>a</sup> represents the reduction percentage of signal intensity of the Linoleum emission because of adsorption effect, estimated by considering the difference between the supposed signal intensity factor of the Linoleum emission at the given area-specific ventilation rates and the measured/assessed signal intensity factor (i.e. factor value difference between supposed factor and measured factor / supposed factor  $\times$  100).

<sup>b</sup> Another two-material mixture case with the same specimens of Linoleum and Gypsum described in Table 1 and under the test conditions of 1.03 l/min, 22°C and 31% RH.

## 4.4 Conclusions

The results of this study demonstrate the feasibility of identifying emission sources with high success rates when multiple materials are present indoors by utilizing the PTR-MS and an effective signal processing method under laboratory indoor conditions. The following conclusions could be derived from the findings of the study (*Stage 2*) described in Chapter 4:

- ◆ In a controlled environment, material emission sources could be identified at reasonably high success rates even for seven-material mixtures co-located at the same time, with their individual relative source strengths (expressed in PTR-MS signal intensities) estimated by the developed technique.
- ◆ The effect of VOC mixture emissions might be superposed in the mass spectrum domain of PTR-MS because of small interactions among material emissions and the conservation of individual material emission pattern even in the presence of emission interactions such as sorption.
- ◆ The sorption effect among material emissions could be quantitatively assessed using the new technique proposed.

## † CHAPTER 5. VARIATION OF ESs OVER TIME AND ITS IMPACT ON SOURCE IDENTIFICATION

---

### 5.1 Introduction

Volatile organic compounds (VOCs) have multiple indoor sources. VOC emitting materials can introduce carcinogens, chemical mutagens, endocrine disruptors, neurotoxins, reproductive toxins and other harmful chemicals into indoor air. The understanding and knowledge on emissions from building materials are becoming more important than before to global and local air quality personnel such as environmental policy makers, product manufacturers, building professionals, air quality managers and regulators because of large portion of these materials' emitting surface area occupied in buildings, their permanent exposure to indoor occupants and the distinguishing lifestyle of the contemporary people in developed countries (i.e. spending most of their time in indoor environments).

The levels of indoor VOCs can be differentiated by the primary and secondary emissions of VOCs from materials. The primary emission is VOCs released directly from the materials into indoor air. This is the highest level of VOC emissions from the materials, and typically decays relatively quickly initially over the first week and then decays slowly



over a long period of time (e.g. more than a year) after the introduction of a product in indoor environments. This emission is a direct result of chemical constituents from the materials. On the other hand, the secondary VOC emission can occur when other indoor materials adsorb emitted VOCs and then continue to re-emit them slowly over a long period of time, when other harmful compounds (e.g. formaldehyde) are produced via chemical reactions (Particularly, ozone related; see Morrison and Nazaroff, 2002), when air velocity or ventilation rate increases, or when certain materials contain chemicals that maintain a slow but steady emission rate for a long-term period. For some materials, secondary emissions may exist for many years and have a greater impact on the long-term indoor air quality than materials with higher primary emission rates. As a result, human residents can experience long-term exposure to these secondary VOC emissions for a long time, which draws more attention and care for improving human's comfort, health and performance.

To support long-term future developments for the improvement of human's life and welfare, the evaluation of the chemical long-term impacts of building materials on air quality may be vital and change the custom and protocols in the establishment of global guidelines and standards, manufacturing practices of building materials, material selection strategies for indoor use, labeling and quality control schemes, and material preparation/testing/validation methods. Hodgson et al. (2000) reported that source reduction treatment via substitution of building materials with low-polluting products or modification of building practices could be generally the preferred method for reducing occupants' exposure to VOCs. They identified several compounds including acetic acid as important compounds having great potency to human's health and perception, but were

not certain about the sources of the identified active compounds in the studied houses. There is a special need to identify and clearly pinpoint VOC emission sources for establishing an effective countermeasure against unwanted VOC emissions. If there is a VOC related problem in an indoor air environment, different relevant sources can be identified and screened individually by an on-line analytical monitoring device (e.g. Proton Transfer Reaction – Mass Spectrometry, or PTR-MS). Finding the source(s) would help eliminating the problem efficiently and effectively. An advantage of this approach is that it may find the sources invisible or hidden when a building with problems of indoor air quality is suspected.

The consideration of long-term VOC emissions from building materials can also impact the source identification study. A considerable step toward source identification of certain indoor VOCs of concern has been taken via several related studies (Han et al., 2010, 2011) to show the existence of stable and unique emission signatures (ES) for different types of building materials and to develop a methodology for separating and identifying the individual material emission signatures from mixture emissions. As far as the possibility of the emission signature change over a long period of time is concerned, the proper estimation and prediction of emission signatures at a later time are considered as essential to extend to a field condition the applicability of the methodology for indoor source identification developed in the previous study (Chapter 4 and Han et al., 2011). The pattern change of material emission signatures over long-term emissions may be accounted for by using appropriate emission source models. The objectives of the study in Chapter 5 were to explore the change of long-term VOC emission profiles of building materials and to develop a methodology to improve the identification of individual indoor

emission sources based on the measurements of mixed air samples with emissions from aged materials and the emission signatures of individual new building materials determined by PTR-MS.

## 5.2 Materials and Methods

### 5.2.1 Overview

In the previous study (Han et al., 2010), chamber exhaust air polluted by the emissions from nine individual building materials in a 50-l small-scale chamber was sampled by PTR-MS at low, medium and high airflow rates to establish an initial library of material emission signatures stable over different sampling time and even over different area-specific ventilation rates in terms of relative signal intensities and overall shape of emissions, and also to determine their variances because of measurement noise. The emission signature (ES) is the PTR-MS ion mass ( $m/z$ , which is a physical quantity denoting the mass-to-charge ratio widely used in the electrodynamics of charged species) spectrum of the air sampled from each material, constructed after subtracting the background air signal from the measured and removing any ion mass components within the measurement uncertainty ( $< 3$  sigma of the background signal). Emissions of all VOCs composing the ES for each material were traced by using source models over the course of long-term emissions to estimate the long-term ESs for the individual materials. Actual combined emissions from three multi-material mixtures were studied to assess the effect of the consideration of long-term ES change on the ES separation and identification

performance. The two algorithms previously developed based on signal processing principles (Chapter 4 and Han et al., 2011) were utilized.

### 5.2.2 Environmental chamber conditions

A 50-l small-scale environmental chamber ( $0.5\text{ m} \times 0.4\text{ m} \times 0.25\text{ m}$  high) made of electro-polished stainless steel was used with a precise airflow controller and a humidity controller. The chamber was maintained at a constant stable temperature in the range of  $19.87\text{-}25.99^\circ\text{C}$  (with a small variation of  $< \pm 0.02^\circ\text{C}$  during each sampling period) and at a controlled relative humidity of  $31 \pm 0.3\%$  RH during the 9-month period of the experiment. The background concentrations of individual VOCs in the empty chamber were maintained clean to be less than  $1\text{ }\mu\text{g}/\text{m}^3$ .

### 5.2.3 Test specimens

Nine typical building materials were investigated including carpet, ceiling material, gypsum board, linoleum, paint 1 (water-based acrylic), paint 2 (with linseed oil), polyolefine, PVC and wood. The detailed descriptions for the specimens can be found elsewhere (Chapter 3 and Han et al., 2010). Specimens were cut and prepared according to the sizes specified in [Table 5.1](#). The prepared specimens were placed vertically, parallel with the airflow in the chamber. The range of area-specific ventilation rates was set by adjusting the airflow to the chamber while keeping the size of specimen unchanged.

**Table 5.1 Flow rates and specimen areas for the PTR-MS experiments.**

Material (ID#)	Flow rate – $Q_v$ (l/min) / Specimen area – $A$ (cm <sup>2</sup> ) $Q_v/A$ (l/s/m <sup>2</sup> )					
	Meas. #1	Meas. #2	Meas. #3	Meas. #4	Meas. #5	Meas. #6
<b>Ceiling (3)</b>	0.50 / 290.7 0.29	1.55 / 290.7 0.89	4.64 / 290.7 2.66			
<b>Wood (9)</b>	0.50 / 265.5 0.31	1.30 / 265.5 0.81	3.85 / 265.5 2.42	1.21 / 265.5 0.76		1.28 / 265.5 0.80
<b>Carpet (7)</b>	0.50 / 240 0.35	1.28 / 240 0.89	3.83 / 240 2.66		1.28 / 240 0.89	
<b>Linoleum (8)</b>	0.50 / 240 0.35	1.28 / 240 0.89	3.83 / 240 2.66	1.21 / 240 0.84	1.28 / 240 0.89	1.28 / 240 0.89
<b>PVC (2)</b>	0.50 / 240 0.35	1.28 / 240 0.89	3.83 / 240 2.66			
<b>Polyolefine (1)</b>	0.50 / 240 0.35	1.28 / 240 0.89	3.83 / 240 2.66			
<b>Gypsum (4)</b>	0.50 / 416 0.20	1.03 / 416 0.41	3.08 / 416 1.23			
<b>Paint 1 (5)</b>	0.50 / 402 0.21	0.99 / 402 0.41	2.97 / 402 1.23			
<b>Paint 2 (6)</b>	0.50 / 490.2 0.17	1.21 / 490.2 0.41	3.63 / 490.2 1.23	1.21 / 490.2 0.41		

\* Meas. stands for 'Measurement'.

\* Measurements #1-3: from single material tests.

\* Measurements #4-6: from material mixture tests with the selected materials put in the chamber together.

#### 5.2.4 PTR-MS setting

A PTR-MS device (*Ionicon Analytik high-sensitivity model with a detection limit as low as 1 pptv, Austria*) was operated at the standard conditions (Drift tube pressure:  $2.20 \pm$

1.9e-5 mbar, PC: 355 mbar, FC: 7.0 STP cc/min, U SO: 85 V, U S: 120 V, Drift tube voltage: 600 V and Source: 6.0 mA). Lindinger et al. (1998) describes the detailed explanations on the device and its principle. The normalized product ion count rate (*ncps*) was used in this study to quantify the VOC concentrations.

### 5.2.5 Test procedure

The nine building materials were previously studied at three different area-specific ventilation rates (Measurements #1, #2 and #3) to establish an initial ES library by PTR-MS specific to each individual material. One year after the experiment for establishing the initial ES library, the long-term experiment using the same nine materials preserved for one year in a well-conditioned storage space has been performed for nine months. Three multi-material mixture measurements were collected (Measurements #4-#6) after the long-term experiment to obtain actual combined emission signatures and to assess the effects of the long-term emission signature change on the source identification performance of the developed algorithms. The ES measurements for the long-term experiment were collected at D-0 to D-2 (designated as Long-term 1 measurement) around 2 hours (to get a quasi-steady state concentration level) after the start of continuous ventilation in a well-controlled ventilation space (keeping a constant surface velocity at 100 ft/min, or 0.51 m/s), 7-month (Long-term 2), 8-month (Long-term 3) and 9-month (Long-term 4), which are illustrated in [Figure 5.1](#).

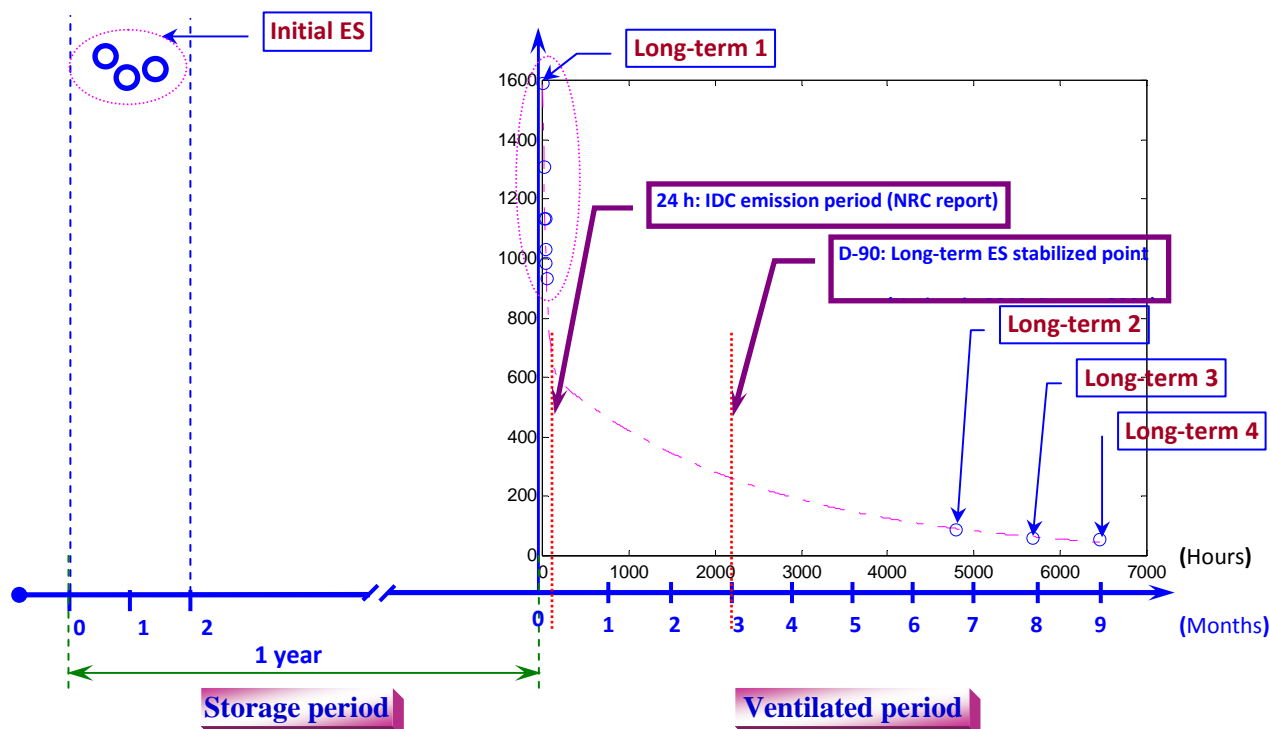


**Figure 5.1 Measurement schedule for constructing 9-month long-term emission signatures.**

\* ES: Emission signature, IDC: Internal-diffusion controlled.

For each measurement except for the Long-term 1 measurement (which was a continuous measuring test with a sampling interval of 24 s for two days), the mass spectra for the background emission signal from the empty chamber and for the sample emission signal with each prepared specimen inside the chamber were measured all after three volumetric air changes from the start of ventilation to allow concentrations in the chamber to reach over 95% of the quasi-steady state level. PTR-MS was set to scan from  $m/z = 21$  to  $m/z = 250$  once every 12 s with an ion mass resolution interval of 50 ms. The total sampling period was 10 min (600 s) with 50 ion mass spectra collected for each dataset. During each measurement, another set of duplicate mass spectra was scanned to verify the collected data.

### 5.3 Results and Discussion

The previous study (Han et al., 2010) determined the specificity and identification of each ion mass with a related VOC by using GC/MS and PTR-MS together. Now, each ion mass of PTR-MS represents a VOC, and its signal intensity (*ncps*) indicates the corresponding concentration level of the VOC. This study used the emission signatures collected at Measurement #2 (medium airflow rate) as a reference, and the variance of the emission signature for a given material was determined based on the variations of all the scanned ion mass peaks from the reference signature for the material.

#### 5.3.1 Emission pattern at each long-term period

##### 5.3.1.1 2-day (D-0 ~ D-2) emission profile (Long-term 1)

(a) Linoleum (ID number = [8])

PTR-MS raw signals were filtered to effectively remove PTR-MS measurement noise by utilizing a moving-average method with 11 samples (corresponding to the sampling period of 264 s) for each measuring point. The detailed descriptions on the filtering technique used can be found in the previous study (Chapter 3 and Han et al., 2010).

**Figure 5.2** exemplifies the raw and filtered signal patterns over two-day emissions of Linoleum. Contrary to the raw signal patterns for several major VOC compounds emitted from Linoleum ( $m/z = 47,61,43$ ), the filtered signals showed clear trends of exponential decay as shown in **Figure 5.2**. The fluctuations shown in the middle of the trends might be caused by the temperature change during the two-day experiment, because the



temperature in the testing facility was not strictly controlled (other environmental conditions were controlled), hence could slowly fluctuate within a limited range. Background components showed almost no change in their concentration levels during the two-day emission test as exemplified in **Figure 5.2** (for  $m/z = 29$ ).

**Figure 5.3** shows the emission patterns of several major compounds emitted from Linoleum for two days. Ethanol ( $m/z = 47,75$ ), acetic acid ( $m/z = 61,43$ ), acetaldehyde ( $m/z = 45$ ), etc. were those indicating higher emission concentrations. Most of the VOC emissions followed the exponential decay profile at a similar decay rate (50% of initial concentrations were decayed after two days). Among them, methanol ( $m/z = 33$ ) showed a faster decay over time than other compounds (as shown in **Figure 5.3**), which might impact the shape change of the emission signature for Linoleum at a later time. Except for this ion mass peak, the emission signature of Linoleum during this two-day period kept a very stable and consistent shape (< 2% variance with regard to the maximum peak of the reference signature).

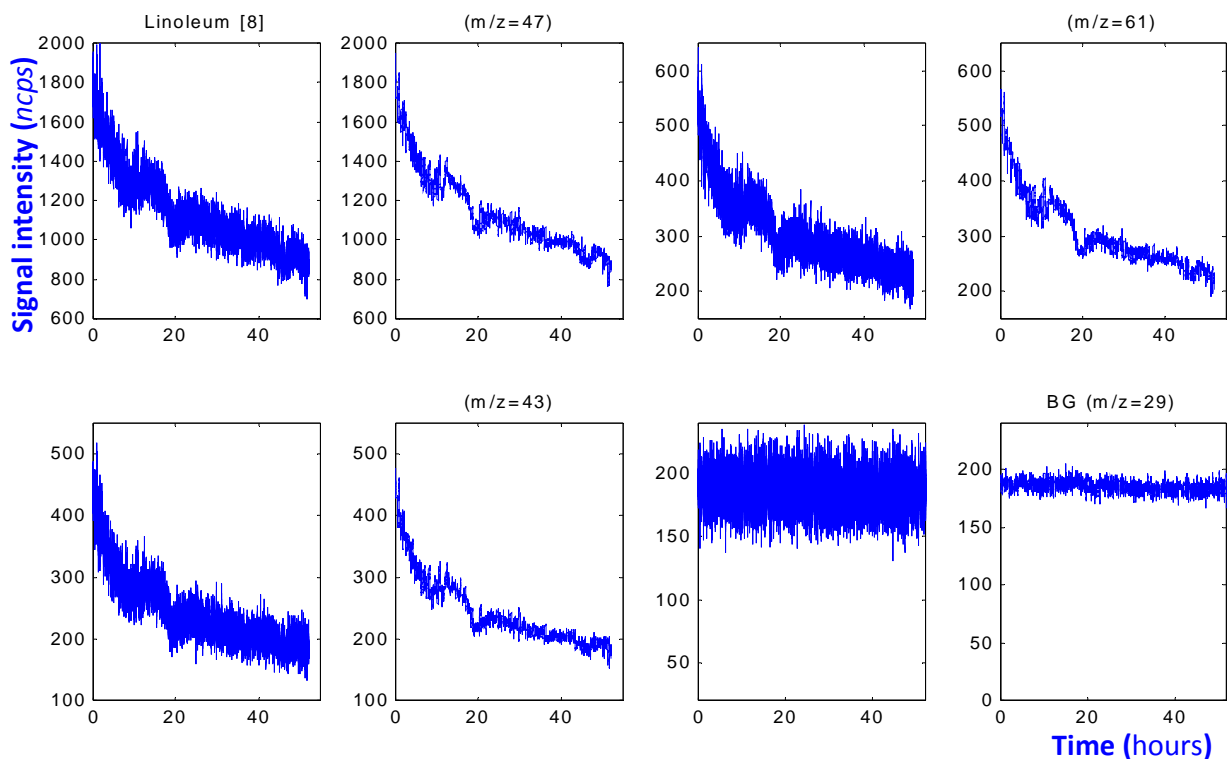


**Figure 5.2** PTR-MS raw emission signal vs. filtered signal patterns of the major ion masses for Linoleum.

\* For each pair of figures, the left figure is the raw signal, and the right the filtered one by utilizing a moving-average method.

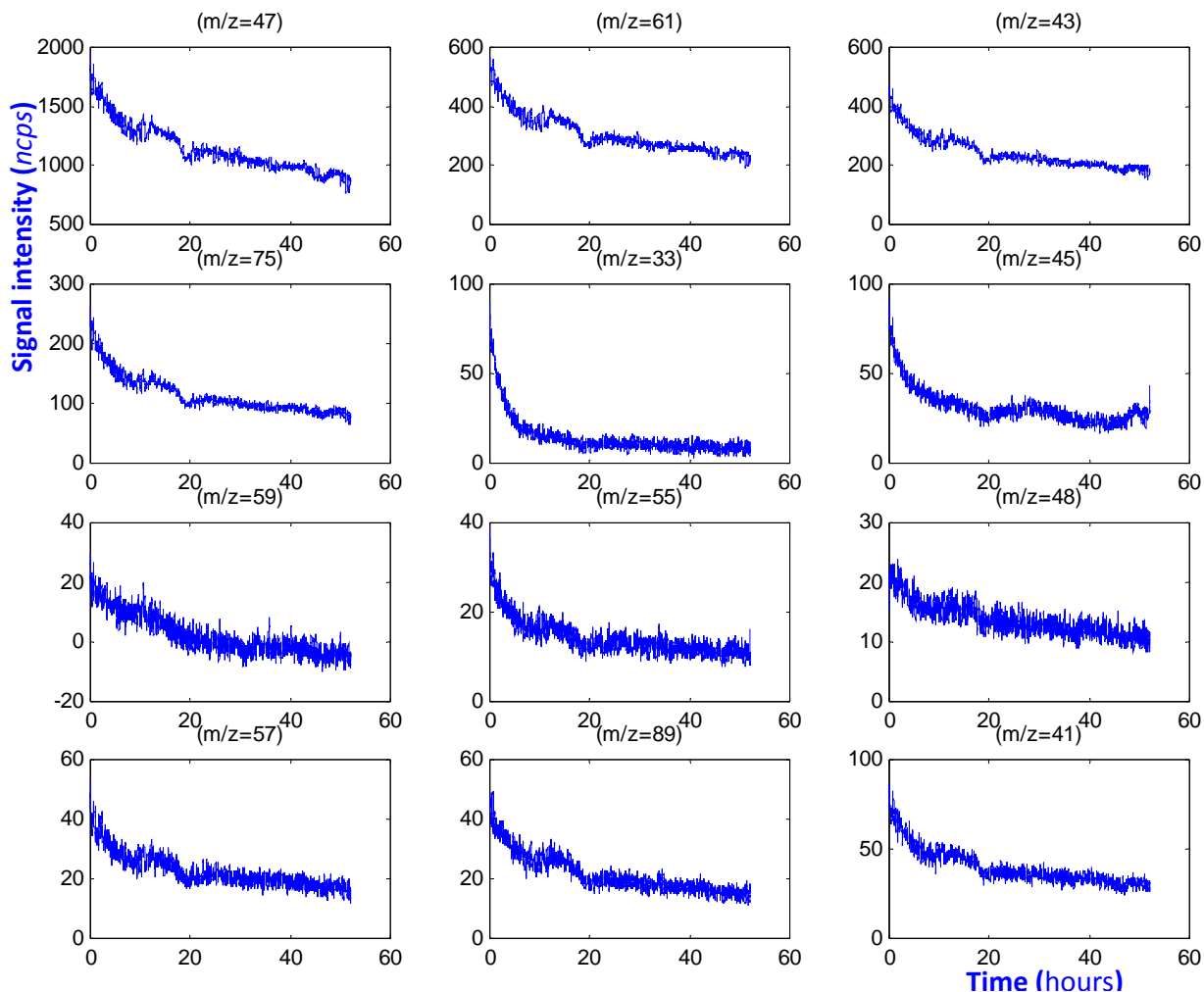


**Figure 5.3** Emission patterns of major compounds from Linoleum during the initial 2 days.

(b) Paint 2 (ID number = [6])

The PTR-MS raw signals measured from VOC emissions of Paint 2 were also filtered in the same way as the Linoleum case to attenuate the noise in the measurements. **Figure 5.4** shows the raw and filtered signal patterns for Paint 2 over two-day emissions. Contrary to the raw signal patterns for several major ion masses of Paint 2 ( $m/z = 41, 43, 61$ ), the filtered signals exhibited clear trends of fast exponential decay. The concentrations of background components (e.g.  $m/z = 29$ ) showed almost no change during the emission experiment.

**Figure 5.5** shows the emission patterns of several major compounds emitted from Paint 2 during the initial two-day ventilation period. Isopropanol ( $m/z = 41,43,39$ ), acetic acid ( $m/z = 61,43$ ), ethanol ( $m/z = 47,75$ ), propanoic acid ( $m/z = 75$ ), etc. were those indicating higher emission concentrations. Most of the major VOC emissions in terms of emission concentration levels showed fast exponential decay profiles, especially for isopropanol and methanol (More than 70% of initial concentrations were decayed after two days). Still, several compounds such as acetic acid ( $m/z = 61$ ) and ethanol ( $m/z = 47$ ) showed a slower decay over time than those fast decayed compounds (as shown in **Figure 5.5**), which led a huge effect on the shape change of the emission signature for Paint 2 at a later time. The emission signature for Paint 2 at the end of this two-day period had a quite different shape compared with the initial emission signature, or the reference emission signature for this material. For this kind of case, the pattern change of material emission signatures over a long-term period may be accounted for by using appropriate emission source models. This issue will be dealt with in a later section.

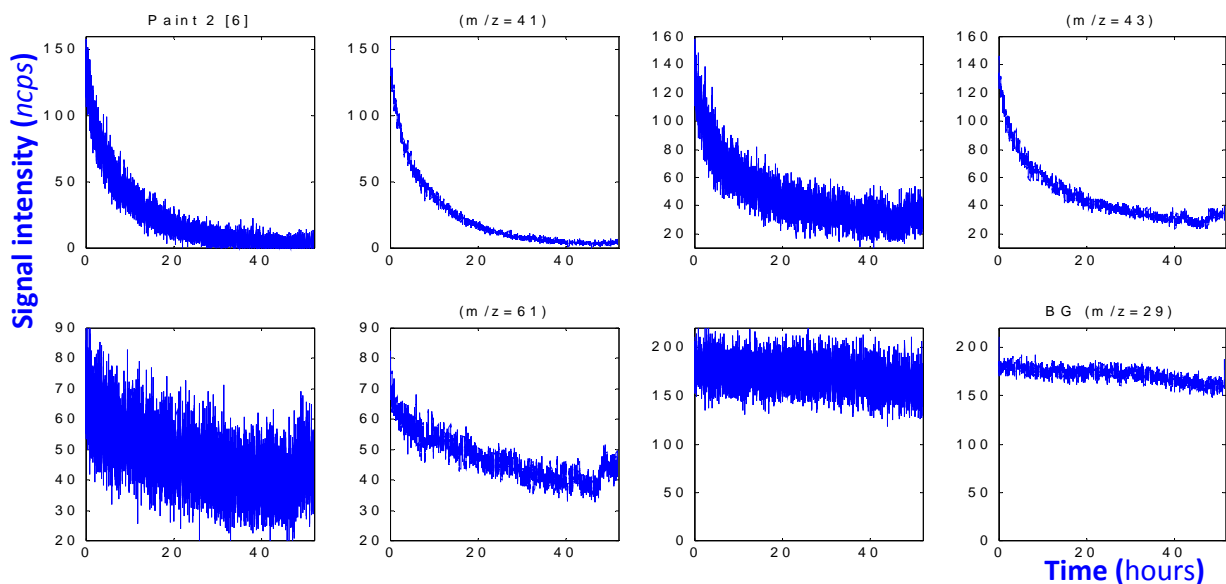


Figure 5.4 PTR-MS raw vs. filtered signal patterns of the major ion masses for Paint 2.

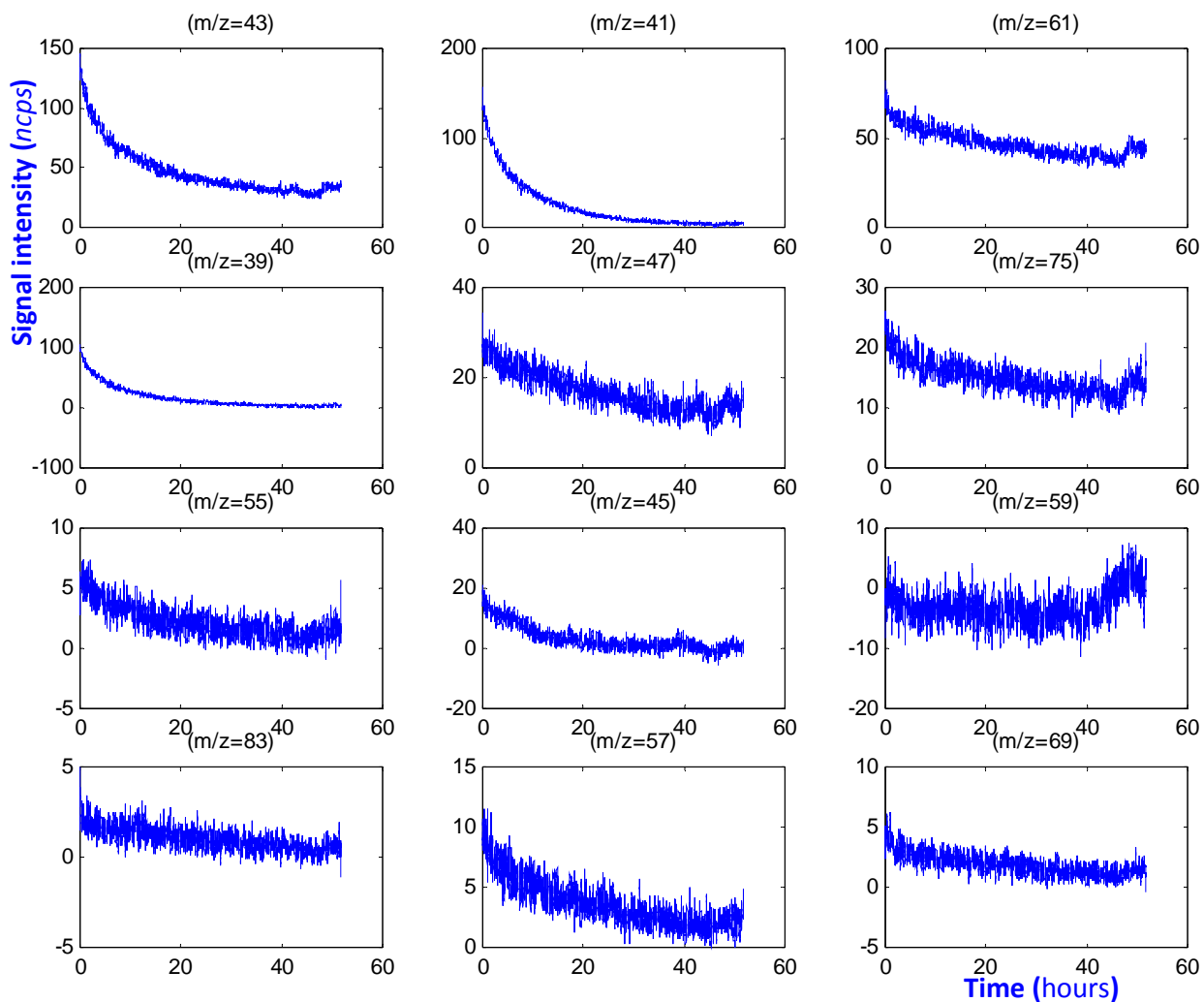


Figure 5.5 Emission patterns of major compounds from Paint 2 during the initial 2 days.

### 5.3.1.2 At 7-month (Long-term 2), 8-month (Long-term 3) and 9-month (Long-term 4)

The emission signatures for the building materials studied in this study were found to change over time. However, the long-term emission signatures for these materials appeared to be stabilized again after a certain period of time (~ 3 months or 90 days, demonstrated in Herbarth and Matysik, 2010) if the emission signal intensities by PTR-MS were high enough compared with those for the background air in the empty chamber (or having a high enough signal-to-noise ratio, SNR). The results of long-term emission signatures obtained for these periods implied that there might be three types of materials in terms of the change of long-term emission signatures: *Type 1* - Materials with a single stable ES from the beginning, *Type 2* - Materials with a stable initial ES and another stable ES for long-term emissions, and *Type 3* - unstable long-term ES due to low SNR. The first type of materials had its own stable emission signature from the early stage of emissions, and kept the similar shape of ES with a small variation in the ES until the end of the long-term emission experiment (up to 9 months in this study). An example of this material type was Wood. Most of the materials belonged to the second type, which had a stable initial ES and another stable long-term ES after a certain elapsed time. Examples of this type of materials were Paint 1, Paint 2, Carpet and Linoleum. If materials themselves initially had a low-polluting property, the emission signals (or SNR) were measured in a very low level and kept decreasing over time. After a certain period of time, the signals from these materials became far below the background signal level (i.e.  $< 10$  *ncps*, or  $1.4$  *ppbv*, whereas the level of the background air signals was around  $50\sim 60$  *ncps*, or  $7\sim 8$  *ppbv*), and the corresponding ESs could not be stable due to relatively high level of noise (low SNR). All the low-polluting materials in this study showed this trend including Polyolefine, PVC, Ceiling and Gypsum.

(a) Paint 2 (ID number = [6])

This belonged to the type 2 material. Because of fast initial decay, the initial ES for this material could not be kept similar even after two days, but after a certain period of time, another stabilized long-term ES could be established as illustrated in [Figure 5.6](#). The variance among these long-term ESs was less than 4% with regard to the maximum peak of the ES at 7 months(Long-term 2).

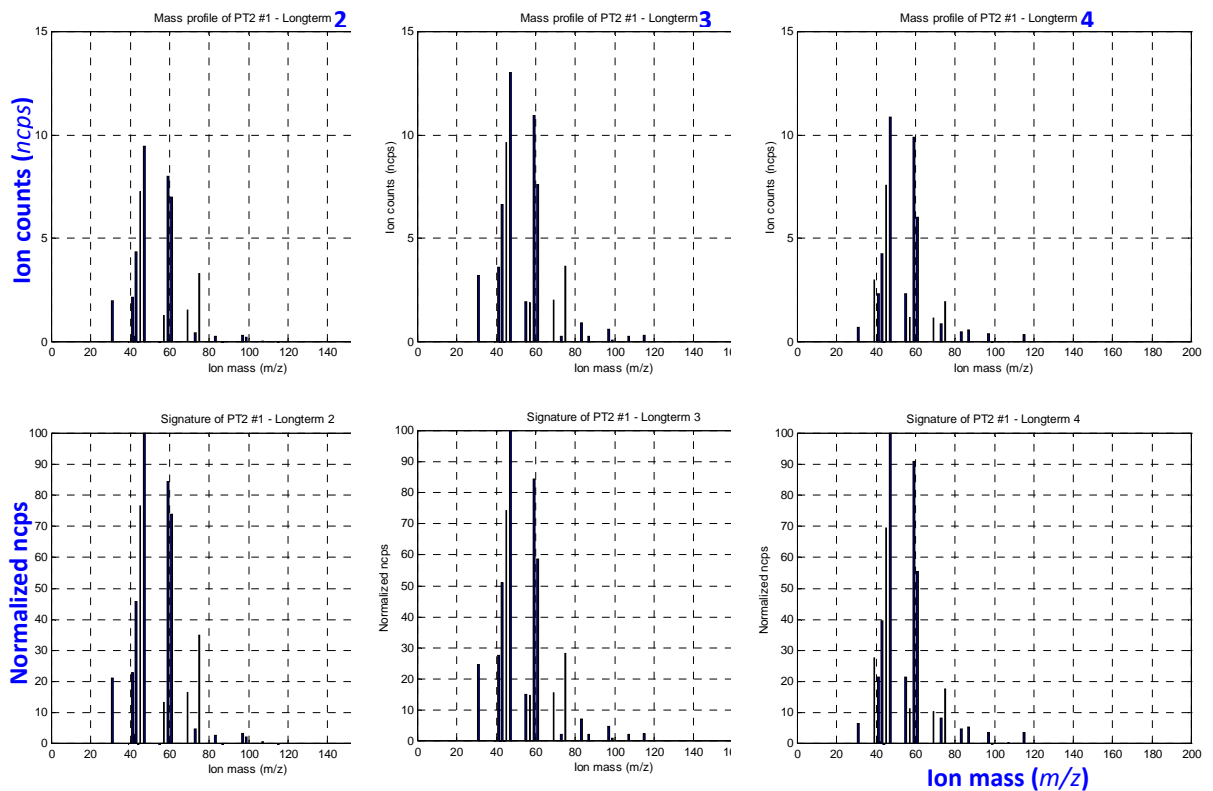


**Figure 5.6** Stable emission signatures for Paint 2 after 7-month long-term emissions.

(b) Carpet (ID number = [7])

This belonged to the type 2 material. The stable long-term ES was quite different with the initial ES for this material. However, after a certain period of time, another stabilized long-term ES existed as shown in [Figure 5.7](#). The variance among these long-term ESs

was less than 8% with regard to the maximum peak of the ES for this material at 7 months (Long-term 2).

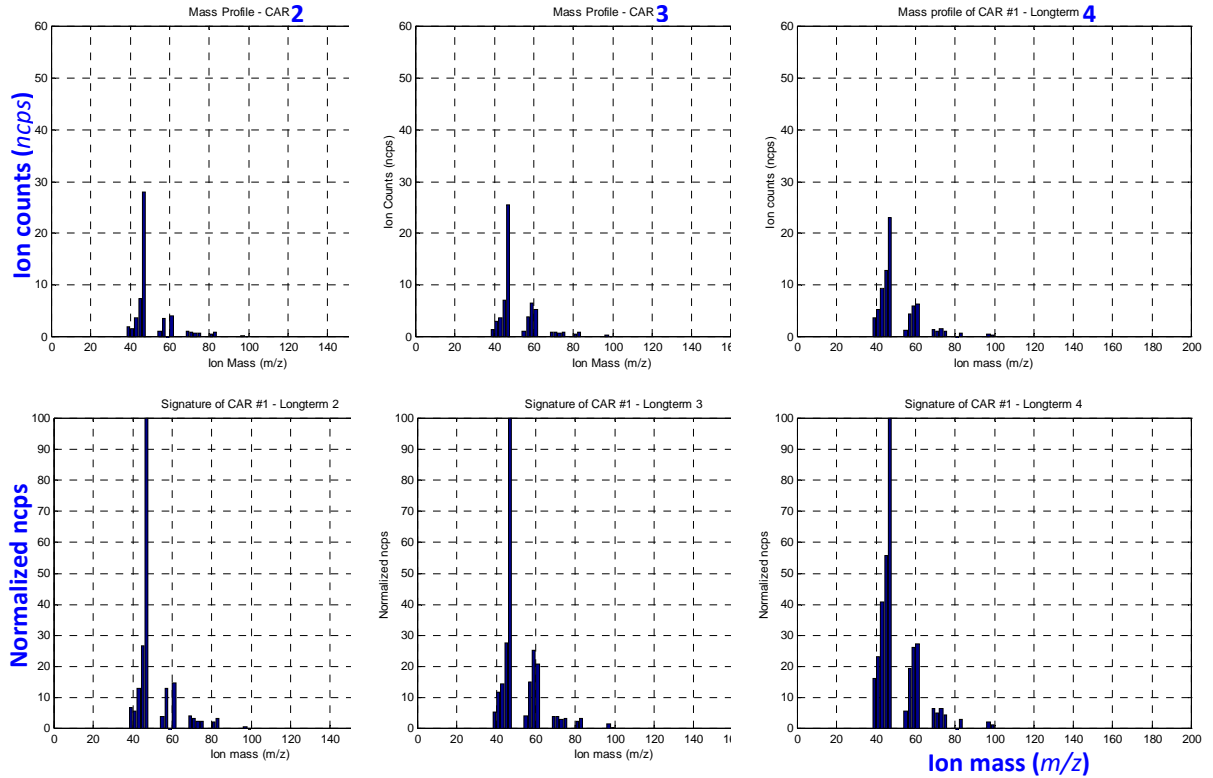


**Figure 5.7** Stable emission signatures for Carpet after 7-month long-term emissions.

(c) Linoleum (ID number = [8])

This belonged to the type 2 material. Because of the steady initial decay of VOC emissions, the shape of the long-term ES kept quite similar to that of the initial ES even after the 9-month ventilation period. The long-term ESs for this material were quite stable and consistent as demonstrated in [Figure 5.8](#). The variance among these long-term ESs was less than 1% (when not considering  $m/z = 59$ ) with regard to the maximum peak of the ES at 7 months (Long-term 2).



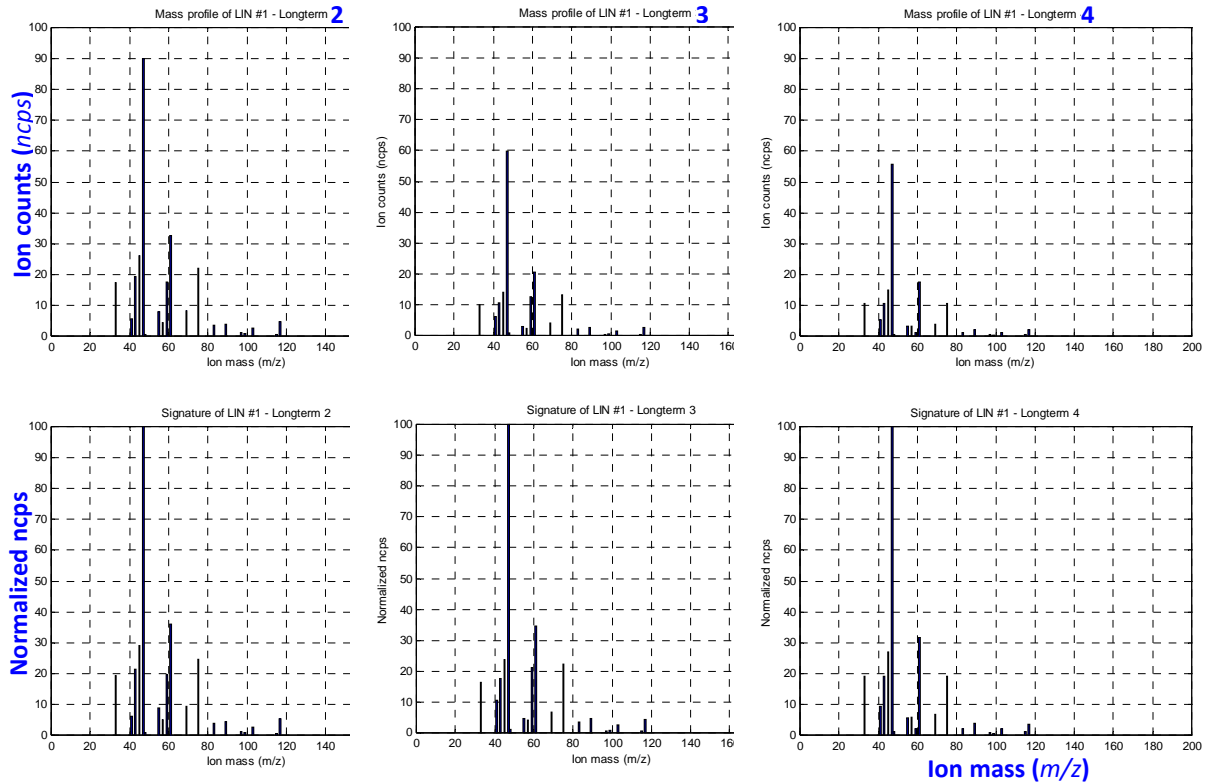


**Figure 5.8** Stable emission signatures for Linoleum after 7-month long-term emissions.

(d) Wood (ID number = [9])

This belonged to the type 1 material. The initial stable ES could be sustained even after the 9-month long-term emissions. Initially, Linoleum was the highest polluting material in the sense of VOC concentration levels, and Wood was the second. After 7 months, however, this material became the highest one due to the low decay rates of its VOC emissions compared with other materials (See the maximum peak levels of Linoleum in [Figure 5.8](#) and of Wood at 7 months in [Figure 5.9](#), 90 *ncps* vs. 140 *ncps*, which were initially 2974 *ncps* for Linoleum vs. 1070 *ncps* for Wood). The long-term ESs for this material were stable and consistent as illustrated in [Figure 5.9](#). The variance among these long-term ESs was less than 5% with regard to the maximum peak of the ES for this material at 7 months (Long-term 2).

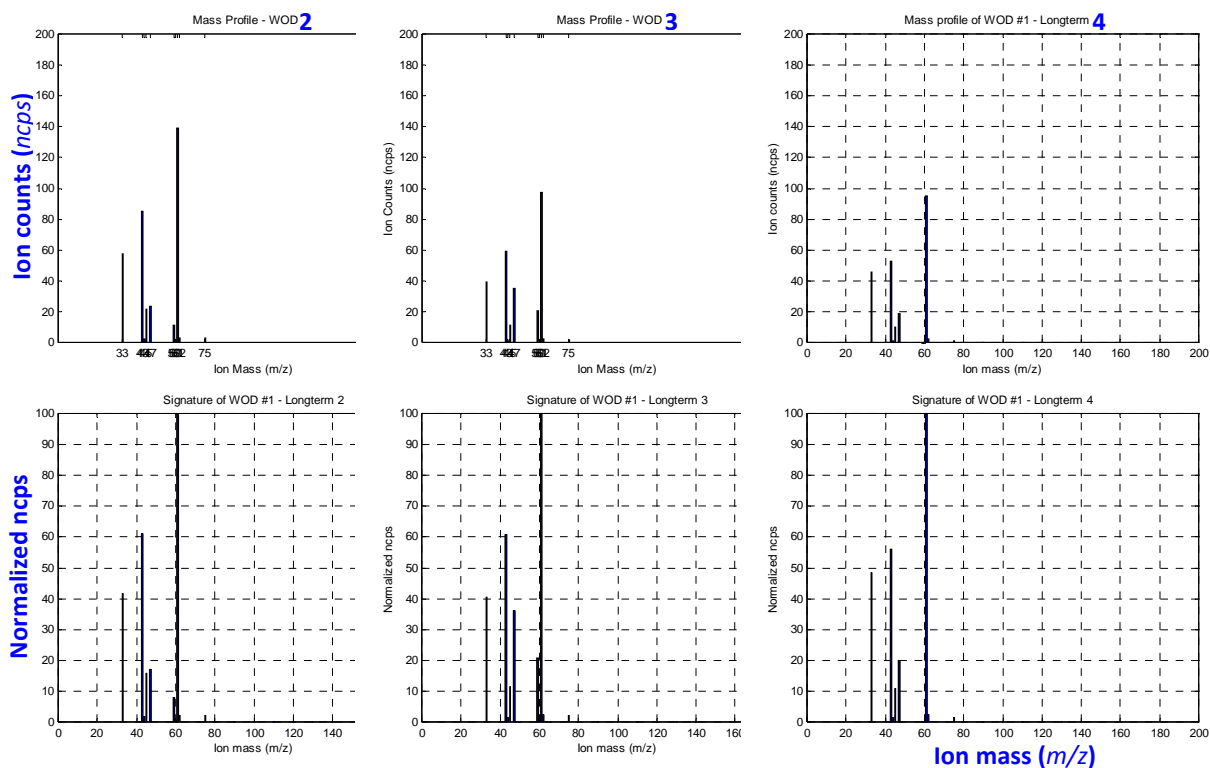


**Figure 5.9** Stable emission signatures for Wood after 7-month long-term emissions.

(e) Gypsum (ID number = [6]) – An example of materials with unstable long-term ESs

This belonged to the type 3 material. The initial stable ES could not be found in any of the long-term ESs shown in [Figure 5.10](#), and also the measured long-term ESs were quite different from each other. [Figure 5.10](#) illustrates the low level of its signal intensities all below 5 *ncps* (< 1 *ppbv*), far lower than that of the background air signals (50~60 *ncps*, or 7~8 *ppbv*). Materials having the concentration level lower than 10 *ncps* might get susceptible to the background signal change and measurement noise, making it infeasible to obtain a stable signature. In this study, we are dealing with trace level of VOCs from building materials, having tens of ppb level of concentrations, and this level became lower than even 1 ppb after the 9-month ventilation. For either case, it may be hard for human subjects to detect the effects of VOCs, or far below the detection limits of human sensory systems. If we deal with much higher concentration levels than the present ones

even for several type 3 materials classified in this study, a stable long-term ES for each case might be obtainable, considering that the stabilizing trends for long-term ESs appeared to exist in other materials and that these type 3 materials also had a stable initial ES for each case when the pollution level was relatively high in its early stage of emissions.

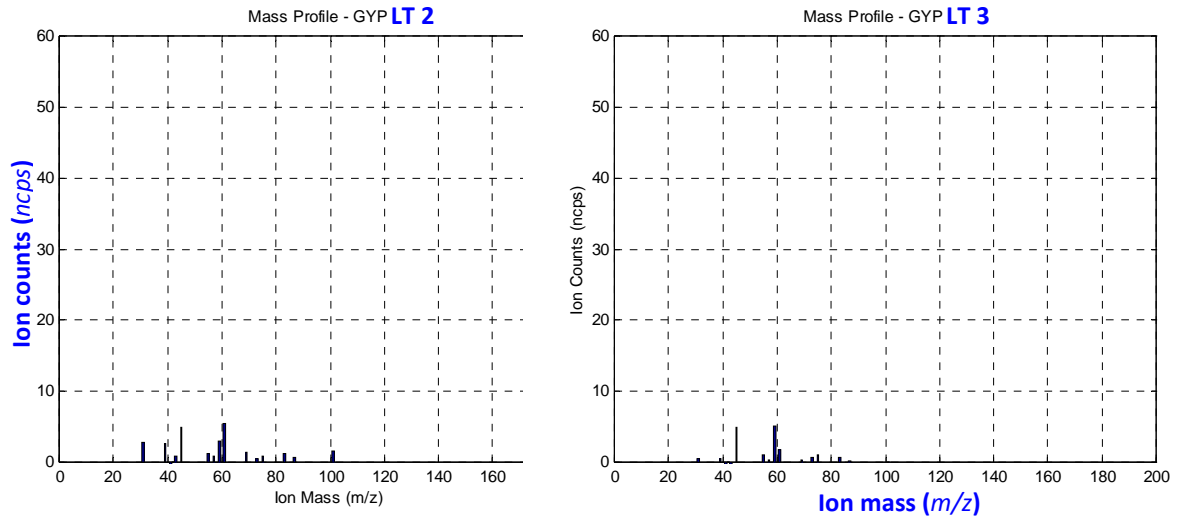


Figure 5.10 Unstable emission signatures for Gypsum at 7 & 8 months due to low SNR.

### 5.3.2 Long-term ES estimations by using source models

Can the long-term emission signatures at a later period of time be estimated by using some information on the initial material emission signatures? This section will challenge this question, providing mathematical approaches (i.e. source models) to reach possible answers and recommending a practical procedure for establishing a library of long-term emission signatures for future researches on this topic.

#### 5.3.2.1 By Double-exponential decay model

Brown (1999, 2002) used source models (i.e. double-exponential and power-law decay models) in his study for exploring persistent low levels of VOC concentrations in established dwellings due to long-term emissions from building materials. The present study investigated the feasibility of the estimation of long-term emission signatures by using collected measurements and source models. Two materials – Linoleum and Paint 2 were selected and studied in this aspect because these two materials are representative of two characteristic material types distinct by a steady (or slow) emission decay and a fast emission decay over time, respectively. First, the double-exponential decay model was applied to the long-term emission measurements for the two materials, defined as follows:

$$EF = EF_0 \cdot \exp(-k_0 \cdot t) + EF_1 \cdot \exp(-k_1 \cdot t) \quad (5.1)$$

where  $EF$  represents the emission factor for source materials in the unit of  $\mu\text{gm}^{-2}\text{h}^{-1}$ ,  $EF_0$  is the initial emission factor of short-term emissions,  $EF_1$  that of long-term emissions

( $\mu\text{gm}^{-2} \text{h}^{-1}$ ),  $k_0$  and  $k_1$  indicate the corresponding decay constants for the short-term and long-term emissions, respectively ( $\text{h}^{-1}$ ), and  $t$  is the elapsed ventilation time (h).

(a) Linoleum

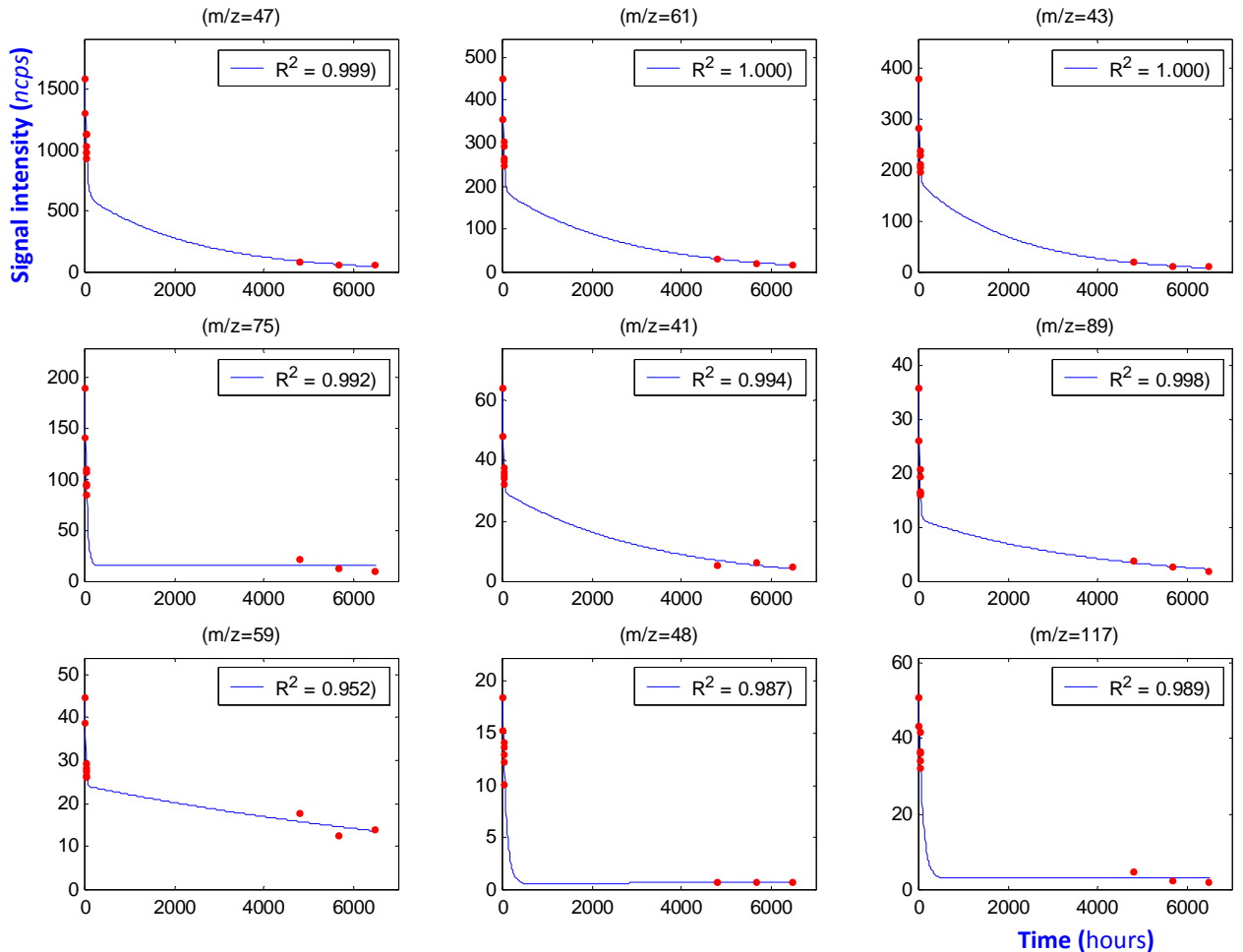


**Figure 5.11 Long-term emission fitting by the double-exponential model for major compounds of Linoleum.**

\* The blue lines indicate the fits using the model, and the red dots represent the actual measurements.

\*  $R^2$ , or COD (coefficient of determination) was presented in each legend of the figure.

For this case, the measurements at  $t_{meas} = [1, 14, 24, 29, 34, 39, 44 \text{ hours}, 7\text{-month}, 8\text{-month and } 9\text{-month}]$  were sampled to evaluate the fitting performance by the source model used. The four unknown control variables for fitting were searched in the sense of

least squared error between the estimated values and the measured ones, by using *Powell* search algorithm (Powell, 1964) customized by the author of the present study via Matlab. The model fitted the measurements with high values of COD (coefficient of determination) for all selected compounds emitted from Linoleum ( $> 0.95$ ) as demonstrated in **Figure 5.11**.

(b) Paint 2

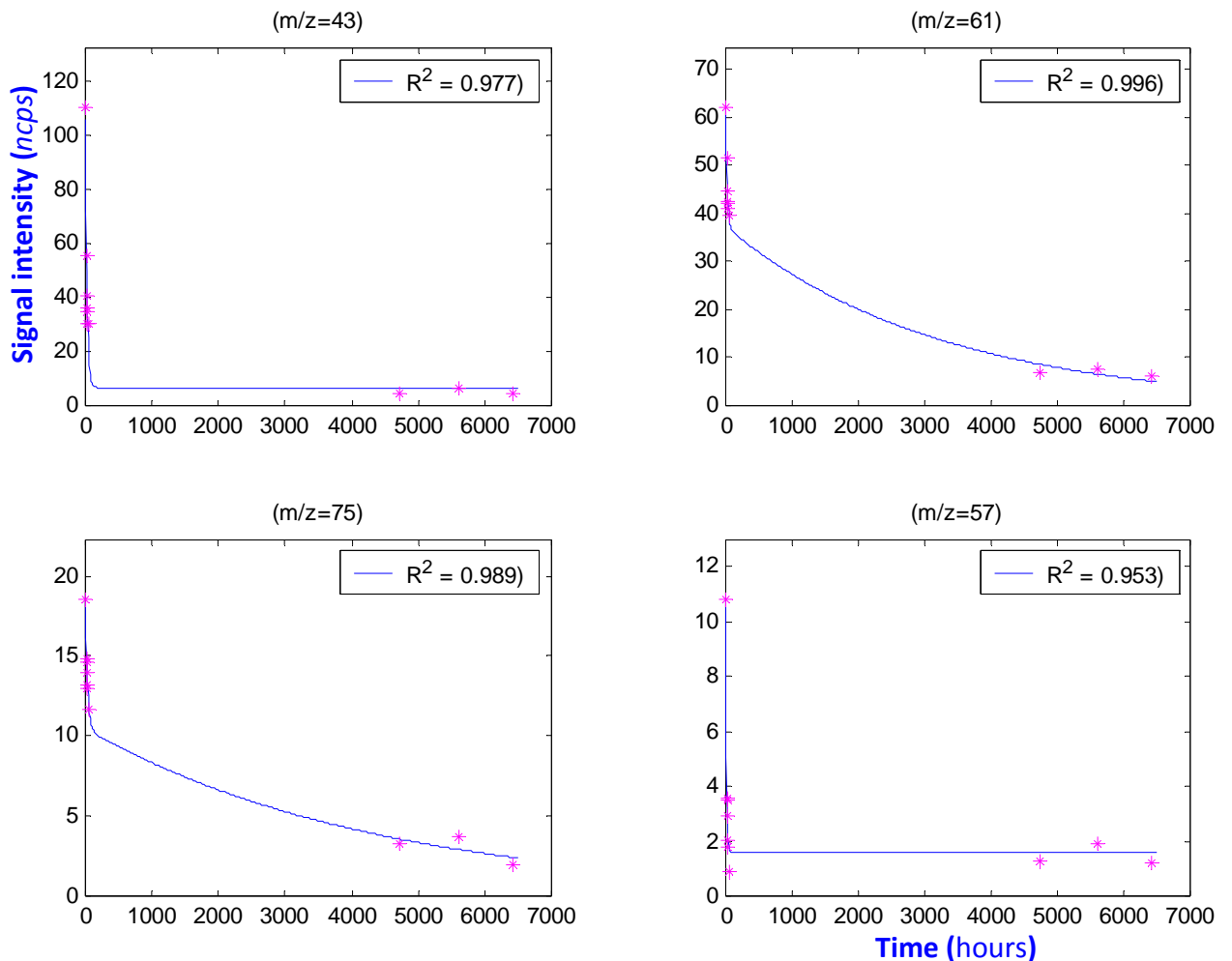


**Figure 5.12 Long-term emission fitting by the double-exponential model for several major compounds of Paint 2.**

\* The blue lines indicate the fits using the source model, and the magenta stars represent the actual measurements.

\*  $R^2$ , or COD (coefficient of determination) was presented in each legend of the figure.

For this case, the measurements at  $t_{meas} = [1, 14, 24, 29, 34, 39, 44 \text{ hours, 7-month, 8-month, and 9-month}]$  were collected to check the fitting performance of the source model. The fitting variables were determined via the least square *Powell* search. The model quite well fitted the measurements with high levels of COD for all selected compounds emitted from Paint 2 ( $> 0.95$ ). The initial concentrations of the presented compounds decayed at very steep rates as shown in **Figure 5.12**.

### 5.3.2.2 By Power-law decay model

Now, the power-law decay model was applied to the long-term emission measurements, defined as follows:

$$EF = a \times t^{-b} \quad (5.2)$$

where  $EF$  represents the emission factor for source materials in the unit of  $\mu\text{gm}^{-2}\text{h}^{-1}$ ,  $a$  and  $b$  are empirical constants in the power-law equation, and  $t$  is the elapsed ventilation time (h).

According to a NRC report published by National Research Council of Canada (Zhang et al., 1999), most of their tested emission cases for building materials appeared to follow internal-diffusion controlled emissions after 24 hours from the start of ventilation. This phenomenon could also be found in most of the tested cases of the present study. In this regard, for this power-law implementation, the measurement data only after the elapse time of 24 hours were used.

## (a) Linoleum

For this case, the measurements at  $t_{meas} = [24, 29, 34, 39, 44 \text{ hours}, 7\text{-month}, 8\text{-month and } 9\text{-month}]$  were sampled to evaluate the fitting performance by the source model used. The two unknown control variables for the fitting were searched in terms of least squared error between the estimated values and the measured ones, by using *Powell* search algorithm customized by using Matlab. The model was fast and stable in obtaining proper fitting variables, and well fitted with the measurements as shown in [Figure 5.13](#). This model showed a less performance than the double-exponential one, but could fit the measurements still with high COD values for all selected compounds emitted from Linoleum ( $> 0.93$ ).

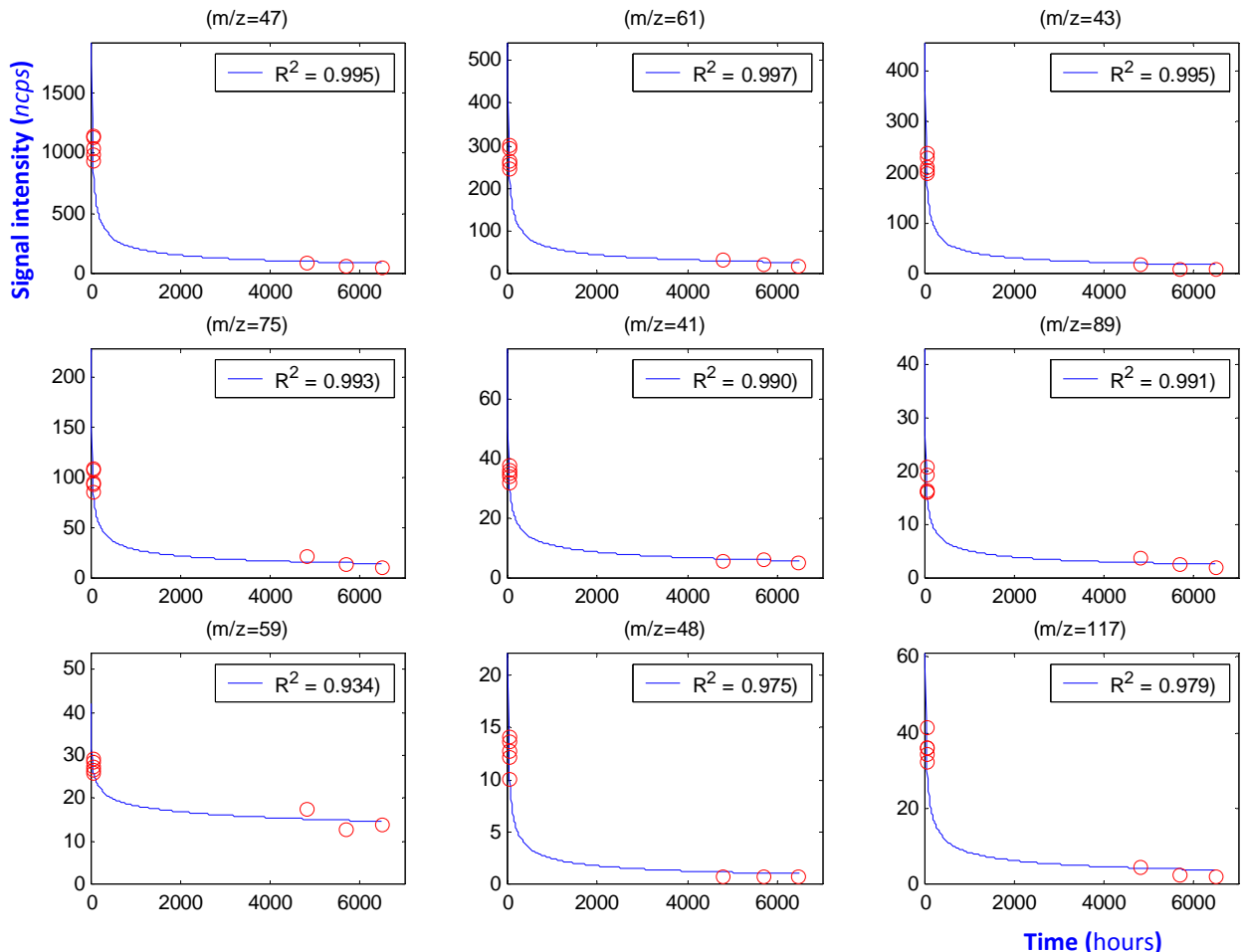




**Figure 5.13 Long-term emission fitting by the power-law model for major compounds of Linoleum.**

\* The blue lines indicate the fits using the source model, and the red circles represent the actual measurements.

\*  $R^2$ , or COD (coefficient of determination) was presented in each legend of the figure.

(b) Paint 2

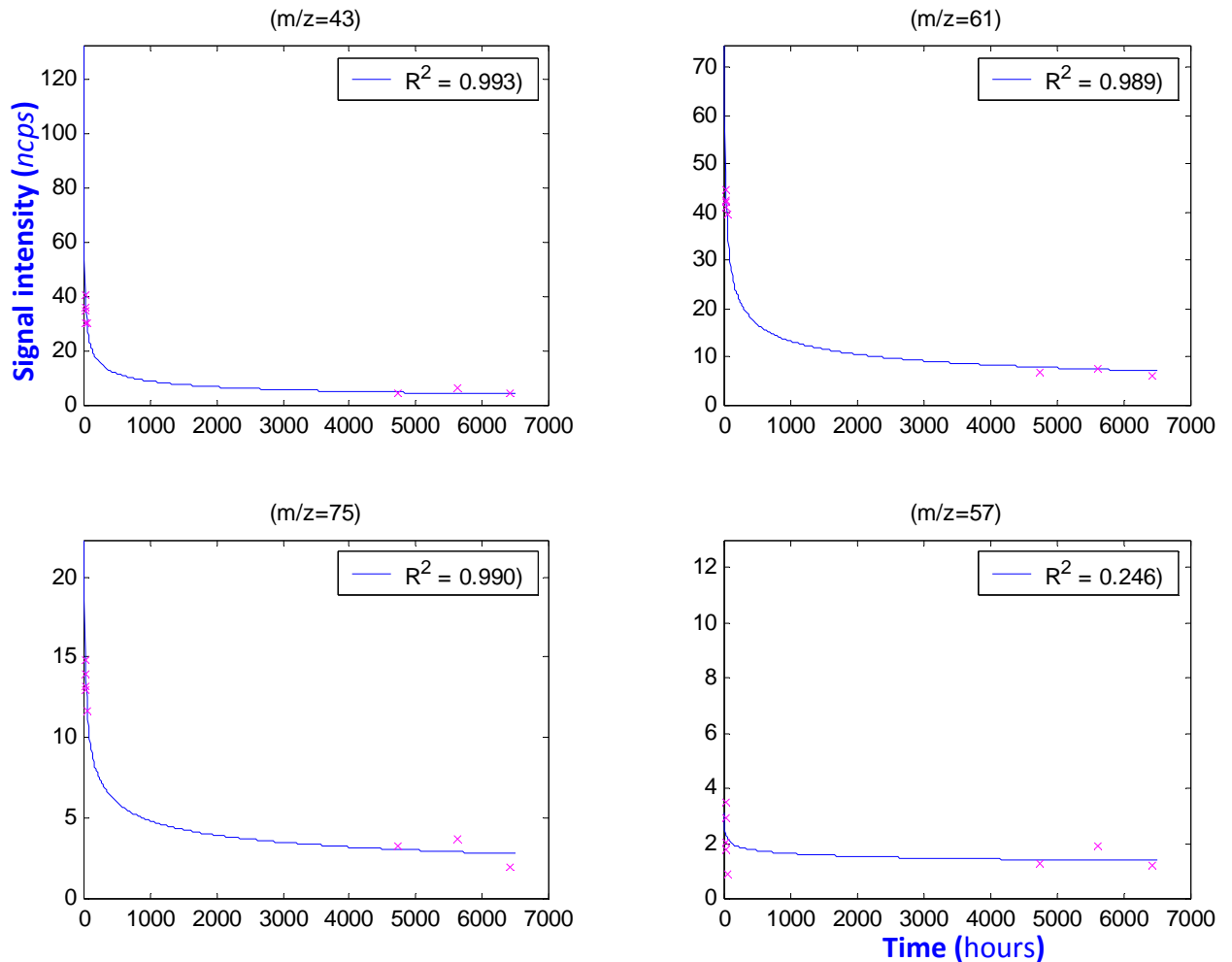


**Figure 5.14 Long-term emission fitting by the power-law model for several major compounds of Paint 2.**

\* The blue lines indicate the fits using the source model, and the magenta 'X's represent the actual measurements.

\*  $R^2$ , or COD (coefficient of determination) was presented in each legend of the figure.

For this case, the measurements at  $t_{meas} = [24, 29, 34, 39, 44 \text{ hours, 7-month, 8-month, and 9-month}]$  were collected to evaluate the fitting performance by this source model.

The fitting variables were determined via the least square *Powell* search in a faster and more stable way than the double-exponential model. The model showed a good fitting performance with reasonably high COD values for most of the selected compounds from Paint 2 ( $> 0.98$ ), but for some compounds, the COD values were low as exemplified in **Figure 5.14** for acrolein ( $m/z = 57$ ).

### 5.3.2.3 Summary of the performance of long-term ES estimations

By utilizing the source models to trace the change of VOC emissions for all compounds composing an emission signature for a given material, long-term ESs can be estimated at a certain given time. To show the feasibility of this approach in estimating long-term ESs, Linoleum and Paint 2 were selected, and this mathematical approach was applied to evaluate the estimation performance. The long-term ESs may also be predicted by using a short-term dataset of ESs at an early period (e.g.  $< 1$ -month). This prediction approach will be dealt with in a later section. After estimating the long-term ESs for a given set of material mixtures used, the dataset of ESs can be re-established, and used in effectively separating and identifying emission signatures for improving the performance of source identification throughout long-term emissions. This approach will be verified in the next section.

**Figure 5.15** exemplifies the approach for emission signature estimations and the performance result using a source model for Linoleum at the 7<sup>th</sup> month. The figure implies that with some information on the measured profile of material emission signatures over time, the long-term change of ESs for a given material at a specific elapsed time can be effectively estimated and may be used for enhancing the performance

of source identification. The estimation performance of long-term ESs was summarized in **Table 5.2** with different source models used and at different elapsed times for the two materials. Except for an outlier, the error variances of the ES estimations were less than 5%.

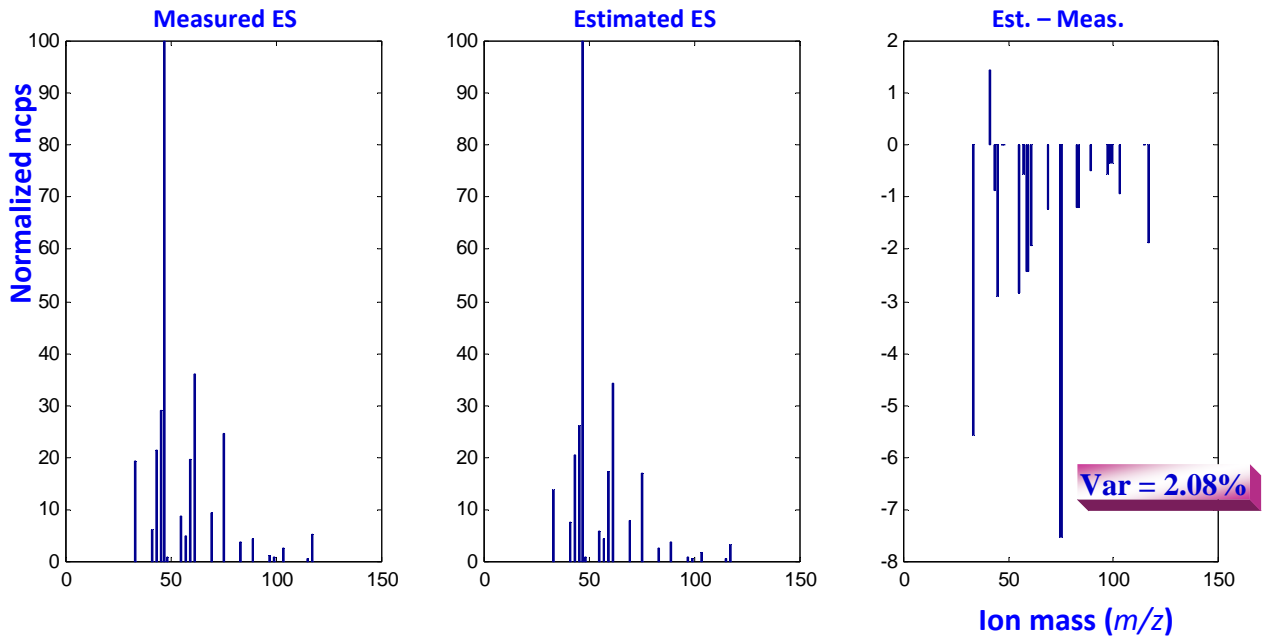


**Figure 5.15** Estimation of emission signatures exemplified by the Linoleum case using the double-exponential model at the time of 7 months (Long-term 2).

**Table 5.2** Summary of emission signature estimation results by source models.

□	Long-term 2 of LIN (7-month)	Long-term 3 of LIN (8-month)	Long-term 4 of LIN (9-month)	Long-term 2 of PT2 (7-month)	Long-term 3 of PT2 (8-month)	Long-term 4 of PT2 (9-month)
<b>Double</b>	2.08%	1.71%	4.11%	3.24%	3.72%	6.86%
<b>Power</b>	3.29%	2.29%	2.54%	4.93%	4.66%	5.98%

\* LIN: Linoleum, PT2: Paint 2.

\* The percentage values in the table represent the error variances between the estimated emission signatures and the measured ones at a given time. The smaller the values, the better the estimation performance.

### 5.3.3 ES separation performance with the consideration of long-term ES change

The mathematical approach described in the previous section for the estimation of emission signatures with the source models may improve the ES separation and identification over the course of long-term emissions. First, the dataset of ESs for a given set of materials can be established again at a specific time by considering the long-term emissions of all composing VOCs for each material and be used for enhancing ES separation and identification. The corresponding performance can be assessed by using the three indices defined in the previous chapter (Chapter. 4) as follows:

$$Err \equiv E \left\{ \left\| \bar{\alpha}_{est} - \bar{\alpha}_{true} \right\|_2 \right\}, \quad Score \equiv E \{scr(N)\}, \quad SR \equiv (N - N_{fail}) \times 100 / N \quad (5.3)$$

## 5.3.3.1 Reconstructed library of ES

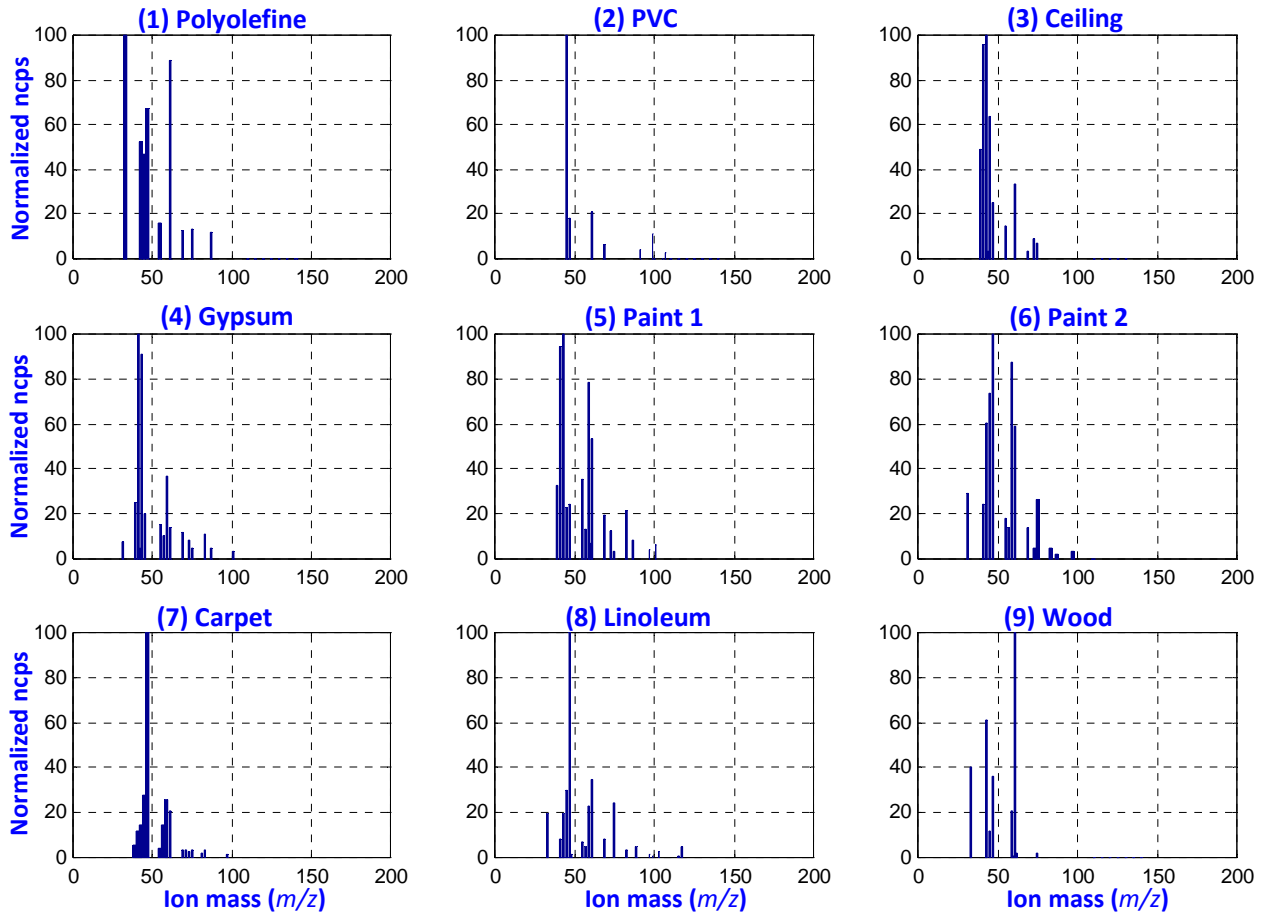


**Figure 5.16 Reconstructed emission signatures based on the estimation results at the time of 9 months.**

\* This library was estimated for the 9-month period by use of the double-exponential decay model with the full long-term emission measurements.

\* The changes of emission signatures for Materials 1 to 4 were not reflected because of their low signal intensities ( $< 1$  ppbv).

## 5.3.3.2 Summary of the identification performance

**Table 5.3 Comparison of signature separation performance results of the two algorithms for various cases.**

Ground truths	ID <sub>est1</sub> → $\alpha_{est1}$ <sup>a</sup>	ID <sub>est2</sub> → $\alpha_{est2}$ <sup>a</sup>	Err1 <sup>b</sup>	Err2 <sup>b</sup>	Score1	Score2	SR1 (%)	SR2 (%)
[6 8 9] w/ INIT	[6 7 8 9] → [0.20 <sub>2</sub> 0.17 <sub>7</sub> 0.05 <sub>6</sub> 0.09 <sub>9</sub> ]	[6 7 8 9] → [0.06 <sub>7</sub> 0.15 <sub>4</sub> 0.19 <sub>4</sub> 0.32 <sub>3</sub> ]	0.42	0.26	25.20	23.00	28.00	26.00
[6 8 9] w/ LT → [0.12 0.39 0.49]	[3 6 8 9] → [0.03 <sub>2</sub> 0.14 <sub>3</sub> 0.08 <sub>4</sub> 0.07 <sub>5</sub> ]	[3 6 8 9] → [0.08 <sub>0</sub> 0.10 <sub>6</sub> 0.31 <sub>2</sub> 0.25 <sub>0</sub> ]	0.46	0.27	52.20	81.80	56.00	<b>90.00</b>
[7 8] w/ INIT	[6 7 8] → [1.09 <sub>1</sub> 0.53 <sub>5</sub> 2.57 <sub>7</sub> ]	[6 7 8] → [0.63 <sub>0</sub> 0.48 <sub>1</sub> 2.84 <sub>9</sub> ]	0.95	0.76	45.00	44.60	50.00	50.00
[7 8] w/ LT → [0.60 2.53]	[3 7 8 9] → [0.26 <sub>5</sub> 1.40 <sub>6</sub> 2.34 <sub>3</sub> 0.14 <sub>8</sub> ]	[3 7 8 9] → [0.20 <sub>2</sub> 0.93 <sub>8</sub> 1.80 <sub>4</sub> 0.02 <sub>9</sub> ]	0.84	0.82	73.60	83.00	<b>92.00</b>	<b>98.00</b>
[8 9] w/ INIT	[3 6 8 9] → [0.05 <sub>7</sub> 0.57 <sub>4</sub> 2.03 <sub>5</sub> 3.09 <sub>4</sub> ]	[6 7 8 9] → [0.70 <sub>4</sub> 0.13 <sub>2</sub> 2.35 <sub>6</sub> 3.08 <sub>1</sub> ]	1.37	1.28	73.00	66.60	88.00	88.00
[8 9] w/ LT → [2.50 4.25]	[1 3 7 8 9] → [0.20 <sub>5</sub> 0.32 <sub>4</sub> 0.46 <sub>2</sub> 1.90 <sub>7</sub> 4.01 <sub>9</sub> ]	[1 3 7 8 9] → [0.13 <sub>6</sub> 0.29 <sub>6</sub> 0.288 <sub>8</sub> 1.29 <sub>1</sub> 3.66 <sub>2</sub> ]	0.82	1.38	65.80	61.60	88.00	88.00

<sup>a</sup> To exemplify the form of the results from the two algorithms, these estimation results (material ID set and the corresponding signal intensity factor vector) were presented in the table, which were obtained when applying the algorithms to the representative (i.e. by averaging the measured 50 samples) emission signature measured for each given material mixture. However, the three performance indices shown in the table were calculated using 50 measured samples for each mixture, following the definitions of the three indices as shown in Equation (5.3). <sup>b</sup> 1: of Algorithm 1, 2: of Algorithm 2.

\* w/ INIT: with initial ESs; w/ LT: with the consideration of long-term emissions.

At the 9-month period, the emissions from three material mixtures were measured under the conditions defined in **Table 5.1** (Measurement #4-6). For each mixture, 50 emission samples were measured by PTR-MS and processed by following the signal processing procedures described in the previous study (Han et al., 2010) to get the corresponding emission signatures for the mixtures. The PTR-MS ESs measured for these combined

emissions were applied to the developed algorithms with and without the consideration of long-term ES change, and the performance of ES separation and identification for each case was assessed by the performance indices (Eq. 5.3). The comparison results were summarized in **Table 5.3**.

The case of the three-material mixture (i.e. [6 8 9] = Paint 2 + Linoleum + Wood, Measurement #4) without the long-term ES consideration ([6 8 9] with the initial ESs) showed the lowest performance with low success rates (< 28%). The number of materials and the large change of ESs especially for Paint 2 appeared to contribute to the resulting low performance. On the other hand, the proper estimation close to the true shapes of the long-term ESs using the source models seemed to improve the separation/identification performance as demonstrated in **Table 5.3**. With Algorithm 2, the success rate was improved up to 90% from 26% before. This improvement could also be observed in the two-material mixture (i.e. [7 8] = Carpet + Linoleum, Measurement #5). The long-term ES for Carpet was also quite different from the initial one, so the adequate estimation of the long-term ES for this material could improve the overall performance. For another two-material mixture (i.e. [8 9] = Linoleum + Wood, Measurement #6), however, there was a small difference between with and without the long-term ES consideration. The reason for this small difference may be that the ES for Wood did not change much along the course of long-term emissions (belonging to the *Type 1* material) and also the ES for Linoleum showed a small variation between the initial and the long-term ES even though this material belonged to the *Type 2* material. These small changes in ESs between the initial and long-term ones made no marked difference in the consideration of long-term emissions for this case.

### 5.3.4 Recommendations on the practical establishment of a long-term ES library

#### 5.3.4.1 Data analysis for the validation of 'measurement generation' approach

The study had been conducted to collect and process the long-term emission data for 9 months, and additional material mixture measurements were collected for applying and validating the consideration of long-term emission signature change to enhance the source identification performance of the developed methodology. As an additional consideration, we are trying to recommend a practical testing schedule for the establishment of an ES library for future works. To suggest this practical timeline for collecting ESs over time, we need several data points in an early stage (i.e. 1-month test data), which were missed in the present measurements because of the unexpected not-readiness of the measuring system at that time. We can generate these needed data points based on the present actual measurements, but to make this suggestion more concrete, we took another set of experiments to validate the following approach for suggesting a practical testing schedule for the ES collection:

\* Assumption: The present fitting function follows the actual measurement trend for each selected ion mass. In other words, the decay constant, or  $k_0$  (Refer to Equation 5.1) of each selected ion mass for a given material is similar even in different measurement groups of the same material.

Because the storage periods of the two specimen groups (the present one and the one to be newly measured) are different, the initial surface quantity ( $M_0$ ) of the two may not be



the same even though the same material is to be used under similar environmental conditions. After normalizing the measured  $EF$  values by the  $EF$  value at the beginning measurement time (i.e. at 24 hours) for each group, if the generated values from the fitting functions determined by the present measurements are aligned with the measured values from the new experiment within a 10% deviation from the generated trajectory, we may validate the assumption declared above and use the data generation approach at least within the validated period (i.e. 1-month).

Two materials, Linoleum and Paint 2, were selected and studied in this aspect because these two materials are representative of two characteristic types of building materials – slow and fast decay.

(a) Linoleum

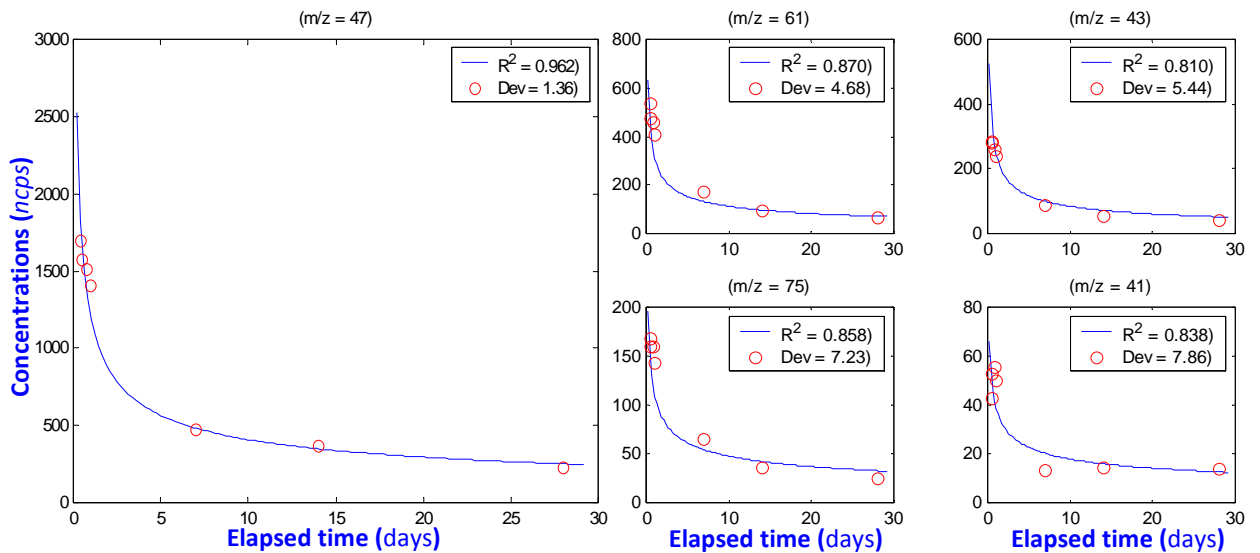


**Figure 5.17 Comparison of the emission profiles of the two different groups of measurements for selected ion masses of Linoleum.**

\*  $R^2$ , coefficient of determination, was calculated for the new measurements with respect to the corresponding fitting lines determined by the previous measurements, and presented in each legend box of the figure.

\* 'Dev' stands for the mean deviation of the new measurements at Day 7, Day 14 and Day 28 from the corresponding fitting lines, and its magnitude was presented in percentage with regard to the concentration level at 24 hours, or Day 1.

**Figure 5.17** shows the comparison results between the new measurement trends and the fitting lines determined by the power-law decay model with the previous measurements for several major compounds emitted from Linoleum. For each case, the  $R^2$  values for the whole samples presented and the mean deviations of the new measurements at Day 7, 14 and 28 are included in the figure. The power-law model appeared to be more physically realistic than the double-exponential model, so the fitting lines by the power-law were used in this comparison. The generated values from the power-law fitting functions by the previous measurements are well aligned with the new measurements within an 8% deviation from the trajectory ( $> 0.81$  of  $R^2$ ).

(b) Paint 2

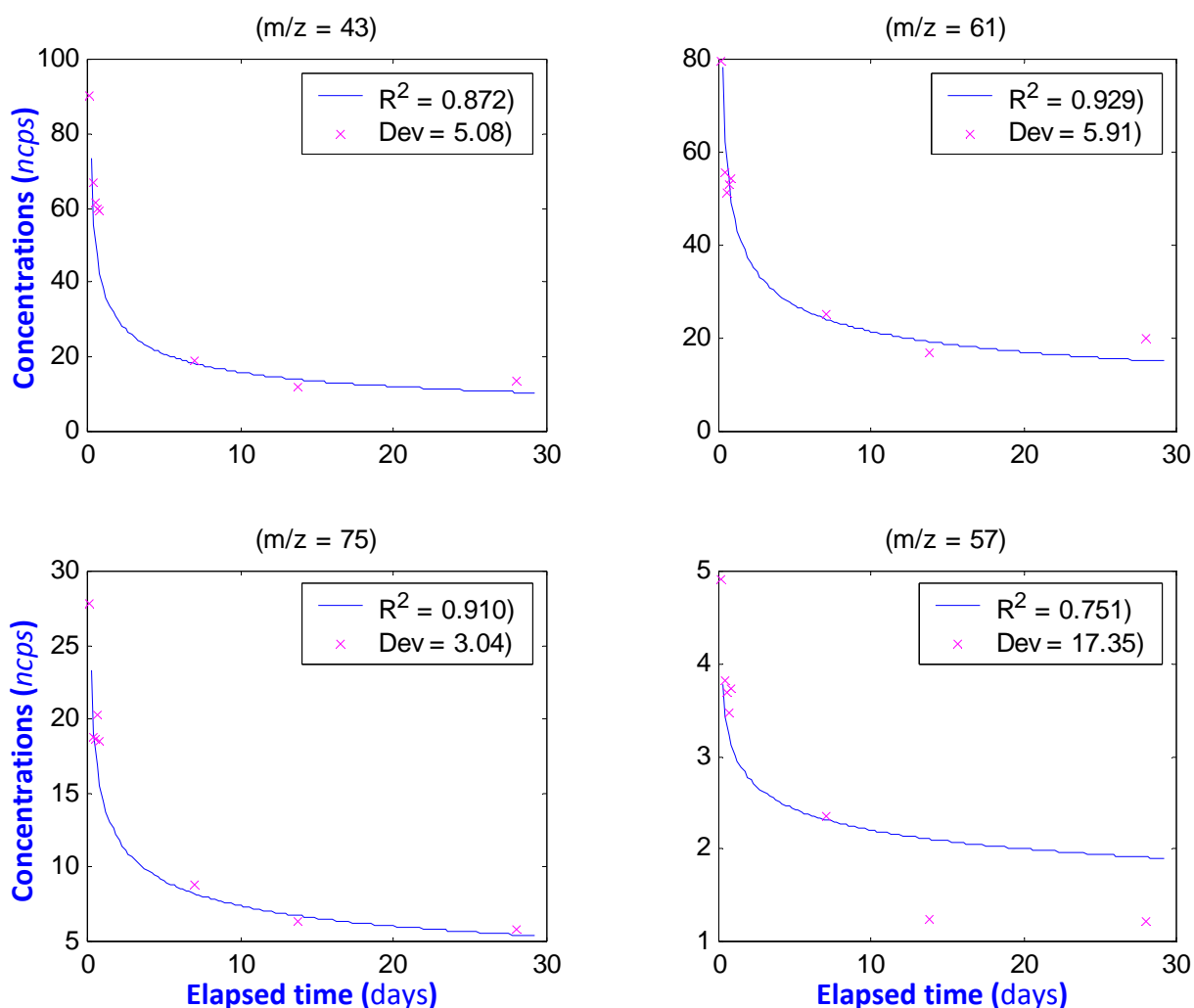


**Figure 5.18** Comparison of the emission profiles of the two different groups of measurements for selected ion masses of Paint 2.

\*  $R^2$ , coefficient of determination, was calculated for the new measurements with respect to the corresponding fitting lines determined by the previous measurements, and presented in each legend box of the figure.

\* 'Dev' stands for the mean deviation of the new measurements at Day 7, Day 14 and Day 28 from the corresponding fitting lines, and its magnitude was presented in percentage with regard to the concentration level at 24 hours, or Day 1.

**Figure 5.18** shows the comparison results for Paint 2. The fitting lines indicate a good alignment with the new measurements within a 6% deviation from the trajectory except for an outlier, and with high levels of fitting determination ( $> 0.75$  of  $R^2$ ).

From this investigation, the calculated decay rates showed a good repeatability even in the two different measurement groups having more than 1 year gap between the two measurements, which can validate the assumption declared in the beginning of this section, confirming the possibility of the data generation approach for a later study at least within the validated period (i.e. 1-month).

#### 5.3.4.2 Recommendations on a practical testing period for the ES library

This section is intended to suggest a practical short-term testing schedule for collecting a set of valid emission signatures for materials. The sampling period generally accepted in the practice for predicting long-term emissions will be explored, which is to collect emission measurements at Day 0-2, Day 7, Day 14 and Day 28 from the start of ventilation (after the pre-conditioning period).

##### (a) Linoleum

The measurements at  $t_{meas} = [1, 14, 24, 29, 34, 39, 44 \text{ hours, Day 7, Day 14, Day 28}]$  were sampled for this material. The source models, Double-exponential and Power-law decay models, were applied to get the optimal fitting line for each case in terms of least squared error, and the results were used for predicting the long-term emission concentrations at 7, 8 and 9 months. For the fitting with the power-law model, only the measurements after 24 hours were used. The prediction errors were assessed with regard to the concentration level at 24 hours in the profile of each case.

**Figure 5.19** is well exemplifying this approach with the case of ethanol ( $m/z = 47$ ) from Linoleum. The figure demonstrates that, because of measurement noise, the

determination of sampling interval may affect the resulting trend of fitting line in a significant way, especially in the case of dealing with very low levels of VOC concentrations (due to low signal-to-noise ratio), which did happen many times in this study due to trace VOCs. The double-exponential model seemed to fit the initial response of the long-term emission concentration profile more adequately than the power-law model when the sampling schedule to be explored in this section was used. The number of control parameters to be estimated for this model (4 parameters) is more than that of the power-law (2 parameters), which can make the fitting process of this model harder and more time-consuming (sometimes, infeasible) than the case with the power-law, requiring more number of samples to be used for the fitting. In addition, the fitting results from this model appeared to become more mathematically oriented than those of the power-law mainly due to the short-term measurements, not physically oriented, finding the final solution with the least error to the given measurements. On the other hand, the power-law model seemed to represent more properly the physical decay property of long-term VOC emissions (Note: when samples only after 24 hours were used) for most of the cases investigated than the double-exponential.

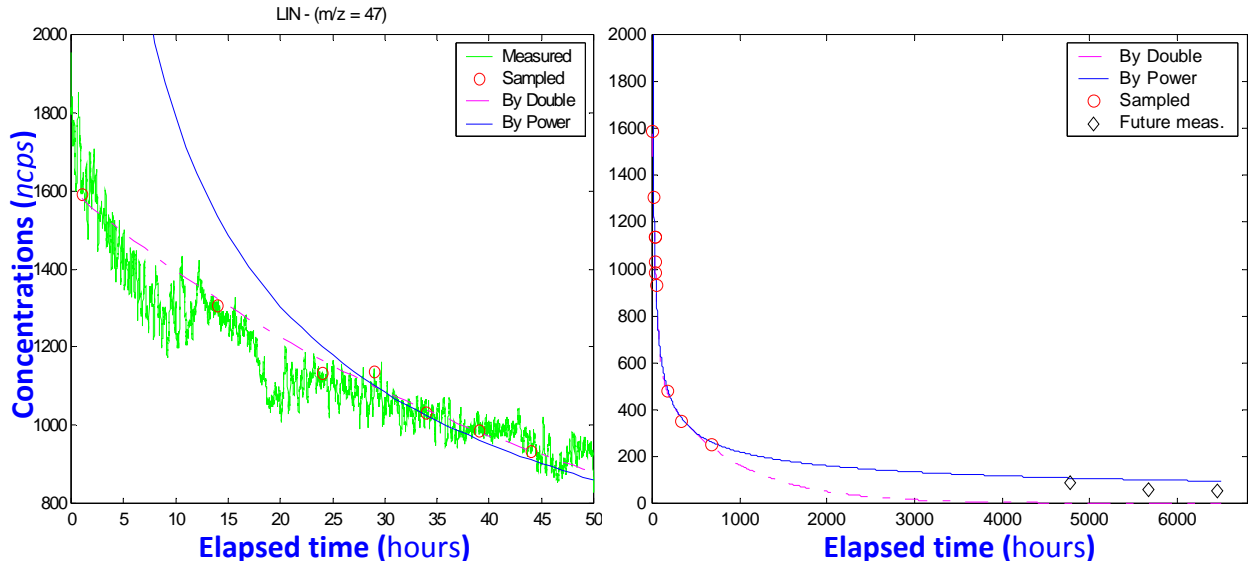


Figure 5.19 Prediction of the future concentrations at 7, 8 & 9 months by source models with short-term meas. exemplified with ethanol ( $m/z=47$ ) from Linoleum.

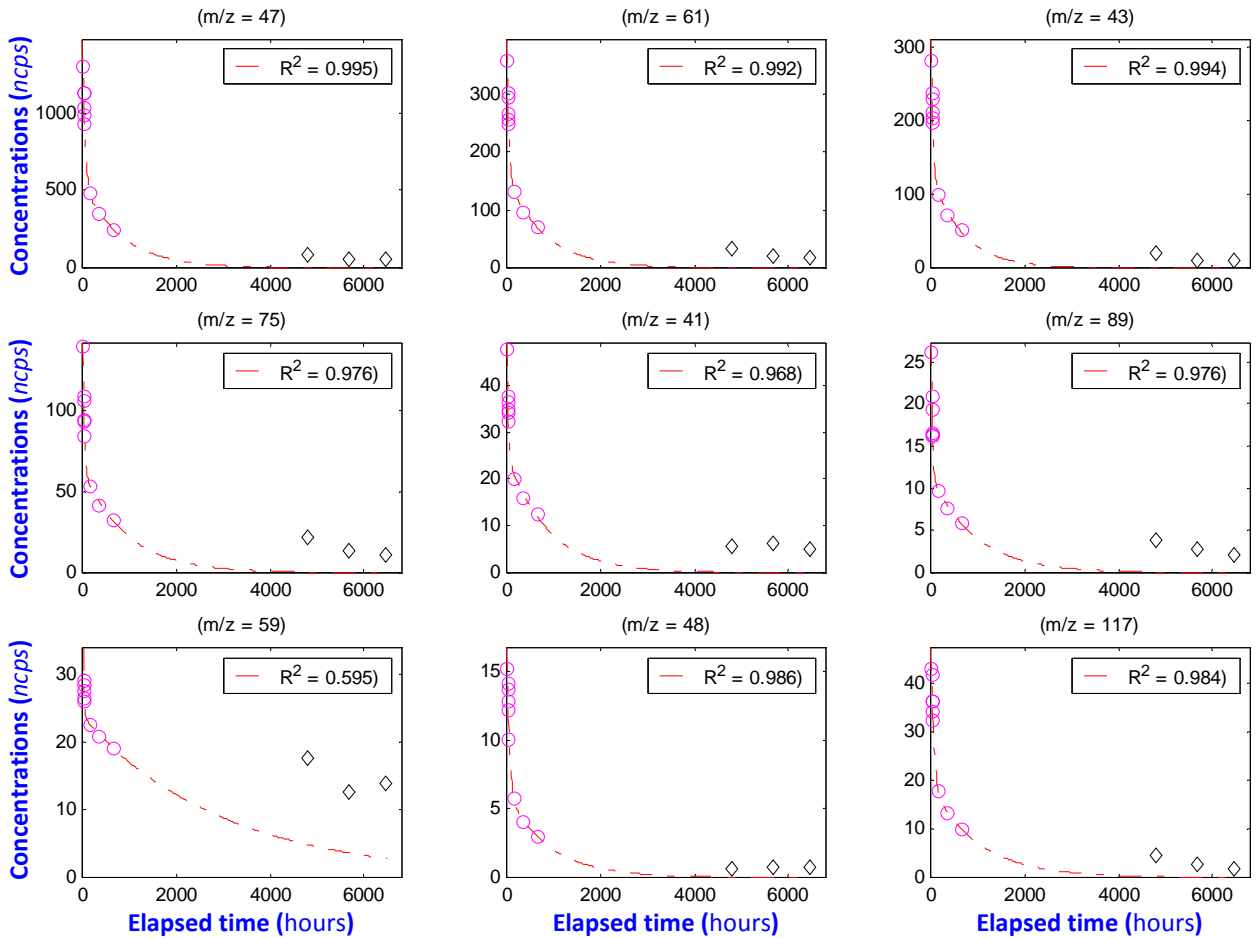
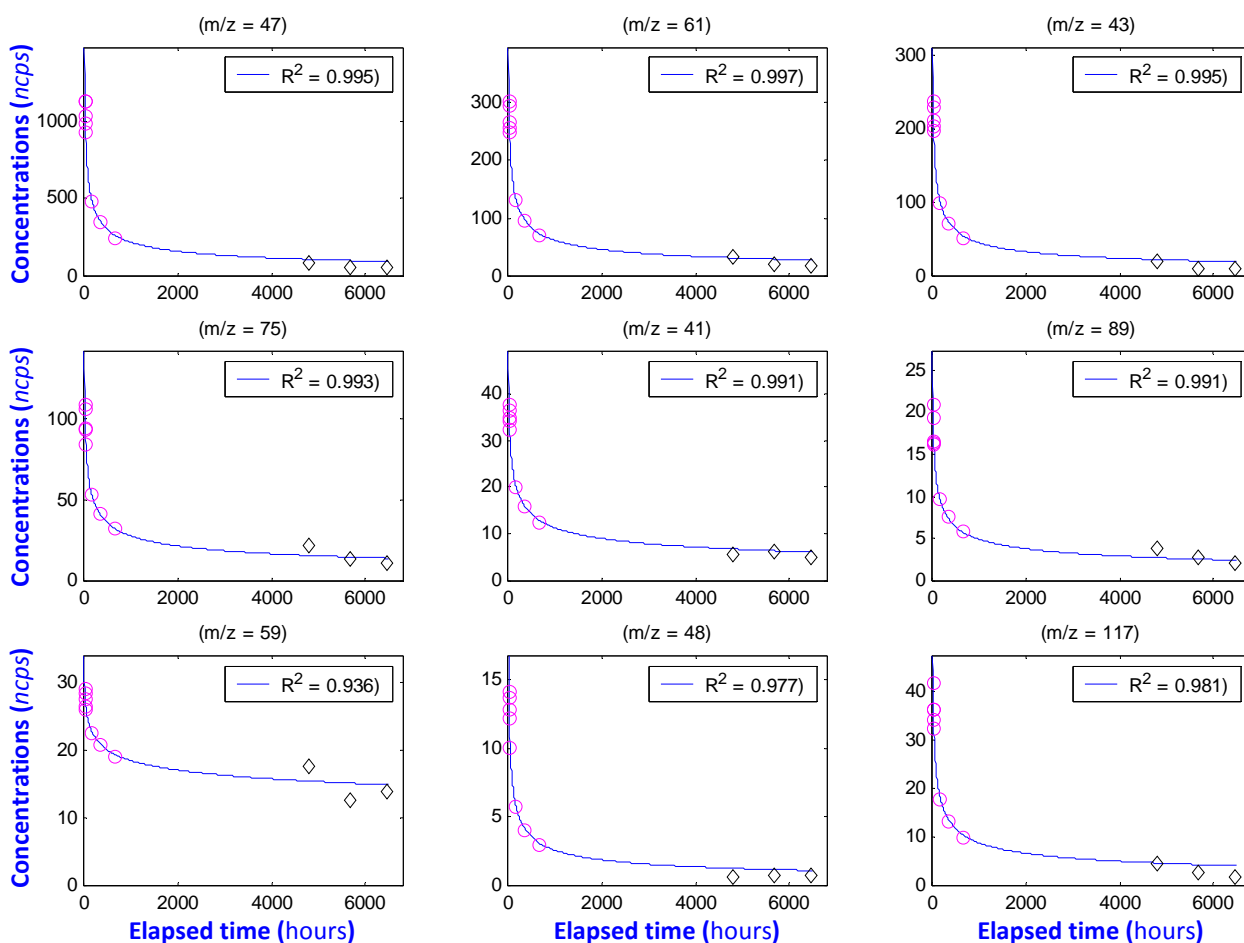


Figure 5.20 Conc. predictions by the double-exp for selected compounds of Linoleum.

\*  $R^2$  is calculated for all the points presented (i.e. the sampled and future measurements).

Because of this attractive property of this model reflecting the proper physical decay even with short-term measurements, the prediction of long-term emissions by the power-law model had lower errors than that from the double-exponential, which can be seen in **Figures 5.19, 5.20** and **5.21**, and summarized in **Table 5.4**. This model showed a fast convergence and a high success rate in finding the final solution with a given tolerance level. **Figures 5.20** and **5.21** show the prediction trends for other major compounds of Linoleum with the double-exponential and power-law decay models, respectively.



**Figure 5.21** Conc. predictions by the power-law model for selected compounds of Linoleum.

\*  $R^2$  is calculated for all the points presented (i.e. the sampled and future measurements).

(b) Paint 2

Same as the case of Linoleum, the measurements at  $t_{meas} = [1, 14, 24, 29, 34, 39, 44$  hours, Day 7, Day 14, Day 28] were sampled also for this material. Even though this material had a different decay property from that of Linoleum, similar fitting trends and prediction performance results could be observed as the case of Linoleum. **Figure 5.22** well indicates the fitting trends and the prediction errors for this material with the case of propanoic acid ( $m/z = 75$ ) emitted from Paint 2. The figure indicates that the sampling interval may be important due to noise in determining the fitting functions like the case of Linoleum. The double-exponential model followed the initial response more adequately than the power-law, but the power-law model seemed to reflect the physical decay property of long-term VOC emissions for Paint 2 more properly. **Figures 5.22, 5.23** (with the double-exponential model) and **5.24** (with the power-law) show the trends and prediction errors for other major compounds of Paint 2, and **Table 5.4** summarizes the prediction performance for the long-term emissions for Paint 2. Both source models quite well fitted the measurements with high coefficient values of fitting determination (i.e.  $> 0.91$  of  $R^2$  with the double-exponential,  $> 0.86$  of  $R^2$  with the power-law), but the power-law appeared to have a better performance in predicting the long-term emissions for Paint 2 (i.e. The prediction error percentage is  $< 8\%$  versus  $< 26\%$  with the double-exponential model) as shown in **Figures 5.22** and **5.23**, and as summarized in **Table 5.4**.



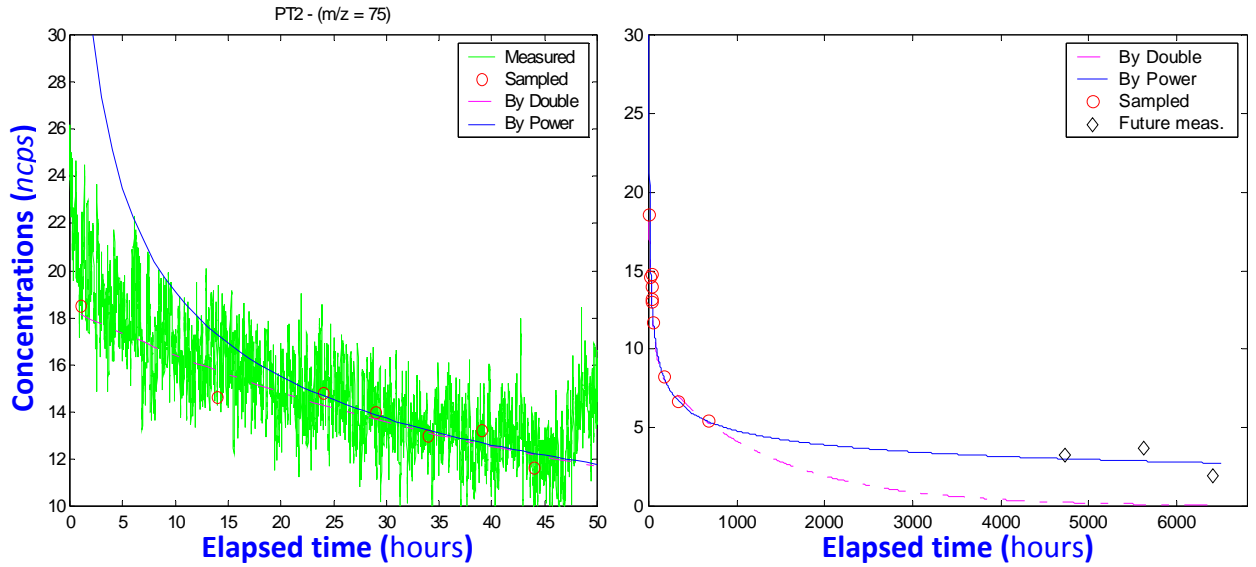
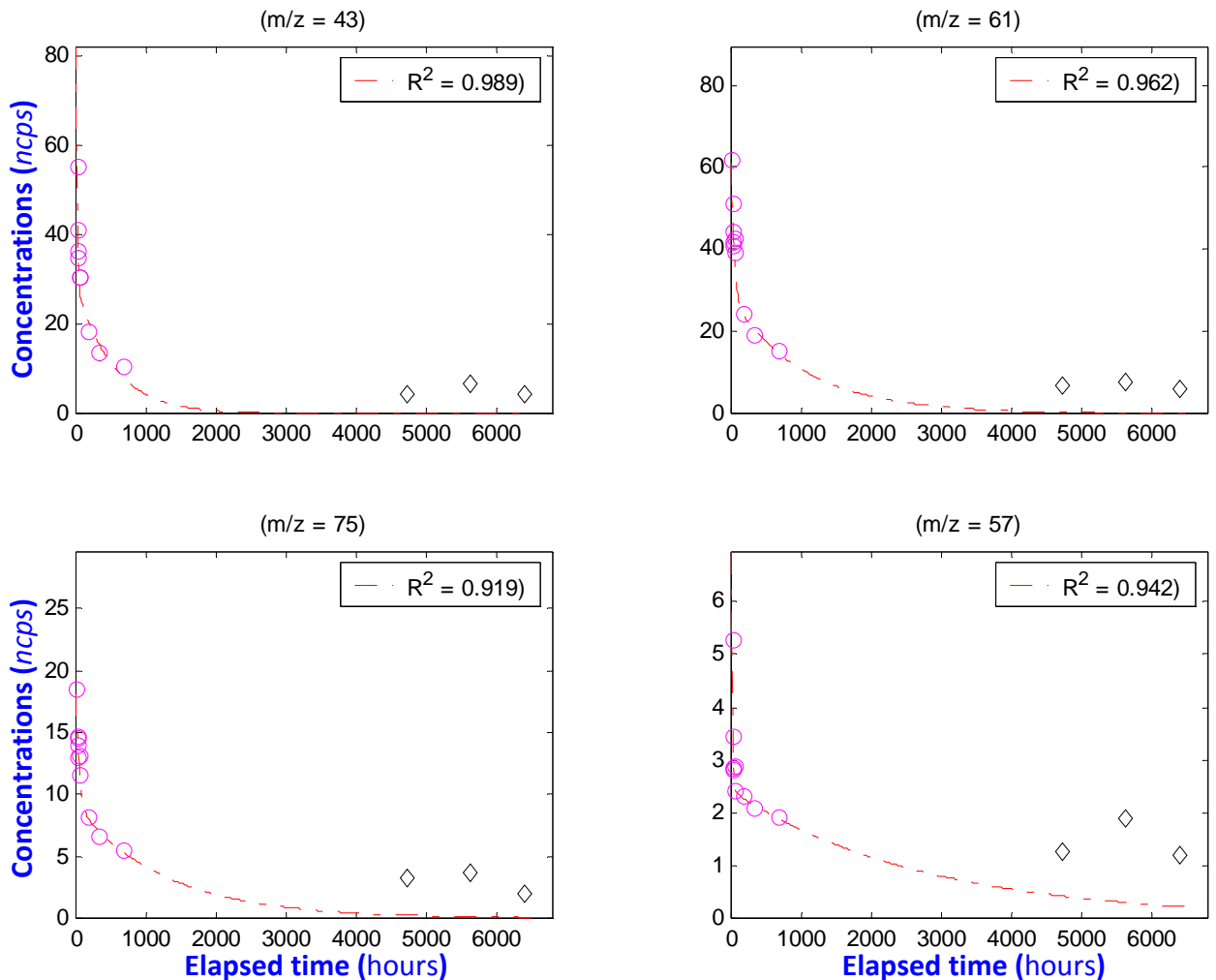
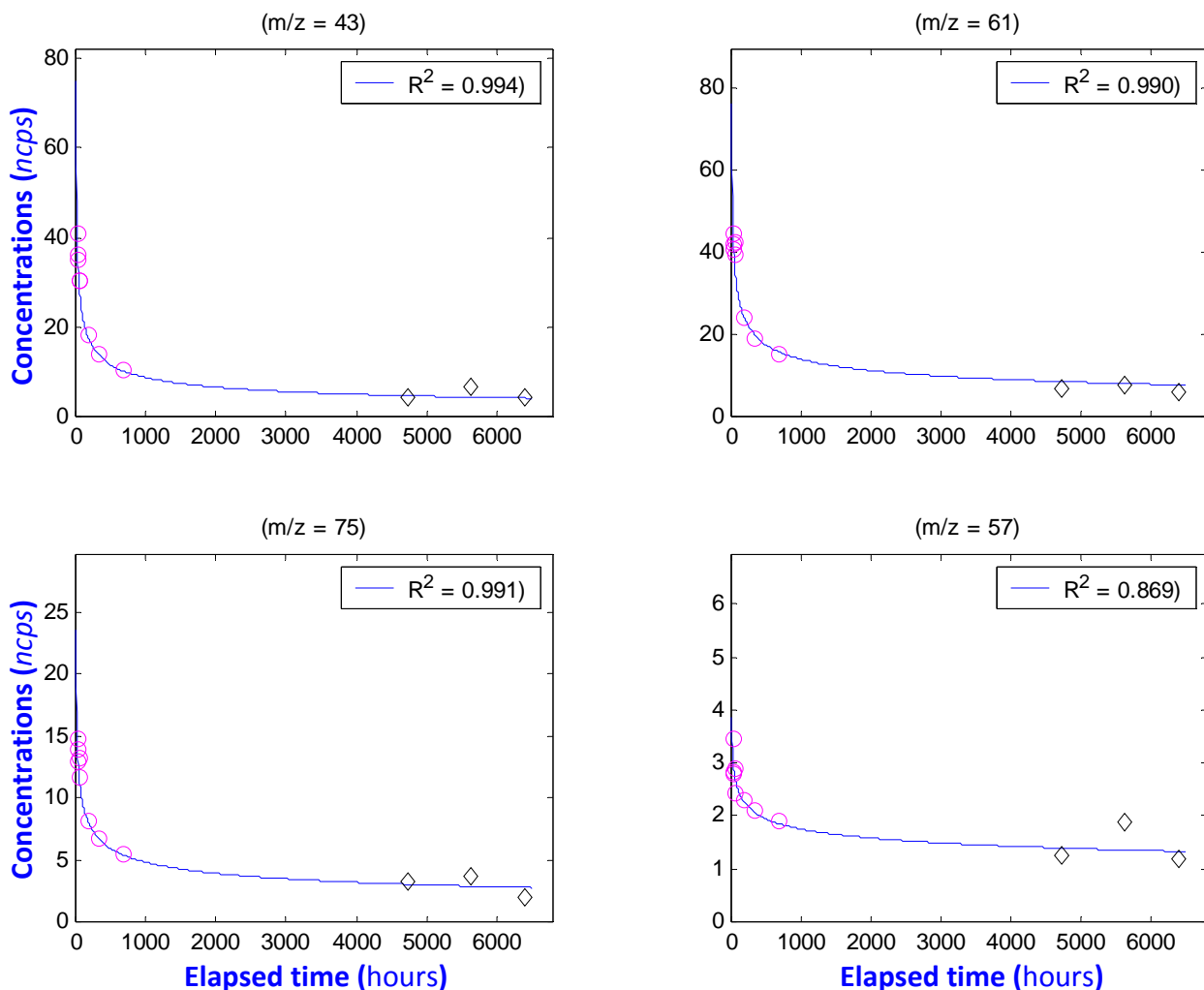


Figure 5.22 Prediction of the future concentration trends at 7, 8 & 9 months by source models with short-term measurements ( $\leq$  Day 28) exemplified with propanoic acid (with a small portion of ethanol,  $m/z=75$ ) from Paint 2.



**Figure 5.23 Conc. predictions by the double-exp for selected compounds of Paint 2.**

\*  $R^2$  is calculated for all the points presented (i.e. the sampled and future measurements).

**Figure 5.24 Conc. predictions by the power-law model for selected compounds of Paint 2.**

\*  $R^2$  is calculated for all the points presented (i.e. the sampled and future measurements).

(c) Summary of the prediction error results

**Table 5.4** summarizes the prediction performance of the long-term emissions by the double-exponential and power-law decay models at the periods of 7, 8 and 9 months, when the proposed short-term sampling schedule ( $\leq 28$  days) was used for Linoleum and Paint 2 which represent the two different emission characteristics of building materials investigated in this study. Except for an outlier, the mean percentage of prediction error at the target months with the double-exponential model was  $< 15\%$  for Linoleum and  $< 19.1\%$  for Paint 2, whereas that with the power-law was  $< 3.3\%$  for Linoleum and  $< 4.1\%$  for Paint 2. The absolute magnitude of this prediction error was calculated in percentage with regard to the concentration level at 24 hours of each case.

**Table 5.4 Summary of the prediction errors by two source models (w/ short-term data).**

	LIN						PT2						
	7 months		8 months		9 months		7 months		8 months		9 months		
	Db	Pw	Db	Pw	Db	Pw	Db	Pw	Db	Pw	Db	Pw	
m/z=47	7.55	1.52	5.07	3.36	4.75	3.23	10.65	0.77	16.31	5.83	10.54	0.47	m/z=43
61	10.38	0.38	6.62	2.73	5.69	3.16							
43	7.78	1.21	4.27	4.06	4.31	3.55	14.49	3.20	16.21	0.90	12.92	3.63	61
75	18.99	5.75	11.48	1.38	9.18	3.21							
41	13.85	3.06	15.51	0.57	12.91	2.61	21.36	1.86	24.74	5.37	13.00	5.67	75
89	18.16	5.59	12.85	0.70	9.72	2.01							
59	41.61	7.79	29.35	8.69	36.48	3.18	24.64	4.42	46.76	17.46	28.80	4.18	57
48	4.71	3.98	5.56	2.65	5.11	2.66							
117	11.38	0.05	6.31	4.34	4.76	5.39							
<b>Mean</b>	14.93%	<b>3.26%</b>	10.78%	<b>3.16%</b>	10.32%	<b>3.22%</b>	17.78%	<b>2.56%</b>	26.00%	<b>7.39%</b>	16.31%	<b>3.49%</b>	

\* Db: By Double-exponential decay model, Pw: By Power-law decay model.

\* The underlined in the table are considered as outliers.

\* The presented values in the table are the deviation percentage from the measurements at the corresponding times with regard to the concentration level at 24 hours of the corresponding concentration profiles.

**Table 5.5 Summary of ES predictions by the power-law model (w/ 28-day short-term data).**

□	Long-term 2 of LIN <sup>a</sup> (7-month)	Long-term 3 of LIN (8-month)	Long-term 4 of LIN (9-month)	Long-term 2 of PT2 <sup>a</sup> (7-month)	Long-term 3 of PT2 (8-month)	Long-term 4 of PT2 (9-month)
<b>Power</b>	3.91% <sup>b</sup>	2.85%	3.16%	4.92%	5.96%	6.87%
<b>It was<sup>c</sup></b>	3.29%	2.29%	2.54%	4.93%	4.66%	5.98%

<sup>a</sup> LIN: Linoleum, PT2: Paint 2.

<sup>b</sup> The percentage values in the table represent the error variances between the estimated emission signatures and the measured ones at a given time. The smaller the values, the better the prediction performance is.

<sup>c</sup> The values in this row are the ES estimation results using the full long-term emission measurements, and presented here for the comparison purpose with the prediction results.

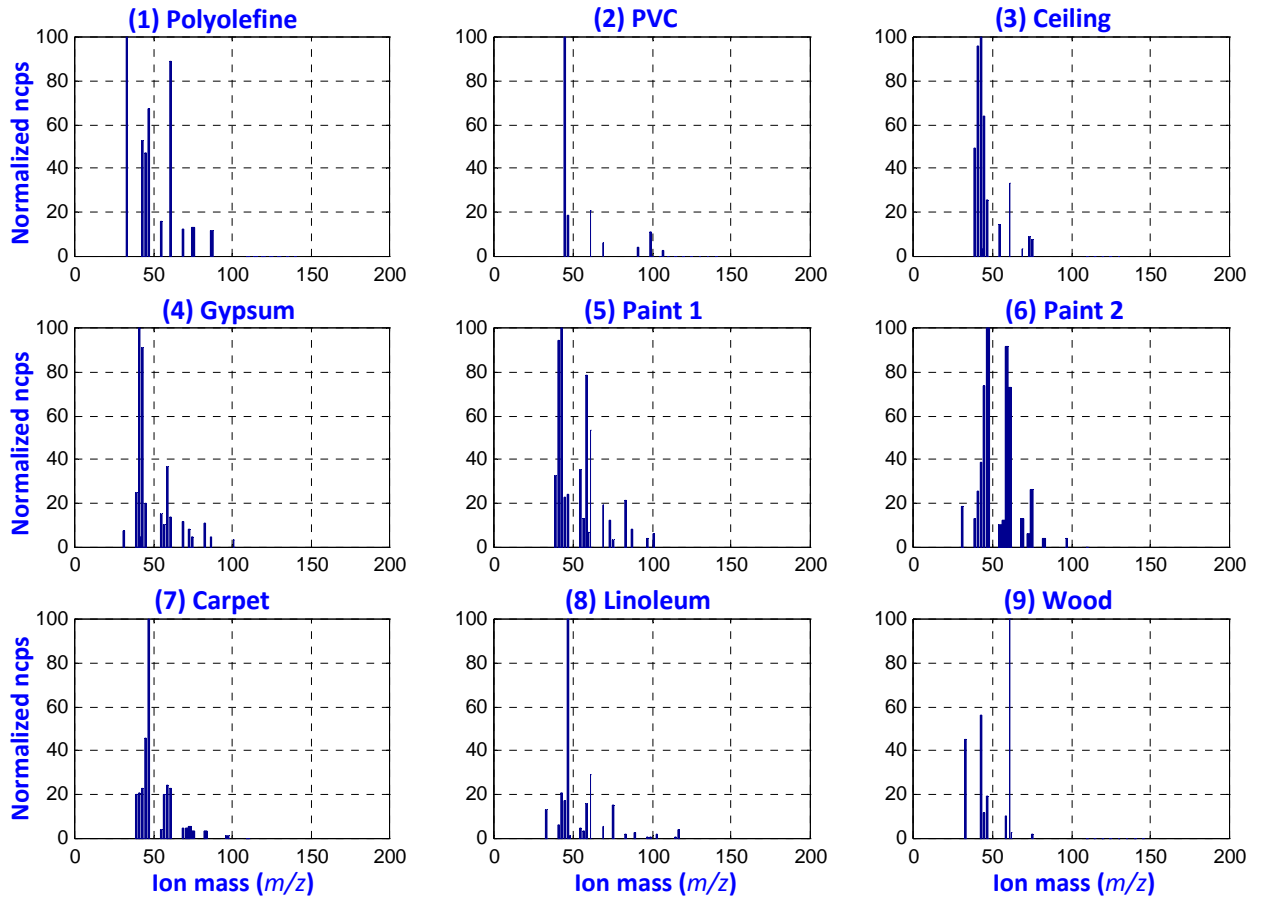


**Figure 5.25** Reconstructed emission signatures based on the prediction results at 9 months (w/ short-term data).

\* This library was predicted for the 9-month period by use of the power-law decay model with a short-term emission dataset ( $\leq 28$  days).

**Table 5.5** shows the ES prediction results when the power-law decay model was used with the 28-day short-term emission dataset. For comparison, the estimation results by the power-law with the full long-term measurements are also presented in the table. There was only slight degradation in the ES prediction performance when a short-term emission dataset was utilized as shown in the table. Except for an outlier, the error variances of the ES predictions were less than 6% (But, it was  $< 5\%$ ). Now, by use of this prediction approach with a short-term emission dataset, the change of source identification performance can be assessed. **Figure 5.25** is the predicted library of ESs at

the 9-month period by utilizing the power-law decay model and the 28-day short-term emission measurements. The previous three measurements of actual material mixture emissions were again used to assess the source identification performance of the algorithms when the ES library was predicted and reconstructed by use of the short-term emission dataset. The performance results are summarized in **Table 5.6**. As the cases of the ES estimations with the full long-term emission measurements, the adequate prediction close to the true shapes of the long-term ESs at a given time via source models seemed to improve the separation/identification performance as demonstrated in **Table 5.6**. With Algorithm 2, the success rate was improved to 76% from 26% before for the three-material mixture (i.e. [6 8 9], Measurement #4) and to 96% from 50% before for the Carpet and Linoleum mixture (i.e. [7 8], Measurement #5). For the three-material mixture, the source separation/identification performance was slightly decreased when compared with the ES estimation case using the full long-term emission measurements. However, for other two-material mixtures, the prediction approach with the short-term dataset showed a similar performance to the full measurement case. In terms of Error level and Score, this prediction approach with the short-term dataset showed a slightly better performance than the estimation with the full measurements. The reason for this odd happening may be attributed to the use of the different source models for the two cases; the double-exponential decay model was used for the full case, and the power-law for the prediction with the short-term dataset. As shown in **Table 5.2**, the double-exponential decay model provided good ES fitting results for an early period, but degraded its fitting performance for a later period at a faster pace than that of the power-law (i.e. at the 9-month period).

**Table 5.6 Comparison of source identification performance by the ES prediction of the power-law at the 9-month period via the two algorithms for various emission mixtures (w/ 28-day short-term data).**

Ground truths	ID <sub>est1</sub> → $\alpha_{est1}$ <sup>a</sup>	ID <sub>est2</sub> → $\alpha_{est2}$ <sup>a</sup>	Err1 <sup>b</sup>	Err2 <sup>b</sup>	Score1	Score2	SR1 (%)	SR2 (%)
[6 8 9] w/ ST <sup>c</sup>	[3 6] → [0.04 <sub>0</sub> <b>0.38</b> <sub>4</sub> ]	[3 6 8 9] → [0.05 <sub>1</sub> <b>0.17</b> <sub>1</sub> <b>0.20</b> <sub>0</sub> <b>0.26</b> <sub>8</sub> ]	0.40	0.28	27.20	66.00	30.00 <sup>d</sup> (28.00)	<b>76.00</b> <sup>d</sup> (26.00)
[6 8 9] w/ LT <sup>c</sup> → [0.12 0.39 0.49]	[3 6 8 9] → [0.03 <sub>2</sub> <b>0.14</b> <sub>3</sub> <b>0.08</b> <sub>4</sub> <b>0.07</b> <sub>5</sub> ]	[3 6 8 9] → [0.08 <sub>0</sub> <b>0.10</b> <sub>6</sub> <b>0.31</b> <sub>2</sub> <b>0.25</b> <sub>0</sub> ]	0.46	0.27	52.20	81.80	56.00	90.00
[7 8] w/ ST	[3 7 8] → [0.18 <sub>3</sub> <b>0.34</b> <sub>3</sub> <b>3.00</b> <sub>2</sub> ]	[3 7 8] → [0.16 <sub>3</sub> <b>0.46</b> <sub>0</sub> <b>2.80</b> <sub>2</sub> ]	0.61	0.38	86.00	83.60	<b>96.00</b> (50.00)	<b>96.00</b> (50.00)
[7 8] w/ LT → [0.60 2.53]	[3 7 8 9] → [0.26 <sub>5</sub> <b>1.40</b> <sub>0</sub> <b>2.34</b> <sub>3</sub> 0.14 <sub>8</sub> ]	[3 7 8 9] → [0.20 <sub>2</sub> <b>0.93</b> <sub>8</sub> <b>1.80</b> <sub>4</sub> 0.02 <sub>9</sub> ]	0.84	0.82	73.60	83.00	92.00	98.00
[8 9] w/ ST	[1 3 8 9] → [0.05 <sub>8</sub> 0.26 <sub>1</sub> <b>2.87</b> <sub>5</sub> <b>3.79</b> <sub>1</sub> ]	[3 8 9] → [0.29 <sub>9</sub> <b>2.43</b> <sub>1</sub> <b>3.66</b> <sub>1</sub> ]	0.63	0.72	72.00	74.20	<b>88.00</b> (88.00)	<b>88.00</b> (88.00)
[8 9] w/ LT → [2.50 4.25]	[1 3 7 8 9] → [0.20 <sub>5</sub> 0.32 <sub>4</sub> 0.46 <sub>2</sub> <b>1.90</b> <sub>7</sub> <b>4.01</b> <sub>9</sub> ]	[1 3 7 8 9] → [0.13 <sub>6</sub> 0.29 <sub>6</sub> 0.288 <sub>8</sub> <b>1.29</b> <sub>1</sub> <b>3.66</b> <sub>2</sub> ]	0.82	1.38	65.80	61.60	88.00	88.00

<sup>a</sup> To exemplify the form of the results from the two algorithms, these estimation results (material ID set and the corresponding signal intensity factor vector) were presented in the table, which were obtained when applying to the algorithms the representative (i.e. by averaging the measured 50 samples) emission signature measured for each given material mixture. However, the three performance indices shown in the table were calculated using 50 measured samples for each mixture, following the definitions of the three indices as shown in Equation (5.3).

<sup>b</sup> 1: of Algorithm 1, 2: of Algorithm 2.

<sup>c</sup> w/ ST: with a short-term emission dataset via the power-law; w/ LT: with the full long-term emission measurements via the double-exponential.

<sup>d</sup> The values in the parenthesis come from Table 5.3 when without the long-term consideration.

### 5.3.4.3 How is the mechanistic diffusion model (CHAMPS-BES) different compared with the empirical source models (double-exponential and power-law decay models)?

Many studies have been conducted to describe VOC emission processes by empirical source models (Brown, 1999, 2002; Colombo et al., 1990). For example, Colombo et al. (1990) used double-exponential transient mass-balance equations to estimate four control parameters for each emission case by a nonlinear least-squares regression, and obtained close fitting lines. However, such empirical approaches typically involve chamber studies, which can be time-consuming, expensive and subject to several limitations due to the lack of physical basis. These empirical methods provide little insight on the controlling mechanism governing VOC source behaviors, and, as a result, are of little value when extrapolating to other environmental conditions not covered by the chamber experiments. On the other hand, for indoor sources controlled by internal diffusion processes, a mechanistic diffusion model has great potential and considerable promise for predicting emission characteristics when compared to empirical models (Cox et al., 2002), because diffusion is one of the most important mechanisms governing VOC source emissions.

A simple physically based diffusion model, which assumes that all of the material emissions are coming from the constituents of the materials, was utilized in this study to evaluate the potential and advantages of this diffusion model approach for predicting the long-term VOC emissions and the resulting emission signatures, over the two empirical source models. The detailed descriptions for this diffusion source model can be found elsewhere (Little et al., 1994). The basic model parameters (i.e. the initial concentration of VOC in a material  $C_0$ , the equilibrium partition coefficient  $K_v$ , and the diffusion



coefficient  $D$ ) for each case were obtained from the iterating process using *Powell* searching method via Matlab, minimizing the least squared error between the estimation results and the actual measurements at the given sampling times. Two representative materials, Linoleum (on  $m/z = 47$ ) and Paint 2 (on  $m/z = 75$ ), were selected and studied with this diffusion model. The measurements at  $t_{meas} = [1, 14, 24, 29, 34, 39, 44$  hours, Day 7, Day 14, Day 28] same as the previous ones were sampled and utilized for this examination. Finally, the resulting optimal profile of long-term emissions for each case was checked again by utilizing CHAMS-BES (Coupled Heat, Air, Moisture and Pollutant Simulation for Built Environmental Systems) with the three optimal model parameters obtained.

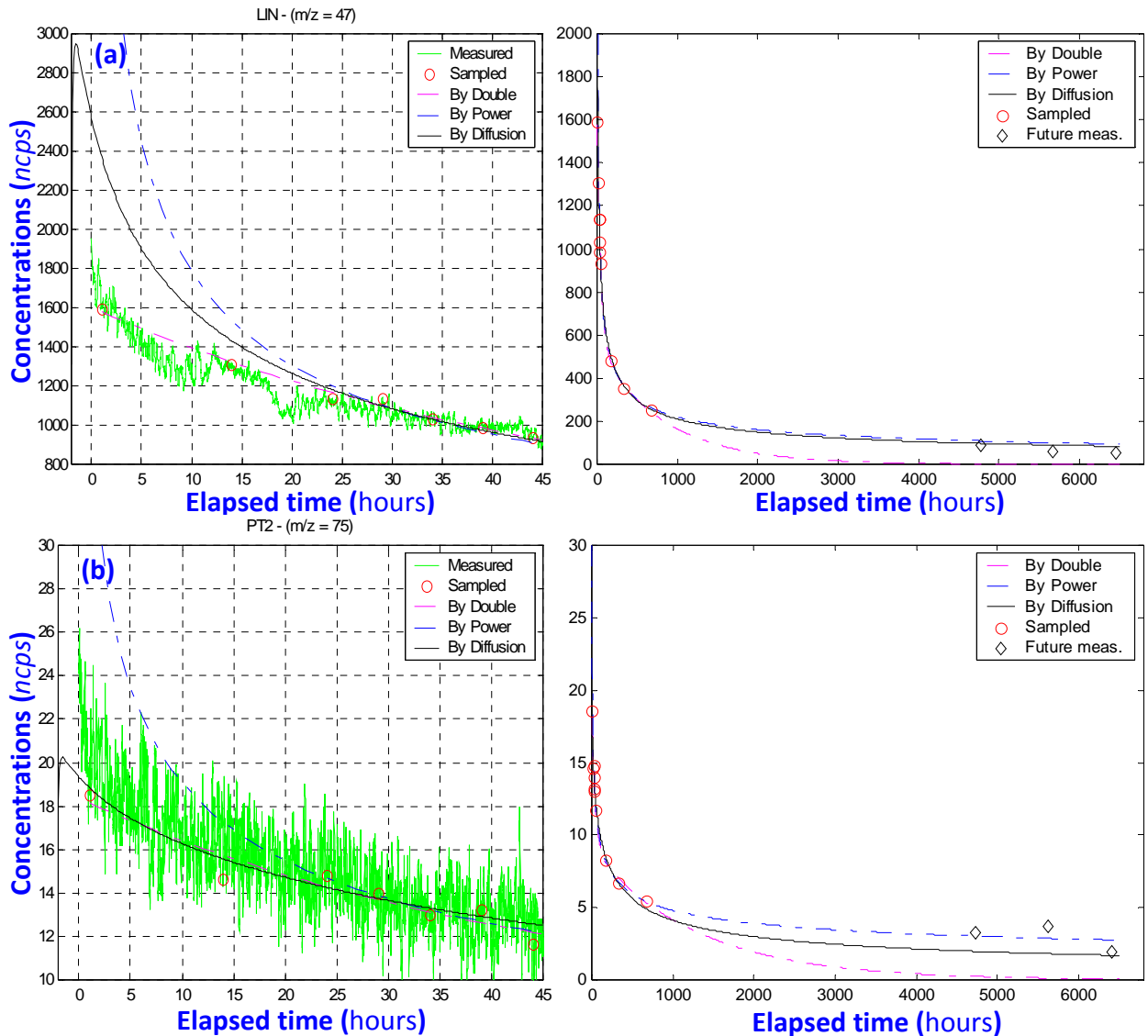


**Figure 5.26 Prediction of the long-term emissions at 7, 8 & 9 months by a mechanistic diffusion model with short-term measurements ( $\leq$  Day 28).**

(a) Ethanol ( $m/z=47$ ) from Linoleum. (b) Propanoic acid (with a small portion of ethanol,  $m/z=75$ ) from Paint 2.

**Figure 5.26** demonstrates the prediction performance of the diffusion source model, comparing this approach with the two empirical source models. The black lines represent the optimal profiles resulted from the diffusion model. The mechanistic diffusion model showed a better initial response than the power-law and a similar initial fitting performance equivalent to the double-exponential. This model could show the up-and-

down concentration change at an early stage of VOC emissions, well representing the behind physics of VOC emission characteristics as illustrated in **Figure 5.26**. The long-term emission predictions at 7, 8 and 9 months were good and for some cases, better than the power-law. Like the case of the double-exponential decay model, the fitting process was hard and time-consuming (due to the use of partial differential equations), and even infeasible with a bad-conditioned initial guess of the model parameters. The good prediction property of this diffusion model for the entire emission period was very encouraging because the model parameters could also be measured using procedures completely independent of the chamber studies and their measurements, or obtained from the comparison with expected values, where possible (Cox et al., 2002; Little et al., 1994). Because of this attractive property of this approach, a shorter term of emission measurements than 28 days might be used to predict the long-term emission signatures for a longer period of VOC emissions. The estimated model parameters for the cases of Linoleum (**Figure 5.26a**) and Paint 2 (**Figure 5.26b**) and the corresponding prediction errors at 7, 8 and 9 months are as follows:

(a) Ethanol ( $m/z = 47$ ) from Linoleum

The loading factor  $L$  for this case and its air change rate  $N$  can be calculated using the given information (See **Table 5.1**) as  $L = 0.48$  ( $\text{m}^{-1}$ ) and  $N = 1.5360$  ( $\text{h}^{-1}$ )

- $[C_0, K_v, D] = [6.05 \times 10^8$  (ncps),  $1.39 \times 10^5$ ,  $1.09 \times 10^{-12}$  ( $\text{m}^2/\text{s}$ )].

- $R^2 = 0.812$ .

\* Note:  $R^2$  is calculated for all the points presented (i.e. the sampled and future measurements).

- Deviation = 0.57% at 7 months, 2.45% at 8 months, and 2.33% at 9 months with regard to the concentration level at 24 hours.

\* Note: The prediction performance is better than that of the power-law for this case.

(b) Propanoic acid ( $m/z = 75$ ) from Paint 2

The calculated loading factor  $L$  and the air change rate  $N$  for this case are  $L = 0.9804$  ( $\text{m}^{-1}$ ) and  $N = 1.4520$  ( $\text{h}^{-1}$ )

- $[C_0, K_v, D] = [4.54 \times 10^6$  (ncps),  $2.00 \times 10^5$ ,  $1.75 \times 10^{-12}$  ( $\text{m}^2/\text{s}$ )].

- $R^2 = 0.977$ .

\* Note:  $R^2$  is calculated for all the points presented (i.e. the sampled and future measurements).

- Deviation = 9.26% at 7 months, 12.94% at 8 months, and 1.58% at 9 months with regard to the concentration level at 24 hours.

## 5.4 Conclusions

The following conclusions could be drawn from the study (Stage 3) performed in Chapter 5:

- ◆ Two types of materials studied in this study were observed and differentiated by using PTR-MS, a whole-pictured on-line monitoring device with a wide detection window for indoor VOCs: most of the major composing VOCs in the materials steadily decaying over time (e.g. Linoleum) or fast decaying over time (e.g. Paint 2).
- ◆ The emission signatures representing individual building materials could change over time, but the long-term emission signatures for most of the building materials studied (if with a high enough signal intensity) appeared to exist stable and consistent after a certain period of long-term emissions (Especially, during the dominant period of the secondary VOC emissions when the relative difference of the emission rate changes over time for the composing VOCs of a given material becomes small).
- ◆ The long-term material emission signatures could be estimated and predicted by using empirical and mechanistic diffusion source models, which could help enhance the performance of source identification.
- ◆ For the prediction of the long-term VOC emissions and the corresponding emission signatures, the power-law decay model was recommendable to use because of its good representation of the internal-diffusion controlled emissions and its computationally efficient solution (Note: The emission signature for a material consists of tens of VOC components).

◆ The testing schedule generally used in the practice for predicting long-term emissions (i.e. Day 0-2, Day 7, Day 14 and Day 28) was found to be valid and practical also for the collection of material emission signatures to establish a library of long-term ESs for materials. Because of its physical basis, the mechanistic diffusion model might far shorten the minimum period of required measurements for this prediction purpose.

This page is intentionally left blank.

## † CHAPTER 6. SUMMARY AND CONCLUSIONS

---

### 6.1 Summary and Conclusions

A new methodology and procedures using PTR-MS were developed to determine the emission signatures specific and consistent over time to individual building materials, connecting the on-line measurements by PTR-MS to the acceptability of air quality assessed by human subjects. A VOC odor index (VOI) was proposed to assess the impact of individual material emissions on human perceived air quality, which correlated well with the acceptability assessed by human subjects for the materials tested.

In addition, this study demonstrated the feasibility of identifying VOC emission sources of concern with high success rates when multiple materials were present indoors by utilizing the PTR-MS and an effective signal processing technique under laboratory indoor conditions. A database of emission signatures for nine typical building materials was established as a foundation for source identification in mixture emissions from the materials. The measured emission signatures from material mixtures were compared to the established database of emission signatures for each single material through the process of two proposed source identification algorithms. These algorithms were tested



and validated by measurement-based Monte-Carlo simulations and by actual measurements of five material mixtures.

The source identification could also be valid throughout VOC long-term emissions by considering the pattern change of material emission signatures over the long-term period, accounted for by appropriate emission source models. The following overall conclusions could be derived from this study:

- A stable VOC emission signature specific to each type of building material appeared to exist by utilizing PTR-MS with the signal processing method and procedure developed. The emission signatures for building materials tested were found not to vary much with different area-specific ventilation rates for the duration and conditions of testing. The signatures might change over a long period of time, but the shape change of emission signatures could be compensated.
- The sum of odor indices for selected major individual VOCs determined by PTR-MS could show a reasonable correlation with the acceptability of air quality assessed by human subjects, and hence may provide a feasible approach to assessing perceived indoor air quality in real-time. This on-line assessment will open a new gate in understanding the role of VOC emissions from building materials on perceived air quality, forming a good foundation to develop real-time or near real-time methods for standard material emission testing and labeling, quality control of emissions from materials, and assessing the acceptability of air quality in buildings.

- The material ranking of pollution based on the VOI using the PTR-MS measurements provided a similar ranking for the tested materials to that in terms of acceptability, and may be used for evaluating the impact of each material on human-perceived air quality in a faster and more efficient way.
- In a controlled environment, the identification of indoor emission sources was found feasible with the estimations of their individual relative source strengths when the developed technique was utilized with a limited number of materials for composing a mixture.
- The effect of VOC mixture emissions in indoor air might be superposed in the mass-spectral domain of PTR-MS because of small interactions among material emissions and the conservation of individual material emission patterns even under mixture conditions. For this reason, the adsorption effect among material emissions could be quantitatively assessed in an accurate way by using the new technique proposed.
- The long-term material emission signatures could be estimated and predicted by using empirical and mechanistic diffusion source models, which could help enhance the performance of VOC source identification. The power-law decay model was recommendable for this purpose with short-term a priori measurements (i.e.  $\leq 28$  days) because of its computationally-efficient characteristics with reasonably-well reflecting the long-term emission decay of VOCs.
- The general testing schedule for predicting VOC long-term emissions (i.e. Day 0-2, Day 7, Day 14 and Day 28) was found to be valid and practical also for the

establishment of a library of long-term emission signatures for building materials studied.

## 6.2 Practical Implications

The present study shows that unique emission patterns may exist for different types of building materials. These patterns, or signatures, can be established by PTR-MS, an on-line analytical monitoring device. The sum of selected major individual VOC odor indices determined by PTR-MS correlates well with the acceptability of air quality assessed by human subjects, and hence provides a feasible approach to assessing perceived indoor air quality with PTR-MS on-line measurements. This on-line assessment will open a new gate in understanding the role of VOC emissions from building materials on perceived air quality, forming a good foundation to develop real-time or near real-time methods for standard material emission testing and labeling, quality control of emissions from materials, and assessing the acceptability of air quality in buildings.

If there is a VOC related problem in an indoor air environment, different relevant sources can be identified and screened individually by PTR-MS. Finding the source(s) would help eliminating the problem efficiently and effectively. The results of this study demonstrate the feasibility of identifying emission sources with high success rates when multiple materials (up to seven-material mixtures with the concentration difference of about 430 times between the lowest and the highest polluting materials) are present indoors by utilizing the PTR-MS and an effective signal processing method under

laboratory indoor conditions. An advantage of this technique is that it may find the sources invisible or hidden when a building with problems of indoor air quality is suspected. In real indoor environments, the identification becomes more challenging than in controlled indoor environments because of the higher number of possible emission sources, the adsorption and desorption effects and the change of emission pattern over time for a given source, and hence require further development of the present identification method.

### 6.3 Limitations

The correlation derived in this study between the PTR-MS on-line measurements and the human odor assessments on perceived air quality may be valid only for the nine building materials studied here because the materials investigated appeared to have similar types of odors. The selection of up to three dominant VOCs in calculating VOC odor index (VOI) can be somewhat arbitrary, and its implementation may be difficult in some cases if the VOCs detected are not known or the corresponding odor thresholds are not determined yet.

The source identification methodology presented in this study considered the possible change of emission signatures over a long period of time as a main possible contributor of the change in a field condition. However, there are other possible causes affecting the change of emission signatures such as temperature, relative humidity, surface velocity over materials, large portion of chemical reactions among material emissions, etc. The source identification technique may break down in a mixture condition having a certain

large number of materials (e.g. 30 materials) or in a highly reactive environment like ozone-initiated chemical-reaction dominant space. In addition, for some materials, any stable emission signature may not be established somehow. If some materials have heavy VOCs as major compounds for their emission signatures, the measured signature from their mixtures may be distorted from the superposed emission signature mainly due to different adsorption phenomena, leading to a breakdown of the method.

For this reason, a broader range of materials and types of odors should be investigated before this new approach can be widely applied.

# † CHAPTER 7. RECOMMENDATIONS FOR FUTURE RESEARCH AND APPLICATIONS

---

## 7.1 Recommendations for Future Works

The following subjects should be further studied:

- 1) Validation of the source identification technique in a field condition
- 2) Development of low cost and portable mass spectrometry for applying the source identification method

During the present study, the appropriate handling of the background air was found to be crucial in getting a well-conditioned stable and consistent emission signature for a target material. Different from the background air well controlled and conditioned under indoor laboratory conditions with a dedicated filter system, the general indoor background air in field environments might be substantially time-varying with higher concentration levels and various noise effects. A well-designed study on the background air profile under field conditions can produce a special technique to extract meaningful and stable signals for the emissions of materials of concern from measured signals in a field condition.

The present validation of this technique for indoor source identification under a laboratory condition can be extended and become significant by applying and

demonstrating the source identification method in a full-scale built environment (e.g. Syracuse CoE headquarters building). Many different materials and furniture have been used in the construction and furnishing of the building. The air distribution inside the building will also affect the identification of sources and the locations of emission sources. A refined procedure should be developed by considering the complexity in its airflow patterns.

To be utilized as a rapid and influential tool in a field condition, the overall signal processing for this technique should be implemented with a real-time processing programming package (e.g. C++ or real-time JAVA). In addition, if this methodology can be proven valid even with the use of a low-cost portable mass spectrometry, the application of this technique can make a great impact on many research and industrial areas. For example, a) the detection and analysis of VOCs on remediation sites are possible in a fast manner prior to site renewal. Any dangerous and toxic materials such as asbestos can be screened as b) a rapid threat screening tool. This method can be used as c) emergency response testing to identify unknown materials in a fast unambiguous way. d) Material verification is also possible. Raw material testing and identity verification are critical steps in the quality control process with tremendous impact on human health and safety. Global pharmaceutical manufacturers are seeking technology that will allow them to approach the goal of 100 percent raw material inspection without additional staff or prohibitive financial investments. Real-time material identity verification will open a new gate to the users in this need. This cost-effective solution will allow the users to quickly develop corresponding adequate procedures, enabling the immediate release of raw materials into production. e) Forensic investigation will also be impacted by this on-

line cost-effective identification method, identifying accelerants used in arson at a fire scene with ease and accuracy.

## 7.2 Possible Applications using the Emission Signature Technique

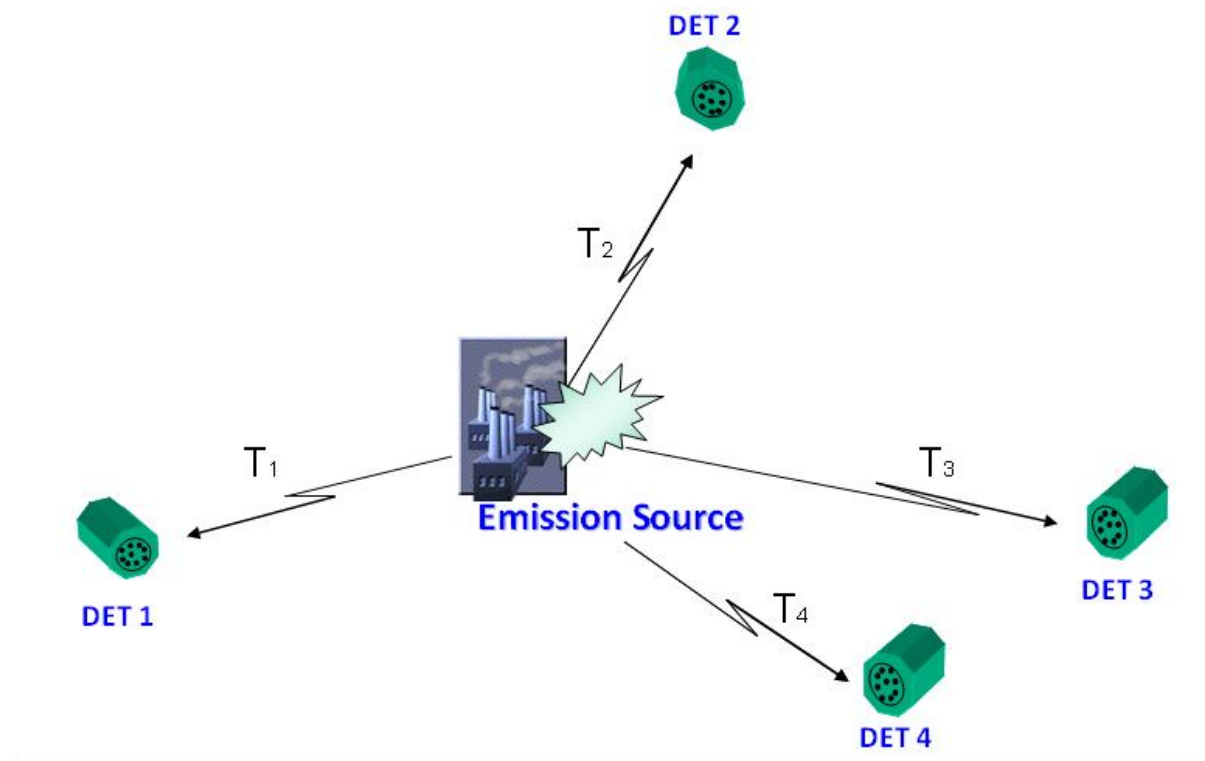


**Figure 7.1** Schematic diagram of a source detection/localization system for VOC emissions.

One of the feasible and novel applications based on this new technique might be a real-time localization system of indoor emission sources. Not only can this technique detect and identify each source material from a bunch of combined emissions emitted from material mixtures, but also the position of an emission source with problematic effects can be traced within a reasonable positioning accuracy if some typical indoor conditions in a huge space are assumed. A toxic and hazardous emission or a target emission to be



traced can be detected and identified, and moreover the position of the emission source in a working space or in a huge storage space can be localized in a real-time basis. **Figure 7.1** shows the schematic concept of this approach with four detectors.

## REFERENCES

- Amoore, J.E. and Hautala, E. (1983). "Odor as an aid to chemical safety: Odor thresholds compared to threshold limit values for 214 industrial chemicals in air and water dilution." *J. Appl. Toxicol.*, **3**, 272-290.
- Andersen, T.E., Knudsen, H.N., Tirkkonen, T., Orko, I., Saarela, K., Clausen, G. and Ganger, P.O. (1996). "Air pollutant concentration effects on VOC emission rates of building and furnishing materials." In: *Proc. of Indoor Air '96*, Nagoya, Japan, **1**, pp. 559-564.
- Arhami, M., Minguillon, M.C., Polidori, A., Schauer, J.J., Delfino, R.J. and Sioutas, C. (2010). "Organic compound characterization and source apportionment of indoor and outdoor quasi-ultrafine particulate matter in retirement homes of the Los Angeles Basin." *Indoor Air*, **20**, 17-30.
- Begum, B.A., Kim, E., Biswas, S.K. and Hopke, P.K. (2004). "Investigation of sources of atmospheric aerosol at urban and semi-urban areas in Bangladesh." *Atmos. Environ.*, **38**, 3025-3038.
- Berglund, L. and Cains, W.S. (1989). "Perceived air quality and thermal environment. In the human equation: health and comfort." Atlanta: *ASHEAE*, 93-99.
- Biasioli, F., Granitto, P.M., Aprea, E., Mott, D., Furlanello, C., Mark, T.D. and Gasperi, F. (2007). "Rapid and non-destructive identification of strawberry cultivars by direct PTR-MS headspace analysis and data mining techniques." *Sensor. and Actuat. B-Chem*, **121**, 379-85.
- Blake, R.S., Monks, P.S. and Ellis, A.M. (2009). "Proton transfer reaction - mass spectrometry." *Chem. Rev.*, **109**, 861-896.
- Bluyssen, P.M., Cornelissen, H.J.M., Hoogeveen, A.W., Wouda, P. and van der Wal, J.F. (1996). "The effect of temperature on the chemical and sensory emission of indoor materials." In: *Proc. of Indoor Air '96*, Nagoya, Japan, **3**, pp. 619-624.

- Boscaini, E., Mikoviny, T., Wisthaler, A., Hartungen, E.V. and Märk, T.D. (2004). "Characterization of wine with PTR-MS." *Int J Mass Spectrom*, **239**, 215-219.
- Brasseur, G., Orlando, J. and Tyndall, G. (1999). *Atmospheric chemistry and global change*, Oxford University Press, New York.
- Brown, S.K. (1999). "Chamber assessment of formaldehyde and VOC emissions from wood-based panels." *Indoor Air*, **9**, 209-215.
- Brown, S.K. (2002). "Volatile organic pollutants in new and established buildings in Melbourne, Australia." *Indoor Air*, **12**, 55-63.
- Bunge, M., Araghipour, N., Mikoviny, T., Dunkl, J., Schnitzhofer, R., Hansel, A., Schinner, F., Wisthaler, A., Margesin, R. and Märk, T.D. (2008). "On-line monitoring of microbial volatile metabolites by proton transfer reaction - mass spectrometry." *Appl. Environ. Microbiol.*, **74**, 2179-2186.
- Buzcu, B. and Fraser, M.P. (2006). "Source identification and apportionment of volatile organic compounds in Houston, TX." *Atmos. Environ.*, **40**, 2385-2400.
- Cain, W.S. and Schmidt, R. (2009). "Can we trust odor databases? Example of t- and n-butyl acetate." *Atmos. Environ.*, **43**, 2591-2601.
- Cass, G.R. (1998). "Organic molecular tracers for particulate air pollution sources." *Trends Anal. Chem.*, **17**, 356-366.
- Christian, T., Kleiss, B., Yokelson, R., Holzinger, R., Crutzen, P., Hao, W., Shirai, T. and Blake, D. (2004). "Comprehensive laboratory measurements of biomass-burning emissions: 2. First intercomparison of open-path FTIR, PTR-MS, and GC-MS/FID/ECD." *J Geophysical Res Atmos.*, 109(doi:10.1029/2003JD003874).
- Cincinelli, A., Mandorlo, S., Dickhut, R.M. and Lepri, L. (2003). "Particulate organic compounds in the atmosphere surrounding an industrialised area of Prato (Italy)." *Atmos. Environ.*, **37**, 3125-3133.

- Cohen, J., Cohen P., West, S.G. and Aiken, L.S. (2003). *Applied multiple regression/correlation analysis for the behavioral sciences*. (2<sup>nd</sup> ed.), Hillsdale, NJ: Lawrence Erlbaum Associates.
- Corbett, J.J., Winebrake, J.J., Green, E.H., Kasibhatla, P., Eyring, V. and Lauer, A. (2007). "Mortality from ship emissions: A global assessment." *Environ. Sci. Technol.*, **41**, 8512–8518.
- Clausen, P.A., Wolkoff, P., Hoist, E. and Nielsen, P.A. (1991). "Long-term emission of volatile organic compounds from waterborne paints - methods of comparison." *Indoor Air*, **1**, 562–576.
- Clausen, G., Pejtersen, J., Saarela, K., Tirkkonen, T., Tahtinen, M. and Dickson, D. (1995). *European Data Base on Indoor Air Pollution Sources in Buildings: Protocol for testing of building materials*, Version 1.0, November 28.
- Clausen, G., Fernandes, E. de O. and Fanger, P.O. (1996). "European database on indoor air pollution sources in buildings." In: Yoshizowa, S., Kimura, K., Ikeda, K., Tanabe, S. and Iwata, T. (eds), *Proc. of Indoor Air '96*, Nagoya, **2**, pp. 639–644.
- Clausen, P.A., Knudsen, H.N., Larsen, K., Kofoed-Sorensen, V., Wolkoff, P. and Wilkins, C.K. (2008). "Use of thermal desorption gas chromatography-olfactometry/mass spectrometry for the comparison of identified and unidentified odor active compounds emitted from building products containing linseed oil." *J. Chromatogra. A*, **1210**, 203-211.
- Colombo, A., de Bortolh, M., Pecchio, E., Schauenburg, H., Schlitt, H. and Vissers, H. (1990). "Chamber testing of organic emissions from building and furnishing materials." *Sci. total Envir.*, **91**, 237-249.
- Cox, S.S., Little, J.C. and Hodgson, A.T. (2002). "Predicting the emission rate of volatile organic compounds from vinyl flooring." *Environ. Sci. Technol.*, **36**, 709-714.
- de Gouw, J., Warneke, C., Karl, T., Eerdeken, G., van derVeen, C. and Fall, R. (2003). "Sensitivity and specificity of atmospheric trace gas detection by proton transfer reaction - mass spectrometry." *Int J Mass Spectrom*, **223**, 365-382.

- de Gouw, J. and Warneke, C. (2007). "Measurements of volatile organic compounds in the earth's atmosphere using proton transfer reaction - mass spectrometry." *Mass Spectrom Rev.*, **26**, 223-257.
- Didyk, B.M., Simoneit, B.R.T., Pezoa, L.A., Riveros, M.L. and Flores, A.A. (2000). "Urban aerosol particles of Santiago, Chile: Organic content and molecular characterization." *Atmos. Environ.*, **34**, 1167-1179.
- Doren and Jorn F.M. (2006). "Reduced-order optimal control of water flooding using proper orthogonal decomposition." *Comput. Geosci.*, **10**, 137-158.
- Edwards, R.D., Jurvelin, J., Koistinen, K., Saarela, K. and Jantunen, M. (2001). "VOC source identification from personal and residential indoor, outdoor and workplace microenvironment samples in EXPOLIS-Helsinki, Finland." *Atmos. Environ.*, **35**, 4829-4841.
- Ellison, S.L.R., Rosslein, M. and Williams, A. (2000). Quantifying Uncertainty in Analytical Measurement (QUAM) – 2<sup>nd</sup> Edition. *EURACHEM/CITAC*.
- EPA (1996). *Air Quality Criteria for Particulate Matter*, Research Triangle Park, National Center for Environmental Assessment Office of Research and Development, US EPA.
- EPA (2009). Technical Support Document, Chapter 3: Impacts of shipping emissions on air quality, health and the environment. *Proposal to Designate an Emission Control Area for Nitrogen Oxides, Sulfur Oxides and Particulate Matter*. Ed. Office of Transportation and Air Quality Assessment and Standards Division, U.S. Environmental Protection Agency.
- Everson, R. and Sirovich, L. (1995). "Karhunen-Loeve procedure for gappy data." *J. Opt. Soc. Am. A*, **12**, 1657-64.
- Fang, L., Clausen, G. and Fanger, P.O. (1996). "The impact of temperature and humidity on perception and emission of indoor air pollutants." In: *Proc. of Indoor Air '96*, Nagoya, Japan, **4**, pp. 349-354.

- Fang, L., Zhang, G. and Wisthaler, A. (2008). "Desiccant wheels as gas-phase absorption (GPA) air cleaners: Evaluation by PTR-MS and sensory assessment." *Indoor Air*, **18**, 375-385.
- Fernandes, D.L.A. and Gomes, M.T.S.R. (2008). "Development of an electronic nose to identify and quantify volatile hazardous compounds." *Talanta*, **77**, 77-83.
- Filella, I. and Penuelas, J. (2006). "Daily, weekly, and seasonal time courses of VOC concentrations in a semi-urban area near Barcelona." *Atmos. Environ.*, **40**, 7752-7769.
- Frey, H.C., Zhang, K. and Roupail, N.M. (2010). "Vehicle-specific emissions modeling based upon on-road measurements." *Environ. Sci. Technol.*, **44**, 3594-3600.
- Friedlander, S.K. (1973). "Chemical element balances and identification of air pollution sources." *Environ. Sci. Technol.*, **7**, 235-240.
- Fujita, E.M., Campbell, D.E., Zielinska, B., Sagebiel, J.C., Bowen, J.L., Goliff, W.S., Stockwell, W.R. and Lawson, D.R. (2003). "Diurnal and weekday variations in the source contributions of ozone precursors in California's South coast air basin." *J. Air & Waste Manage. Assoc.*, **53**, 844-863.
- Gohlke, R.S. (1959). "Time-of-flight mass spectrometry and gas-liquid partition chromatography." *Anal. Chem.*, **31**, 535-41.
- Graham, B., Falkovich, A.H., Rudich, Y., Maenhaut, W., Guyon, P. and Andreae, M.O. (2004). "Local and regional contributions to the atmospheric aerosol over Tel Aviv, Israel: a case study using elemental, ionic and organic tracers." *Atmos. Environ.*, **38**, 1593-1604.
- Granitto, P.M., Biasioli, F., Aprea, E., Mott, D., Furlanello, C., Märk, T.D. and Gasperi, F. (2007). "Rapid and non-destructive identification of strawberry cultivars by direct PTR-MS headspace analysis and data mining techniques." *Sens. Actuators B: Chem.*, **121**, 379-385.
- Granitto, P.M., Biasioli, F., Furlanello, C. and Gasperi, F. (2008). "Efficient feature selection for PTR-MS fingerprinting of agroindustrial products." In: *Proc. of 18th International Conference on Artificial Neural Networks, ICANN 2008, September 03-September 06*, Springer Verlag, pp. 42-51.

- Gunnarsen, L. and Fanger, P.O. (1992). "Adaptation to indoor air pollution." *Environment International*, **18**, 43-54.
- Gunnarsen, L., Nielsen, P.A., Nielson, J.B., Wolkoff, P., Knudsen, H. and Thøgersen, K. (1993). "The influence of specific ventilation rate on the emissions from construction products." In: *Proc. of Indoor Air '93*, Helsinki, Finland, **2**, pp. 501-506.
- Haghighat, F. and Donnini, G. (1993). "Emissions of indoor pollution from building materials: State-of-the-art review." *Archit. Sci. Rev.*, **36**, 13-22.
- Haghighat, F. and DeBellis, L. (1998). "Material emission rates: Literature review and the impact of indoor air, temperature and relative humidity." *Build. Environ.*, **33**, 261-277.
- Haghighat, F. and Zhang, Y. (1999). "Modeling of emission of volatile organic compounds from building materials - estimation of gas-phase mass transfer coefficient." *Build. Environ.*, **34**, 377-389.
- Haghighat, F., Sakr, W., Gunnarsen, L. and Grunau, M.Von. (2001). "The impact of combinations of building materials and intermittent ventilation on perceived air quality." *ASHRAE Trans.*, **107**(AT-01-13-4), 821-835.
- Hagler, G.S.W., Bergin, M.H., Salmon, L.G., Yu, J.Z., Wan, E.C.H., Zheng, M., Zeng, L.M., Kiang, C.S., Zhang, Y.H., Lau, A.K.H. and Schauer, J.J. (2006). "Source areas and chemical composition of fine particulate matter in the Pearl River Delta Region of China." *Atmos. Environ.*, **40**, 3802-15.
- Han, K.H., Zhang, J.S., Wargocki, P., Knudsen, H.N. and Guo, B. (2010). "Determination of material emission signatures by PTR-MS and their correlations with odor assessments by human subjects." *Indoor Air*, **20**, 341-354.
- Han, K.H., Zhang, J.S., Knudsen, H.N., Wargocki, P., Chen, H., Varshney, P.K. and Guo, B. (2011). "Development of a novel methodology for indoor emission source identification." *Atmos. Environ.*, **in review**.

- Han, K.H., Zhang, J.S., Knudsen, H.N., Wargocki and Guo, B. (2011b). "Consideration of the change of material emission signatures due to long-term emissions for enhancing VOC source identification." In: *Proc. of Indoor Air '11*, Austin, Texas.
- Hansel, A. (2004). "Proton transfer mass spectrometer." *Europhys. News*, **35**, 197-9.
- Herbarth, O. and Matysik, S. (2010). "Decreasing concentrations of volatile organic compounds (VOC) emitted following home renovations." *Indoor Air*, **20**, 141-146.
- Hewitt, C. (1999). *Reactive Hydrocarbons in the Atmosphere*, Academic Press, San Diego.
- Hewitt, C., Hayward, S. and Tani, A. (2003). "The application of proton transfer reaction - mass spectrometry (PTR-MS) to the monitoring and analysis of volatile organic compounds in the atmosphere." *J. Environ. Monit.*, **5**, 1-7.
- Hodgson, A.T., Rudd A.F., Beal, D. and Chandra, S. (2000). "Volatile organic compound concentrations and emission rates in new manufactured and site-built houses." *Indoor Air*, **10**, 178-192.
- Holy S. (BC 1446-AD 96). *The Holy Bible*, NIV-version.
- Huang, S., Rahn, K.A. and Arimoto, R., (1999). "Testing and optimizing two factor-analysis techniques on aerosol at Narragansett, Rhode Island." *Atmos. Environ.*, **33**, 2169–2185.
- Ilka, T.B. (2005). *Volatile Organic Compound (VOC) Emissions from Sources in a Partitioned Office Environment and Their Impact on Indoor Air Quality (IAQ)*. MS Thesis of Syracuse University, New York, USA.
- ISO/IEC (2008). *Guide to the expression of uncertainty in measurement (GUM)*.
- Iwashita, G. and Kimura, K. (1994). "Experimental study on surface emission rate of perceived air pollutants: Influence of air velocity." In: *Proc. of the 3rd Healthy Building Conf.*, Budapest, Hungary, **1**, pp. 469-474.
- Jensen, B. and Wolkoff, P. (1996). "VOCBASE - odor thresholds, mucous membrane irritation thresholds and physico-chemical parameters of VOCs." A PC program, Version 2.1, National Institute of Occupational Health, Copenhagen.



- Jia, C., Batterman, S., Godwin, C., Charles, S. and Chin, J.Y. (2010). "Sources and migration of volatile organic compounds in mixed-use buildings." *Indoor Air*, **20**.
- Jobson, B.T., Alexander, M.L., Maupin, G.D. and Muntean, G.G. (2005). "On-line analysis of organic compounds in diesel exhaust using a proton transfer reaction - mass spectrometer (PTR-MS)." *Int J Mass Spectrom*, **245**, 78-89.
- Jordan, C., Fitz, E., Hagan, T., Sive, B., Frinak, E., Haase, K., Cottrell, L., Buckley, S. and Talbot, R. (2009). "Long-term study of VOCs measured with PTR-MS at a rural site in New Hampshire with urban influences." *Atmos. Chem. Phys.*, **9**, 4677-4697.
- Karl, T., Fall, R., Crutzen, P.J., Jordan, A. and Lindinger, W. (2001). "High concentrations of reactive biogenic VOCs at a high altitude site in late Autumn." *Geophysical Res Lett*, **28**, 507-510.
- Kato, S., Miyakawa, Y., Kaneko, T. and Kajii, Y. (2004). "Urban air measurements using PTR-MS in Tokyo area and comparison with GC-FID Measurements." *Int J Mass Spectrom*, **235**, 103-110.
- Kenney, J.F. and Keeping, E.S. (1962). "Chapter 14.2. Moving averages." *Mathematics of Statistics, Pt 1, 3<sup>rd</sup> ed*, Princeton, NJ: Van Nostrand, pp. 221-223.
- Kim, Y.M., Harrad, S. and Harrison, R.M. (2001). "Concentrations and sources of VOCs in urban domestic and public microenvironments." *Environ. Sci. Technol.*, **35**, 997-1004.
- Kim, E., Hopke, P.K. and Edgerton, E. (2003). "Source identification of Atlanta aerosol by positive matrix factorization." *J. Air & Waste Manage. Assoc.*, **53**, 731-739.
- Kim, E. and Hopke, P.K. (2004). "Source apportionment of fine Particles at Washington, DC utilizing temperature resolved carbon fractions." *J. Air & Waste Manage. Assoc.*, **54**, 773-785.
- Kim, E. and Hopke, P.K. (2008). "Source characterization of ambient fine particles at multiple sites in the Seattle area." *Atmos. Environ.*, **42**, 6047-6056.

- Knudsen, H.N., Valbjorn, O. and Nielsen, P.A. (1998). "Determination of exposure-response relationships for emissions from building products." *Indoor Air*, **8**, 264-275.
- Knudsen, H.N., Kjaer, U.D., Nielsen, P.A. and Wolkoff, P. (1999). "Sensory and chemical characterization of VOC emissions from building products: Impact of concentration and air velocity." *Atmos. Environ.*, **33**, 1217-1230.
- Knudsen, H.N., Wargocki, P. and Vondruskova, J. (2006). "Effect of ventilation on perceived quality of air polluted by building materials – a summary of reported Data." In: *Proc. of Healthy Buildings 2006*, **1**, pp. 57-62.
- Knudsen, H.N., Clausen, P.A., Wilkins, C.K. and Wolkoff, P. (2007). "Sensory and chemical evaluation of odorous emissions from building products with and without linseed oil." *Build. Environ.*, **42**, 4059-4067.
- Knudsen, H.N. and Wargocki, P. (2008). "The effect of using low-polluting building materials on perceived air quality and ventilation requirements in real rooms." In: *Proc. of Indoor Air 2008*, CD-Rom.
- Lamb, B., Velasco, E., Allwine, E., Westberg, H., Herndon, S., Knighton, B., Grimsrud, E., Jobson, T., Alexander, M. and Prezeller, P. (2004). "Ambient VOC measurements in Mexico city." In: *Proc., 5th Symposium on the Urban Environment*, American Meteorological Society, Boston, MA 02108-3693, United States, pp. 851-857.
- Lee, C.S., Haghighat, F. and Ghaly, W.S. (2005). "A study on VOC source and sink behavior in porous building materials – analytical model development and assessment." *Indoor Air*, **15**, 183-196.
- Lewis, C.W., Klouda, G.A. and Ellenson, W.D. (2004). "Radiocarbon measurement of the biogenic contribution to summertime PM<sub>2.5</sub> ambient aerosol in Nashville, TN." *Atmos. Environ.*, **38**, 6053-6061.
- Li, F. and Niu, J. (2007). "Control of volatile organic compounds indoors: Development of an integrated mass-transfer-based model and its application." *Atmos. Environ.*, **41**, 2344-2354.

- Lin, C., Yu, K., Zhao, P. and Whei-May Lee, G. (2009). "Evaluation of impact factors on VOC emissions and concentrations from wooden flooring based on chamber tests." *Build. Environ.*, **44**, 525-533.
- Lin, L., Lee, M. and Eatough, D. (2010). "Review of recent advances in detection of organic markers in fine particulate matter and their use for source apportionment." *J. Air & Waste Manage. Assoc.*, **60**, 3-25.
- Lindinger, C., Labbe, D., Pollien, P., Rytz, A., Juillerat, M.A., Yeretian, C. and Blank, I. (2008). "When machine tastes coffee: Instrumental approach to predict the sensory profile of espresso coffee." *Anal. Chem.*, **80**, 1574-1581.
- Lindinger, W., Hansel, A. and Jordan, A. (1998). "On-line monitoring of volatile organic compounds at pptv levels by means of proton transfer reaction - mass spectrometry (PTR-MS) - medical applications, food control and environmental research." *Int J Mass Spectrom*, **173**, 191-241.
- Lindinger, W., Fall, R. and Karl, T. (2001). "Environmental, food and medical applications of proton transfer reaction - mass spectrometry (PTR-MS)." In: Adams, N.G. and Babcock, L.M. (eds) *Advances in Gas-Phase Ion Chemistry*, Amsterdam, Elsevier, pp. 1-48.
- Lirk, P., Bodrogi, F. and Rieder, J. (2004). "Medical applications of proton transfer reaction - mass spectrometry: Ambient air monitoring and breath analysis." *Int J Mass Spectrom*, **239**, 221-6.
- Little, J.C., Hodgson, A.T. and Gadgil, A.J. (1994). "Modeling emissions of volatile organic compounds from new carpets." *Atmos. Environ.*, **28**, 227-234.
- Liu, X. and Zhai, Z. (2007). "Inverse modeling methods for indoor airborne pollutant tracking: literature review and fundamentals." *Indoor Air*, **17**, 419-438.
- Liu, X. and Zhai, Z. (2008). "Location identification for indoor instantaneous point contaminant source by probability-based inverse Computational Fluid Dynamics modeling." *Indoor Air*, **18**, 2-11.

- Mayr, D., Margesin, R., Schinner, F. and Märk, T.D. (2003). "Detection of the spoiling of meat using PTR-MS." *Int J Mass Spectrom*, **223-224**, 229-235.
- Miller, M.S., Friedlander, S.K. and Hidy, G.M. (1972). "A chemical element balance for the Pasadena aerosol." *J. Colloid Interface Sci.*, **39**, 65–176.
- Morrison, G.C. and Nazaroff, W.W. (2002). "Ozone interactions with carpet: Secondary emissions of Aldehydes." *Environ. Sci. Technol.*, **36**, 2185-2192.
- Moularat, S., Robine, E., Ramalho, O. and Oturan, M.A. (2008). "Detection of fungal development in a closed environment through the identification of specific VOC: Demonstration of a specific VOC fingerprint for fungal development." *Sci. Total Environ.*, **407**, 139-146.
- Nagata, Y. (2003). "Measurement of odor threshold by triangle odor bag method." *Odor Measurement Review*, Japan Ministry of the Environment, 118-127.
- Paatero, P. and Tapper, U. (1994). "Positive matrix factorization: a nonnegative factor model with optimal utilization of error estimates of data values." *Environmetrics*, **5**, 111–126.
- Paatero, P. (1999). "The multilinear engine - A table-driven, least squares program for solving multilinear problems, including the n-way parallel factor analysis model." *J. Comput. Graphical Stat.*, **8**, 854–888.
- Paatero, P. (2000). *User's Guide for Positive Matrix Factorization Programs PMF2 and PMF3, Part 1: tutorial*. University of Helsinki, Finland.
- Pearson, K. (1901). "[On Lines and Planes of Closest Fit to Systems of Points in Space](#)." (PDF). *Philosophical Magazine*, **2**, 559–572.
- Peter Prazeller (2003). "Proton transfer reaction ion trap mass spectrometer." *Rapid Commun. Mass Spectrom.*, **17**, 1593–1599.
- Pope, C.A . III and Dockery, D.W. (2007). "Health effects of fine particulate air pollution: Lines that connect." *J. Air & Waste Manage. Assoc.*, **57**, 709-742.

- Powell, M.J.D. (1964). "An efficient method for finding the minimum of a function of several variables without calculating derivatives." *Computer Journal*, **7**, 152–162.
- Qu, G., Omotoso, M.M., El-Din, M.G. and Feddes, J.J.R. (2008). "Development of an integrated sensor to measure odors." *Environmental Monitoring and Assessment*, **144**, 277-283.
- Quinche, N. and Margot, P. (2010). "Coulrier, Paul-Jean (1824-1890): A precursor in the history of fingerprint detection and their potential use for identifying their source", *Journal of Forensic Identification*, **60**, 129-134.
- Ramadan, Z., Song, X.H. and Hopke, P.K. (2000). "Identification of sources of Phoenix aerosol by positive matrix factorization." *J. Air & Waste Manage. Assoc.*, **50**, 1308–1320.
- Ravindran, S.S. (1999). *Proper Orthogonal Decomposition in Optimal Control of Fluids*, NASA, Langley Research Center.
- Reinikainen, L.M. (1993). "The effect of humidification on perceived indoor air quality assessed by an untrained odor panel." In: *Proc. of Indoor Air '93*, Helsinki, Finland, **1**, pp. 101-105.
- Roels, S. and Janssen, H. (2006). "A comparison of the Nordtest and Japanese test methods for the moisture buffering performance of building materials." *J. Build. Phys.*, **30**, 137-161.
- Sakr, W., Weschler, C.J. and Fanger, P.O. (2006). "The impact of sorption on perceived indoor air quality." *Indoor Air*, **16**, 98-110.
- Schauer, J.J., Rogge, W.F., Hildemann, L.M., Mazurek, M.A., Cass, G.R. and Simoneit, B.R.T. (1996). "Source apportionment of airborne particulate matter using organic compounds as tracers." *Atmos. Environ.*, **30**, 3837-3855.
- Sheynin, O. (2004). "Fechner as a statistician." *The British Journal of Mathematical and Statistical Psychology*, **57**, 53-72
- Simoneit, B.R.T. (2002). "Biomass burning - a review of organic tracers for smoke from incomplete combustion." *Appl. Geochem.*, **17**, 129-162.
- Sirovich, L. (1987). "Turbulence and the dynamics of coherent structures. I. Coherent structures." *Q Appl Math*, **45**, 561-70.

- Sirovich, L. (1987). "Turbulence and the dynamics of coherent structures II. Symmetries and transformations." *Q Appl Math*, **45**, 573-82.
- Sirovich, L. (1987). "Turbulence and the dynamics of coherent structures. III. Dynamics and scaling." *Q Appl Math*, **45**, 583-90.
- Smith, L.I. (2002). *A Tutorial on Principal Component Analysis*.
- Steeghs, M., Bais, H.P., de Gouw, J., Goldan, P., Kuster, W., Northway, M., Fall, R. and Vivanco, J.M. (2004). "Proton transfer reaction - mass spectrometry as a new tool for real time analysis of root-secreted volatile organic compounds in Arabidopsis." *Plant Physiol.*, **135**, 47-58.
- Steinbacher, M., Dommen, J., Ammann, C., Spirig, C., Neftel, A. and Prevot, A.S.H. (2004). "Performance characteristics of a proton transfer reaction - mass spectrometer (PTR-MS) derived from laboratory and field measurements." *Int J Mass Spectrom*, **239**, 117-128.
- Taipale, R., Ruuskanen, T.M., Rinne, J., Kajos, M.K., Hakola, H., Pohja, T. and Kulmala, M. (2008). "Technical note: Quantitative long-term measurements of VOC concentrations by PTR-MS - measurement, calibration, and volume mixing ratio calculation methods." *Atmos. Chem. Phys. Discuss.*, **8**, 9435-9475.
- Tarman, I.H. and Sirovich, L. (1998). "Extensions to Karhunen-Loeve based approximation of complicated phenomena." *Comput. Methods Appl. Mech. Eng.*, **155**, 359-68.
- Van Ruth, S.M., Koot, A., Akkermans, W., Araghpour, N., Rozijn, M., Baltussen, M., Wisthaler, A., Mark, T.D. and Frankhuizen, R. (2007). "Butter and butter oil classification." *Eur. Food Res. Technol.*, **227**, 307-317.
- Viana, M., Amato, F., Alastuey, A., Querol, X., Moreno, T., Dos Santos, S.G., Hecce, M.D. and Fernandez-Patier, R. (2009). "Chemical tracers of particulate emissions from commercial shipping." *Environ Sci Technol.*, **43**, 7472-7477.
- Wang, X., Zhang, Y. and Zhao, R. (2006). "Study on characteristics of double surface VOC emissions from dry flat-plate building materials." *Chinese Science Bulletin*, **51**, 2287-93.

- Wang, Z. and Stout, S.A. (2007). "Emerging CEN methodology for oil spill identification." *Oil Spill Environmental Forensics: Fingerprinting and Source Identification*, Academic Press, pp. 229-256.
- Wargocki, P. and Wyon, D.P. (2006). "Effects of HVAC on student performance." *ASHRAE J.*, **48**, 22-28.
- Wargocki, P., Knudsen, H.N. and Zuczek, P. (2007). "Effect of using low-polluting building materials and increasing ventilation on perceived indoor air quality." In: *Proc. of CLIMA 2007*, Helsinki, Finland.
- Wargocki, P., Knudsen, H.N. and Frontczak, M. (2008). "The effect of using low-polluting building materials on ventilation requirements and energy use in buildings." DTU.
- Warneke, C., de Gouw, J., Kuster, W., Goldan, P. and Fall, R. (2003). "Validation of atmospheric VOC measurements by proton transfer reaction - mass spectrometry using a gas-chromatographic pre-separation method." *Environ Sci Technol.*, **37**, 2494-2501.
- Watson, J.G., Robinson, N.F., Chow, J.C., Henry, R.C., Kim, B.M., Pace, T.G., Meyer, E.L. and Nguyen, Q. (1990). "The USEPA/DRI chemical mass balance receptor model, CMB 7.0." *Environmental Software*, **5**, 38-49.
- Webber, G.A., Handler, R.A. and Sirovich, L. (1997). "The Karhunen-Loeve decomposition of minimal channel flow." *Phys. Fluids*, **9**, 1054-66.
- Wehinger, A., Schmid, A., Mechtcheriakov, S., Ledochowski, M., Grabmer, C., Gastl, G.A. and Amann, A. (2007). "Lung cancer detection by proton transfer reaction - mass spectrometric analysis of human breath gas." *Int J Mass Spectrom*, **265**, 49-59.
- Weschler, C.J., Wisthaler, A., Cowlin, S., Tamas, G., Strom-Tejsen, P., Hodgson, A.T., Destailats, H., Herrington, J., Zhang, J.J. and Nazaroff, W.W. (2007). "Ozone-initiated chemistry in an occupied simulated aircraft cabin." *Environ Sci Technol.*, **41**, 6177-6184.

- Whyte, C., Wyche, K.P., Kholia, M., Ellis, A.M. and Monks, P.S. (2007). "Fast fingerprinting of arson accelerants by proton transfer reaction time-of-flight mass spectrometry." *Int J Mass Spectrom*, **263**, 222-232.
- Winchester, J.W. and Nifong, G.D. (1971). "Water pollution in Lake Michigan by trace elements from pollution aerosol fallout." *Water, Air, Soil Pollut.*, **1**, 50-64.
- Wisthaler, A., Strom-Tejse, P., Fang, L., Arnaud, T.J., Hansel, A., Mark, T.D. and Wyon, D.P. (2007). "PTR-MS assessment of photocatalytic and sorption-based purification of recirculated cabin air during simulated 7-h flights with high passenger density." *Environ Sci Technol.*, **41**, 229-234.
- Wolkoff, P., Clausen, P.A., Nielsen, P.A. and Molhave, L. (1991). "The Danish twin apartment study: Part 1, formaldehyde and long-term VOC measurements." *Indoor Air*, **1**, 478-490.
- Wolkoff, P. (1998). "Impact of air velocity, temperature, humidity and air on long-term VOC emissions from building products." *Atmos. Environ.*, **32**, 2659-2668.
- Wolkoff, P. and Nielsen, G.D. (2001). "Organic compounds in indoor air - their relevance for perceived indoor air quality." *Atmos. Environ.*, **35**, 4407-4417.
- Wu, C., Larson, T.V., Wu, S., Williamson, J., Westberg, H.H. and Liu, L.S. (2007). "Source apportionment of PM<sub>2.5</sub> and selected hazardous air pollutants in Seattle." *Sci. Total Environ.*, **386**, 42-52.
- Yaglou, C.P., Riley, E.C. and Coggins, D.I. (1936). "Ventilation requirements." *ASHRAE Trans.*, **42**, 133-162.
- Yang, X., Chen, Q., Zhang, J.S., Magee, R., Zeng, J. and Shaw, C.Y. (2001). "Numerical simulation of VOC emissions from dry materials." *Build. Environ.*, **36**, 1099-1107.
- Zhang, J.S., Shaw, C.Y., Sander, D. and Zhu, J.P. (1999). "MEDB-IAQ: A material emission database and single-zone IAQ simulation program – A tool for building designers, engineers and managers." *CMEIAQ Report 4.2, IRC/NRC*, Ottawa, Canada.

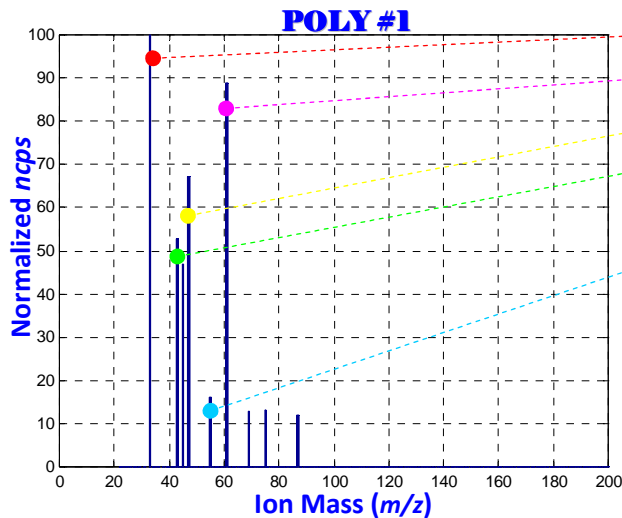


- Zhang, J.S., Zhu, J.P. and Shaw, C.Y. (1999). *CMEIAQ Report 1.1, 1.2, 1.3, 3.1, 4.1, IRC/NRC*, Ottawa, Canada.
- Zhang, T. and Chen, Q. (2007). "Identification of contaminant sources in enclosed spaces by a single sensor." *Indoor Air*, **17**, 439-449.
- Zhang, Y. and Haghighat, F. (1997). "The impact of surface air movement on material emissions." *Build. Environ.*, **32**, 551-556.
- Zhao, W., Hopke, P.K., Gelfand, E.W. and Rabinovitch, N. (2007). "Use of an expanded receptor model for personal exposure analysis in schoolchildren with Asthma." *Atmos. Environ.*, **41**, 4084-4096.
- Zhu, J.P., Magee, R.J., Lusztyk, E., Zhang, J.S. and Shaw, C.Y. (1999). "Material emission data for typical building materials: Small environmental chamber tests." *CMEIAQ Report 4.1, IRC/NRC*, Ottawa, Canada.

## APPENDIX A. A Library of ESs by PTR-MS for Nine Building Materials tested.

### (a) Polyolefine:

1. Material ID & Name: (1) POLY, Polyolefine
2. Description on material: 2.0-mm homogenous polyolefine-based resilient flooring, reinforced with polyurethane
3. Test conditions:  
 $T = 23.8 \pm 0.07^\circ\text{C}$ ,  $\text{RH} = 31.0 \pm 0.03\%$



●	<u>33: (100) Methanol</u>
●	<u>61: (88.90) Acetic Acid</u>
●	<u>47: (67.09) Ethanol</u>
●	<u>43: (52.71) Acetic Acid</u>
●	45: (46.88) Acetaldehyde
●	55: (16.04) Hexanal
●	75: (13.33) Ethanol
●	69: (12.84) Nonanal
●	87: (11.95) Pentanal

- \* In the order of Ion Mass, Magnitude, VOC Name above.
- \* Range of  $Q_v/A = 0.35, 0.89 \text{ \& } 2.66 \text{ (L/s/m}^2\text{)}$ .
- \* The underlined above are the major peaks.
- \* Oxirane ( $m/z=73$ ): Within the uncertainty.
- \* Benzaldehyde ( $m/z=107$ ): Within the uncertainty.

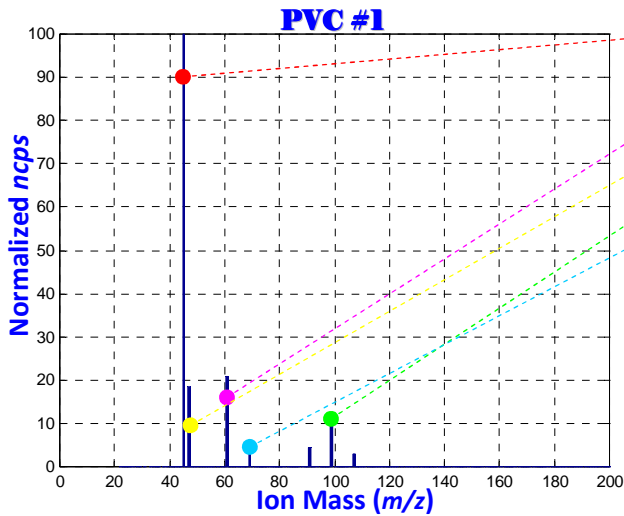
GC/MS Analysis VOC Compound	<input type="checkbox"/> M.W.	<input type="checkbox"/> Formula	<input type="checkbox"/> CAS#	<input type="checkbox"/> Detected <sup>a</sup> <input type="checkbox"/> (Yes/No)	Threshold <sup>b</sup> ppb	Threshold <sup>b</sup> ug/m <sup>3</sup>
OXIRANE, ETHYL- ACETIC ACID, ANHYDRIDE WITH FORMIC ACID	72	C4H8O	106-88-7	<input type="checkbox"/> Yes	<input type="checkbox"/>	<input type="checkbox"/>
PENTANAL	86	C5H10O	110-62-3	<input type="checkbox"/> Yes	6.03	21.90
ETHANOL, 2-NITRO-, PROPIONATE (ESTER)	147	C5H9O4N	5390-28-3	<input type="checkbox"/> (No)	<input type="checkbox"/>	<input type="checkbox"/>
HEXANAL	100	C6H12O	66-25-1	<input type="checkbox"/> Yes	13.80	57.5
BUTANOIC ACID	88	C4H8O2	107-92-6	<input type="checkbox"/> (No)	3.9	14.50
HEPTANAL	114.2	C7H14O	111-71-7	<input type="checkbox"/> (No)	4.79	22.90
CYCLOTETRASIOXANE, OCTAMETHYL-	296	C8H24O4Si4	556-67-2	<input type="checkbox"/> Yes	<input type="checkbox"/>	<input type="checkbox"/>
PENTANOIC ACID	102	C5H10O2	109-52-4	<input type="checkbox"/> (No)	4.79	20.40
BENZALDEHYDE	106	C7H6O	100-52-7	<input type="checkbox"/> Yes	41.70	186.00
HEXANOIC ACID	116	C6H12O2	142-62-1	<input type="checkbox"/> (No)	12.60	60.30
NONANAL	142	C9H18O	124-19-6	<input type="checkbox"/> Yes	2.24	13.5

<sup>a</sup>  $Q_v/A=0.89 \text{ (L/s/m}^2\text{)}$ ,  $T=23.8^\circ\text{C}$ ,  $\text{RH}=31\%$ .

<sup>b</sup> Odor threshold based on "VOCBASE" database by the Danish National Institute of Occupational Health.

**(b) PVC:**

1. Material ID & Name: (2) PVC, Polyvinyl
2. Description on material: 2.0-mm homogenous single layered vinyl flooring, reinforced with polyurethane
3. Test conditions:  
 $T = 23.7 \pm 0.03^\circ\text{C}$ ,  $\text{RH} = 31.0 \pm 0.07\%$



- 45: (100) Acetaldehyde
- 61: (20.72) Acetic Acid
- 47: (18.46) Ethanol
- 99: (10.90) Cyclohexanone
- 69: (6.13) Nonanal
- 91: (4.45) ???
- 107: (2.87) Benzaldehyde

\* In the order of Ion Mass, Magnitude, VOC Name above.  
 \* Range of  $Q_w/A = 0.89 \text{ (L/s/m}^2\text{)}$ .  
 \* The underlined above are the major peaks.

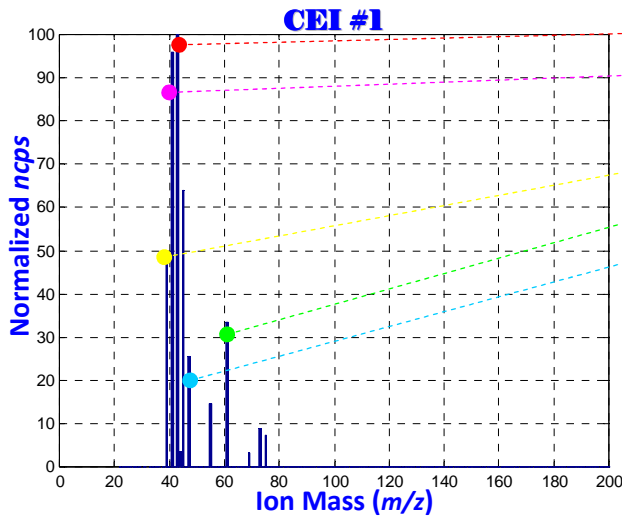
GC/MS Analysis VOC Compound	<input type="checkbox"/> M.W.	<input type="checkbox"/> Formula	<input type="checkbox"/> CAS#	<input type="checkbox"/> [ Detected <sup>a</sup> [ (Yes/No)	Threshold <sup>b</sup> ppb	Threshold <sup>b</sup> ug/m <sup>3</sup>
OXIRANE, ETHYL-	72	C4H8O	106-88-7	<input type="checkbox"/> (No)	<input type="checkbox"/>	<input type="checkbox"/>
ACETIC ACID, ANHYDRIDE WITH FORMIC ACID	88	C3H4O3	2258-42-6	<input type="checkbox"/> (No)	<input type="checkbox"/>	<input type="checkbox"/>
PENTANAL	86	C5H10O	110-62-3	<input type="checkbox"/> (No)	6.03	21.90
ETHANOL, 2-NITRO-, PROPIONATE (ESTER)	147	C5H9O4N	5390-28-3	<input type="checkbox"/> (No)	<input type="checkbox"/>	<input type="checkbox"/>
HEXANAL	100	C6H12O	66-25-1	<input type="checkbox"/> (No)	13.80	57.5
BUTANOIC ACID	88	C4H8O2	107-92-6	<input type="checkbox"/> (No)	3.9	14.50
HEPTANAL	114.2	C7H14O	111-71-7	<input type="checkbox"/> (No)	4.79	22.90
CYCLOTETRAILOXANE, OCTAMETHYL-	296	C8H24O4Si4	556-67-2	<input type="checkbox"/> (No)	<input type="checkbox"/>	<input type="checkbox"/>
PENTANOIC ACID	102	C5H10O2	109-52-4	<input type="checkbox"/> (No)	4.79	20.40
BENZALDEHYDE	106	C7H6O	100-52-7	<input type="checkbox"/> <b>Yes</b>	41.70	186.00
HEXANOIC ACID	116	C6H12O2	142-62-1	<input type="checkbox"/> (No)	12.60	60.30
NONANAL	142	C9H18O	124-19-6	<input type="checkbox"/> <b>Yes</b>	2.24	13.5

<sup>a</sup>  $Q_w/A=0.89 \text{ (L/s/m}^2\text{)}$ ,  $T=23.7^\circ\text{C}$ ,  $\text{RH}=31\%$ .

<sup>b</sup> Odor threshold based on "VOCBASE" database by the Danish National Institute of Occupational Health.

(c) Ceiling:

1. Material ID & Name: (3) CEI, Ceiling
2. Description on material: 10-mm plain gypsum board covered with plastic coated material
3. Test conditions:  
 $T = 24.7 \pm 0.02^\circ\text{C}$ ,  $\text{RH} = 31.0 \pm 0.1\%$



- 43: (100) Isopropanol, Acetic Acid
- 41: (95.93) Isopropanol
- 45: (63.93) Acetaldehyde
- 39: (49.08) Isopropanol
- 61: (33.55) Acetic Acid
- 47: (25.46) Ethanol
- 55: (14.71) Hexanal
- 73: (8.79) Oxirane
- 75: (7.33) Ethanol
- 44: (3.59) ???
- 69: (3.28) Nonanal

\* In the order of Ion Mass, Magnitude, VOC Name above.  
 \* Range of  $Q_w/A = 0.29, 0.89 \text{ \& } 2.66 \text{ (L/s/m}^2\text{)}$ .  
 \* The underlined above are the major peaks.  
 \* Pentanal ( $m/z=87$ ): Within the uncertainty.  
 \* Benzaldehyde ( $m/z=107$ ): Within the uncertainty.  
 \* Methanol ( $m/z=33$ ): Rapidly decayed.

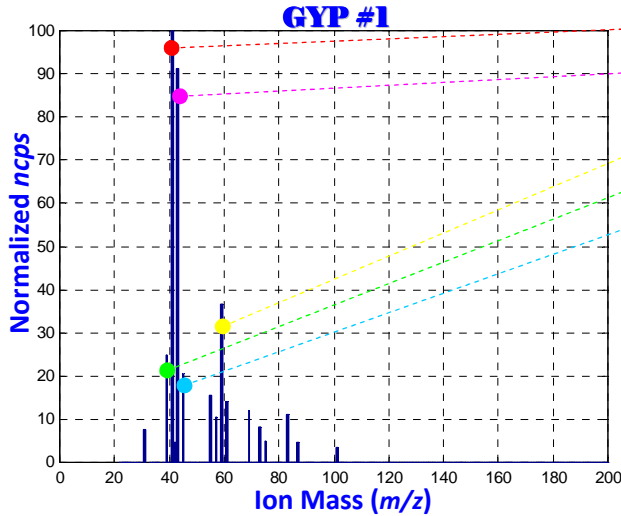
GC/MS Analysis VOC Compound	<input type="checkbox"/> M.W.	<input type="checkbox"/> Formula	<input type="checkbox"/> CAS#	<input type="checkbox"/> Detected <sup>a</sup> <input type="checkbox"/> (Yes/No)	Threshold <sup>b</sup> ppb	Threshold <sup>b</sup> ug/m <sup>3</sup>
OXIRANE, ETHYL- ACETIC ACID, ANHYDRIDE WITH FORMIC ACID	72 88	C4H8O C3H4O3	106-88-7 2258-42-6	<input type="checkbox"/> Yes <input type="checkbox"/> Yes	<input type="checkbox"/> <input type="checkbox"/>	<input type="checkbox"/> <input type="checkbox"/>
PENTANAL	86	C5H10O	110-62-3	<input type="checkbox"/> Yes	6.03	21.90
ETHANOL, 2-NITRO-, PROPIONATE (ESTER)	147	C5H9O4N	5390-28-3	<input type="checkbox"/> (No)	<input type="checkbox"/>	<input type="checkbox"/>
HEXANAL	100	C6H12O	66-25-1	<input type="checkbox"/> Yes	13.80	57.5
BUTANOIC ACID	88	C4H8O2	107-92-6	<input type="checkbox"/> (No)	3.9	14.50
HEPTANAL	114.2	C7H14O	111-71-7	<input type="checkbox"/> (No)	4.79	22.90
CYCLOTETRAILOXANE, OCTAMETHYL-	296	C8H24O4Si4	556-67-2	<input type="checkbox"/> Yes	<input type="checkbox"/>	<input type="checkbox"/>
PENTANOIC ACID	102	C5H10O2	109-52-4	<input type="checkbox"/> (No)	4.79	20.40
BENZALDEHYDE	106	C7H6O	100-52-7	<input type="checkbox"/> Yes	41.70	186.00
HEXANOIC ACID	116	C6H12O2	142-62-1	<input type="checkbox"/> (No)	12.60	60.30
NONANAL	142	C9H18O	124-19-6	<input type="checkbox"/> Yes	2.24	13.5

<sup>a</sup>  $Q_w/A=0.89 \text{ (L/s/m}^2\text{)}$ ,  $T=24.7^\circ\text{C}$ ,  $\text{RH}=31\%$ .

<sup>b</sup> Odor threshold based on "VOCBASE" database by the Danish National Institute of Occupational Health.

**(d) Gypsum:**

1. Material ID & Name: (4) GYP, Gypsum board
2. Description on material: 13-mm plain gypsum board lined with cardboard
3. Test conditions:  
 $T = 24.5 \pm 0.09^\circ\text{C}$ ,  $\text{RH} = 31.0 \pm 0.03\%$



●	41: (100) <u>Isopropanol</u>
●	43: (91.28) <u>Isopropanol</u> , Acetic Acid
●	59: (36.67) <u>Acetone</u>
●	39: (24.85) <u>Isopropanol</u>
●	45: (20.42) <u>Acetaldehyde</u>
●	55: (15.43) Hexanal
●	61: (14.14) Acetic Acid
●	69: (12.03) Nonanal
●	83: (11.01) Hexanal
●	57: (10.58) Acrolein
●	73: (8.27) Oxirane
●	31: (7.72) Formaldehyde
●	75: (5.03) Propanoic Acid
●	42: (4.69) Acetonitrile
●	87: (4.66) Pentanal
●	101: (3.55) Hexanal

\* In the order of Ion Mass, Magnitude, VOC Name above.  
 \* Range of  $Q_w/A = 0.20, 0.41, 1.23 \text{ \& } 3.70 \text{ (L/s/m}^2\text{)}$ .  
 \* The underlined above are the major peaks.  
 \* Benzaldehyde ( $m/z=107$ ): Within the uncertainty.  
 \* Methanol ( $m/z=33$ ): Rapidly decayed.

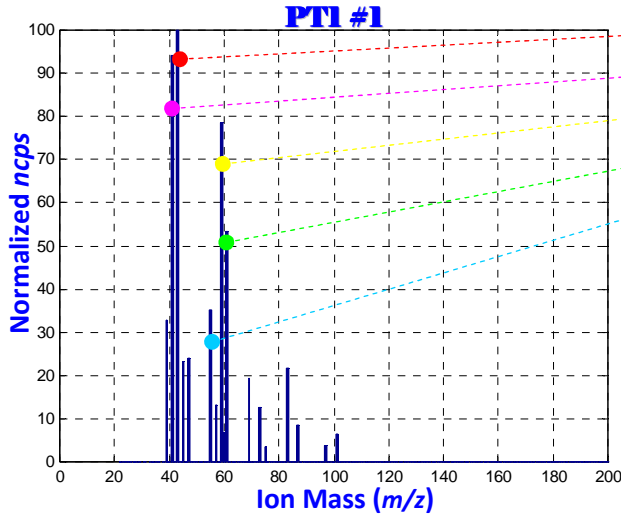
GC/MS Analysis VOC Compound	<input type="checkbox"/> M.W.	<input type="checkbox"/> Formula	<input type="checkbox"/> CAS#	<input type="checkbox"/> Detected <sup>a</sup> <input type="checkbox"/> (Yes/No)	Threshold <sup>b</sup> ppb	Threshold <sup>b</sup> ug/m <sup>3</sup>
OXIRANE, ETHYL-	72	C4H8O	106-88-7	<input type="checkbox"/> Yes	<input type="checkbox"/>	<input type="checkbox"/>
ACETIC ACID, ANHYDRIDE WITH FORMIC ACID	88	C3H4O3	2258-42-6	<input type="checkbox"/> (No)	<input type="checkbox"/>	<input type="checkbox"/>
PENTANAL	86	C5H10O	110-62-3	<input type="checkbox"/> Yes	6.03	21.90
ETHANOL, 2-NITRO-, PROPIONATE (ESTER)	147	C5H9O4N	5390-28-3	<input type="checkbox"/> (No)	<input type="checkbox"/>	<input type="checkbox"/>
HEXANAL	100	C6H12O	66-25-1	<input type="checkbox"/> Yes	13.80	57.5
BUTANOIC ACID	88	C4H8O2	107-92-6	<input type="checkbox"/> (No)	3.9	14.50
HEPTANAL	114.2	C7H14O	111-71-7	<input type="checkbox"/> (No)	4.79	22.90
CYCLOTETRASIOXANE, OCTAMETHYL-	296	C8H24O4Si4	556-67-2	<input type="checkbox"/> Yes	<input type="checkbox"/>	<input type="checkbox"/>
PENTANOIC ACID	102	C5H10O2	109-52-4	<input type="checkbox"/> (No)	4.79	20.40
BENZALDEHYDE	106	C7H6O	100-52-7	<input type="checkbox"/> Yes	41.70	186.00
HEXANOIC ACID	116	C6H12O2	142-62-1	<input type="checkbox"/> (No)	12.60	60.30
NONANAL	142	C9H18O	124-19-6	<input type="checkbox"/> Yes	2.24	13.5

<sup>a</sup>  $Q_w/A=0.41 \text{ (L/s/m}^2\text{)}$ ,  $T=24.5^\circ\text{C}$ ,  $\text{RH}=31\%$ .

<sup>b</sup> Odor threshold based on "VOCBASE" database by the Danish National Institute of Occupational Health.

(e) Paint 1:

1. Material ID & Name: (5) PT1, Paint 1
2. Description on material: 13-mm plain gypsum board painted with one coat (0.14 l/m<sup>2</sup>) of water-based acrylic wall paint
3. Test conditions:  
 T = 24.5 ± 0.04°C, RH = 31.0 ± 0.03%



- 43: (100) Isopropanol, Acetic Acid
- 41: (94.20) Isopropanol
- 59: (78.59) Acetone
- 61: (53.48) Acetic Acid
- 55: (35.24) Hexanal
- 39: (32.78) Isopropanol
- 47: (24.00) Ethanol
- 45: (23.11) Acetaldehyde
- 83: (21.74) Hexanal
- 69: (19.41) Nonanal
- 57: (13.15) Acrolein
- 73: (12.53) Oxirane
- 87: (8.62) Pentanal
- 60: (6.65) ???
- 101: (6.57) Hexanal
- 97: (3.85) Heptanal
- 75: (3.51) Ethanol

\* In the order of Ion Mass, Magnitude, VOC Name above.  
 \* Range of Q<sub>v</sub>/A = 0.21, 0.41, 1.23 & 3.70 (L/s/m<sup>2</sup>).  
 \* The underlined above are the major peaks.  
 \* Benzaldehyde (m/z=107): Within the uncertainty.  
 \* Methanol (m/z=33): Rapidly decayed.

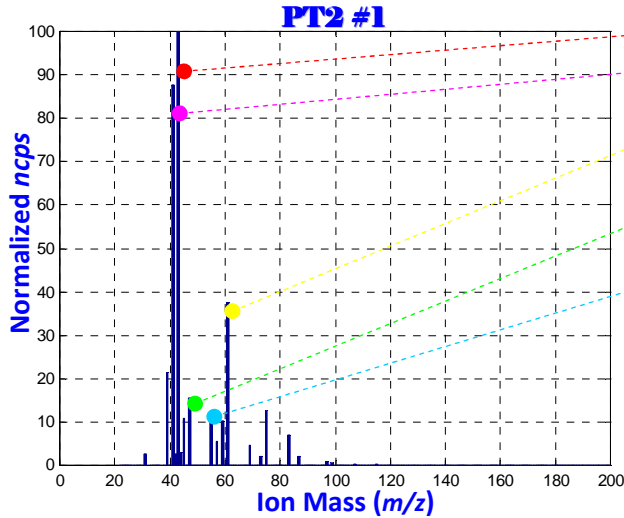
GC/MS Analysis VOC Compound	<input type="checkbox"/> M.W.	<input type="checkbox"/> Formula	<input type="checkbox"/> CAS#	<input type="checkbox"/> Detected <sup>a</sup> <input type="checkbox"/> (Yes/No)	Threshold <sup>b</sup> ppb	Threshold <sup>b</sup> ug/m <sup>3</sup>
OXIRANE, ETHYL- ACETIC ACID, ANHYDRIDE WITH FORMIC ACID	72 88	C4H8O C3H4O3	106-88-7 2258-42-6	<input type="checkbox"/> Yes <input type="checkbox"/> (No)	<input type="checkbox"/> <input type="checkbox"/>	<input type="checkbox"/> <input type="checkbox"/>
PENTANAL	86	C5H10O	110-62-3	<input type="checkbox"/> Yes	6.03	21.90
ETHANOL, 2-NITRO-, PROPIONATE (ESTER)	147	C5H9O4N	5390-28-3	<input type="checkbox"/> (No)	<input type="checkbox"/>	<input type="checkbox"/>
HEXANAL	100	C6H12O	66-25-1	<input type="checkbox"/> Yes	13.80	57.5
BUTANOIC ACID	88	C4H8O2	107-92-6	<input type="checkbox"/> (No)	3.9	14.50
HEPTANAL	114.2	C7H14O	111-71-7	<input type="checkbox"/> Yes	4.79	22.90
CYCLOTETRASILOXANE, OCTAMETHYL-	296	C8H24O4Si4	556-67-2	<input type="checkbox"/> Yes	<input type="checkbox"/>	<input type="checkbox"/>
PENTANOIC ACID	102	C5H10O2	109-52-4	<input type="checkbox"/> (No)	4.79	20.40
BENZALDEHYDE	106	C7H6O	100-52-7	<input type="checkbox"/> Yes	41.70	186.00
HEXANOIC ACID	116	C6H12O2	142-62-1	<input type="checkbox"/> (No)	12.60	60.30
NONANAL	142	C9H18O	124-19-6	<input type="checkbox"/> Yes	2.24	13.5

<sup>a</sup> Q<sub>v</sub>/A=0.41 (L/s/m<sup>2</sup>), T=24.5°C, RH=31%.

<sup>b</sup> Odor threshold based on "VOCBASE" database by the Danish National Institute of Occupational Health.

(f) Paint 2:

1. Material ID & Name: (6) PT2, Paint 2
2. Description on material: 13-mm plain gypsum board painted with one coat (0.14 l/m<sup>2</sup>) of water-based wall paint with linseed oil
3. Test conditions:  
T = 24.5 ± 0.04°C, RH = 31.0 ± 0.1%



- 43: (100) Isopropanol, Acetic Acid
- 41: (87.75) Isopropanol
- 61: (37.66) Acetic Acid
- 39: (21.46) Isopropanol
- 47: (15.68) Ethanol
- 75: (12.57) Propanoic Acid, Ethanol
- 55: (11.07) Hexanal
- 45: (10.71) Acetaldehyde
- 59: (10.29) Acetone
- 83: (6.96) Hexanal
- 57: (5.57) Acrolein
- 69: (4.63) Nonanal
- 44: (2.96) ???
- 42: (2.77) Acetonitrile
- 31: (2.75) Formaldehyde
- 73: (2.11) Oxirane
- 87: (2.10) Pentanal
- 97, 115: (1.34) Heptanal
- 99: (0.52) Decane
- 107: (0.31) Benzaldehyde

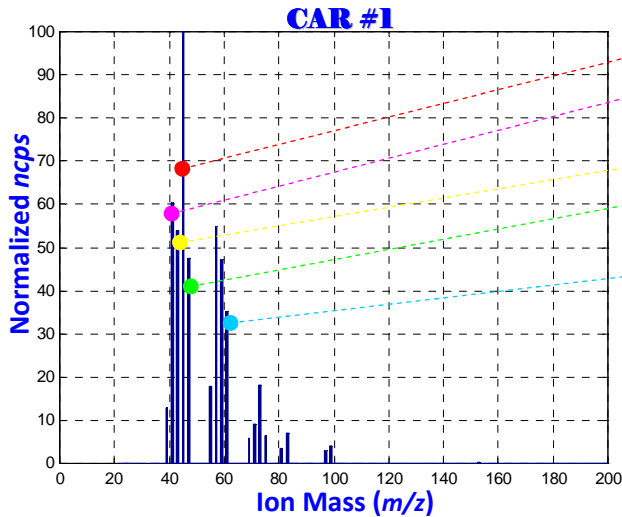
\* In the order of Ion Mass, Magnitude, VOC Name above.  
 \* Range of Q<sub>w</sub>/A = 0.17, 0.41, 1.23 & 3.70 (L/s/m<sup>2</sup>).  
 \* The underlined above are the major peaks.

GC/MS Analysis VOC Compound	M.W.	Formula	CAS#	Detected <sup>a</sup> (Yes/No)	Threshold <sup>b</sup> ppb	Threshold <sup>b</sup> ug/m <sup>3</sup>
OXIRANE, ETHYL- ACETIC ACID, ANHYDRIDE WITH FORMIC ACID	72 88	C4H8O C3H4O3	106-88-7 2258-42-6	<input type="checkbox"/> Yes <input type="checkbox"/> Yes	<input type="checkbox"/> <input type="checkbox"/>	<input type="checkbox"/> <input type="checkbox"/>
PENTANAL	86	C5H10O	110-62-3	<input type="checkbox"/> Yes	6.03	21.90
ETHANOL, 2-NITRO-, PROPIONATE (ESTER)	147	C5H9O4N	5390-28-3	<input type="checkbox"/> (No)	<input type="checkbox"/>	<input type="checkbox"/>
HEXANAL	100	C6H12O	66-25-1	<input type="checkbox"/> Yes	13.80	57.5
BUTANOIC ACID	88	C4H8O2	107-92-6	<input type="checkbox"/> (No)	3.9	14.50
HEPTANAL	114.2	C7H14O	111-71-7	<input type="checkbox"/> Yes	4.79	22.90
CYCLOTETRASIOXANE, OCTAMETHYL-	296	C8H24O4Si4	556-67-2	<input type="checkbox"/> Yes	<input type="checkbox"/>	<input type="checkbox"/>
PENTANOIC ACID	102	C5H10O2	109-52-4	<input type="checkbox"/> (No)	4.79	20.40
BENZALDEHYDE	106	C7H6O	100-52-7	<input type="checkbox"/> Yes	41.70	186.00
HEXANOIC ACID	116	C6H12O2	142-62-1	<input type="checkbox"/> (No)	12.60	60.30
NONANAL	142	C9H18O	124-19-6	<input type="checkbox"/> Yes	2.24	13.5

<sup>a</sup> Q<sub>w</sub>/A=0.41 (L/s/m<sup>2</sup>), T=24.5°C, RH=31%.  
<sup>b</sup> Odor threshold based on "VOCBASE" database by the Danish National Institute of Occupational Health.

## (g) Carpet:

1. Material ID & Name: (7) CAR, Carpet
2. Description on material: 6.4-mm tufted loop polyamide carpet with supporting layer of polypropylene web and polypropylene backing
3. Test conditions:  
T = 23.5 ± 0.05°C, RH = 31.0 ± 0.1%



- 45: (100) Acetaldehyde
- 41: (60.47) Propanal, Isopropanol
- 57: (54.88) Acrolein
- 43: (53.90) Acetic Acid, Isopropanol
- 47: (47.59) Ethanol
- 59: (47.26) Acetone, Propanal
- 61: (35.17) Acetic Acid
- 73: (18.14) Oxirane
- 55: (17.79) Hexanal
- 39: (12.91) Isopropanol
- 71: (8.95) Methacrolein
- 83: (6.91) Hexanal
- 75: (6.44) Ethanol
- 69: (5.90) Nonanal
- 99: (4.10) Decane
- 81: (3.44) Limonene
- 97: (3.03) Heptanal

\* In the order of Ion Mass, Magnitude, VOC Name above.  
 \* Range of Q<sub>w</sub>/A = 0.35, 0.89 & 2.66 (L/s/m<sup>2</sup>).  
 \* The underlined above are the major peaks.

GC/MS Analysis VOC Compound	<input type="checkbox"/> M.W.	<input type="checkbox"/> Formula	<input type="checkbox"/> CAS#	<input type="checkbox"/> Detected <sup>a</sup> <input type="checkbox"/> (Yes/No)	Threshold <sup>b</sup> ppb	Threshold <sup>b</sup> ug/m <sup>3</sup>
OXIRANE, ETHYL- ACETIC ACID, ANHYDRIDE WITH FORMIC ACID	72	C4H8O	106-88-7	<input type="checkbox"/> Yes	<input type="checkbox"/>	<input type="checkbox"/>
PENTANAL	86	C5H10O	110-62-3	<input type="checkbox"/> (No)	6.03	21.90
ETHANOL, 2-NITRO-, PROPIONATE (ESTER)	147	C5H9O4N	5390-28-3	<input type="checkbox"/> (No)	<input type="checkbox"/>	<input type="checkbox"/>
HEXANAL	100	C6H12O	66-25-1	<input type="checkbox"/> Yes	13.80	57.5
BUTANOIC ACID	88	C4H8O2	107-92-6	<input type="checkbox"/> (No)	3.9	14.50
HEPTANAL	114.2	C7H14O	111-71-7	<input type="checkbox"/> Yes	4.79	22.90
CYCLOTETRASILOXANE, OCTAMETHYL-	296	C8H24O4Si4	556-67-2	<input type="checkbox"/> (No)	<input type="checkbox"/>	<input type="checkbox"/>
PENTANOIC ACID	102	C5H10O2	109-52-4	<input type="checkbox"/> (No)	4.79	20.40
BENZALDEHYDE	106	C7H6O	100-52-7	<input type="checkbox"/> (No)	41.70	186.00
HEXANOIC ACID	116	C6H12O2	142-62-1	<input type="checkbox"/> (No)	12.60	60.30
NONANAL	142	C9H18O	124-19-6	<input type="checkbox"/> Yes	2.24	13.5

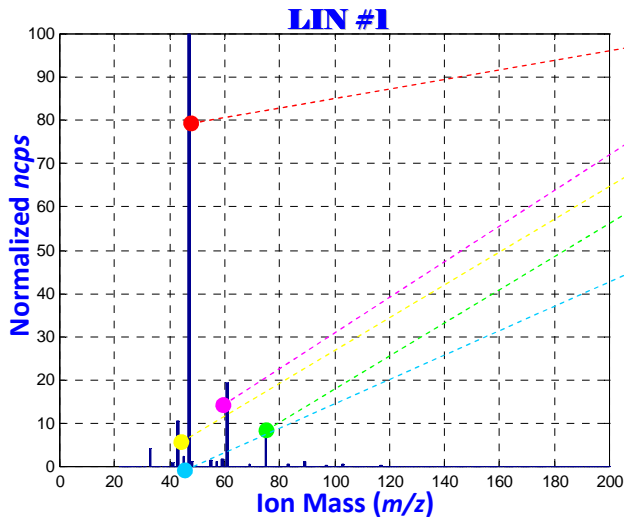
<sup>a</sup> Q<sub>w</sub>/A=0.89 (L/s/m<sup>2</sup>), T=23.5°C, RH=31%.

<sup>b</sup> Odor threshold based on "VOCBASE" database by the Danish National Institute of Occupational Health.



## (h) Linoleum:

1. Material ID & Name: (8) LIN, Linoleum
2. Description on material: 2.5-mm linseed-oil-based flooring, 52% wood meal
3. Test conditions:  
 $T = 23.9 \pm 0.02^\circ\text{C}$ ,  $\text{RH} = 31.0 \pm 0.03\%$



●	<u>47: (100) Ethanol</u>
●	<u>61: (19.21) Acetic Acid</u>
●	<u>43: (10.42) Acetic Acid</u>
●	<u>75: (6.71) Ethanol</u>
●	33: (4.06) Methanol
●	<u>45: (2.34) Acetaldehyde</u>
●	59: (1.74) Acetone, Propanal
●	55: (1.35) Hexanal
●	48: (1.26) Some Isotope
●	57: (1.25) Acrolein
●	89: (1.23) Butanoic Acid
●	41: (0.98) Propanal
●	83: (0.72) Hexanal
●	103: (0.71) Pentanoic Acid
●	69: (0.58) Nonanal
●	117, 99: (0.51) Hexanoic Acid
●	97, 115: (0.32) Heptanal

\* In the order of Ion Mass, Magnitude, VOC Name above.

\* Range of  $Q_w/A = 0.35, 0.89 \text{ \& } 2.66 \text{ (L/s/m}^2\text{)}$ .

\* The underlined above are the major peaks.

\* Benzaldehyde ( $m/z=107$ ): Within the uncertainty.

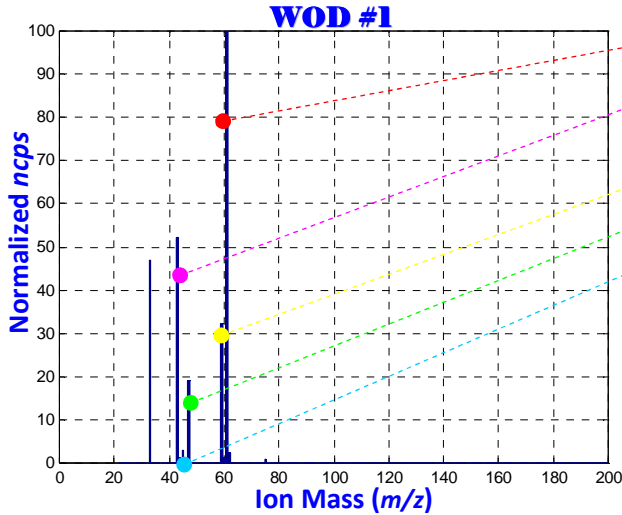
GC/MS Analysis VOC Compound	<input type="checkbox"/> M.W.	<input type="checkbox"/> Formula	<input type="checkbox"/> CAS#	<input type="checkbox"/> Detected <sup>a</sup> <input type="checkbox"/> (Yes/No)	Threshold <sup>b</sup> ppb	Threshold <sup>b</sup> ug/m <sup>3</sup>
OXIRANE, ETHYL-	72	C4H8O	106-88-7	<input type="checkbox"/> (No)	<input type="checkbox"/>	<input type="checkbox"/>
ACETIC ACID, ANHYDRIDE WITH FORMIC ACID	88	C3H4O3	2258-42-6	<input type="checkbox"/> Yes	<input type="checkbox"/>	<input type="checkbox"/>
PENTANAL	86	C5H10O	110-62-3	<input type="checkbox"/> Yes	6.03	21.90
ETHANOL, 2-NITRO-, PROPIONATE (ESTER)	147	C5H9O4N	5390-28-3	<input type="checkbox"/> Yes	<input type="checkbox"/>	<input type="checkbox"/>
HEXANAL	100	C6H12O	66-25-1	<input type="checkbox"/> Yes	13.80	57.5
BUTANOIC ACID	88	C4H8O2	107-92-6	<input type="checkbox"/> Yes	3.9	14.50
HEPTANAL	114.2	C7H14O	111-71-7	<input type="checkbox"/> Yes	4.79	22.90
CYCLOTETrasiloxane, OCTAMETHYL-	296	C8H24O4Si4	556-67-2	<input type="checkbox"/> (No)	<input type="checkbox"/>	<input type="checkbox"/>
PENTANOIC ACID	102	C5H10O2	109-52-4	<input type="checkbox"/> Yes	4.79	20.40
BENZALDEHYDE	106	C7H6O	100-52-7	<input type="checkbox"/> Yes	41.70	186.00
HEXANOIC ACID	116	C6H12O2	142-62-1	<input type="checkbox"/> Yes	12.60	60.30
NONANAL	142	C9H18O	124-19-6	<input type="checkbox"/> Yes	2.24	13.5

<sup>a</sup>  $Q_w/A=0.89 \text{ (L/s/m}^2\text{)}$ ,  $T=23.9^\circ\text{C}$ ,  $\text{RH}=31\%$ .

<sup>b</sup> Odor threshold based on "VOCBASE" database by the Danish National Institute of Occupational Health.

(i) Wood:

1. Material ID & Name: (9) WOD, Wood
2. Description on material: 14-mm untreated beech wood parquets
3. Test conditions:  
 $T = 24.5 \pm 0.04^\circ\text{C}$ ,  $\text{RH} = 31.0 \pm 0.03\%$



- 61: (100) Acetic Acid
- 43: (52.07) Acetic Acid
- 33: (30~47) Methanol
- 59: (32.11) Acetone
- 47: (19.13) Ethanol
- 45: (2.93) Acetaldehyde
- 62: (2.36) Some Isotope
- 44: (1.12) Some Isotope
- 60: (1.08) ???
- 75: (1.02) Ethanol

\* In the order of Ion Mass, Magnitude, VOC Name above.  
 \* Range of  $Q_v/A = 0.31, 0.81, 2.42 \text{ \& } 7.14 \text{ (L/s/m}^2\text{)}$ .  
 \* The underlined above are the major peaks.

GC/MS Analysis VOC Compound	<input type="checkbox"/> M.W.	<input type="checkbox"/> Formula	<input type="checkbox"/> CAS#	<input type="checkbox"/> Detected <sup>a</sup> <input type="checkbox"/> (Yes/No)	Threshold <sup>b</sup> ppb	Threshold <sup>b</sup> ug/m <sup>3</sup>
OXIRANE, ETHYL-	72	C4H8O	106-88-7	<input type="checkbox"/> Yes	<input type="checkbox"/>	<input type="checkbox"/>
ACETIC ACID, ANHYDRIDE WITH FORMIC ACID	88	C3H4O3	2258-42-6	<input type="checkbox"/> Yes	<input type="checkbox"/>	<input type="checkbox"/>
PENTANAL	86	C5H10O	110-62-3	<input type="checkbox"/> (No)	6.03	21.90
ETHANOL, 2-NITRO-, PROPIONATE (ESTER)	147	C5H9O4N	5390-28-3	<input type="checkbox"/> (No)	<input type="checkbox"/>	<input type="checkbox"/>
HEXANAL	100	C6H12O	66-25-1	<input type="checkbox"/> Yes	13.80	57.5
BUTANOIC ACID	88	C4H8O2	107-92-6	<input type="checkbox"/> (No)	3.9	14.50
HEPTANAL	114.2	C7H14O	111-71-7	<input type="checkbox"/> (No)	4.79	22.90
CYCLOTETRAILOXANE, OCTAMETHYL-	296	C8H24O4Si4	556-67-2	<input type="checkbox"/> (No)	<input type="checkbox"/>	<input type="checkbox"/>
PENTANOIC ACID	102	C5H10O2	109-52-4	<input type="checkbox"/> (No)	4.79	20.40
BENZALDEHYDE	106	C7H6O	100-52-7	<input type="checkbox"/> (No)	41.70	186.00
HEXANOIC ACID	116	C6H12O2	142-62-1	<input type="checkbox"/> (No)	12.60	60.30
NONANAL	142	C9H18O	124-19-6	<input type="checkbox"/> (No)	2.24	13.5

<sup>a</sup>  $Q_v/A=0.81 \text{ (L/s/m}^2\text{)}$ ,  $T=24.5^\circ\text{C}$ ,  $\text{RH}=31\%$ .

<sup>b</sup> Odor threshold based on "VOCBASE" database by the Danish National Institute of Occupational Health.

## Biographical Sketch

### KWANG H. HAN

Ph. D., Building Energy and Environmental Systems Laboratory (BEESL), Dept. of Mechanical and Aerospace Engineering, Syracuse University; 263 Link Hall, Syracuse, New York 13244; Phone: (315) 450-2704; Fax: (315) 443-9099; e-mail: [kwhan@syr.edu](mailto:kwhan@syr.edu)

#### AREA OF EXPERTISE:

Integrated Built Environmental Systems; Material Emissions and Indoor Air Quality; Design and Implementation of Optimal Control System; Signal Processing; GPS/INS as a Positioning and Navigation Sensor

#### PROFESSIONAL PREPARATION:

Syracuse University, Syracuse, NY	Mechanical & Aerospace Engineering	Ph.D 2011
Seoul National University, Korea	Aerospace Engineering	MS 2001
Seoul National University, Korea	Mechanical & Aerospace Engineering	BS 1999

#### APPOINTMENTS:

CoE Fellow	Syracuse Center of Excellence headquarters building, Syracuse, NY, May 2010 – May 2011.
Research Assistant	Mechanical and Aerospace Engineering, Syracuse University, Syracuse, NY, Sep 2007 – Aug 2010.
Chief Liaison Officer (First Lieutenant, O-2)	Air Force Logistics Command of Republic of Korea, Daegu, Korea, Mar 2001 – Jun 2004.
Develop. Engineer & Technical Instructor	National Institute of Agricultural Engineering, Suwon, Korea, Jul 2000 – Mar 2001.
Teaching Assistant	Mechanical and Aerospace Engineering, Seoul National University, Seoul, Korea, Mar 1999 – Jul 2000.

#### SELECTED PUBLICATIONS:

- One patent: *New Concept and Development of Sound Positioning System*, KR Patent #10-1999-0011379, Apr 1999.
- **Han, K.H.**, Zhang, J.S., Wargocki, P., Knudsen, H.N. and Guo, B. (2010). "Determination of material emission signatures by PTR-MS and their correlations with odor assessments by human subjects." *Indoor Air*, **20**, 341-354.
- **Han, K.H.**, Zhang, J.S., Knudsen, H.N., Wargocki, P., Chen, H., Varshney, P.K. and Guo, B. (2011). "Development of a novel methodology for indoor emission source identification." *Atmospheric Environment*, [doi:10.1016/j.atmosenv.2011.03.021](https://doi.org/10.1016/j.atmosenv.2011.03.021).
- **Han, K.H.** and Kee, C. (2001). "On Integrating GPS and INS." *Journal of SNU BK21*, Seoul National University, Korea.

#### SYNERGETIC ACTIVITIES:

*Kwang H. Han has over 5 years of research experience in Signal Processing and Control, and 4 years of research experience in Built Environmental Systems (BES). He led a project, a part of the collaborative effort among Syracuse University, Technical University of Denmark, and Danish Building Research Institute, Aalborg University. He demonstrated his collaborative excellence with researchers that have different academic backgrounds. He is a member of ISIAQ and ASHRAE.*

